frontiers | Research Topics

Multidrug gram-negative bacilli : Current situation and future perspective

Edited by
Rafael Franco-Cendejas, Elvira Garza González,
Rodolfo García-Contreras and Luis Esau Lopez Jacome

Published in
Frontiers in Cellular and Infection Microbiology

ISSN 1664-8714
ISBN 978-2-8325-3996-5
DOI 10.3389/978-2-8325-3996-5

About Frontiers

Frontiers is more than just an open access publisher of scholarly articles: it is a pioneering approach to the world of academia, radically improving the way scholarly research is managed. The grand vision of Frontiers is a world where all people have an equal opportunity to seek, share and generate knowledge. Frontiers provides immediate and permanent online open access to all its publications, but this alone is not enough to realize our grand goals.

Frontiers journal series

The Frontiers journal series is a multi-tier and interdisciplinary set of open-access, online journals, promising a paradigm shift from the current review, selection and dissemination processes in academic publishing. All Frontiers journals are driven by researchers for researchers; therefore, they constitute a service to the scholarly community. At the same time, the *Frontiers journal series* operates on a revolutionary invention, the tiered publishing system, initially addressing specific communities of scholars, and gradually climbing up to broader public understanding, thus serving the interests of the lay society, too.

Dedication to quality

Each Frontiers article is a landmark of the highest quality, thanks to genuinely collaborative interactions between authors and review editors, who include some of the world's best academicians. Research must be certified by peers before entering a stream of knowledge that may eventually reach the public - and shape society; therefore, Frontiers only applies the most rigorous and unbiased reviews. Frontiers revolutionizes research publishing by freely delivering the most outstanding research, evaluated with no bias from both the academic and social point of view. By applying the most advanced information technologies, Frontiers is catapulting scholarly publishing into a new generation.

What are Frontiers Research Topics?

Frontiers Research Topics are very popular trademarks of the *Frontiers journals series*: they are collections of at least ten articles, all centered on a particular subject. With their unique mix of varied contributions from Original Research to Review Articles, Frontiers Research Topics unify the most influential researchers, the latest key findings and historical advances in a hot research area.

Find out more on how to host your own Frontiers Research Topic or contribute to one as an author by contacting the Frontiers editorial office: frontiersin.org/about/contact

Multidrug gram-negative bacilli : Current situation and future perspective

Topic editors

Rafael Franco-Cendejas — National Institute of Rehabilitation Luis Guillermo Ibarra Ibarra, Mexico

Elvira Garza González — Autonomous University of Nuevo León, Mexico

Rodolfo García-Contreras — National Autonomous University of Mexico, Mexico

Luis Esau Lopez Jacome — PhD. Coordinador de Laboratorio de Infectología. Instituto Nacional de Rehabilitación., Mexico

Citation

Franco-Cendejas, R., González, E. G., García-Contreras, R., Jacome, L. E. L., eds. (2023). *Multidrug gram-negative bacilli : Current situation and future perspective*. Lausanne: Frontiers Media SA. doi: 10.3389/978-2-8325-3996-5

Table of contents

frontiers | Frontiers in Cellular and Infection Microbiology

TYPE Editorial
PUBLISHED 09 November 2023
DOI 10.3389/fcimb.2023.1327413

OPEN ACCESS

EDITED AND REVIEWED BY
Costas C. Papagiannitsis,
University of Thessaly, Greece

*CORRESPONDENCE
Elvira Garza-González
elvira_garza_gzz@yahoo.com;
elvira.garzagn@uanl.edu.mx

RECEIVED 24 October 2023
ACCEPTED 31 October 2023
PUBLISHED 09 November 2023

CITATION
López-Jácome LE, Franco-Cendejas R, García-Contreras R and Garza-González E (2023) Editorial: Multidrug gram-negative bacilli : current situation and future perspective.
Front. Cell. Infect. Microbiol. 13:1327413.
doi: 10.3389/fcimb.2023.1327413

Editorial: Multidrug gram-negative bacilli : current situation and future perspective

Luis Esaú López-Jácome[1], Rafael Franco-Cendejas[1], Rodolfo García-Contreras[2] and Elvira Garza-González[3]*

[1]Laboratorio de Infectología, Instituto Nacional de Rehabilitación, Ciudad de México, Mexico, [2]Departamento de Microbiología y Parasitología, Facultad de Medicina, Universidad Nacional Autónoma de México (UNAM), Mexico City, Mexico, [3]Laboratorio de Microbiología Molecular, Facultad de Medicina, Universidad Autónoma de Nuevo León, Monterrey, Mexico

KEYWORDS

drug resistance, multidrug-resistant, carbapenems, acinetobacter, carbapenemase

Editorial on the Research Topic
Multidrug gram-negative bacilli : current situation and future perspective

Drug resistance in Gram-negative is increasing worldwide, complicating therapies of infections, and is associated with increased morbidity and mortality (Antimicrobial Resistance Collaborators, 2023). The World Health Organization designed and proposed a unified One Health approach for the study of resistance to antibiotics. This concept involves the interaction of humans and animals in the environment (Accessed on October 23, 2023).

In this topic we were dedicated to the study of multidrug-resistant Gram negatives and nine original articles from 69 authors were included. Among Gram-negative bacilli with multi-drug resistance, 3 studies included *Acinetobacter* and other studies included other relevant genera (*Salmonella*, *Proteus*, *Klebsiella*, and *Campylobacter*). Among the nine studies, one was a clinical study, specifically in patients with acute pancreatitis, two analyzed the colonization by drug-resistant organisms in humans and chickens and 6 other studies analyzed the molecular characteristics of particular strains. In this scenario, we included the study of multidrug-resistant bacteria in humans and animals with which we approach the One Health concept.

In the clinical study, Yan et al. established a model for early prediction of the risk of death in patients with acute pancreatitis infected with Gram negatives. In the results of this study, four variables were selected, but only two of them had an adequate confidence interval, with the carbapenem resistance showing the highest odds ratio value (OR 7.99), followed by the presence of septic shock (OR 6.33). This result underlined the importance of drug resistance in the outcome of patients, specially for broad-spectrum antibiotics such as carbapenems.

Also, two studies of carriers of drug-resistance genes were included, with one of them analyzing carriers in humans and the other in chickens. The first carriers study determined the relationship between the intestinal loads of $bla_{\text{CTX-M-1}}$, $bla_{\text{OXA-1}}$, $bla_{\text{OXA-48}}$, and bla_{VIM} genes and antibiotic consumption among 90 pediatric critically ill patients (Dahdouh et al.). In this study, 74.45% of patients were positive for at least one of the tested genes. Also, consumption of

carbapenems, non-carbapenem β-lactams, and glycopeptides was associated with a negative result for *bla*$_{CTX-M-1}$ and *bla*$_{OXA-1}$ and the consumption of trimethoprim/sulfamethoxazole and aminoglycosides was associated with a negative result for bla$_{OXA-48.}$ The high prevalence of intestinal carriers of some carbapenemase encoding genes (*bla*$_{OXA-48}$ and *bla*$_{VIM)}$ puts the spotlight on the high possibility of dissemination of these genes because being in the intestinal lumen is an easy way to disseminate them to the hospital environment, healthcare providers, and other patients. The second one focused on the description of whole genome sequencing and determination of susceptibility patterns of 13 *Campylobacter jejuni* and 17 *Campylobacter coli* strains isolated from chickens in China. This work was conducted by Xiao et al.. The results showed two dominant clonal complexes in *C. coli* (CC-354 *C. jejuni* and CC-828). All strains were resistant to ciprofloxacin and tetracycline and this phenotype correlated strongly with the presence of the GyrA T86I and *tet(O)*/*tet(L)* mutation, respectively. The high distribution of genes encoding resistance to quinolones and tetracycline in animals of high consumption in humans allows us to understand the relevance of studying animals in conjunction with humans, to, after knowing the magnitude of the problem, design strategies for its control.

Six articles were related to the microbiological and molecular analysis of clinical isolates and is not surprising that 3 of them were related to *Acinetobacter* species, one to *Salmonella enterica*, one for *Proteus mirabilis*, and one to *Klebsiella pneumoniae*.

In the first study Sharma et al., described the susceptibility profile of carbapenem-resistant *A. baumannii* co-harboring *bla*$_{OXA-23}$ and metallo-β-lactamases against standard drugs and some combinations of drugs. They included 356 clinical isolates, with 89.04% being resistant to imipenem, 79.49% to meropenem, 77.80% to doripenem, 71.62% to ampicillin/sulbactam and 2.52% to colistin. The majority (87.69%) were co-producers of classes D and B carbapenemases. Regarding the drug combinations, there was synergy with meropenem-sulbactam (47%) and meropenem-colistin (57%), but reduced synergy was detected for those strains harboring the *bla*$_{NDM}$ gene. The presence of the *bla*$_{NDM}$ gene was a significant cause of synergy loss in meropenem-sulbactam and meropenem-colistin, further reducing therapeutic options for infections due to bacteria that had genes encoding the NDM gene. The presence of the NDM gene, beyond representing resistance to carbapenems and other antibiotics, may hinder the therapeutic efficacy of antibiotic combinations.

Acinetobacter baumannii is one of the species that have shown the worldwide distribution of multi- and extensive drug resistance. For this bacterial species, colistin is one of the few therapeutic alternatives. For the study of colistin resistance in *A. baumannii*, it is common the analysis of colistin-resistant strains, but the study of susceptible isolates is relevant to discriminating which mutations may be associated with resistance and which not. Zafer et al. analyzed 18 multi-/extensively drug-resistant *A. baumannii* isolates by whole genome sequencing with 17 of them being susceptible to colistin. All these strains carried missense mutations in *pmrCAB* and *lpxACD* operons. Overall, 34 mutations were found, 20 strains had substitutions in *pmrC* and no mutations were found in *pmrA* or *lpxA*. This study provides information that may be helpful in the study of colistin resistance mechanisms.

The third work about *Acinetobacter* genus describes the genetic characterization of carbapenem-resistant *Acinetobacter johnsonii*, co-producing NDM-1, OXA-58, and PER-1 collected for sputum. Surprisingly, the strain carried 11 plasmids, with *bla*$_{OXA-58}$ and *bla*$_{PER-1}$ genes located in the pAYTCM-1 plasmid that has been reported in several countries (Tian et al.). The *bla*$_{NDM-}$ gene was located in conjugative plasmids that were stable even after 70 passages under antibiotics-free conditions.

Colistin resistance has been associated with a chromosomal mutation in genes associated with the modification of the lipid A of lipopolysaccharide, the primary target of colistin (DOI: 10.3389/fmicb.2014.00643). A plasmid-mediated colistin resistance was reported in 2015 (DOI: 10.1016/S1473-3099(15)00424-7), and this plasmid has been reported worldwide. Sun et al. reported the characteristics of 12 *mcr*-bearing plasmids in clinical *Salmonella enterica* in China (10 carried the *mcr*-1 and two carried the *mcr*-3). They detected that the *mcr* gene in clinical *Salmonella* was commonly carried by broad-host plasmids and had the potential to transfer into other bacteria by these plasmids.

The last study included the genetic analysis of resistance and virulence characteristics of clinical multidrug-resistant *Proteus mirabilis* isolates and detected 14 MDR bacteria that were susceptible to carbapenems (except imipenem), ceftazidime, and amikacin; as well as most of them were susceptible to aminoglycosides (Li et al.). Genomic analysis showed high genetic diversity, with integrative and conjugative elements commonly detected, carrying abundant antimicrobial resistance genes, including the *bla*$_{CTX-M-65}$. The findings highlight the important roles of antimicrobial resistance genes in mediating the spread of antimicrobial resistance genes in *P. mirabilis* strains.

Finally, the last one detailed the whole bacterial genome of *K. pneumoniae* strain F4 resistant to routinely used antibiotics, including tigecycline associated with the presence of the *oqxAB* gene localized on the F4_chromosome and tmexCD1-toprJ1 on F4_plasmid A (Qu et al.).

This study showed a wide antibiotic resistance of *K. pneumoniae* strain F4 that effective antibiotics were virtually unavailable, therefore their spread and prevalence should be strictly controlled. Together, all these 9 studies contribute to better knowledge about the current situation and perspectives on infections by multidrug-resistant Gram-negative bacilli. Continued education on this topic may allow us to better understand the dynamics of transmission of these infections, and the role of the different participants to better implement control therapies.

Author contributions

LL-J: Methodology, Writing – review & editing. RF-C: Writing – review & editing. RG-C: Writing – review & editing. EG-G: Methodology, Writing – original draft, Writing – review & editing.

Funding

The author(s) declare that no financial support was received for the research, authorship, and/or publication of this article.

Acknowledgments

We thank the contributing authors of this Research Topic for their valuable contributions. To the Frontiers staff for careful follow-up of the submission, review, and editing of articles.

Conflict of interest

The authors declare that the research was conducted in the absence of any commercial or financial relationships that could be construed as a potential conflict of interest.

The author(s) declared that they were an editorial board member of Frontiers, at the time of submission. This had no impact on the peer review process and the final decision.

Publisher's note

Reference

Antimicrobial Resistance Collaborators. (2023). The burden of antimicrobial resistance in the Americas in 2019: a cross-country systematic analysis. *Lancet Reg. Health Am.* 25, 100561. doi: 10.1016/j.lana.2023.100561

frontiers | Frontiers in Cellular and Infection Microbiology

TYPE Original Research
PUBLISHED 10 November 2022
DOI 10.3389/fcimb.2022.1032375

OPEN ACCESS

EDITED BY
Rajat Madan,
University of Cincinnati, United States

REVIEWED BY
Almagul Kushugulova,
Nazarbayev University, Kazakhstan
Kavya Patel,
College of Medicine, University of Cincinnati, United States

*CORRESPONDENCE
Peng Jie
pengjie2014@csu.edu.cn

†These authors have contributed equally to this work and share first authorship

SPECIALTY SECTION
This article was submitted to Clinical Microbiology, a section of the journal Frontiers in Cellular and Infection Microbiology

RECEIVED 31 August 2022
ACCEPTED 25 October 2022
PUBLISHED 10 November 2022

CITATION
Yan J, Yilin H, Di W, Jie W, Hanyue W, Ya L and Jie P (2022) A nomogram for predicting the risk of mortality in patients with acute pancreatitis and Gram-negative bacilli infection. *Front. Cell. Infect. Microbiol.* 12:1032375.
doi: 10.3389/fcimb.2022.1032375

A nomogram for predicting the risk of mortality in patients with acute pancreatitis and Gram-negative bacilli infection

Jia Yan†, Huang Yilin†, Wu Di, Wang Jie, Wang Hanyue, Liu Ya and Peng Jie*

Department of Gastroenterology, Xiangya Hospital, Central South University, Changsha, China

Objective: Gram-negative bacilli (GNB) are common pathogens of infection in severe acute pancreatitis (SAP), and their occurrence increases the mortality of SAP. Early identification of SAP severity and prognosis is of great significance to SAP treatment. This study explored risk factors for mortality in patients with SAP and GNB infection and established a model for early prediction of the risk of death in GNB-infected SAP patients.

Methods: Patients diagnosed with SAP from January 1, 2016, to March 31, 2022, were included, and their baseline clinical characteristics were collected. Univariate logistic regression analysis was performed to screen for death related variables, and concurrently, a Boruta analysis was performed to identify potentially important clinical features associated with mortality. The intersection of the two results was taken for further multivariate logistic regression analysis. A logistic regression model was constructed according to the independent risk factor of death and then visualized with a nomogram. The performance of the model was further validated in the training and validation cohort.

Results: A total of 151 patients with SAP developed GNB infections. Univariate logistic regression analysis identified 11 variables associated with mortality. The Boruta analysis identified 11 clinical features, and 4 out of 9 clinical variables: platelet counts (odds ratio [OR] 0.99, 95% confidence interval [CI] 0.99–1.00; p = 0.007), hemoglobin (OR 0.96, 95% CI 0.92–1; p = 0.037), septic shock (OR 6.33, 95% CI 1.12–43.47; p = 0.044), and carbapenem resistance (OR 7.99, 95% CI 1.66–52.37; p = 0.016), shared by both analyses were further selected as independent risk factors by multivariate logistic regression analysis. A nomogram was used to visualize the model. The model demonstrated good performance in both training and validation cohorts with recognition sensitivity and specificity of 96% and 80% in the training cohort and 92.8% and 75% in the validation cohort, respectively.

Conclusion: The nomogram can accurately predict the mortality risk of patients with SAP and GNB infection. The clinical application of this model

allows early identification of the severity and prognosis for patients with SAP and GNB infection and identification of patients requiring urgent management thus allowing rationalization of treatment options and improvements in clinical outcomes.

KEYWORDS

severe acute pancreatitis, carbapenem-resistant Gram-negative bacilli, septic shock, predictive model, nomogram

Introduction

Acute pancreatitis (AP), an acute inflammatory disease caused by destruction of acinar cells that perform exocrine function of the pancreas, is one of the most common diseases of the digestive system requiring emergency treatment. Its global incidence is on the rise. The overall mortality rate is about 5% (Mederos et al. 2021). About 20% of patients develop severe acute pancreatitis (SAP) with persistent organ failure as the main manifestation, and the fatality rate is as high as 30% to 50% (Garg and Singh, 2019). In patients with SAP, in addition to the high risk of death caused by systemic inflammatory response syndrome and organ failure during the early stages of the disease, local and/or systemic infectious complications and related organ failure during the middle and late stages of the disease compose the second death peak, and gradually become the main cause of death (Johnson and Abu-Hilal, 2004).

Patients with AP are at high risk of infection due to the overuse of early anti-inflammatory and antimicrobial drugs, and infection is a major complication that jeopardizes the course of AP (Moka et al., 2018). Disruption of the intestinal barrier and translocation of intestinal bacteria in patients with AP has been recognized as the main cause of necrotizing infection in pancreatitis. In AP, bacterial and fungal infections resulting from predominantlyPatients with necrotizing Gram-negative bacteria (GNB) can occur in the abdominal cavity, and pancreatic infection is present in approximately one-third of patients with acute necrotizing pancreatitis (van Brunschot et al., 2012). Patients with necrotizing pancreatitis and infection may have more than twice the mortality rate of uninfected group (Baron et al., 2020). Infectious necrotizing pancreatitis (INP) has been identified as a determinant of mortality in acute pancreatitis study (Petrov et al., 2010). Additionally, approximately one third of patients with AP have extra-pancreatic infections (EPI), such as bacteremia, pneumonia, and urinary tract infections (Bakker et al., 2013). Complications of extra pancreatic infections are also associated with increased mortality (Brown et al., 2014). EPIs are considered to be iatrogenic infections acquired by intestinal bacterial translocation into the systemic circulation or through percutaneous drainage tubes, venous catheters, urinary catheters, and others (Wu et al., 2008). EPI have received more and more attention in recent years. In the process of AP treatment, EPI also needs to be actively evaluated and treated.

Despite the improvements in diagnostic and treatment techniques, the high mortality rate for AP, especially SAP, has not declined over the past decade (Lankisch et al., 2015). Early and accurate assessment of the severity and prognosis of SAP, especially when it occurs with a concurrent infection, is of great significance for clinicians to pay attention to the condition of SAP and to prescribe more effective treatment measures for patients whose condition might worsen. Related research mainly focuses on necrotizing pancreatitis and drug-resistant bacterial infection. Few studies exploring mortality prediction in patients with AP and GNB infection are available. Herein, we used machine learning methods to develop a visual and easy-to-use nomogram to predict the risk of death in patients with AP and GNB infection.

Methods

Study design and patients

A retrospective cohort study enrolled cases of moderate SAP and SAP patients confirmed to have infections with GNB and collected relevant clinical data from January 1, 2016, to March 31, 2022, in Xiangya Hospital, Central South University, a 3500-bed tertiary care teaching hospital. At the initial admission, all patients were assessed and managed *via* the multidisciplinary team, including pancreatic surgeons, emergency physicians, gastroenterology physicians, and intensive care unit physicians according to the latest international guidelines (Crockett et al., 2018).

In our cohort, diagnosis and classification of AP were based on the criteria of revised Atlanta classification (Banks et al., 2013). Criteria of etiology are listed: (1) biliary: choledocholithiasis or cholelithiasis by enhanced computed tomography; (2) hypertriglyceridemia: triglyceride >1000 mg/dl; and/or (3)

alcoholic: drinking > 50 g/d for at least one year. Patients who were older than 18 years, diagnosed with AP according to Atlanta criteria, and had GNB infection in the advanced period (disease duration > 2 weeks) would also be enrolled in our study. Patients who were younger than 18 years or older than 75 years, diagnosed with mild acute pancreatitis, pregnant, complicated with malignant tumor, and/or infected before the admission to our hospital were excluded.

Eventually, 151 patients were enrolled for further analysis, and they were randomly allocated as a ratio of 7:3 to training and validation cohorts (Zhang et al., 2020). The variable analysis and model establishment were conducted based on the whole data set and further evaluated in the training and validation cohorts, respectively.

Clinical data collection

Clinical characteristics included general demographic information, etiology, comorbidity, type of acute pancreatitis (recurrent acute pancreatitis [RAP], severe acute pancreatitis), site of infections, bacteria species, laboratory indices, mortality, antibiotic therapy, complications, and the detailed information on admission. Missing data < 20% were subsequently submitted to missing value imputation.

The infection was diagnosed on the basis of clinical presentation and positive culture features according to the criteria of the Centers for Disease Control (Horan et al., 2008). The date of the first positive sample collection was considered as the initiation of the infection. The relevant laboratory data within the initial 24 h after the first positive culture sample were collected, and the worst data were used in the analysis if two or more identical detecting items existed. Commonly used prophylactic anti-infective drugs included broad-spectrum antibiotics ($3^{rd}/4^{th}$ generation cephalosporins and quinolones, carbapenems, and combined antibiotics). In addition, antibiotic therapy was administered for "suspected" infections until further positive culture and drug susceptibility results were available for the selection of a targeted therapy. In general, the whole antibiotic procedure lasted approximately 5 days, including the frequently used drugs carbapenems, tigecycline, penicillin/β-lactamase inhibitors, and their combination.

Microbiological identification of drug resistance was performed using the VITEK-2 system (BiomeRieux, Marcy L'etoile, France). Drug susceptibility and minimum inhibitory concentrations were determined using the Kerby–Bauer disk diffusion and agar dilution methods, respectively. Carbapenem resistance (CR) was defined as acquired insensitivity to meropenem or imipenem; minimum inhibitory concentration ≥ to 2 mg/L (Wu et al., 2020).

Clinical outcomes were divided into mortality and survival according to death event during the time of hospitalization.

Ethics statement

Because of the retrospective nature of this cohort study, the Institutional Review Boards of Xiangya Hospital (no. 202105092) waived the need for direct patient enrollment and informed consent. Information was gathered from electrical medical systems in an anonymous manner in which all authors could ensure the confidentiality of patient data. The study was strictly performed in accordance with the Declaration of Helsinki.

Feature analysis and selection

Using logistic regression analysis

Variables were subjected to univariate logistic regression analysis to calculate odds ratio (OR) and evaluated whether the characteristic factor was significant.

Based on random forest

Concurrently, to clarify the exact clinical characteristics concerning with mortality at a probability excelling random, a Boruta analysis was conducted to remove unusable features that could create unnecessary noise. The Boruta analysis is a random forest-based feature selection algorithm (Kursa, 2014) in which the basic logic is to evaluate the importance of each feature variable through a loop method by copying the original feature set and randomly mixing each feature value to construct a shadow feature with randomness; after interactive calculation, the importance of the scores of the original and shadow features were compared, so as to filter out the optimal feature set that can be used for modeling. The final result uses the shadow Max as the screening index. When the feature variable score was greater than the shadow Max, the feature was considered important and accepted; otherwise, the variable was rejected, the remaining variables with importance scores around shadow Max value were divided into a tentative group. All Boruta analyses were performed using the Boruta package version 6.0.0 using the default parameters (ntree = 500, max Runs = 500, p = 0.01).

Development and validation of a logistic regression model

The intersection of variables with statistical significance that were sifted out in the univariate logistic regression analysis and the important variables distinguished by Boruta analyses were selected. Successively, the intersected variables were taken to multivariate logistic regression analysis to determine independent predictors of mortality. Furthermore, a logistic regression model was established based on independent predictors, and a visual version was constructed through the

utilize of a nomogram. Besides, we assessed the model in the training cohort (n = 105) and validation cohort (n = 46), which was determined by the ratio of the patients enrolled into the training cohort and validation cohort in the previous study (Zhang et al., 2020). Predictive performance was assessed by discrimination and calibration.

Statistical analysis

Other missing values were interpolated using the mice package (3.14.0) of R software for multiple imputation (Hayati Rezvan et al., 2015). Normally, distributed continuous variables were expressed as mean ± standard deviation (SD) and compared using Student's t-test, and non-normally distributed continuous variables were expressed as median (inter-quartile range [IQR]) and were compared using the Wilcox Sum Rank test. Categorical variables were expressed as count and percentage, which were compared using a chi-squared or Fisher's exact test.

The intersection of variables with statistical significance sifted out in the univariate logistic regression analysis and the important variables distinguished by Boruta analyses were selected. The intersected variables selected in the previous steps were taken to multivariate logistic regression analysis, to identify the ones with $P < 0.05$ and construct a clinical predictive model. Furthermore, a receiver operating characteristic curve (ROC) was conducted to measure the predictive accuracy of the developed model, and the area under the receiver operating characteristic curve (AUC) was calculated. Finally, this model was assessed using a bootstrap-based calibration process (Wan et al., 2022) to evaluate the relationship between the actual and predicted probabilities of mortality. The statistical analyses mentioned above were performed using the RMS Version 6.2-0 and pROC Version 1.18.0 R package.

All statistical analyses were performed using R software version4.1.2 (www.r-project.org). P-value < 0.05 was considered statistically significant among the relevant analyses.

Results

Baseline characteristics of patients

A total of 151 patients with moderate SAP and SAP developed GNB infection with a mortality rate of 25.8% (39 of 151) and a median age of 48 years over a 6-year period. The ratio of male and female were 70.9% (n = 107) and 29.1% (n = 44), respectively. Hypertriglyceridemia (n = 64, 42.4%) and gallstones (n = 39, 25.8%) were the main etiologies in our cohort. And 23 patients were diagnosed with RAP (15.2%). The most common comorbidities included diabetes (21.2%) and hypertension (20.5%). SAP accounted for 53.6% of the total cases. The pancreas (peri) (64.9%) was the most common site (64.9%) of infection, and *Klebsiella pneumonia* (29.8%) was the most common pathogen. Of the 151 patients, a total of 49% had polymicrobial infections, 51% had multiple site infections, 33.1% had fungal infections, and 30.5% had Gram-positive pathogen infections. Among the Gram-negative pathogens, 47.5% were carbapenem-resistant. Broad-spectrum antibiotics (33.8%) were the most common preventive anti-infective drugs followed by combined antibiotics (30.5%) and carbapenems (29.8%). Carbapenems (35.1%) and carbapenem–tigecycline (29.1%) were the most commonly used treatment protocols for confirmed infection. The incidence of pancreatic leakage and intestinal fistula were 16.6% and 13.9%, respectively. More than one-quarter (31.8%) of patients developed respiratory failure and required mechanical ventilation support, and 17.2% of patients required vasoactive drugs to maintain blood pressure due to septic shock. A comparison of clinical data and laboratory variables between the survival and mortality groups of 151 patients with SAP and GNB infection is shown in Table 1. Among the 151 patients who met the inclusion criteria, 105 patients were included in the training cohort and 46 included in the validation cohort, and no significant differences in baseline clinical characteristics between the training and validation cohorts were found (Supplementary Table 1). The mortality rates of these two cohorts were 23.8% (25 of 105) and 30.4% (14 of 46), respectively. No significant difference in baseline characteristic between the training and validation cohorts were found.

Univariate logistic regression analysis for statistically significant parameters

Risk factors for death in patients with AP and GNB infection were analyzed by univariate logistic regression, and the results are shown in Table 2. Eleven variables, including creatinine, bilirubin, platelets, hemoglobin, carbapenem resistance, septic shock, SAP, therapeutic agents, mechanical ventilation, and the first site of infection were found to be significantly associated with mortality.

Identification of important variables with Boruta analysis

To obtain all relevant classified features according to importance, 32 clinical characteristics were evaluated using the Boruta feature selection method. The hierarchical graph of feature importance is shown in Figure 1. When the feature variable score is above the shadow Max, the feature was accepted; among them, 11 clinical indicators, including SAP, intestinal leakage, etiology, platelet counts, bilirubin, hemoglobin, intubation, procalcitonin, creatinine, carbapenem

TABLE 1 Clinical characteristics and comparison between survival and mortality of 151 AP patients with GNB infections.

Variables [n (%), median (IQR) or mean ± SD]	Total (n =151)	Survival (n =112)	Death (n = 39)	p-value
Gender (Male)	107 (70.9)	78 (69.6)	29 (74.4)	0.724
Age, years	48.44 (12.53)	47.54 (12.49)	51.03 (12.45)	0.136
Comorbidity				
Hypertension	31 (20.5)	21 (18.8)	10 (25.6)	0.492
Diabetes	32 (21.2)	25 (22.3)	7 (17.9)	0.728
Hepatitis	4 (2.6)	2 (1.8)	2 (5.1)	0.274
Etiology				
Gallstones	39 (25.8)	26 (23.2)	13 (33.3)	0.011
Hypertriglyceridemia	64 (42.4)	53 (47.3)	11 (28.2)	
Alcoholism	18 (11.9)	8 (7.1)	10 (25.6)	
Idiopathic	3 (2.0)	3 (2.7)	0 (0.0)	
Others	27 (17.9)	22 (19.6)	5 (12.8)	
RAP	23 (15.2)	21 (18.8)	2 (5.1)	0.075
SAP	81(53.6)	46 (41.1)	35 (89.7)	<0.001
Enteral nutrition, days	2.00 (2.00, 5.00)	2.00 (2.00, 4.50)	2.50 (2.00, 5.00)	0.905
PH	7.44 (7.39, 7.48)	7.45 (7.42, 7.48)	7.40 (7.33, 7.48)	0.031
SCr (mmol/L)	66.80 (52.95, 100.75)	62.40 (51.62, 76.38)	218.60 (79.85, 364.70)	<0.001
ALB (g/L)	29.92 (4.76)	30.20 (4.94)	29.09 (4.17)	0.211
TBil (mmol/L)	15.70 (9.60, 26.87)	14.30 (9.17, 20.48)	24.95 (17.25, 67.38)	<0.001
NE ($\times10^9$/L)	8.20 (5.60, 12.50)	8.00 (5.57, 12.33)	8.60 (6.00, 14.75)	0.563
LYMPH ($\times10^9$/L)	0.90 (0.60, 1.20)	0.90 (0.60, 1.20)	0.80 (0.50, 1.20)	0.413
PLT($\times10^9$/L)	271.99 (132.69)	294.94 (131.79)	206.10 (112.93)	<0.001
Hb (g/L)	88.13 (17.75)	91.79 (17.37)	77.62 (14.44)	<0.001
PCT (ng/L)	1.00 (0.28, 3.71)	0.45 (0.19, 1.75)	6.46 (1.86, 21.34)	<0.001
Temperature,℃	39.00 (38.00, 39.50)	38.95 (37.95, 39.42)	39.20 (38.80, 39.50)	0.06
Carbapenem resistance	69 (45.7)	33 (29.5)	36 (92.3)	<0.001
Septic shock	26 (17.2)	4 (3.6)	22 (56.4)	<0.001
Mechanical ventilation	48 (31.8)	19 (17.0)	29 (74.4)	<0.001
The first infection site				0.012
Pancreas (peri)	98(64.9)	80(71.4)	18(46.1)	
Bloodstream	16 (10.6)	9 (8.0)	7 (17.9)	
Lung	28 (18.5)	15 (13.4)	13 (33.3)	
Urinary system	2 (1.3)	2 (1.8)	0 (0.0)	
Others	7 (4.6)	6 (5.4)	1 (2.6)	
The first infection strain				<0.001
Escherichia coli	32 (21.2)	29 (25.9)	3 (7.7)	
Klebsiella ozaena	45 (29.8)	28 (25.0)	17 (43.6)	
Acinetobacter baumannii	33 (21.9)	18 (16.1)	15 (38.5)	
Pseudomonas aeruginosa	10 (6.6)	9 (8.0)	1 (2.6)	
Others	31 (20.5)	28 (25.0)	3 (7.7)	
Polymicrobial infections	74 (49.0)	50 (44.6)	24 (61.5)	0.103
Concurrent GPB infection	46 (30.5)	35 (31.2)	11 (28.2)	0.878
Fungal infection	50 (33.1)	34 (30.4)	16 (41.0)	0.307
Prophylactic anti-infection				0.3
Wide-spectrum antibiotics	51 (33.8)	38 (33.9)	13 (33.3)	
Carbapenem	45 (29.8)	33 (29.5)	12 (30.8)	
Combined antibiotics	46 (30.5)	32 (28.6)	14 (35.9)	
Antibiotic therapy				0.013

(Continued)

TABLE 1 Continued

Variables [n (%), median (IQR) or mean ± SD]	Total (n =151)	Survival (n =112)	Death (n = 39)	p-value
Carbapenem (high-dose, extended-infusion)	53 (35.1)	42 (37.5)	11 (28.2)	
Carbapenem and tigecycline	44 (29.1)	26 (23.2)	18 (46.2)	
Penicillins/β-lactamase inhibitors	29 (19.2)	27 (24.1)	2 (5.1)	
Carbapenem and penicillins/β-lactamase inhibitors	21 (13.9)	14 (12.5)	7 (17.9)	
Tigecycline	2 (1.3)	1 (0.9)	1 (2.6)	
Carbapenem and sulfonamides	1 (0.7)	1 (0.9)	0 (0.0)	
Tigecycline and polymyxin	1 (0.7)	1 (0.9)	0 (0.0)	
Pancreatic leakage	25 (16.6)	18 (16.1)	7 (17.9)	0.983
Intestinal leakage	21 (13.9)	12 (10.7)	9 (23.1)	0.098

IQR, interquartile ranges; SD, standard deviation; RAP, recurrent acute pancreatitis; SAP, severe acute pancreatitis; PH, potential of hydrogen; SCr, serum creatinine; ALB, albumin; TBil, total bilirubin; NE, neutrophilic granulocyte; LYMPH, lymphocyte; PLT, platelet; Hb, hemoglobin; PCT, procalcitonin; Concurrent GPB infection, Concurrent Gram-positive bacterial infection.

resistance, and septic shock were important. Not surprisingly, carbapenem-resistant GNB infection and septic shock were significantly associated with the risk of death from moderate SAP. All other variables with an importance score lower than the Shadow max were rejected.

Establishment of death prediction nomogram

Furthermore, we added the intersection of these 11 variables identified by univariate logistic regression analysis and the 11 variables selected by Boruta into the multivariate logistic regression analysis. Among them, platelets (OR 0.99, 95% confidence interval [CI] 0.99–1.00; p = 0.007), hemoglobin (OR 0.96, 95% CI 0.921; p = 0.037), septic shock (OR 6.33, 95% CI 1.12–43.47; p = 0.044), and carbapenem resistance (OR 7.99, 95% CI 1.66–52.37; p = 0.016) were confirmed as independent risk factors for mortality in patients with moderately SAP and SAP (Table 3). These factors were used to construct a multivariate logistic regression prediction model for mortality risk, which was further visualized as a nomogram as shown in Figure 2.

Verification of the developed nomogram

Predictive models were internally validated using the bootstrap validation method. The receiver operating characteristic curves (ROC) for prediction model in training and validating cohorts are shown in Figures 3A, B. The nomogram showed good accuracy in estimating the risk of death among patients with SAP who were infected by GNB. In addition, we applied our model to the training and validation cohorts and conducted correlation analysis to evaluate the performance of the nomogram. The calibration plot graphically showed good consistency in the risk estimated by the nomogram and the actual mortality of patients with SAP (Figures 3C, D). The sensitivity and specificity of this nomogram for identifying death in patients requiring GNB infection were 96% and 80% in the training cohort and 92.8% and 75% in the validation cohort, respectively.

Discussion

Local or systemic infection secondary to SAP is the primary cause of exacerbation in the late stage among which GNB ranks the most important causal pathogen while the influence the infection brought to patient prognosis remains unknown. In this study, we conducted a logistic regression analysis and feature selection to identify four variables: (1) septic shock, (2) carbapenem resistance, (3) hemoglobin, and (4) PLT and developed an easy-to-use visual nomogram to predict the risk of mortality in patients with advanced GNB infection in SAP. The nomogram showed good predictive power. To our knowledge, this is the first report of a clinically-applied predictive model for predicting the risk of mortality in patients with SAP and late-stage GNB infections.

In this study, patients with SAP and GNB infection had a mortality rate of 25.8%. In fact, previous study reported a mortality rate of 34.5% for patients with SAP and secondary infections (Tian et al., 2020) and 40% for patients with necrotizing pancreatitis and concurrent infection (Biberci Keskin et al., 2020). The most common etiology of AP was hyperlipidemia (42.4%), which has been reported as the main cause (58.9%) in patients with multidrug-resistant (MDR) pathogen infections (Li et al., 2020). The rate of RAP was 15.2%, which was similar to the previously reported incidence in about 17% (Ahmed Ali et al., 2016). The rate of carbapenem resistance was 45.7%, slightly lower than the ratio of beyond 50% reported by other studies (Chen et al., 2021). The most common site of infection was the pancreas, and the most common causal pathogen was *K. pneumoniae*, which was similar to the previous literature (Wu et al., 2022).

TABLE 2 Univariate logistic regression analysis based on baseline characteristics in the survival group and death group.

Variables	OR	95% CI	p-value
Age	1.02	0.99 - 1.05	0.137
Male	1.26	0.57 - 2.99	0.577
Etiology	1.078	0.813-1.428	0.603
RAP	0.23	0.04 - 0.85	0.058
SAP	12.55	4.63 - 44.16	< 0.001
Hypertension	1.49	0.61 - 3.48	0.361
Diabetes	0.76	0.28 - 1.86	0.566
Hepatitis	2.97	0.35 - 25.50	0.284
Temperature	1.44	1.01 - 2.12	0.052
PH	0.29	0.03 - 2.64	0.266
SCr	1.01	1.00 - 1.01	< 0.001
ALB	0.95	0.87 - 1.03	0.211
TBil	1.01	1.00 - 1.02	0.016
NE	1	0.95 - 1.03	0.819
LYMPH	0.84	0.42 - 1.10	0.551
PLT	0.99	0.99 - 1.00	< 0.001
PCT	1.03	1.01 - 1.06	0.009
Hb	0.94	0.91 - 0.97	< 0.001
The first infection strain	0.891	0.683-1.162	0.395
Polymicrobial infections	1.98	0.95 - 4.25	0.071
The first infection site	1.316	1.02-1.697	0.035
Fungal infection	1.6	0.74 - 3.39	0.225
Concurrent GPB infection	0.86	0.38 - 1.90	0.722
Carbapenem resistance	28.73	9.52 - 125.01	< 0.001
Prophylactic anti-infection	1.33	0.888-1.992	0.166
Antibiotic therapy	1.293	1.025-1.632	0.03
Eternal nutrition	0.95	0.86 - 1.02	0.251
Septic shock	34.94	11.75 - 131.18	< 0.001
Mechanical ventilation	14.19	6.13 - 35.43	< 0.001
Pancreatic leakage	1.14	0.41 - 2.89	0.786
Intestinal leakage	2.5	0.94 - 6.49	0.06

OR, odds ratio; CI, confidence interval; RAP, recurrent acute pancreatitis; SAP, severe acute pancreatitis; PH, potential of hydrogen; SCr, serum creatinine; ALB, albumin; TBil, total bilirubin; NE, neutrophilic granulocyte; LYMPH, lymphocyte; PLT, platelet; PCT, procalcitonin; Hb, hemoglobin; Concurrent GPB infection, Concurrent Gram-positive bacterial infection.

The translocation of intestinal bacteria (namely, intestinal bacteria passing through the intestinal mucosal barrier, and invading the systemic circulation and extra-intestinal organs) could cause damage to extra-intestinal organs, which led to secondary multiple organ failure and eventually to sepsis (Wang et al., 2019). Septic shock was the most serious infectious complication of bloodstream infection. GNB was most likely to elicit inflammatory reactions within the bloodstream when they discharge large amounts of endotoxin-containing membrane blebs (Munford, 2006). In our study, septic shock was found to be an independent predictive risk factor in patients with SAP and Gram-negative organism infection, manifesting as systemic inflammatory response and secondary multi-organ failure. In fact, septic shock was reported associating with higher mortality in patients with AP and multidrug-resistant *K. pneumonia* infection (Devani et al., 2018), which was consistent with our results. Together with the previous study and our findings, patients with SAP and septic shock should receive prompt and rational treatment, not least antibiotic therapy, as explicit guidelines for early initiation of antiseptic shock therapy are available (Permpikul et al., 2019).

It has been reported that carbapenem has been considered as the last-line regimen for AP patients with "suspected" pancreatic infections (Guo et al., 2022). Due to relative resistance to hydrolysis by most β-lactamases, carbapenems are regarded as the most active and potent agents against multidrug-resistant (MDR) gram-negative pathogens with a wide antibacterial spectrum (El-Gamal et al., 2017).However, the inappropriate use of the antimicrobial drugs has led to the rise of the drug-resistant pathogens, which, according to the reporting

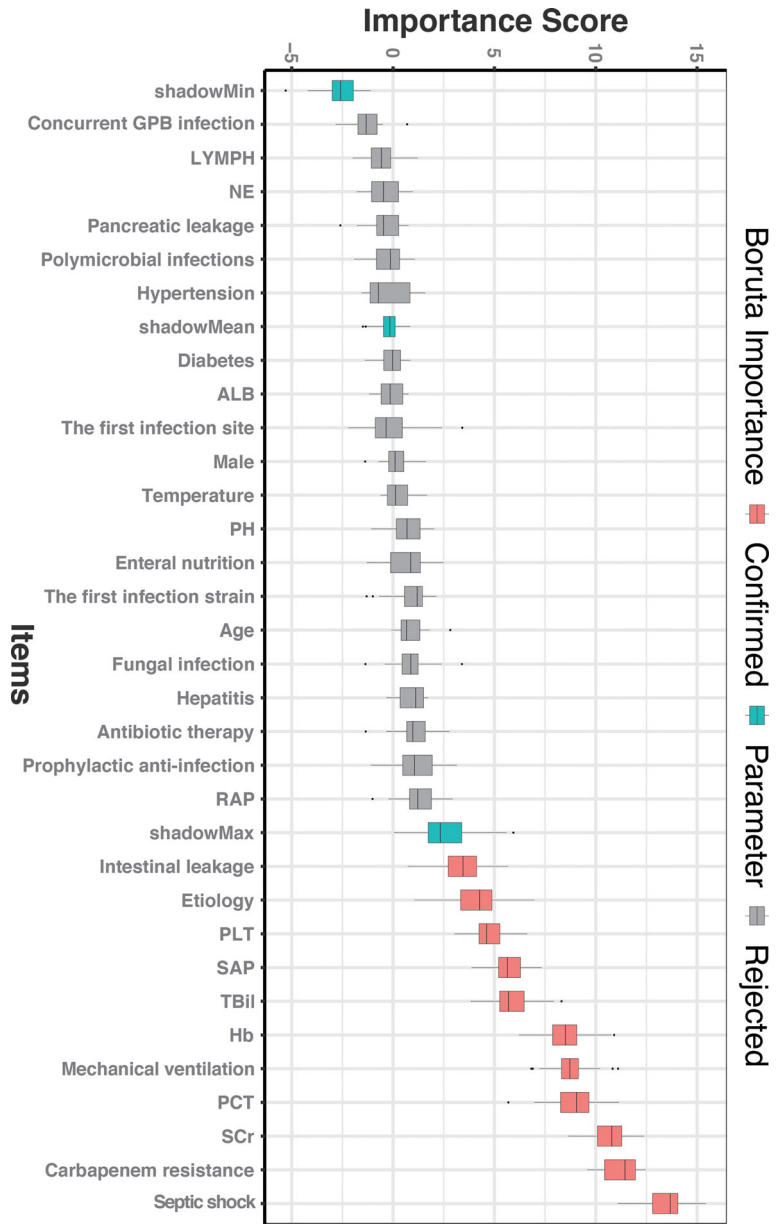

FIGURE 1
The feature importance in the Boruta feature selection process. The red box represents the feature that is confirmed as important, the green box represents the Boruta parameter, and the gray box represents the feature that is rejected. SCr, serum creatinine; PCT, procalcitonin; Hb, hemoglobin; TBil, total bilirubin; SAP, severe acute pancreatitis; PLT, platelet; RAP, recurrent acute pancreatitis; PH, potential of hydrogen; ALB, albumin; NE, neutrophilic granulocyte; LYMPH, lymphocyte; Concurrent GPB infection, Concurrent Gram-positive bacterial infection.

frequency, are sorted from high to low as Carbapenem-resistant *Enterobacteria* (CRE), Carbapenem-resistant *Pseudomonas aeruginosa* (CRPA), and Carbapenem-resistant *Acinetobacter baumannii* (CRAB) complex (Tacconelli et al., 2018). The overuse of antibiotics in China ranks first in the world; hence, Chinese patients with AP were more susceptible to drug-resistant pathogen infections (Párniczky et al., 2019). Over the past decade, CRE infections have caused high mortality, thus placing tremendous economic burden in the global healthcare system (Durante-Mangoni et al., 2019). The GNB acquired resistance to certain drugs occurs *via* multiple methods: (1) production of carbapenemases, (2) over-expression of some efflux pumps, (3) increase in membrane permeability as a result of special porins loss. (Higgins et al., 2004, Cornaglia

TABLE 3 Multivariate logistic regression analysis of mortality based on baseline characteristics in the survival group and death group.

Variables	OR	95% CI	p-value
SCr	1	0.99 - 1.00	0.808
TBil	1.01	1.00 - 1.02	0.093
PLT	0.99	0.99 - 1.00	0.007
Hb	0.96	0.92 - 1.00	0.037
PCT	1.04	0.99 - 1.10	0.143
Carbapenem resistance	7.99	1.66 - 52.37	0.016
Septic shock	6.33	1.12 - 43.47	0.044
SAP	4.86	0.87 - 42.19	0.097
Mechanical ventilation	1.53	0.35 - 6.34	0.556

OR, odds ratio; CI, confidence interval; SCr, serum creatinine; TBil, total bilirubin; PLT, platelet; Hb, hemoglobin; PCT, procalcitonin; SAP, severe acute pancreatitis.

et al., 2007, Zhanel et al., 2007, Nikaido and Pagès, 2012). Thus, carbapenem resistance in Gram-negative pathogens poses a special clinical challenge. Some previous studies elucidated that infection caused by CR- or carbapenemase-producing (CP)-GNB likely led to high mortality rates (Cheng et al., 2015, Liu et al., 2016). Jain et al. revealed that MDR bacterial infection was an independent predictor of mortality in patients with AP and infected pancreatic necrosis (Jain et al., 2018), which was consistent with our findings. Together with previous studies, our data supported the idea that close attention should be devoted to the appropriate use of antibiotics. Although some "last line" antibiotics, such as tigecycline, colistin, minocycline, and ceftazidime–avibactam and others might be available for treating CR-GNB under certain conditions (Doi, 2019), and an animal study demonstrated high dosages of aztreonam might work in the future clinical practice (Bellais et al., 2002).Our results showed that prophylactic antibiotic use was not an independent risk factor for death. Nevertheless, the prophylactic use of antibiotics, especially carbapenems, may not be recommended in AP for the prevention of infectious complication.

Platelet count was found as an independent risk factor for death in the patients with SAP and GNB infection. The inflammatory cascade in the AP could cause damage to the vascular endothelium, activate platelet, induce thrombosis, and conversely promote the progression of AP (Beyazit et al., 2012). The abnormality of platelet count could be considered as an assessing indicator of coagulation function and disease severity (Lei et al., 2017). In addition to participating in the hemostasis process, platelets were important players in host defense during infection and battle with invading pathogens *via* various mechanisms, which included interacting with neutrophils or directly with bacteria (Amison et al., 2018). Hematopoietic inhibition, autoimmune attack, and micro thrombosis depletion might contribute to the occurrence of thrombocytopenia (Kelton et al., 1979; Zhang et al.,

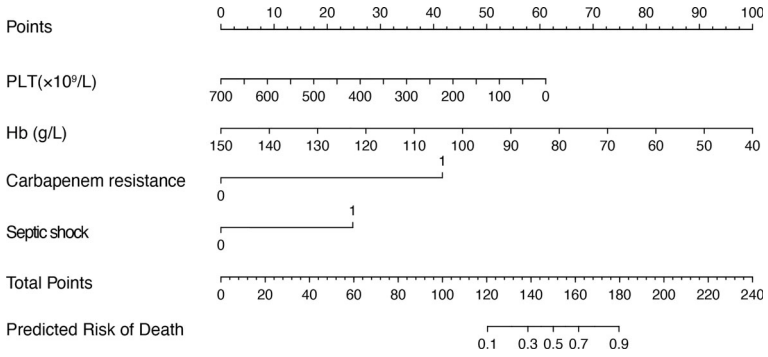

FIGURE 2
Nomogram for predicting the mortality risk in patients with SAP and GNB infection. To evaluate the risk of mortality *via* the nomogram, draw a line perpendicular to the specific axis of each parameter until it reaches the top line marked "Points", sum up the number of points for all parameters, and draw a line descending from the axis marked "Total Points" until it reaches the bottom line to determine the predictive risk of death. PLT, platelet; Hb, hemoglobin.

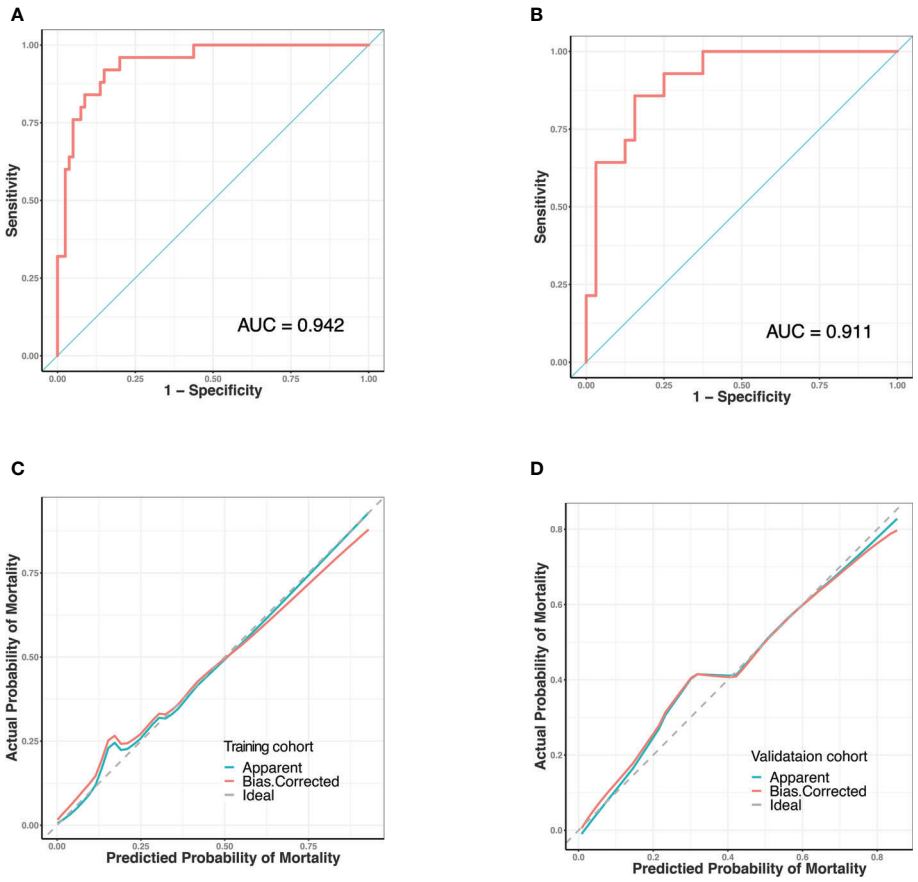

FIGURE 3
Receiver operating characteristic (ROC) curves and predictive performance of the nomogram for predicting mortality risk in SAP patients with GNB infection. **(A)** ROC curve for the predictive model of the training cohort. Area under the curve was 0.942. **(B)** ROC curve for the predictive model of the validation cohort. Area under the curve was 0.911. **(C)** Validity of the predictive performance of the nomogram in estimating the risk of mortality in the training cohort. **(D)** Validity of the predictive performance of the nomogram in estimating the risk of mortality in the validation cohort. ROC, receiver operating characteristic.

2020).However, the specific mechanism remains obscure. In a real-world study, thrombocytopenia was also described as a predictor of death in GNB infection, and closely related to ICU mortality (Jonsson et al., 2021; Ni et al., 2022). It implies that more attention should be paid to the platelet count variation in the clinical practice.

The long-term course of SAP leads to accelerated catabolism, increased caloric and nutrient requirements, and in many cases, nutritional deficiencies, which causes an increase in the incidence and mortality of infections. An important and sensitive indicator reflecting nutritional deficiencies was anemia, and severe anemia was associated with poor prognosis in patients with SAP (Ibrahim et al., 2017; Oh et al., 2021). A study of risk factors for mortality in patients with AP also found that lower hemoglobin was associated with an increase in mortality, which was consistent with our conclusion (Popa et al., 2016). Inflammatory responses were found to influence hemoglobin levels through various approaches, including suppressed erythropoiesis, shortened erythrocyte survival, and decreased erythropoietin production (Ganz, 2019). Besides, the endotoxin released by GNB could also damage the vascular endothelium and even cause disseminated intravascular coagulation, resulting in impaired hemostatic function and blood loss (Schrottmaier et al., 2016). Anemia might affect the prognosis of an individual with infection. When hemoglobin was at a low level, oxygen delivered to major organs was reduced, leading to tissue hypoxia, which can ultimately contribute to multiple organ dysfunction in infected patients (Cavezzi et al., 2020). A related study in patients with sepsis further supported our findings (Muady et al 2016), indicating anemia will lead to a higher risk of increased mortality in patients with infection.

Univariate logistic regression analysis showed that serum creatinine, bilirubin levels, PCT, SAP, and mechanical ventilation were associated with patient mortality, a finding that is consistent with the results of real-world studies, while in our multivariate logistic regression analysis, these several parameters were not independently associated with the risk of mortality. Confounding factors such as platelets, hemoglobin, septic shock, and carbapenem-resistant infections might play an important role in mortality. Multiple organ failure concomitant with septic shock leads to secondary associations between laboratory biochemical markers and mortality. Carbapenem-resistant pathogen infections lead to an increase in the occurrence of mechanical ventilation (Zilberberg et al., 2017). Our results suggest that the above variables did not by themselves directly affect the risk of mortality even though they were closely associated with disease severity. The higher comorbidity burden and greater severity of illness might contribute to wider use of antibiotics in the death group when compared with the survival group.

The purpose of our study was to develop a visual and quantitative nomogram to predict the risk of death in patients with SAP and GNB infections. The application of a nomogram to assess the risk of death in patients with SAP is a new concept. Our predictive model is sensitive and easy to use, enabling efficient and accurate identification in clinical practice. Moreover, the model has good predictive performance. By calculating a total score based on four objective clinical variables (septic shock, carbapenem resistance, platelet counts, and hemoglobin levels), physicians can quantify the mortality in patients with SAP and GNB infections, contributing to more timely and comprehensive diagnosis and treatment.

The calibration curve fits well. The use of this predictive model can provide important guidance for clinical decision making and optimal allocation of medical resources which is expected to improve patient prognosis and quality of life. Using this predictive model to accurately identify patients with high risk of death can enhance clinical symptom warning, optimize the allocation of medical resources, facilitate clinical decision-making, and possibly improve the clinical outcomes of patients with SAP.

Several limitations should be discussed. First, clinical data from patients in the cohort were retrospectively collected; therefore, inherent biases were unavoidable. Second, external and prospective validation in a new large cohort is required to determine diagnostic accuracy and clinical application. Finally, the recapitulative nomogram was used to predict mortality risk for all types of GNB infection, which might temper the efficacy of our nomogram. It would be more precise to expand the sample size in the future study and promote the nomogram according to the specific causal GNB.

Conclusion

We developed a clinically applicable nomogram for predicting the risk of mortality in patients with SAP and GNB infection. This nomogram enables early and efficient assessment of mortality risk in patients with SAP infected by GNB, which may provide guidance for clinical decision-making.

Data availability statement

The original contributions presented in the study are included in the article/Supplementary Material. Further inquiries can be directed to the corresponding author.

Ethics statement

The studies involving human participants were reviewed and approved by the Institutional Review Board of Xiangya Hospital, Central South University. Written informed consent for participation was not required for this study in accordance with the national legislation and the institutional requirements.

Author contributions

Study concept and design: JY. Acquisition of data: JY, WD, WJ, and WH. Statistical analysis: JY. Analysis and interpretation of data: JY and HY. Drafting of the manuscript: HY and JY. Critical revision of the manuscript: PJ. All authors contributed to the article and approved the submitted version.

Funding

This work was supported by grants from the Fundamental Research Funds for the Central Universities of Central South University (2021zzts0352), and National Natural Science Foundation of China (Grant No. 82170661).

Acknowledgments

We appreciate the professionalism and compassion demonstrated by all the healthcare workers involved in patient care. We also acknowledge all the patients for their involvement in this study.

Conflict of interest

The authors declare that the research was conducted in the absence of any commercial or financial relationships that could be construed as a potential conflict of interest.

Publisher's note

All claims expressed in this article are solely those of the authors and do not necessarily represent those of their affiliated organizations, or those of the publisher, the editors and the reviewers. Any product that may be evaluated in this article, or claim that may be made by its manufacturer, is not guaranteed or endorsed by the publisher.

Supplementary material

The Supplementary Material for this article can be found online at: https://www.frontiersin.org/articles/10.3389/fcimb.2022.1032375/full#supplementary-material

References

Ahmed Ali, U., Issa, Y., Hagenaars, J. C., Bakker, O. J., van Goor, H., Nieuwenhuijs, V. B., et al. (2016). Risk of recurrent pancreatitis and progression to chronic pancreatitis after a first episode of acute pancreatitis. *Clin. Gastroenterol. Hepatol.* 14 (5), 738–746. doi: 10.1016/j.cgh.2015.12.040

Amison, R. T., O'Shaughnessy, B. G., Arnold, S., Cleary, S. J., Nandi, M., Pitchford, S. C., et al. (2018). Platelet depletion impairs host defense to pulmonary infection with pseudomonas aeruginosa in mice. *Am. J. Respir. Cell Mol. Biol.* 58 (3), 331–340. doi: 10.1165/rcmb.2017-0083OC

Bakker, O. J., van Santvoort, H., Besselink, M. G., Boermeester, M. A., van Eijck, C., Dejong, K., et al. (2013). Extrapancreatic necrosis without pancreatic parenchymal necrosis: a separate entity in necrotising pancreatitis? *Gut* 62 (10), 1475–1480. doi: 10.1136/gutjnl-2012-302870

Banks, P. A., Bollen, T. L., Dervenis, C., Gooszen, H. G., Johnson, C. D., Sarr, M. G., et al. (2013). Classification of acute pancreatitis–2012: revision of the Atlanta classification and definitions by international consensus. *Gut* 62 (1), 102–111. doi: 10.1136/gutjnl-2012-302779

Baron, T. H., DiMaio, C. J., Wang, A. Y., and Morgan, K. A. (2020). American Gastroenterological association clinical practice update: Management of pancreatic necrosis. *Gastroenterology* 158 (1), 67–75.e61. doi: 10.1053/j.gastro.2019.07.064

Bellais, S., Mimoz, O., Léotard, S., Jacolot, A., Petitjean, O., and Nordmann, P. (2002). Efficacy of beta-lactams for treating experimentally induced pneumonia due to a carbapenem-hydrolyzing metallo-beta-lactamase-producing strain of pseudomonas aeruginosa. *Antimicrob. Agents Chemother.* 46 (6), 2032–2034. doi: 10.1128/aac.46.6.2032-2034.2002

Beyazit, Y., Sayilir, A., Torun, S., Suvak, B., Yesil, Y., Purnak, T., et al. (2012). Mean platelet volume as an indicator of disease severity in patients with acute pancreatitis. *Clin. Res. Hepatol. Gastroenterol.* 36 (2), 162–168. doi: 10.1016/j.clinre.2011.10.003

Biberci Keskin, E., Okay, G., Muhiddin, D., Sharif, R., Taşlidere, B., and Şentürk, H. (2020). The microbiology of necrotizing pancreatitis and its impact on in-hospital and 1-year all-cause mortality. *Eur. J. Gastroenterol. Hepatol.* 32 (6), 695–700. doi: 10.1097/meg.0000000000001687

Brown, L. A., Hore, T. A., Phillips, A. R., Windsor, J. A., and Petrov, M. S. (2014). A systematic review of the extra-pancreatic infectious complications in acute pancreatitis. *Pancreatology* 14 (6), 436–443. doi: 10.1016/j.pan.2014.09.010

Cavezzi, A., Troiani, E., and Corrao, S. (2020). COVID-19: hemoglobin, iron, and hypoxia beyond inflammation. *A Narrat. Rev. Clin. Pract.* 10 (2), 1271. doi: 10.4081/cp.2020.1271

Cheng, A., Chuang, Y. C., Sun, H. Y., Sheng, W. H., Yang, C. J., Liao, C. H., et al. (2015). Excess mortality associated with colistin-tigecycline compared with colistin-carbapenem combination therapy for extensively drug-resistant acinetobacter baumannii bacteremia: A multicenter prospective observational study. *Crit. Care Med.* 43 (6), 1194–1204. doi: 10.1097/ccm.0000000000000933

Chen, S., Shi, J., Chen, M., Ma, J., Zeng, Z., Wang, R., et al. (2021). Characteristics of and risk factors for biliary pathogen infection in patients with acute pancreatitis. *BMC Microbiol.* 21 (1), 269. doi: 10.1186/s12866-021-02332-w

Cornaglia, G., Akova, M., Amicosante, G., Cantón, R., Cauda, R., Docquier, J. D., et al. (2007). Metallo-beta-lactamases as emerging resistance determinants in gram-negative pathogens: open issues. *Int. J. Antimicrob. Agents* 29 (4), 380–388. doi: 10.1016/j.ijantimicag.2006.10.008

Crockett, S. D., Wani, S., Gardner, T. B., Falck-Ytter, Y., and Barkun, A. N. (2018). American Gastroenterological association institute guideline on initial management of acute pancreatitis. *Gastroenterology* 154 (4), 1096–1101. doi: 10.1053/j.gastro.2018.01.032

Devani, K., Charilaou, P., Radadiya, D., Brahmbhatt, B., Young, M., and Reddy, C. (2018). Acute pancreatitis: Trends in outcomes and the role of acute kidney injury in mortality- a propensity-matched analysis. *Pancreatology* 18 (8), 870–877. doi: 10.1016/j.pan.2018.10.002

Doi, Y. (2019). Treatment options for carbapenem-resistant gram-negative bacterial infections. *Clin. Infect. Dis.* 69 (Suppl 7), S565–s575. doi: 10.1093/cid/ciz830

Durante-Mangoni, E., Andini, R., and Zampino, R. (2019). Management of carbapenem-resistant enterobacteriaceae infections. *Clin. Microbiol. Infect.* 25 (8), 943–950. doi: 10.1016/j.cmi.2019.04.013

El-Gamal, M. I., Brahim, I., Hisham, N., Aladdin, R., Mohammed, H., and Bahaaeldin, A. (2017). Recent updates of carbapenem antibiotics. *Eur. J. Med. Chem.* 131, 185–195. doi: 10.1016/j.ejmech.2017.03.022

Ganz, T. (2019). Anemia of inflammation. *N Engl. J. Med.* 381 (12), 1148–1157. doi: 10.1056/NEJMra1804281

Garg, P. K., and Singh, V. P. (2019). Organ failure due to systemic injury in acute pancreatitis. *Gastroenterology* 156 (7), 2008–2023. doi: 10.1053/j.gastro.2018.12.041

Guo, D., Dai, W., Shen, J., Zhang, M., Shi, Y., Jiang, K., et al. (2022). Assessment of prophylactic carbapenem antibiotics administration for severe acute pancreatitis: An updated systematic review and meta-analysis. *Digestion* 103 (3), 183–191. doi: 10.1159/000520892

Hayati Rezvan, P., Lee, K. J., and Simpson, J. A. (2015). The rise of multiple imputation: A review of the reporting and implementation of the method in medical research. *BMC Med. Res. Methodol.* 15, 30. doi: 10.1186/s12874-015-0022-1

Higgins, P. G., Wisplinghoff, H., Stefanik, D., and Seifert, H. (2004). Selection of topoisomerase mutations and overexpression of adeB mRNA transcripts during an outbreak of acinetobacter baumannii. *J. Antimicrob. Chemother.* 54 (4), 821–823. doi: 10.1093/jac/dkh427

Horan, T. C., Andrus, M., and Dudeck, M. A. (2008). CDC/NHSN surveillance definition of health care-associated infection and criteria for specific types of infections in the acute care setting. *Am. J. Infect. Control* 36 (5), 309–332. doi: 10.1016/j.ajic.2008.03.002

Ibrahim, M. K., Zambruni, M., Melby, C. L., and Melby, P. C. (2017). Impact of childhood malnutrition on host defense and infection. *Clin. Microbiol. Rev.* 30 (4), 919–971. doi: 10.1128/cmr.00119-16

Jain, S., Mahapatra, S. J., Gupta, S., Shalimar,, and Garg, P. K. (2018). Infected pancreatic necrosis due to multidrug-resistant organisms and persistent organ failure predict mortality in acute pancreatitis. *Clin. Transl. Gastroenterol.* 9 (10), 190. doi: 10.1038/s41424-018-0056-x

Johnson, C. D., and Abu-Hilal, M. (2004). Persistent organ failure during the first week as a marker of fatal outcome in acute pancreatitis. *Gut* 53 (9), 1340–1344. doi: 10.1136/gut.2004.039883

Jonsson, A. B., Rygård, S. L., Hildebrandt, T., Perner, A., Møller, M. H., and Russell, L. (2021). Thrombocytopenia in intensive care unit patients: A scoping review. *Acta Anaesthesiol. Scand.* 65 (1), 2–14. doi: 10.1111/aas.13699

Kelton, J. G., Neame, P. B., Gauldie, J., and Hirsh, J. (1979). Elevated platelet-associated IgG in the thrombocytopenia of septicemia. *N Engl. J. Med.* 300 (14), 760–764. doi: 10.1056/nejm197904053001404

Kursa, M. (2014). Robustness of random forest-based gene selection methods. *BMC Bioinf.* 15, 8. doi: 10.1186/1471-2105-15-8

Lankisch, P. G., Apte, M., and Banks, P. A. (2015). Acute pancreatitis. *Lancet* 386 (9988), 85–96. doi: 10.1016/s0140-6736(14)60649-8

Lei, J. J., Zhou, L., Liu, Q., Xiong, C., and Xu, C. F. (2017). Can mean platelet volume play a role in evaluating the severity of acute pancreatitis? *World J. Gastroenterol.* 23 (13), 2404–2413. doi: 10.3748/wjg.v23.i13.2404

Li, X., Li, L., Liu, L., Hu, Y., Zhao, S., Sun, J., et al. (2020). Risk factors of multidrug resistant pathogens induced infection in severe acute pancreatitis. *Shock* 53 (3), 293–298. doi: 10.1097/shk.0000000000001371

Liu, C. P., Shih, S. C., Wang, N. Y., Wu, A. Y., Sun, F. J., Chow, S. F., et al. (2016). Risk factors of mortality in patients with carbapenem-resistant acinetobacter baumannii bacteremia. *J. Microbiol. Immunol. Infect.* 49 (6), 934–940. doi: 10.1016/j.jmii.2014.10.006

Mederos, M. A., Reber, H. A., and Girgis, M. D. (2021). Acute pancreatitis: A review. *Jama* 325 (4), 382–390. doi: 10.1001/jama.2020.20317

Moka, P., Goswami, P., Kapil, A., Xess, I., Sreenivas, V., and Saraya, A. (2018). Impact of antibiotic-resistant bacterial and fungal infections in outcome of acute pancreatitis. *Pancreas* 47 (4), 489–494. doi: 10.1097/mpa.0000000000001019

Muady, G. F., Bitterman, H., Laor, A., Vardi, M., Urin, V., and Ghanem-Zoubi, N. (2016). Hemoglobin levels and blood transfusion in patients with sepsis in internal medicine departments. *BMC Infect. Dis.* 16 (1), 569. doi: 10.1186/s12879-016-1882-7

Munford, R. S. (2006). Severe sepsis and septic shock: the role of gram-negative bacteremia. *Annu. Rev. Pathol.* 1, 467–496. doi: 10.1146/annurev.pathol.1.110304.100200

Nikaido, H., and Pagès, J. M. (2012). Broad-specificity efflux pumps and their role in multidrug resistance of gram-negative bacteria. *FEMS Microbiol. Rev.* 36 (2), 340–363. doi: 10.1111/j.1574-6976.2011.00290.x

Ni, S., Xu, P., Zhang, K., Zou, H., Luo, H., Liu, C., et al. (2022). A novel prognostic model for malignant patients with gram-negative bacteremia based on real-world research. *Sci. Rep.* 12 (1), 11644. doi: 10.1038/s41598-022-15126-5

Oh, T. K., Song, K. H., and Song, I. A. (2021). History of anemia and long-term mortality due to infection: a cohort study with 12 years follow-up in south Korea. *BMC Infect. Dis.* 21 (1), 674. doi: 10.1186/s12879-021-06377-0

Párniczky, A., Lantos, T., Tóth, E. M., Szakács, Z., Gódi, S., Hágendorn, R., et al. (2019). Antibiotic therapy in acute pancreatitis: From global overuse to evidence based recommendations. *Pancreatology* 19 (4), 488–499. doi: 10.1016/j.pan.2019.04.003

Permpikul, C., Tongyoo, S., Viarasilpa, T., Trainarongsakul, T., Chakorn, T., and Udompanturak, S. (2019). Early use of norepinephrine in septic shock resuscitation (CENSER). *A Randomized Trial Am. J. Respir. Crit. Care Med.* 199 (9), 1097–1105. doi: 10.1164/rccm.201806-1034OC

Petrov, M. S., Shanbhag, S., Chakraborty, M., Phillips, A. R., and Windsor, J. A. (2010). Organ failure and infection of pancreatic necrosis as determinants of mortality in patients with acute pancreatitis. *Gastroenterology* 139 (3), 813–820. doi: 10.1053/j.gastro.2010.06.010

Popa, C. C., Badiu, D. C., Rusu, O. C., Grigorean, V. T., Neagu, S. I., and Strugaru, C. R. (2016). Mortality prognostic factors in acute pancreatitis. *J. Med. Life* 9 (4), 413–418. doi: 10.22336/jml.2016.0416

Schrottmaier, W. C., Kral, J. B., Zeitlinger, M., Salzmann, M., Jilma, B., and Assinger, A. (2016). Platelet activation at the onset of human endotoxemia is undetectable *in vivo*. *Platelets* 27 (5), 479–483. doi: 10.3109/09537104.2015.1119814

Tacconelli, E., Carrara, E., Savoldi, A., Harbarth, S., Mendelson, M., Monnet, D. L., et al. (2018). Discovery, research, and development of new antibiotics: the WHO priority list of antibiotic-resistant bacteria and tuberculosis. *Lancet Infect. Dis.* 18 (3), 318–327. doi: 10.1016/s1473-3099(17)30753-3

Tian, H., Chen, L., Wu, X., Li, F., Ma, Y., Cai, Y., et al. (2020). Infectious complications in severe acute pancreatitis: Pathogens, drug resistance, and status of nosocomial infection in a university-affiliated teaching hospital. *Dig. Dis. Sci.* 65 (7), 2079–2088. doi: 10.1007/s10620-019-05924-9

van Brunschot, S., Bakker, O. J., Besselink, M. G., Bollen, T. L., Fockens, P., Gooszen, H. G., et al. (2012). Treatment of necrotizing pancreatitis. *Clin. Gastroenterol. Hepatol.* 10 (11), 1190–1201. doi: 10.1016/j.cgh.2012.05.005

Wan, R., Bai, L., Yan, Y., Li, J., Luo, Q., Huang, H., et al. (2022). A clinically applicable nomogram for predicting the risk of invasive mechanical ventilation in pneumocystis jirovecii pneumonia. *Front. Cell Infect. Microbiol.* 12. doi: 10.3389/fcimb.2022.850741

Wang, C., Li, Q., and Ren, J. (2019). Microbiota-immune interaction in the pathogenesis of gut-derived infection. *Front. Immunol.* 10. doi: 10.3389/fimmu.2019.01873

Wu, D., Chen, C., Liu, T., and Wan, Q. (2020). Risk factors for acquisition of carbapenem-resistant klebsiella pneumoniae and mortality among abdominal solid organ transplant recipients with k. pneumoniae infections. *Med. Sci. Monit.* 26, e922996. doi: 10.12659/msm.922996

Wu, D., Huang, Y., Xiao, J., Qin, G., Liu, H., and Peng, J. (2022). Risk factors for mortality among critical acute pancreatitis patients with carbapenem-resistant organism infections and drug resistance of causative pathogens. *Infect. Dis. Ther.* 11 (3), 1089–1101. doi: 10.1007/s40121-022-00624-w

Wu, B. U., Johannes, R. S., Kurtz, S., and Banks, P. A. (2008). The impact of hospital-acquired infection on outcome in acute pancreatitis. *Gastroenterology* 135 (3), 816–820. doi: 10.1053/j.gastro.2008.05.053

Wu, J., Zhang, H., Li, L., Hu, M., Chen, L., Xu, B., et al. (2020). A nomogram for predicting overall survival in patients with low-grade endometrial stromal sarcoma: A population-based analysis. *Cancer Commun. (Lond)* 40 (7), 301–312. doi: 10.1002/cac2.12067

Zhanel, G. G., Wiebe, R., Dilay, L., Thomson, K., Rubinstein, E., Hoban, D. J., et al. (2007). Comparative review of the carbapenems. *Drugs* 67 (7), 1027–1052. doi: 10.2165/00003495-200767070-00006

Zhang, Y., Zeng, X., Jiao, Y., Li, Z., Liu, Q., Ye, J., et al. (2020). Mechanisms involved in the development of thrombocytopenia in patients with COVID-19. *Thromb. Res.* 193, 110–115. doi: 10.1016/j.thromres.2020.06.008

Zilberberg, M. D., Nathanson, B. H., Sulham, K., Fan, W., and Shorr, A. F. (2017). Carbapenem resistance, inappropriate empiric treatment and outcomes among patients hospitalized with enterobacteriaceae urinary tract infection, pneumonia and sepsis. *BMC Infect. Dis.* 17 (1), 279. doi: 10.1186/s12879-017-2383-z

frontiers | Frontiers in Cellular and Infection Microbiology

TYPE Original Research
PUBLISHED 06 January 2023
DOI 10.3389/fcimb.2022.1068840

OPEN ACCESS

EDITED BY
Luis Esau Lopez Jacome,
Instituto Nacional de Rehabilitación, Mexico

REVIEWED BY
Luis Fernando Espinosa-Camacho, Universidad Nacional Autónoma de México, Mexico
Amina Abdelhadi, Zagazig University, Egypt
Rapee Thummeepak, Naresuan University, Thailand

*CORRESPONDENCE
Tuhina Banerjee
drtuhina@yahoo.com

SPECIALTY SECTION
This article was submitted to Antibiotic Resistance and New Antimicrobial drugs, a section of the journal Frontiers in Cellular and Infection Microbiology

RECEIVED 13 October 2022
ACCEPTED 20 December 2022
PUBLISHED 06 January 2023

CITATION
Sharma S, Banerjee T, Yadav G and Kumar A (2023) Susceptibility profile of *bla*$_{OXA-23}$ and metallo-β-lactamases co-harbouring isolates of carbapenem resistant *Acinetobacter baumannii* (CRAB) against standard drugs and combinations.
Front. Cell. Infect. Microbiol. 12:1068840.
doi: 10.3389/fcimb.2022.1068840

Susceptibility profile of *bla*$_{OXA-23}$ and metallo-β-lactamases co-harbouring isolates of carbapenem resistant *Acinetobacter baumannii* (CRAB) against standard drugs and combinations

Swati Sharma[1], Tuhina Banerjee[1]*, Ghanshyam Yadav[2] and Ashok Kumar[3]

[1]Department of Microbiology, Institute of Medical Sciences, Banaras Hindu University, Varanasi, India, [2]Department of Anaesthesiology, Institute of Medical Sciences, Banaras Hindu University, Varanasi, India, [3]Department of Pediatrics, Institute of Medical Sciences, Banaras Hindu University, Varanasi, India

Background: The rapid emergence of carbapenem resistant *Acinetobacter baumannii* (CRAB) has resulted in an alarming situation worldwide. Realizing the dearth of literature on susceptibility of CRAB in genetic context in the developing region, this study was performed to determine the susceptibility profile against standard drugs/combinations and the association of *in-vitro* drug synergy with the prevalent molecular determinants.

Methods and findings: A total of 356 clinical isolates of *A. baumannii* were studied. Confirmation of the isolates was done by amplifying *recA* and ITS region genes. Susceptibility against standard drugs was tested by Kirby Bauer disc diffusion. Minimum inhibitory concentration (MIC), MIC$_{50}$ and MIC$_{90}$ values against imipenem, meropenem, doripenem, ampicillin/sulbactam, minocycline, amikacin, polymyxin B, colistin and tigecycline was tested as per guidelines. Genes encoding enzymes classes A (*bla*$_{GES}$, *bla*$_{IMI/NMC-A}$, *bla*$_{SME}$, *bla*$_{KPC}$), B (*bla*$_{IMP}$, *bla*$_{VIM}$, *bla*$_{NDM}$) and D (*bla*$_{OXA-51}$, *bla*$_{OXA-23}$ and *bla*$_{OXA-58}$) were detected by multiplex polymerase chain reaction. Synergy against meropenem-sulbactam and meropenem-colistin combinations was done by checkerboard MIC method. Correlation of drug synergy and carbapenemase encoding genes was statistically analyzed.

Results: Of the total, resistance above 90% was noted against gentamicin, ciprofloxacin, levofloxacin, ceftazidime, cefepime, ceftriaxone, cotrimoxazole and piperacillin/tazobactam. By MIC, resistance rates from highest to lowest was seen against imipenem 89.04% (n=317), amikacin 80.33% (n=286), meropenem 79.49% (n=283), doripenem 77.80% (n=277), ampicillin/sulbactam 71.62% (n=255), tigecycline 55.61% (n=198), minocycline 14.04%

(n=50), polymyxin B 10.11% (n=36), and colistin 2.52% (n=9). CRAB was 317 (89.04%), 81.46% (n=290) were multidrug resistant and 13.48% (n=48) were extensively drug resistant. All the CRAB isolates harboured *bla*$_{OXA-51}$ gene (100%) and 94% (n=298) *bla*$_{OXA-23}$ gene. The *bla*$_{IMP}$ gene was most prevalent 70.03% (n=222) followed by *bla*$_{NDM,}$ 59.62% (n=189). Majority (87.69%, 278) were co-producers of classes D and B carbapenemases, *bla*$_{OXA-23}$ with *bla*$_{IMP}$ and *bla*$_{NDM}$ being the commonest. Synergy with meropenem-sulbactam and meropenem-colistin was 47% and 57% respectively. Reduced synergy (p= <0.0001) was noted for those harbouring *bla*$_{OXA-51}$+bla$_{OXA-23}$with *bla*$_{NDM}$ gene alone or co-producers.

Conclusion: Presence of *bla*$_{NDM}$ gene was a significant cause of synergy loss in meropenem-sulbactam and meropenem-colistin. In *bla*$_{NDM}$ endemic regions, tigecycline, minocycline and polymyxins could be viable options against CRAB isolates with more than one carbapenemase encoding genes.

KEYWORDS

bla$_{NDM}$, minocycline, meropenem, synergy, endemic

1 Introduction

The rapid emergence and widespread dissemination of carbapenem resistance in Gram negative bacilli has posed real challenges in the management of infection caused by them. In this regard, the emergence of carbapenem resistant *Acinetobacter baumannii* (CRAB) has been very significant not only because of the carbapenem resistance acquired by these organisms but also due to the fact that acquisition of this resistance has made the otherwise 'insignificant colonizers', a potential pathogen. The impact has been so severe that both the World Health Organization (WHO) in its global priority pathogen list and India in its Indian Pathogen Priority List has labelled CRAB as 'critical priority pathogen' for further research (World Health Organization Press [WHO], 2017; WHO and DBT, Indian Priority Pathogen List [IPPL], 2021). According to Global Antimicrobial Resistance Surveillance System (GLASS) report 2019, 68-82% percentage of CRAB isolates have been reported from Saudi Arabia, Egypt, South Africa, Argentina, Brazil, Iran, Pakistan, and Italy (GLASS, 2019). Moreover, the data from Central Asian and Eastern European surveillance of Antimicrobial Resistance (CAESAR) 2019, showed 80%-91% of CRAB isolates in Russia, Ukraine and Belarus (CAESAR, 2019). Similarly, the China Antimicrobial Surveillance network (CHINET) 2017 reported 82% CRAB isolates (CHINET, 2017) (OneHealth Trust).

Carbapenem group of drugs are the last resort therapeutic option in many low resource settings especially, in developing regions. However, as has been the case in India or for that matter most of the developing countries, the broad-spectrum property of this important group of drugs has encouraged excessive inappropriate use in form of over-the-counter scale or those without valid prescriptions (Laxminarayan and Chaudhury, 2016). Among the different enzymatic and non-enzymatic mechanisms of carbapenem resistance in CRAB like Ambler classes A/B/D, porin channels, and efflux pumps, Ambler class B metallo-beta lactamases (MBLs) like *bla*$_{NDM-1}$, has been reported as most worrisome (López et al., 2019). In addition to this, in Indian scenario, CRAB is very different from other parts of the world. Not only the molecular determinants of carbapenem resistance varies, the combination of resistance genes and availability of alternative therapeutic options also pose huge challenge in deciding for their appropriate management (Bartal et al., 2022). Several studies, though limited by heterogeneity in methods and sample size, have reported synergistic effect of antibiotics combinations (Ayoub Moubareck and Hammoudi Halat, 2020; Mohd Sazlly Lim et al., 2021). Despite there is lack of epidemiological data and experimental studies on susceptibility to alternative options in Indian context which indirectly promotes empirical use of antibiotics and hence emergence of carbapenem resistant organisms.

We have previously identified and studied the endemicity of CRAB in the intensive care unit (ICU) of the present study center against a background of high empirical carbapenem use (Banerjee et al., 2018). We have also studied sustained outbreak of CRAB wherein, it was shown that intense carbapenem use within the ICU facilitated the persistence of the CRAB isolates in the hospital environment causing repeated outbreaks (Sharma et al., 2021a). We then studied colistin resistance in CRAB isolates wherein all the resistant isolates were reported in

patients with prior carbapenem therapy (Sharma et al., 2021b). To meet the heavy empirical carbapenem use we also tried to restrict the empirical therapy by detecting biomass through a low-cost hand-held microscope (Foldscope) (Sharma et al., 2022). However, even though the challenge of CRAB infection was elucidated through this series of related studies, no consensus could be reached on the therapeutic options of these resistance strains. Realizing the scarcity of data in Indian context, the present study was conducted to determine the susceptibility profile of CRAB against available standard drugs and their combinations and to determine association of *in-vitro* drug synergy with the widely prevalent molecular determinants of carbapenem resistance. To the best of our knowledge, this study provides the data on drug synergy and epidemiology on the largest number of CRAB isolates.

2 Materials and methods

2.1 Study site

This prospective cross-sectional study was conducted in the Department of Microbiology, Institute of Medical Sciences, Banaras Hindu University, and the associated 2000 bedded tertiary care hospital, Varanasi. The work was approved by Institute ethical committee (Dean/2017/EC/186) and prior to sample collection an informed consent was taken from each subject or their guardian.

2.2 Bacterial isolates

Isolates of *A. baumannii* from different clinical specimens were included in the study. The isolates were collected from various samples from the patients admitted to different wards and ICUs of the hospital over a period of 15 months (January 2018-March 2019). The sample size was calculated by the formula 'n=Z^2pq/d^2' (n=minimum sample size, Z= standard score based on given confidence level, p=prevalence rate, q=1-p, d= standard error), considering the previous prevalence data of *A. baumannii* in the study center (Banerjee et al., 2018; Sharma et al., 2022). More than required isolates were included to increase the power of study and to eliminate any bias. The detailed demographic data of the patients were also noted.

2.3 Inclusion and exclusion criteria

Only those isolates were considered which were collected from patients with clinical suspicion of infections like pneumonia, skin and soft tissue infection, sepsis, and urinary tract infection. Only the first isolate from the samples were included. *A. baumannii* isolated from mixed infections and those suggesting colonization were excluded.

2.4 Isolation and identification

All the isolates were phenotypically characterized by standard microbiological methods as culture on MacConkey agar and Leeds *Acinetobacter* agar base media (HiMedia Laboratories Pvt Ltd, India), Gram staining and biochemical reactions. The molecular identification as *A. baumannii* was done by multiplex PCR, targeting *recA* gene and species specific ITS-region gene (Fallon and Young, 1996; Chen et al., 2014).

2.5 Antimicrobial susceptibility testing

2.5.1 Disc diffusion method

Susceptibility towards gentamicin (10 µg), ciprofloxacin (5 µg), levofloxacin (5 µg), ceftazidime (30 µg), cefepime (30 µg) ceftriaxone (30 µg), cotrimoxazole (1.25/23.75 µg), piperacillin/tazobactam (100/10 µg), ampicillin/sulbactam (10/10 µg), imipenem (10 µg), meropenem (10 µg) and amikacin (HiMedia Laboratories Pvt. Ltd, India) was tested by Kirby Bauer disc diffusion method.

2.5.2 Determination of minimum inhibitory concentration (MIC) against selected drugs

MIC for imipenem, meropenem, doripenem, ampicillin, sulbactam, tigecycline, colistin (Sigma-Aldrich Chemicals Pvt. Ltd, India), polymyxin B (Bharat serums & vaccines Ltd, India), amikacin (Aristo Pharmaceuticals Ltd. India) and minocycline (Gufic Biosciences Ltd, India) was performed by agar dilution or broth microbroth dilution methods as per recommendation by Clinical Laboratory Standards Institute (CLSI) guidelines (CLSI, 2020). The bacterial inoculum was prepared by inoculating, 2-3 pure isolated colonies from overnight growth into Luria Bertani (LB) broth medium (HiMedia Laboratories Pvt Ltd, India) and incubated at 37°C with constant shaking at 180 rpm for 2 hours. The turbidity was adjusted according to 0.5 McFarland standards and 0.01 mL suspension was used as inoculum. The test was performed in cation-adjusted Mueller Hinton broth and agar medium (HiMedia Laboratories Pvt Ltd, India). The drug potency was calculated as described elsewhere and antibiotic stock solution was prepared by dissolving antibiotic powders into appropriate solvent (Biswas and Rather, 2019). *Escherichia coli* ATCC® 25922, *Pseudomonas aeruginosa* ATCC® *27853* and *Acinetobacter baumannii* ATCC® *19606* were used as quality controls. The results were interpreted according to CLSI guidelines 2020 (CLSI, 2020). For tigecycline, isolates with ≥4 µg/ml MIC were considered as resistant isolates (Marchaim et al., 2014).

2.6 Determination of MIC_{50} and MIC_{90}

For each tested antibiotic the MIC_{50} and MIC_{90} value was calculated. The MIC_{50} is equivalent to median MIC value and calculated as n x 0.5 (n=no. of test isolates). The MIC_{90} is the 90^{th} percentile of the MIC value and calculated as n x 0.9, if the resulting number wasn't an integer, therefore the subsequent integer next to the respective value represented the MIC_{90} (Biswas and Rather, 2019).

2.7 Definitions and determination of multiple antibiotic resistance (MAR) index

CRAB was defined as, an isolate resistant to anyone carbapenem (imipenem or meropenem). Multi-drug resistant *A. baumannii* (MDRAb) and extensively-drug resistant *A. baumannii* (XDRAb) was defined as an isolate showing non-susceptibility to at least 1 agent in ≥3 antimicrobial categories and at least 1 agent in all but <2 or fewer antimicrobial categories, respectively including penicillins, ß-lactam combination agents, cephems, carbapenems, lipopeptides, aminoglycoside, tetracyclines, fluoroquinolones, and folate pathway antagonists (Magiorakos et al., 2012). The result of disc diffusion method was used for the above classification except for lipopeptides and tetracyclines which were not tested by disc diffusion method.

The MAR index was determined by using the formula MAR = a/b, where 'a' is the number of antibiotics to which the test isolate showed resistance and 'b' is the total number of antibiotics to which the test isolate was exposed. Values >0.2 MAR index represents high risk source of contamination is where antibiotics are frequently used (Sandhu et al., 2016).

2.8 Detection of carbapenemase encoding genes

The phenotypically carbapenem resistant isolates as detected by their MICs were subjected to genotypic characterization of carbapenemases encoding genes. Four different multiplex PCR was performed for detection of class A (bla_{GES}, $bla_{IMI/NMC-A}$, bla_{SME}, bla_{KPC}), class B (bla_{IMP}, bla_{VIM}, bla_{NDM}) and class D ($bla_{OXA-51,}$ bla_{OXA-23} and bla_{OXA-58}) genes. Each single reaction mixture (25 µL) contained 2.5 µL Taq DNA buffer, 2 µL of dNTP, and 1 µL of each primer (10 picomole; Eurofins Scientific India Pvt. Ltd.), 0.3 µL of Taq DNA polymerase (Genei Laboratories Pvt. Ltd., India). To maintain volume, 5 µL of template DNA (100 ng/mL) and nuclease free water was added. The reactions were run under the following conditions: For bla_{GES}, $bla_{IMI/NMC-A}$, bla_{SME}, and bla_{KPC} genes, initial denaturation at 94°C for 5 min, 25 cycles at 94°C for 30 sec, 50°C for 30 sec, 72°C for 60 sec, and final extension at 72°C for 7 min (Hong et al., 2012). For bla_{IMP}, bla_{VIM}, and bla_{NDM} genes, initial denaturation at 94°C for 10 min, 36 cycles at 94°C for 30 sec, 52°C for 40 sec, 72°C for 50 sec, and final extension at 72°C for 5 min (Poirel et al., 2011). For $bla_{OXA-51,}$ and bla_{OXA-23} genes, initial denaturation at 94°C for 3 min, 35 cycles at 94°C for 45 sec, 57°C for 45 sec, 72°C for 60 sec, and final extension at 72°C for 5 min (Turton et al., 2006). For bla_{OXA-58} gene, initial denaturation at 94°C for 5 min, 30 cycles at 94°C for 25 sec, 52°C for 40 sec, 72°C for 50 sec, and final extension at 72°C for 6 min (Woodford et al., 2006). The primer pairs used in the study have been shown in Table 1.

2.9 Drug combination testing

For 100 selected CRAB isolates with different genetic profile, synergy testing was performed in 96-well microtiter plate by checkerboard MIC method. The selection of antibiotics for synergy testing was done after reviewing the antibiogram of the tertiary care center and literature on potentially potent antibiotic combinations for CRAB isolates (Laishram et al., 2017; Banerjee et al., 2018; Ayoub Moubareck and Hammoudi Halat, 2020). The synergy was investigated for combination of meropenem with sulbactam and meropenem with colistin. The concentration used for meropenem-sulbactam combination ranged from 2-256 µg/ml for meropenem and 2-128 µg/ml for sulbactam. For meropenem-colistin combination, the concentration for meropenem used was same as above and for colistin the concentration ranged from 0.5-2 µg/ml. Single agent MIC was also determined during the checkerboard assay. The fractional inhibitory concentration index (FICI) was calculated and interpreted as described earlier (Biswas and Rather, 2019).

2.10 Molecular typing

The clonal relationship of 100 CRAB isolates included for combination testing was studied by repetitive extragenic palindromic polymerase chain reaction (Rep-PCR) as described earlier (Fitzpatrick et al., 2016). The primer pair Rep1and Rep2 was used for the amplification. The reaction was run under the following condition, initial denaturation at 94°C for 3 min, 30 cycles at 94°C for 60 sec, 40°C for 60 sec, 65°C for 8 min, and final extension at 72°C for 16 min. Each single reaction mixture (25 µl) contained 2.5 µl Taq DNA buffer, 2 µl of dNTP, and 2µl of each primer (10 picomole; Eurofins Scientific, India), 0.3 µl of Taq DNA polymerase (Genei, Bangalore, India). To maintain volume, 5 µl of template DNA (100 ng/mL) and nuclease free water was added. The amplified PCR products were run on 1.8% agarose gel electrophoresis (BioRad Laboratories India Pvt. Ltd, India). Further the isolates showing similar band pattern were considered as one Rep cluster while isolates with

TABLE 1 Primer sequences used in the study.

S.No.	Primer pairs	Sequence (5′-3′)	Target	Base-pair	Ref.
1	P-rA1 P-rA2	CCTGAATCTTCTGGTAAAAC GTTTCTGGGCTGCCAAACATTAC	*recA*	425	Chen et al., 2014
2	P-Ab-ITSF P-Ab-ITSB	CATTATCACGGTAATTAGTG AGAGCACTGTGCACTTAAG	ITS	208	
3	GES-F GES-MR	GCTTCATTCACGCACTATT CGATGCTAGAAACCGCTC	$bla_{GES1-9,\ 11-20}$	323	Hong et al., 2012
4	IMI(NMC)-F1 IMI(NMC)-R1	TGCGGTCGATTGGAGATAAA CGATTCTTGAAGCTTCTGCG	bla_{IMI13} and bla_{NMC-A}	399	
5	SME-F1 SME-R1	ACTTTGATGGGAGGATTGGC ACGAATTCGAGCATCACCAG	bla_{SME1-3}	551	
6	KPCF2 KPCFR	GTATCGCCGTCTAGTTCTGC GGTCGTGTTTCCCTTTAGCC	$bla_{KPC2-13}$	638	
7	IMP-F IMP-R	GGAATAGAGTGGCTTAAYTCTC GGTTTAAYAAAACAACCACC	bla_{IMP}	232	Poirel et al., 2011
8	VIM-F VIM-R	GATGGTGTTTGGTCGCATA CGAATGCGCAGCACCAG	bla_{VIM}	390	
9	NDM-F NDM-R	GGTTTGGCGATCTGGTTTTC CGGAATGGCTCATCACGATC	bla_{NDM}	621	
10	OXA-23-like F OXA-23-like R	GATCGGATTGGAGAACCAGA ATTTCTGACCGCATTTCCAT	bla_{OXA-23}	501	Turton et al., 2006
11	OXA-51-like F OXA-51-like R	TAATGCTTTATCGGCCTTG TGGATTGCACTTCATCTTGG	bla_{OXA-51}	353	
12	OXA-58-like F OXA-58-like R	AAGTATTGGGGCTTGTGCTG CCCCTCTGCGCTCTACATAC	bla_{OXA-58}	599	Woodford et al., 2006
13	Rep1 Rep2	IIIGCGCCGICATCAGGC ACGTCTTATCAGGCCTAC	–	–	Fitzpatrick et al., 2016

inconsistent bands were grouped into different Rep cluster based on the dendrogram.

2.11 Statistical analysis

Fisher's exact test was employed with the help of MedCalc® statistical software version 19.6.3.0., to compare the synergistic effect of drug combination with the phenotypic resistance profile and molecular determinants of carbapenem resistance in the CRAB isolates respectively.

3 Results

3.1 Bacterial isolates

A total of 356 A. *baumannii* isolates confirmed by *recA* and *ITS* gene amplification were studied, among which majority were from the ICU 71.91% (n=256) followed by surgical wards 14.60% (n=52), and medical wards 13.48% (n=48). The most frequent site of infection was the lower respiratory tract. The demographic details of the patients showed, 71.1% (n=253) were males and 28.9% (n=103) were female with the mean age of 35.6 and 40.4 years respectively. The distribution of isolates among different clinical specimens and department has been shown in Figure 1.

3.2 Susceptibility

3.2.1 Disc diffusion method

Among the 356 isolates, resistance was noted against gentamicin 93.25% (n=332), ciprofloxacin 96.06% (n=342), levofloxacin 92.13% (n=328), ceftazidime 94.66% (n=337), cefepime 96.34% (n=343), ceftriaxone 97.75% (n=348), cotrimoxazole 91.85% (n= 327), piperacillin/tazobactam 93.25% (n=332), ampicillin/sulbactam 76.93% (n=274), imipenem 92.41% (n=329), meropenem 87.35% (n=311) and amikacin 85.67% (n=305) by disc diffusion assay.

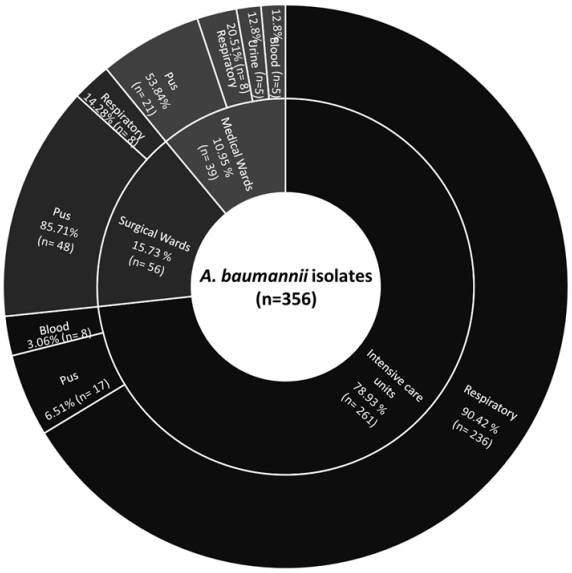

FIGURE 1
Sunburst chart showing distribution of *A. baumannii* isolates among different departments and clinical specimen.

3.2.2 Determination of minimum inhibitory concentration (MIC) against selected drugs

By MIC, highest resistance was seen against imipenem 89.04% (n=317) followed by amikacin 80.33% (n=286), meropenem 79.49% (n=283), doripenem 77.80% (n=277), ampicillin/sulbactam 71.62% (n=255), tigecycline 55.61% (n=198), minocycline 14.04% (n=50), polymyxin B 10.11% (n=36), and colistin 2.52% (n=9). The MIC results were considered for those drugs that were tested by both the methods, in case of discrepancy. The total number of isolates that were classified as CRAB were 317 (89.04%). Among 356 isolates, 81.46% (n=290) were reported as MDRAb, and 13.48% (n=48) as XDRAb. The exact MIC range, MIC_{50} and MIC_{90} values for each antimicrobial agent has been summarized in Table 2.

MAR index revealed 36 drug resistance patterns against 9 antimicrobial agents and >2 MAR index in 54.77% isolates (Supplementary Table 1). All of them were isolated from the ICU.

3.3 Carbapenemase encoding determinants

The genotypic characterization of 317 CRAB isolates showed that all were carrying bla_{OXA-51} gene (100%) and 94% (n=298) of the isolates were harbouring bla_{OXA-23} gene. Among class B carbapenemases, bla_{IMP}gene was most prevalent 70.03% (n=222) in the CRAB isolates followed by $bla_{NDM,}$ 59.62% (n=189) and bla_{VIM}, 31.23% (n=99) genes. Majority of isolates, 87.69% (n=278) were co-producers of class D and class B carbapenemases in multiple combinations (Figure 2). The most common combination was bla_{OXA-23} with bla_{IMP} and bla_{NDM} gene. None of the isolate was found positive for class A carbapenemases genes and bla_{OXA-58}. The association between phenotypic carbapenem resistance profile and genotypic resistance profile of CRAB isolates has been shown in Table 3.

3.4 Drug combination testing

The reduction in MIC range, MIC_{50} and MIC_{90} was noted against the antibiotics in combination as compared to antibiotics as single agent (Table 4).The MIC_{50} and MIC_{90} of meropenem and sulbactam was reduced four-fold when tested in combination. The combination of meropenem-sulbactam was synergistic against 47% CRAB isolates and indifference against 53% CRAB isolates. When meropenem was combined with colistin, eight-fold and four-fold reduction in MIC_{50} and MIC_{90} of meropenem and colistin was noted respectively. The meropenem-colistin combination showed 57% synergy and 43%

TABLE 2 Minimum inhibitory concentration range, MIC_{50} and MIC_{90} values of *A.baumannii* isolates.

Antimicrobial Agents	MIC range (µg/ml)	MIC_{50}	MIC_{90}
Ampicillin/sulbactam	0.5 – >128	64	128
Imipenem	0.5 – >256	128	256
Meropenem	0.5 – >128	64	>128
Doripenem	0.5 – >128	32	128
Polymyxin B	0.5 – 64	1	4
Colistin	0.5 – 64	1	2
Amikacin	4 – >512	128	512
Minocycline	0.5 – 64	4	16
Tigecycline	0.5 – 128	32	64

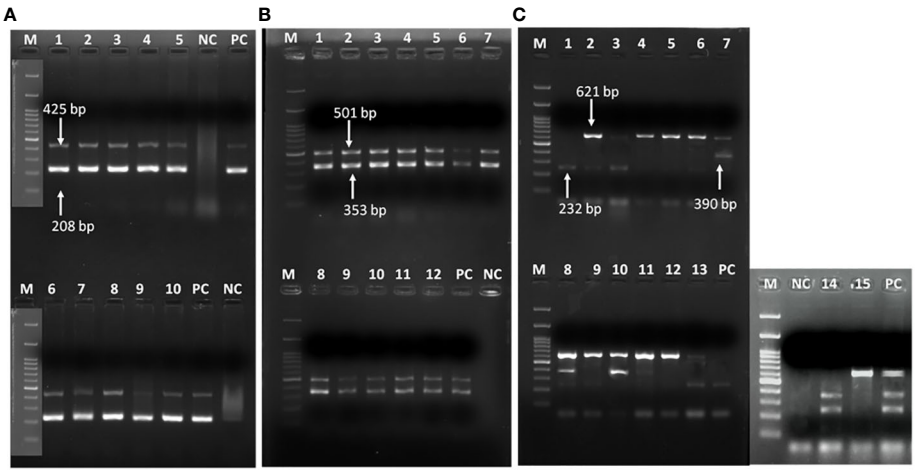

FIGURE 2
Representative gel image showing **(A)** *recA* and ITS genes in *A baumannii*; **(B)** $bla_{\text{OXA-51}}$ and $bla_{\text{OXA-23}}$ genes; **(C)** multiple class B carbapenemases. **(A)** Lane M: Marker 100 bp; Lane 1-5,6-10: *recA* (425bp) & *ITS* gene (208bp); NC: negative control PCR-grade water; PC: positive control *A. baumannii* ATCC 19606. **(B)** class D carbapenemase genes; Lane M: Marker 100 bp; Lane 1-12: $bla_{\text{OXA-51}}$ (353 bp) & Lane 1-12: $bla_{\text{OXA-23}}$ (501 bp); NC: negative control PCR-grade water; PC: previously confirmed & published isolate positive for $bla_{\text{OXA-51}}$ & $bla_{\text{OXA-23}}$ genes **(C)** class B carbapenamse genes; Lane M: Marker 100 bp; Lane 1-3,6,8, 13, 14: bla_{IMP} (232 bp), Lane 7-8,10-11, 14: bla_{IMP} (390 bp) & Lane 2-13, 15: bla_{NDM} (621 bp); PC: previously confirmed & published isolate positive for bla_{IMP}, bla_{VIM} and bla_{NDM} genes.

indifference against CRAB isolates. None of the combination showed antagonistic effect (Supplementary Table 2).

The synergistic effect of drug combinations was compared with the molecular mechanism of carbapenem resistance in CRAB isolates (Table 5). For both the combinations meropenem-sulbactam and meropenem-colistin 90-100% synergy was observed for isolates carrying $bla_{\text{OXA-51}}$+$bla_{\text{OXA-23}}$ and $bla_{\text{OXA-51}}$+$bla_{\text{OXA-23}}$with bla_{VIM} or bla_{IMP} genes. However, significantly lower synergy (p= <0.0001) was noted for the isolates harbouring $bla_{\text{OXA-51}}$+$bla_{\text{OXA-23}}$ with bla_{NDM} gene alone or co-producing other metallo-β-lactamases (MBLs). When the association of synergism with various phenotypic resistance patterns to other drug classes were compared, no significant association was seen with any profile (Table 6).

3.5 Molecular typing

Based on Rep-PCR, 18 different clusters consisting of 2 to 5 isolates with 100% similarity were detected in the 100 CRAB isolates. Besides, 57 singletons were detected with 50-90% similarity as shown in Supplementary Figure 1.

TABLE 3 The comparison of the phenotypic carbapenem resistance profile and genotypic resistance profile of CRAB isolates.

Phenotypic resistance profile	n	Genotypic profile	N
IPM/MEM/DOR	272	$bla_{\text{OXA-51}}$+$bla_{\text{OXA-23}}$+bla_{IMP}+bla_{NDM}+bla_{VIM}	28
		$bla_{\text{OXA-51}}$+$bla_{\text{OXA-23}}$+bla_{IMP}+bla_{NDM}	114
		$bla_{\text{OXA-51}}$+$bla_{\text{OXA-23}}$+bla_{IMP}+bla_{VIM}	62
		$bla_{\text{OXA-51}}$+$bla_{\text{OXA-23}}$+bla_{NDM}	46
		$bla_{\text{OXA-51}}$+$bla_{\text{OXA-23}}$+bla_{IMP}	13
		$bla_{\text{OXA-51}}$+$bla_{\text{OXA-23}}$+bla_{VIM}	9
IPM/MEM	11	$bla_{\text{OXA-51}}$+$bla_{\text{OXA-23}}$ +bla_{NDM} $bla_{\text{OXA-51}}$+$bla_{\text{OXA-23}}$	1 10
IPM/DOR	5	$bla_{\text{OXA-51}}$+$bla_{\text{OXA-23}}$+bla_{IMP}	5
IPM	29	$bla_{\text{OXA-51}}$+$bla_{\text{OXA-23}}$	10
		$bla_{\text{OXA-51}}$	19

IPM, imipenem; MEM, meropenem; DOR, doripenem.

TABLE 4 Summarized results for drug combinations tested by checkerboard method against 100 CRAB isolates.

	Single agent MIC (µg/ml)			MEM+SUL Combination MIC (µg/ml)		MEM+SUL ΣFICI	Interpretation	MEM+COL Combination MIC (µg/ml)		MEM +COL ΣFICI	Interpretation
	MEM	SUL	COL	MEM	SUL			MEM	COL		
Range	8-256	16-128	0.5-2	2-128	1-64	0.31-1.5	47% synergy 53% indifference	0.5-32	0.25-2	0.13-1.12	57% synergy 43% indifference
MIC_{50}	128	64	1	32	16	–		16	0.5	–	
MIC_{90}	256	128	2	64	32	–		32	1	–	

MIC, minimum inhibitory concentration; MEM, meropenem; SUL, sulbactam; COL, colistin; FICI, fractional inhibitory concentration index.

4 Discussion

The study highlights the extent of antimicrobial resistance in *A. baumannii*, dissemination of carbapenem resistance determinants and more importantly the synergistic effect of drug combinations on molecular determinants of carbapenem resistance. The study is significant as it is the first extensive study on *in-vitro* susceptibility of alternative drugs and their combinations on a large number of CRAB isolates from this part of the globe. The most striking finding is the existence of multiple carbapenemase encoding genes in these isolates with presence of bla_{NDM} significantly accounting for the loss of synergy in the combination therapies against these isolates.

Both, intrinsic and acquired class D carbapenemases like $bla_{OXA\text{-}51}$ and $bla_{OXA\text{-}23}$, are the most prevalent enzymes in CRAB worldwide. A recent study on population structure of CRAB circulating in the US hospital systems under the Study Network of *Acinetobacter* as a Carbapenem-Resistant Pathogen (SNAP) study has revealed the predominance of $bla_{\text{OXA-23}}$ followed by other class D enzymes. In these isolates, MBLs were rare (Iovleva et al., 2022). The situation is in contrast in South and Southeast Asia where MBLs, with comparatively broader spectrum of activity, are quite prevalent (Hsu et al., 2017). This study showed that not only bla_{NDM}, others like bla_{IMP}, which was considered rare in CRAB almost 10 years back, has emerged rapidly (Viehman and Nguyen, 2014).

The endemic burden of CRAB has become a major cause of healthcare associated infections (HAIs) in large referral hospitals worldwide. In this study considerable resistance (70% - >90%) against cephalosporins, fluoroquinolones, cotrimoxazoles, piperacillin/tazobactam, carbapenems, amikacin and ampicillin/sulbactam was revealed. Currently the therapeutic options for CRAB might be cefiderocol or colistin in combination with carbapenems or minocycline or tigecycline (Monnheimer et al., 2021). The study showed appreciable *in-vitro* activity of tigecycline (44.39%), minocycline (85.96%), polymyxin B (89.89%) and colistin (97.48%) against CRAB isolates, the use of which could be rationalized for the most effective management of these isolates. In this regard minocycline, as a non-polymyxin based therapeutic agent, has been promising for treatment of CRAB infections. Two large surveillance-based studies on minocycline activity have shown similarly high susceptibility towards *A. baumannii* isolates. However, both these studies were from developed nations where molecular epidemiology of the isolates were different from the present study (Lashinsky et al., 2017). Nevertheless,

TABLE 5 Comparison of drug synergy and molecular determinants of CRAB isolates.

Molecular determinants of CRAB	No. of CRAB isolates	Meropenem + Sulbactam		Meropenem + Colistin	
		Synergy n (%)	Indifference n (%)	Synergy n (%)	Indifference n (%)
$bla_{\text{OXA-51}}$+$bla_{\text{OXA-23}}$+bla_{IMP}+bla_{NDM}+bla_{VIM}*	20	4 (20)	16 (80)	5 (25)	15 (75)
$bla_{\text{OXA-51}}$+$bla_{\text{OXA-23}}$+bla_{IMP}+bla_{NDM}*	30	8 (26.66)	22 (73.33)	11 (36.66)	19 (63.33)
$bla_{\text{OXA-51}}$+$bla_{\text{OXA-23}}$+bla_{IMP}+bla_{VIM}	20	14 (70)	6 (30)	17 (85)	3 (15)
$bla_{\text{OXA-51}}$+$bla_{\text{OXA-23}}$+ bla_{IMP}	10	9 (90)	1 (10)	10 (100)	0
$bla_{\text{OXA-51}}$+$bla_{\text{OXA-23}}$+bla_{NDM}*	10	2 (20)	8 (80)	4 (40)	6 (60)
$bla_{\text{OXA-51}}$+$bla_{\text{OXA-23}}$+bla_{VIM}	5	5 (100)	0	5 (100)	0
$bla_{\text{OXA-51}}$+$bla_{\text{OXA-23}}$	5	5 (100)	0	5 (100)	0

*p= <0.0001; Fisher's exact test applied.

TABLE 6 Comparison of drug synergy and phenotypic non-carbapenem resistance profile of 100 CRAB isolates.

S. no.	Phenotypic resistance profile (n=100)	No. of Isolates n (%)	Meropenem + Sulbactam		Meropenem + Colistin	
			Synergy n (%)	Indifference n (%)	Synergy n (%)	Indifference n (%)
1	AMS^r/AMK^r/MIN^r, TGC^r	2 (2)	0	2 (100)	0	2 (0)
2	AMS^r/AMK^r/MIN^r	5 (5)	0	5 (100)	1 (20)	4 (80)
3	AMS^r/AMK^r/TGC^r	14 (14)	3 (21.42)	11 (78.57)	2 (14.28)	12 (85.71)
4	AMS ^{r}/MIN^r/TGC^r	2 (2)	0	2 (100)	0	2 (100)
5	AMK^r/MIN^r/TGC^r	4 (4)	1 (25)	3 (25)	2 (50)	2 (50)
6	AMK^r/TGC^r	2 (2)	2 (100)	0	2 (100)	0
7	AMK^r/MIN^r	1 (1)	1 (100)	0	1 (100)	0
8	AMK^r/AMS ^{r}	24 (24)	13 (54.16)	11 (78.57)	17 (70.83)	7 (29.16)
9	AMS ^{r}/TGC^r	1 (1)	0	1 (100)	1 ()	0
10	TGC^r	1 (1)	1 (100)	0	1 (100)	0
11	AMS ^{r}	13 (13)	7 (53.84)	6 (46.15)	9 (69.23)	4 (30.76)
12	AMK^r	27 (27)	19 (70.37)	8 (29.62)	21 (77.77)	6 (22.22)

^{r} resistance; AMS, ampicillin/sulbactam; AMK, amikacin; MIN, minocycline; TGC, Tigecycline.

minocycline was effective in the CRAB isolates with multiple carbapenemase genes. A systematic review of effectiveness of minocycline treatment reported clinical and microbiological success rates of 72.6% and 60.2% respectively. Most of the infections treated were of pneumonia (Fragkou et al., 2019). Susceptibility against tigecycline, another non-polymyxin therapeutic agent, was also tested, as according to clinical practice guidelines by the Infectious Disease Society of America and the American Thoracic Society (ATS-IDSA), the use of tigecycline for the treatment of ventilator associated pneumonia (VAP) in adult patients is recommended (Kalil et al., 2016). Clinical trials to measure the efficacy of tigecycline with comparators are scarce in literature, though one of the largest case series have shown the utility of early initiation of tigecycline in reducing severity of infections due to XDRAb (Lee et al., 2013). However, there has been concern regarding development of resistance with the use of tigecycline as monotherapy. The present study showed more than 50% resistance against tigecycline, though a similar study conducted in an adjacent country (Nepal) showed 100% susceptibility (Joshi et al., 2017). However, smaller sample size in the latter study could be the reason for the difference.

Comparable rates of polymyxin B and colistin resistance ranging from 0%-4% from a multicenter study in European countries has been reported (Wang et al., 2022). Besides, surveillance data from countries of US and Europe have also documented lower rate of polymyxins resistance even in XDR CRAB (Piperaki et al., 2019; Wang et al., 2022). Similarly, in polymyxin based therapies, a recent meta-analysis demonstrated better clinical response as compared to non-polymyxin based therapies (61.7% vs. 39.3%). However, polymyxins being nephrotoxic, showed more adverse events (Lyu et al., 2020).

It should be emphasized that, besides activity, the most important consideration in the above-mentioned antibiotics is the cost. Most of these drugs (minocycline and polymyxins) are not affordable by the people of the developing countries. Access to antibiotics, availability or purchasing power of the population, burden of secondary infection, inadequate healthcare facilities often are the decisive factors for the choice of treatment of CRAB infections (Joshi et al., 2017).

The increasing carbapenem resistance has restricted the antibiotic armamentarium and so combination therapies are frequently being used to increase the antibiotic coverage against MDRAb and XDRAb. The most appropriate combinations suggested against MDRAb and XDRAb in a handful of reports till date is based on testing on a smaller number of isolates than the present study (Laishram et al., 2017). The combinations are of meropenem, imipenem, amikacin or cefepime with sulbactam as it has an intrinsic affinity for penicillin-binding proteins of *A. baumannii*. The other most suggested combination is colistin with carbapenem or colistin-tigecycline (Ayoub Moubareck and Hammoudi Halat, 2020). Based on the hospital setup in this study where meropenem is made available for the treatment free of cost as a part of government supply, synergistic effect for meropenem-sulbactam and meropenem-colistin combinations was studied. The latter showed 57% synergistic effect against the CRAB isolates. Additionally, the colistin combination therapy in comparison with colistin monotherapy has also been found

beneficial for reduction in risk of nephrotoxicity (Ayoub Moubareck and Hammoudi Halat, 2020).

All the four Ambler classes have been described in *A. baumannii* and among them the OXA-type carbapenemases followed by MBLs have been reported as dominant mechanism of resistance around the South and Southeast Asian countries (Hsu et al., 2017). Presence of $bla_{\text{OXA-23}}$ is one of the common causes of resistance conferring the high level of resistance. Usually, MBLs are less frequently detected in developed regions in contrast to the developing regions like India where multiple carabapenemase encoding genes are found in the CRAB isolates without any compensation in fitness (Sharma et al., 2021). Among the genes, $bla_{\text{OXA-23}}$ is highly endemic and the most common carbapenemase encoding gene found in India followed by bla_{NDM} (Vijayakumar et al., 2020). The $bla_{\text{OXA-51}}$ gene is known to be a native chromosomal oxacillinase and was present in all the study isolates. The widespread burden of $bla_{\text{OXA-23}}$ (94%) as seen this study indicates the probable relocation of the gene in chromosome or plasmid (Vijayakumar et al., 2022). The prevalence of bla_{IMP}, gene has already been reported from this study center previously, though infrequent reports have been found from other countries (Alkasaby and Zaki El Sayed, 2017; Banerjee et al., 2018; Fallah et al., 2014). The bla_{NDM} genes was also found in a high percentage (59.62%) of the isolates and are known to be widely disseminated around the globe (Fallah et al., 2014; Alkasaby and Zaki El Sayed, 2017; Vijayakumar et al., 2020). The isolates were found negative for class A beta-lactamases and $bla_{\text{OXA-58}}$ gene, probably because they are the common mechanism of resistance in European or western countries (Vijayakumar et al., 2022). Additionally, it was interesting to note that the predominance of $bla_{\text{OXA-58}}$ was replaced by $bla_{\text{OXA-23}}$ since 2009 in the Mediterranean region, probably due to selective advantage of the latter with higher carbapenemase activity (Djahmi et al., 2014). A more recent study has reported isolates producing $bla_{\text{OXA-23}}$ alone or coproducing $bla_{\text{OXA-23}}$, andbla_{NDM} mostly belonged to international clone (IC) IC1 and IC2 among which IC2 is highly transmissible (Vijayakumar et al., 2022).

The correlation of molecular mechanism of resistance with synergy rate is an important aspect which has been less studied. The study noted high rate of synergy against both meropenem-sulbactam and meropenem-colistin combinations when there is absence of bla_{NDM} gene. The bla_{NDM} gene is known to be most concerning gene among the MBLs because the expression of bla_{NDM} genes not only helps in production of high-level beta-lactamases but also favours fitness cost for bacterial growth (López et al., 2019; Sharma et al., 2021). While the bla_{NDM} gene was first reported from India more than 10 years back, its widespread dissemination is a serious cause of concern (Kumarasamy et al., 2010). Based on this study it can be inferred that in bla_{NDM} endemic regions such combinations might not be appropriate strategy for the management of the CRAB isolates.

The study was not without limitations. It was a single center study though a large number of CRAB isolates were included. In addition, the molecular epidemiology of the isolates was representative of the nation at large as per previous reports. Secondly, this was an *in-vitro* study without any data on the course of actual management of the infections with these isolates. Nevertheless, the study clearly reveals the burden of CRAB with more than one carbapenemase encoding genes, role of bla_{NDM} in failure of combination therapy and possible therapeutic options against the resistant isolates.

5 Conclusion

The study revealed susceptibility of minocycline (85.96%), polymyxin B (89.89%) and colistin (97.48%) against the CRAB isolates with more than one carbapenemase encoding genes from India. Combinations of meropenem-sulbactam and meropenem-colistin showed 47% and 57% synergy respectively. However, presence of bla_{NDM} gene in the CRAB isolates was a significant cause of loss of synergy. Therefore, the bla_{NDM} endemic regions must review the treatment options against CRAB infections with alternatives like tigecycline, minocycline and polymyxins. Despite being limited to *in-vitro* data, the study involves one of the largest data on synergy testing against CRAB isolates harbouring multiple classes of carbapenemases and their alternative therapeutic options.

Data availability statement

The original contributions presented in the study are included in the article/Supplementary Material. Further inquiries can be directed to the corresponding author.

Ethics statement

The studies involving human participants were reviewed and approved by Institute Ethical committee, Institute of Medical Sciences, BHU. Written informed consent to participate in this study was provided by the participants' legal guardian/next of kin. Written informed consent was obtained from the individual(s) for the publication of any potentially identifiable images or data included in this article.

Author contributions

SS performed the experiment and wrote the manuscript. TB conceptualized, designed the study and revised the manuscript. GY and AK supervised the study. All authors contributed to the article and approved the submitted version.

Conflict of interest

The authors declare that the research was conducted in the absence of any commercial or financial relationships that could be construed as a potential conflict of interest.

Publisher's note

All claims expressed in this article are solely those of the authors and do not necessarily represent those of their affiliated organizations, or those of the publisher, the editors and the reviewers. Any product that may be evaluated in this article, or claim that may be made by its manufacturer, is not guaranteed or endorsed by the publisher.

Supplementary material

The Supplementary Material for this article can be found online at: https://www.frontiersin.org/articles/10.3389/fcimb.2022.1068840/full#supplementary-material

SUPPLEMENTARY FIGURE 1
Dendrogram by Rep-PCR of 100 CRAB isolates included in drug synergism testing.

References

Alkasaby, N. M., and Zaki El Sayed, M. (2017). Molecular study of *Acinetobacter baumannii* isolates for metallo-β-lactamases and extended-spectrum-β-lactamases genes in intensive care unit, mansoura university hospital, Egypt. *Int. J. Microbiol.*, 2017, 1–7. doi: 10.1155/2017/3925868

Ayoub Moubareck, C., and Hammoudi Halat, D. (2020). Insights into *Acinetobacter baumannii*: a review of microbiological, virulence, and resistance traits in a threatening nosocomial pathogen. *Antibiotics* 9, 119 1–8. doi: 10.3390/antibiotics9030119

Banerjee, T., Mishra, A., Das, A., Sharma, S., Barman, H., and Yadav, G. (2018). High prevalence and endemicity of multidrug resistant *Acinetobacter* spp. in intensive care unit of a tertiary care hospital, varanasi, India. *J. Pathog.* 2018, 1–8. doi: 10.1155/2018/9129083

Bartal, C., Rolston, K. V. I., and Nesher, L. (2022). Carbapenem-resistant *Acinetobacter baumannii*: Colonization, infection and current treatment options. *Infect. Dis. Ther.* 11, 683–694. doi: 10.1007/s40121-022-00597-w

Biswas, I., and Rather, P. N. *Acinetobacter baumannii*: Methods and Protocols. New York: Springer Humana New York, NY Publisher (2019). doi: 10.1007/978-1-4939-9118-1

Chen, T. L., Lee, Y. T., Kuo, S. C., Yang, S. P., Fung, C. P., and Lee, S. D. (2014). Rapid identification of *Acinetobacter baumannii*, *Acinetobacter nosocomialis* and *Acinetobacter pittii* with a multiplex PCR assay. *J. Med. Microbiol.* 63 (9), 1154–1159. doi: 10.1099/jmm.0.071712-0

CLSI (2020). *Performance standards for antimicrobial susceptibility testing. 30th ed CLSI supplement M100* (Wayne, PA: Clinical and Laboratory Standards Institute).

Djahmi, N., Dunyach-Remy, C., Pantel, A., Dekhil, M., Sotto, A., and Lavigne, J. P. (20142014). Epidemiology of carbapenemase-producing *Enterobacteriaceae* and *Acinetobacter baumannii* in Mediterranean countries. *BioMed. Res. Int.* 2014, 305784. doi: 10.1155/2014/305784

Fallah, F., Noori, M., Hashemi, A., Goudarzi, H., Karimi, A., Erfanimanesh, S., et al. (2014). Prevalence of bla_{NDM}, bla_{PER}, bla_{VEB}, bla_{IMP}, and bla_{VIM} genes among *Acinetobacter baumannii* isolated from two hospitals of Tehran, Iran. *Scientifica* 2014, 1–7. doi: 10.1155/2014/245162

Fallon, R. J., and Young, H. (1996). "Neisseria, moraxella, acinetobacter," in *Mackie & McCartney practical medical microbiology, 14th edition*. Eds. J. G. Collee, A. G. Fraser, B. P. Marmion and A. Simmons (London, UK: Churchill Livingstone), 283–361.

Fitzpatrick, M. A., Ozer, E. A., and Hauser, A. R. (2016). Utility of whole-genome sequencing in characterizing *Acinetobacter* epidemiology and analyzing hospital outbreaks. *J. Clin. Microbiol.* 54, 593–612. doi: 10.1128/JCM.01818-15

Fragkou, P. C., Poulakou, G., Blizou, A., Blizou, M., Rapti, V., Karageorgopoulos, D. E., et al. (2019). The role of minocycline in the treatment of nosocomial infections caused by multidrug, extensively drug and pandrug resistant *Acinetobacter baumannii*: a systematic review of clinical evidence. *Microorganisms* 7, 159. doi: 10.3390/microorganisms7060159

WHO Country Office for India and Department of Biotechnology Government of India. *Indian Priority pathogen list: to guide research, discovery, and development of new antibiotics in India*. (World Health Organization: Geneva, Switzerland) (2021), 1–22. Available at: https://dbtindia.gov.in/sites/default/files/IPPL_final.pdf.

Hong, S. S., Kim, K., Huh, J. Y., Jung, B., Kang, M. S., and Hong, S. G. (2012). Multiplex PCR for rapid detection of genes encoding class a carbapenemases. *Ann. Lab. Med.* 32, 359–361. doi: 10.3343/alm.2012.32.5.359

Hsu, L. Y., Apisarnthanarak, A., Khan, E., Suwantarat, N., Ghafur, A., and Tambyah, P. A. (2017). Carbapenem-resistant *Acinetobacter baumannii* and *Enterobacteriaceae* in south and southeast Asia. *Clin. Microbiol. Rev.* 30, 1–22. doi: 10.1128/CMR.masthead.30-1

Iovleva, A., Mustapha, M. M., Griffith, M. P., Komarow, L., Luterbach, C., Evans, D. R., et al. (2022). Carbapenem-resistant acinetobacter baumannii in US hospitals: diversification of circulating lineages and antimicrobial resistance. *mBio* 13, e0275921. doi: 10.1128/mbio.02759-21

Joshi, P. R., Acharya, M., Kakshapati, T., Leungtongkam, U., Thummeepak, R., and Sitthisak, S. (2017). Co-Existence of bla_{OXA-23} and bla_{NDM-1} genes of *Acinetobacter baumannii* isolated from Nepal: antimicrobial resistance and clinical significance. *Antimicrob. Resist. Infect. Control* 6, 1–7. doi: 10.1186/s13756-017-0180-5

Kalil, A. C., Metersky, M. L., Klompas, M., Muscedere, J., Sweeney, D. A., and Palmer, L. B. (2016). Management of adults with hospital-acquired and ventilator-associated pneumonia: 2016 clinical practice guidelines by the infectious diseases society of America and the American thoracic society. *Clin. Infect. Dis.* 63, e61–111. doi: 10.1093/cid/ciw353

Kumarasamy, K. K., Toleman, M. A., Walsh, T. R., Bagaria, J., Butt, F., and Balakrishnan, R. (2010). Emergence of a new antibiotic resistance mechanism in India, Pakistan, and the UK: a molecular, biological, and epidemiological study. *Lancet Infect. Dis.* 10, 597–602. doi: 10.1016/S1473-3099(10)70143-2

Laishram, S., Pragasam, A. K., Bakthavatchalam, Y. D., and Veeraraghavan, B. (2017). An update on technical, interpretative and clinical relevance of antimicrobial synergy testing methodologies. *Indian J. Med. Microbiol.* 35, 445–468. doi: 10.4103/ijmm.IJMM_17_189

Lashinsky, J. N., Henig, O., Pogue, J. M., and Kaye, K. S. (2017). Minocycline for the treatment of multidrug and extensively drug-resistant *A. baumannii*: a review. *Infect. Dis. Ther.* 6, 199–211. doi: 10.1007/s40121-017-0153-2

Laxminarayan, R., and Chaudhury, R. R. (2016). Antibiotic resistance in India: drivers and opportunities for action. *PloS Med.* 13, e1001974. doi: 10.1371/journal.pmed.1001974

Lee, Y. T., Tsao, S. M., and Hsueh, P. R. (2013). Clinical outcomes of tigecycline alone or in combination with other antimicrobial agents for the treatment of patients with healthcare-associated multidrug-resistant *Acinetobacter baumannii* infections. *Eur. J. Clin. Microbiol. Infect. Dis.* 32, 1211–1220. doi: 10.1007/s10096-013-1870-4

López, C., Ayala, J. A., Bonomo, R. A., González, L. J., and Vila, A. J. (2019). Protein determinants of dissemination and host specificity of metallo-β-lactamases. *Nat. Commun.* 10, 1–11. doi: 10.1038/s41467-019-11615-w

Lyu, C., Zhang, Y., Liu, X., Wu, J., and Zhang, J. (2020). Clinical efficacy and safety of polymyxins based versus non-polymyxins based therapies in the infections caused by carbapenem-resistant *Acinetobacter baumannii*: a systematic review and meta-analysis. *BMC Infect. Dis.* 20, 296. doi: 10.1186/s12879-020-05026-2

Magiorakos, A. P., Srinivasan, A., Carey, R. B., Carmeli, Y., Falagas, M. E., Giske, C. G., et al. (2012). Multidrug-resistant, extensively drug-resistant and pandrug-resistant bacteria: an international expert proposal for interim standard definitions

for acquired resistance. *Clin. Microbiol. Infect.* 18, 268–281. doi: 10.1111/j.1469-0691.2011.03570.x

Marchaim, D., Pogue, J. M., Tzuman, O., Hayakawa, K., Lephart, P. R., Salimnia, H., et al. (2014). Major variation in MICs of tigecycline in gram-negative bacilli as a function of testing method. *J. Clin. Microbiol.* 52, 1617–1621. doi: 10.1128/JCM.00001-14

Mohd Sazlly Lim, S., Heffernan, A. J., Zowawi, H. M., Roberts, J. A., and Sime, F. B. (2021). Semi-mechanistic PK/PD modelling of meropenem and sulbactam combination against carbapenem-resistant strains of *Acinetobacter baumannii*. *Eur. J. Clin. Microbiol. Infect. Dis.* 40, 1943–1952. doi: 10.1007/s10096-021-04252-z

Monnheimer, M., Cooper, P., Amegbletor, H. K., Pellio, T., Groß, U., Pfeifer, Y., et al. (2021). High prevalence of carbapenemase-producing *Acinetobacter baumannii* in wound infections, Ghana 2017/2018. *Microorganisms* 9, 537. doi: 10.3390/microorganisms9030537

One Health Trust (2022) *Resistance map: Antibiotic resistance*. Available at: https://resistancemap.onehealthtrust.org/AntibioticResistance.php/CountryPageSub.php (Accessed November 28, 2022).

Piperaki, E. T., Tzouvelekis, L. S., Miriagou, V., and Daikos, G. L. (2019). Carbapenem-resistant *Acinetobacter baumannii*: in pursuit of an effective treatment. *Clin. Microbiol. Infect.* 25, 951–957. doi: 10.1016/j.cmi.2019.03.014

Poirel, L., Walsh, T. R., Cuvillier, V., and Nordmann, P. (2011). Multiplex PCR for detection of acquired carbapenemase genes. *Diagn. Microbiol. Infect. Dis.* 70, 119–123. doi: 10.1016/j.diagmicrobio.2010.12.002

Sandhu, R., Dahiya, S., and Sayal, P. (2016). Evaluation of multiple antibiotic resistance (MAR) index and doxycycline susceptibility of *Acinetobacter* species among inpatients. *Indian J. Microbiol. Res.* 3 (3), 299. doi: 10.5958/2394-5478.2016.00064.9

Sharma, S., Banerjee, T., Yadav, G., and Chaurasia, R. C. (2022). Role of early foldscopy (microscopy) of endotracheal tube aspirates in deciding restricted empirical therapy in ventilated patients. *Indian J. Med. Microbiol.* 40, 96–100. doi: 10.1016/j.ijmmb.2021.08.004

Sharma, S., Banerjee, T., Yadav, G., and Palandurkar, K. (2021b). Mutations at novel sites in pmrA/B and lpxA/D genes and absence of reduced fitness in colistin-resistant *Acinetobacter baumannii* from a tertiary care hospital, India. *Microb. Drug Resist.* 27, 628–636. doi: 10.1089/mdr.2020.0023

Sharma, S., Das, A., Banerjee, T., Barman, H., Yadav, G., and Kumar, A. (2021a). Adaptations of carbapenem resistant *Acinetobacter baumannii* (CRAB) in the hospital environment causing sustained outbreak. *J. Med. Microbiol.* 70, 1–8. doi: 10.1099/jmm.0.001345

Turton, J. F., Woodford, N., Glover, J., Yarde, S., Kaufmann, M. E., and Pitt, T. L. (2006). Identification of *Acinetobacter baumannii* by detection of the blaOXA-51-like carbapenemase gene intrinsic to this species. *J. Clin. Microbiol.* 44, 2974–2976. doi: 10.1128/JCM.01021-06

Viehman, J. A., and Nguyen, M. H. (2014). Treatment options for carbapenem-resistant and extensively drug-resistant *Acinetobacter baumannii* infections. *Drugs* 74, 1315–1333. doi: 10.1007/s40265-014-0267-8

Vijayakumar, S., Jacob, J. J., Vasudevan, K., Mathur, P., Ray, P., Neeravi, A., et al. (2022). Genomic characterization of mobile genetic elements associated with carbapenem resistance of *Acinetobacter baumannii* from India. *Front. Microbiol.* 13. doi: 10.3389/fmicb.2022.869653

Vijayakumar, S., Wattal, C., Oberoi, J. K., Bhattacharya, S., Vasudevan, K., Anandan, S., et al. (2020). Insights into the complete genomes of carbapenem-resistant *Acinetobacter baumannii* harbouring *bla* $_{OXA-23}$, *bla* $_{OXA-420}$ and *bla* $_{NDM-1}$ genes using a hybrid-assembly approach. *Access Microbiol.* 2, 1–7. doi: 10.1099/acmi.0.000140

Wang, Y., Luo, Q., Xiao, T., Zhu, Y., and Xiao, Y. (2022). Impact of polymyxin resistance on virulence and fitness among clinically important gram-negative bacteria. *Engineering* 13, 178–185. doi: 10.1016/j.eng.2020.11.005

Woodford, N., Ellington, M. J., Coelho, J. M., Turton, J. F., Ward, M. E., Brown, S., et al. (2006). Multiplex PCR for genes encoding prevalent OXA carbapenemases in *Acinetobacter* spp. *Int. J. Antimicrob. Agents* 27, 351–353. doi: 10.1016/j.ijantimicag.2006.01.004

World Health Organization Press (2017) *Global priority list of antibiotic-resistant bacteria to guide research, discovery, and development of new antibiotics*. Available at: https://www.who.int/news/item/27-02-2017-who-publishes-list-of-bacteria-for-which-new-antibiotics-are-urgently-needed.

frontiers | Frontiers in Cellular and Infection Microbiology

TYPE Original Research
PUBLISHED 02 May 2023
DOI 10.3389/fcimb.2023.1180714

OPEN ACCESS

EDITED BY
Rodolfo García-Contreras,
Department of Microbiology and Parasitology, National Autonomous University of Mexico, Mexico

REVIEWED BY
Kokila Kota,
Ramapo College, United States
Friederike Maechler,
Institute of Hygiene, Germany

*CORRESPONDENCE
Elias Dahdouh
elie.dahdouh@gmail.com

SPECIALTY SECTION
This article was submitted to Antibiotic Resistance and New Antimicrobial drugs, a section of the journal Frontiers in Cellular and Infection Microbiology

RECEIVED 06 March 2023
ACCEPTED 13 April 2023
PUBLISHED 02 May 2023

CITATION
Dahdouh E, Cendejas-Bueno E, Ruiz-Carrascoso G, Schüffelmann C, Lázaro-Perona F, Castro-Martínez M, Moreno-Ramos F, Escosa-García L, Alguacil-Guillén M and Mingorance J (2023) Intestinal loads of extended-spectrum beta-lactamase and Carbapenemase genes in critically ill pediatric patients. *Front. Cell. Infect. Microbiol.* 13:1180714. doi: 10.3389/fcimb.2023.1180714

Intestinal loads of extended-spectrum beta-lactamase and Carbapenemase genes in critically ill pediatric patients

Elias Dahdouh[1*], Emilio Cendejas-Bueno[1,2], Guillermo Ruiz-Carrascoso[1,2], Cristina Schüffelmann[3], Fernando Lázaro-Perona[1], Mercedes Castro-Martínez[4], Francisco Moreno-Ramos[5], Luis Escosa-García[2,6], Marina Alguacil-Guillén[1] and Jesús Mingorance[1,2]

[1]Clinical Microbiology and Parasitology Department, Hospital Universitario La Paz, Instituto de Investigación Sanitaria del Hospital Universitario La Paz (IdiPAZ), Madrid, Spain, [2]Centro de Investigación Biomédica en Red de Enfermedades Infecciosas (CIBERINFEC), Instituto de Salud Carlos III, Madrid, Spain, [3]Pediatric Intensive Care Unit, Hospital Universitario La Paz, Madrid, Spain, [4]Preventive Medicine Department, Hospital Universitario La Paz, Madrid, Spain, [5]Department of Pharmacy, Hospital Universitario La Paz, Madrid, Spain, [6]Pediatric Tropical and Infectious Diseases Department, Hospital Universitario La Paz, Madrid, Spain

Introduction: Intestinal colonization by Multi-Drug Resistant Organisms (MDROs) can pose a threat on the health of critically ill patients. The extent of colonization by these organisms is related to previous antibiotic treatments and their ability to cause infections among adult patients. The aim of this study is to determine the relationship between the intestinal Relative Loads (RLs) of selected antibiotic resistance genes, antibiotic consumption and extra-intestinal spread among critically ill pediatric patients.

Methods: RLs of $bla_{\text{CTX-M-1-Family}}$, $bla_{\text{OXA-1}}$, $bla_{\text{OXA-48}}$ and bla_{VIM} were determined in 382 rectal swabs obtained from 90 pediatric critically ill patients using qPCRs. The RLs were compared to the patients' demographics, antibiotic consumption, and detection of MDROs from extra-intestinal sites. 16SrDNA metagenomic sequencing was performed for 40 samples and clonality analyses were done for representative isolates.

Results and discussion: 76 (74.45%) patients from which 340 (89.01%) rectal swabs were collected had at least one swab that was positive for one of the tested genes. Routine cultures did not identify carbapenemases in 32 (45.1%) and 78 (58.2%) swabs that were positive by PCR for $bla_{\text{OXA-48}}$ and blaVIM, respectively. RLs of above 6.5% were associated with extra-intestinal spread of blaOXA-48-harboring MDROs. Consumption of carbapenems, non-carbapenem β-lactams, and glycopeptides were statistically associated with testing negative for $bla_{\text{CTX-M-1-Family}}$ and $bla_{\text{OXA-1}}$ while the consumption of trimethoprim/sulfamethoxazole and aminoglycosides was associated with testing negative for blaOXA-48 ($P<0.05$). In conclusion, targeted qPCRs can be used to determine the extent of intestinal dominance by antibiotic resistant

opportunistic pathogens and their potential to cause extra-intestinal infections among a critically ill pediatric population.

KEYWORDS

intestinal dominance, pediatric patients, β-lactamase genes, relative intestinal load, qPCR, antibiotic consumption, extra-intestinal multi-drug resistant organisms, microbiome

1 Introduction

Intestinal colonization with Multi-Drug Resistant Organisms (MDROs) capable of producing Extended-Spectrum β-Lactamases (ESBLs) and/or carbapenemases is a global concern since these organisms can cause life-threatening opportunistic infections (Weinstein, 2012). Intestinal colonization by MDROs is often a result of antibiotic consumption that selects for these organisms and allows them to overgrow and dominate the intestinal microbiome (Willmann et al., 2019). This dominance poses an additional threat since it is linked to higher rates of infections (Sun et al., 2021) and transmission of MDROs (Lerner et al., 2015). Moreover, the resulting dysbiosis in the gut microbiome could have detrimental effects on human health (Young, 2017), and especially on the healthy development of children (Gaufin et al., 2018).

Recent studies have shown that the degree of intestinal colonization by opportunistic pathogens, especially ESBL- and carbapenemase-producers, can have a direct effect on infection and mortality rates (Dahdouh et al., 2021; Migliorini et al., 2022; Pérez-Nadales et al., 2022). Moreover, this colonization can be occult, *i.e.* present at such low amounts that it is not detected by traditional culture media, but has the potential to quickly expand and dominate the intestinal microbiome in response to antibiotic pressure (Sim et al., 2022). Previous studies have shown associations between high intestinal Relative Loads (RLs) of carbapenemase-producing *Klebsiella pneumoniae*, antibiotic consumption, and development of infections in hospitalized adult patient populations (Migliorini et al., 2022;, Lázaro-Perona et al., 2020), and in pediatric liver transplant patients (Dahdouh et al., 2022). The aim of this study is to use the qPCR assay developed and validated in these previous studies to determine the relationship between the intestinal RLs of selected ESBL and carbapenemase genes, antibiotic consumption, occult colonization, gut microbiome dysbiosis, and extra-intestinal spread of MDROs among critically ill pediatric patients.

2 Materials and methods

2.1 Study design

The study was retrospective and performed at the Hospital Universitario La Paz (HULP) in Madrid, Spain; a 1,200 bed tertiary care center. The pediatric patients included in this study were all those that had at least one stay at the pediatric Intensive Care Unit (pICU) of the hospital between April, 2018 and December, 2019. These patients were then followed throughout the duration of the study even when they were transferred, admitted, or visited other hospital wards at HULP. The samples received from these patients were originally collected for routine epidemiological surveillance and there wasn't any sample that was collected specifically for this study. All the samples were re-used after fulfilling their diagnostic purposes and were analysed in bulk. Also, no results were communicated in real time to neither the clinicians nor the patients, and therefore the results obtained from this study did not interfere with the clinical management of the patients involved. Pediatric liver transplant patients were excluded since they received extensively more antibiotics than other patient groups and were included in a previous study performed by our group (Dahdouh et al., 2022).

During the time of the study, rectal swabs were routinely collected and sent to the microbiology department of HULP to determine the presence of ESBL, OXA-48, and VIM producers was implemented due to an ongoing outbreak caused by carbapenem-resistant *K. pneumoniae* that started in 2010 and has become endemic at the hospital (Pérez-Blanco et al., 2018). The rectal swabs were received from patients whose health condition allow for taking the swab and were initially cultured on MacConkey plates containing 4μg/mL cefotaxime (custom made by Maim®, Madrid, Spain) for the detection of ESBL producers, and on ChromID CARBA SMART™ agar plates (Biomérieux®, Marcy l'étoile, France) for the detection of carbapenemase producers. This was part of the routine epidemiological surveillance performed at HULP. After reaching the clinical conclusions, the same swabs were then collected to be reused in this study. Their contents were suspended in 0.5 mL of TE buffer (10mM Tris and 1mM EDTA; pH = 8.0) through vigorous shaking. The suspension was then stored at -20°C until used, and analysed in batches when a sufficient number of samples was reached. In the cases where the isolates obtained from the rectal swabs were stored in the hospital's bacterial collection, they were recovered. Moreover, all the MDRO isolates that were obtained from clinical samples of the patients included in this study (such as urine, blood, abscesses, etc…), and that were stored in the bacterial collection as part of HULP's routine practice were recovered to be used in this study. These latter isolates are

labelled "extra-intestinal isolates" throughout the rest of the article.

2.2 DNA extraction

100µL of the rectal swab suspensions were diluted with 900µL of TE buffer in order to avoid inhibition of the qPCR reactions. Total DNA was then extracted by heating this suspension at 95°C for 20 minutes, performing mechanical lysis at 7,000rpm for 70 seconds using MagNA Lyser Green Beads and MagNa Lyser™ (Roche®, Mannheim, Germany), and extracted using the MagNA Pure Compact Nucleic Acid Isolation Kit I and MagNA Pure Compact™ system (Roche®, Mannheim, Germany). The DNA was then stored at -20°C.

2.3 Quantification of the relative intestinal loads of $bla_{CTX\text{-}M\text{-}1\text{-}Family}$, $bla_{OXA\text{-}1}$, $bla_{OXA\text{-}48}$, and *bla*$_{VIM}$ genes

The qPCR assays designed in one of our previous studies were used to determine the Relative intestinal Loads (RLs) of the beta-lactamase genes that are endemic at HULP (*bla*$_{CTX\text{-}M\text{-}1\text{-}Family}$, *bla*$_{OXA\text{-}1}$, *bla*$_{OXA\text{-}48}$, and *bla*$_{VIM}$) (Dahdouh et al., 2022). Briefly, reaction mixtures containing 10µl 2X PowerUP™ SYBR® Green Master Mix (Applied Biosystems, Waltham, MA, USA), 0.05µM of each respective primer pair, 6µl H_2O and 2µl DNA were prepared. The CFX Connect™ Real-Time System (BioRad, Madrid, Spain) was used for thermal cycling under the following conditions: 95°C for 3 minutes, then 40 cycles of 95°C for 15 seconds and 60°C for 1 minute; followed by melting curve analyses.

RLs of the tested genes were determined in relation to the C_t values of the *16SrDNA* gene and normalized to the RLs of these genes in pure bacterial cultures using the $2^{-\Delta\Delta Ct}$ method (Livak and Schmittgen, 2001). The RLs were then transformed into an inverse logarithmic scale where 0 represents RLs that are equivalent to pure bacterial cultures, –1 represents 10% of the bacterial population collected in the rectal swab, –2 represents 1%, and so on until –6 which represents 0.0001% of the total bacterial population, and our detection limit. The values are also expressed (where relevant) as percentages (%RL) where the values were converted to percentages using the formula $10^{RL} \times 100$.

2.4 Clonality analyses

Clonality analyses were done using Random Amplified Polymorphic DNA (RAPD) (Hsueh et al., 1998). The primers used were OPA-2 (5'-TGCCGAGCTG-3'), OPA-12 (5'-TCGGCGATAG-3'), and OPA-18 (5'-AGGTGACCGT-3') and the thermal cycling conditions were 94°C for 5 minutes, followed by 45 cycles of 94°C for 1 minute, 37°C for 1 minute, and 72°C for 2 minutes, and a final step at 72°C for 2 minutes. PCR products were then visualized on 2% agarose gels and the resulting profiles obtained were used to determine the clonal relatedness of the isolates.

2.5 Next-generation sequencing

Whole-genomes were sequenced for representative isolates from the most frequent clones (as determined by RAPD). The isolates were cultured overnight on blood agar plates at 37°C and DNA was extracted from 10 single colonies as described previously (section 2.2). The NEBNext® Fast DNA Fragmentation & Library Prep Set for Ion Torrent™ (New England Biolabs, Ipswich MA, USA) was used to prepare the libraries according to the manufacturer's instructions. Mag-Bind® TotalPure NGS beads (Omega Bio-Tek, Norcross GA, USA) was used for the purifications step, and the Ion Chef® and S5® Gene Studio (ThermoFisher Scientic, Waltham MA, USA) were used for sequencing. The reads were assembled using Geneious (v.10.1.3, Biomatter Ltd., Auckland, New Zealand). They were also tested for the presence of antibiotic resistance determinants and plasmids, and were allocated a specific Sequence Type (ST) using the tools available on the Center for Genomic Epidemiology website (https://cge.cbs.dtu.dk).

16SrDNA metagenomic sequencing was performed to rectal swab suspensions that had varying RLs towards the tested genes, and the samples were labelled S1 through S40. Samples S1 to S29 were positive to at least one of the genes tested for, and were ordered in decreasing values of RLs while samples S30 to S40 were negative to all 4 tested genes. The Ion 16S™ Metagenomics Kit and the Ion Plus™ Fragment Library Kit with the Ion Xpress Barcode Adapters (Thermo Fisher, USA) kits were used to prepare the libraries according to the manufacturer's instructions. Sequencing was performed using the same instruments as above and the sequences were analyzed using ION Reporter™ (Thermo Fisher, USA). All the sequences obtained from this study were deposited in Genbank under the Bioproject with the accession number PRJNA911601.

2.6 Patient data

Patient data (age, gender, colonization status, extra-intestinal infections 14 days before or after rectal swab collection, colonisation status upon sample collection, and antibiotics received) were retrieved from the hospital's information system database. The patients were given study-specific codes in such a way that no patient can be identified. Approval of HULP's local ethics committee was obtained for the study (PI-3428).

2.7 Statistical analyses

Normality of the data was tested for using the Kolmogorov-Smirnov (if n>50) and Shapiro-Wilk (if n<50) tests. The RLs of the four tested genes were grouped based on whether or not they correspond to an extra-intestinal infection, whether or not the patients received antibiotics in the 30 days prior to sample collection, and whether or not they correspond to detection of MDROs using the routine screening cultures performed at HULP. Two-sided student T-tests and ANOVA were used for normally distributed quantitative data, and Kruskal-Wallis and Mann-

Whitney U tests were used for non-normally distributed quantitative data. Chi-squared was used for the comparison of categorical variables such as antibiotic consumption in relation to having one or more β-lactamase genes detected in the rectal swab. Receiver Operating Characteristic (ROC) analyses were performed using the easyROC online tool (http://biosoft.erciyes.edu.tr/app/easyROC/) in order to determine cutoff values after which there is an increase rate of detection of extra-intestinal MDROs harbouring the same gene as that detected in the rectal swabs. The Youden method (*i.e.* determining the J value through the formula [sensitivity + specificity – 1] for all the points of the curve) was used in order to determine the cutoff values. Statistical significance was determined when *p* values were less than 0.05 and all the statistical tests were performed using SPSS (version 24.0; IBM, Armonk, NY, USA).

3 Results

3.1 Clinical data and detection of β-lactamase genes

The general characteristics of the patients and the samples included, as well as the qualitative results obtained by routine cultures and qPCRs are presented in Table 1. Of the 90 patients included in this study, 42 were chronic. Of these chronic patients, 19 were transplant patients (9 kidney, 4 multi-organ, 3 hematopoietic, and 3 cardiac transplants). Of the 382 rectal swabs obtained from the 90 patients included in the study, 317 (82.98%) were collected from chronic patients and 65 (17.02%) were collected from acute patients (2 or less swabs from each acute patient that had average hospital stays of less than 1 week). Sixty-seven patients from which 340 rectal swabs were collected had at least one swab that was positive for at least one of the genes tested by PCR. Thirty-eight of these patients had both ESBLs and carbapenemases, 18 had only carbapenemases, and 11 had only ESBLs. Just 3 of the 23 patients that were negative for these genes where chronic patients (15 (4.73%) samples), and the rest were acute patients (40 (61.54%) samples). By routine cultures, 28 patients had at least one sample positive for ESBLs, 24 for carbapenems, and 10 for both carbapenems and ESBLs.

K. pneumoniae was the most frequent species isolated from the rectal swabs (Table 1). To study the relationship between the different isolates, clonality analyses through RAPD was performed for 43 isolates that could be recovered from 21 patients. The most frequent clone comprised 20 isolates originating from 9 different patients, and was found (through whole-genome sequencing) to belong to sequence type (ST) ST39. Another clone was found to belong to ST37 and was detected in 7 isolates from a single patient. A third clone was detected in 2 isolates obtained from a single patient and belonged to ST3155, and a fourth clone that belonged to ST1928 was also detected in 2 isolates obtained from another patient. The rest of the isolates (twelve isolates from nine patients) included in the clonality analyses did not have a profile that was similar to any other isolate.

TABLE 1 Description of the patients and samples included in this study, as well as the qualitative results obtained by routine cultures and qPCRs for the genes included in this study.

General Characteristics of the Patients and Samples Included in the Study	
Number of Patients	90
Chronic Patients[1]	42
Acute Patients[2]	48
Average Age (years)	8.3 (median = 6; range = 3 – 18)
Gender	43 (48.8%) Female
Average of Weeks Followed	11 (median = 6; range = 0.3 – 57)
Average number of Swabs per Patient	4 (range: 1 – 23)
Total Rectal Swabs Collected	382
Paediatric Intensive Care Unit	130 (34%)
Haematology/Oncology Outpatient	54 (14.1%)
Emergency	40 (10.5%)
Haematology/Oncology Inpatient	39 (10.2%)
Paediatrics	36 (9.4%)
Nephrology Inpatient	25 (6.5%)
Gastroenterology	22 (5.8%)
Neonatal	11 (2.9%)
Nephrology Outpatient	10 (2.6%)
Surgery	8 (2.1%)
Cardiology	7 (1.8%)
Routine Epidemiological Screening	
Carbapenemase-Producers	82 (21.5%)
ESBL-Producers	53 (13.9%)
ESBL- and Carbapenemase-Producers	9 (2.4%)
Negative	211 (55.2%)
Not Processed	27 (7.1%)[3]
ESBL Producers Detected by Routine Screening (n = 55)[4,5]	
Klebsiella pneumoniae	45 (81.8%)
Enterobacter cloacae	4 (7.3%)
Others (incidence of 3 or less)	6 (10.9%)
Carbapenemase Producers Detected by Routine Screening (n = 83)[4,5]	
Klebsiella pneumoniae	50 (60.2%)
Enterobacter cloacae	11 (13.3%)
Klebsiella oxytoca	7 (8.4%)
Escherichia coli	9 (10.8%)
Others (incidence of 3 or less)	6 (7.2%)

(Continued)

TABLE 1 Continued

General Characteristics of the Patients and Samples Included in the Study	
Genes Detected by PCR[6]	
$bla_{\text{CTX-M-1-Family}}$	136 (35.6%)
$bla_{\text{OXA-1}}$	109 (28.5%)
$bla_{\text{OXA-48}}$	71 (18.6%)
bla_{VIM}	134 (35.1%)
Negative for all 4 genes	122 (31.9%)

[1]Chronic patients included pediatric transplant (excluding liver transplant) and haematological/oncological patients.
[2]Acute patients included accident victims and neonates with post-partum complications.
[3]These rectal swabs were not processed by routine culture screening because they did not comply with the standard protocols applied at the Hospital Universitario La Paz at time of the study.
[4]There were multiple instances of more than one organism being isolated from a single rectal swab.
[5]8 Klebsiella pneumoniae isolates and 1 K. oxytoca isolate had both ESBL and Carbapenemases.
[6]There were multiple instances of more than one gene detected in the same rectal swab.

In total (out of the 382 rectal swabs), 136 (35.6%) were positive for $bla_{\text{CTX-M-1-Family}}$, 109 (28.5%) for $bla_{\text{OXA-1}}$, 71 (18.6%) for $bla_{\text{OXA-48}}$, and 134 (35.1%) for bla_{VIM} by PCR. Compared to the PCR, the sensitivity of the routine cultures for the detection of OXA-48 producers was 51.52% and its specificity 98.39%. For VIM producers, the sensitivity was 38.1% and the specificity 98.98% (Supplementary Table 1). ESBL-producers were not included in this analysis since ESBL-harboring *E. coli* were reported as negative in the hospital's information system database, according to the activated protocols at the time of the study.

3.2 Relative intestinal loads of the β-lactamase genes

The RLs of the four β-lactamase genes endemic at HULP ($bla_{\text{CTX-M-1-Family}}$, $bla_{\text{OXA-1}}$, $bla_{\text{OXA-48}}$, and bla_{VIM}) were determined through normalizing the Ct values of these genes to that of the *16SrDNA* gene. The RLs of the four genes measured in all the swabs fell within a six log range, from almost pure cultures (0; 100% of bacterial population) to -6 (0.0001% of the total bacterial population). The median RLs of $bla_{\text{CTX-M-1-Family}}$ and $bla_{\text{OXA-1}}$ were significantly higher than those of $bla_{\text{OXA-48}}$ and bla_{VIM} (-1.7 (1.98%) and -1.79 (1.64%) versus -2.49 (0.32%) and -2.41 (0.4%), respectively; $P < 0.05$; Figure 1). The RLs determined for $bla_{\text{OXA-48}}$ and bla_{VIM} were more evenly spread out across the detection ranges, but showed a bi-modal distribution pattern where they clustered in either high RLs (over -2 (*i.e.* 1% of the total bacterial population)) or low RLs (under -4 (*i.e.* 0.001% of the total bacterial population)) (Figure 1). Samples that were PCR-positive for $bla_{\text{CTX-M-1-Family}}$ and $bla_{\text{OXA-1}}$ often showed RLs that were higher than -2 (1% of the total bacterial population). There was no difference in RLs between male and female patients, nor was there any difference based on the age of the patient, the type of disease for which the patient was receiving treatment, the wards in which the patients were admitted to at the time of sampling, and whether or not the patients were critically ill.

There were 75 (70.1%), 32 (45.1%), and 78 (58.2%) swabs positive by PCR for $bla_{\text{CTX-M-1-Family}}$, $bla_{\text{OXA-48}}$, and bla_{VIM} genes, respectively, that were negative in antibiotic-selective cultures. However, according to HULP's protocols at the time of the study, ESBL-harboring *E. coli* were reported as negative in the hospital's information system database, and therefore the total number of positive cultures for ESBL-producing organisms cannot be known. Comparing the RLs of the carbapenemase genes to the results of the routine cultures showed that the median RLs of $bla_{\text{OXA-48}}$ and bla_{VIM} were significantly higher in samples that were positive by PCR and culture as compared to those only positive by PCR (-1.45 (3.2%) and -0.82 (15.1%) versus -4.38 (0.004%) and -4.02 (0.01%); respectively; $P<0.05$; Figure 2). Moreover, the bi-modal distribution pattern disappeared where the RLs of the samples that were positive through both methods clustered in the higher RL ranges while those that were only positive by PCR clustered in the lower RL ranges (Figure 2). The $bla_{\text{OXA-1}}$ gene was not included in this analysis since it was not screened for in the routine cultures.

3.3 Antibiotic consumption and relative intestinal loads of antibiotic resistance genes

Antibiotic consumption data was retrieved from the hospital's information system database for the patients that were included in this study throughout the duration of the study, and 30 days before inclusion. Twenty one (23.33%) patients did not receive any antibiotic throughout the study period, and in 37 (41.11%) patients, all the samples collected from them corresponded to them receiving antibiotics during the previous 30 days. These treatments were not consecutive and were often mixed where different antibiotics were received at different times, but they always received at least one type in the 30 days before sampling. The remaining 32 (35.56%) patients were mixed where some swabs corresponded with antibiotic consumption during the 30 days before sample collection, and others did not. From the first group of 21 patients, 42 (10.99%) rectal swabs were collected, and from the second group of 37 patients 139 (36.39%) swabs were collected. From the third group of mixed patients, 138 (36.12%) rectal swabs corresponded with antibiotic consumption and 63 (16.49%) of them did not correspond with the patient receiving antibiotics in the previous 30 days.

In total, 277 (72.51%) of the rectal swabs corresponded with antibiotic consumption during the 30 days prior to collection, and 105 (27.49%) did not. For 72 rectal swabs, the patients received one type of antibiotic, for 40 rectal swabs the patients received antibiotics from 2 different classes, and for the remaining 165 swabs the patients received 3 or more antibiotics from different classes. Table 2 shows the type of antibiotics that the patients received before sample collection. In the majority of the incidents (82%), the antibiotics were administered intravenously, in 14.5% of the incidents antibiotics were received orally and intravenously, and in 3.5% of the incidents the antibiotics were only administered orally.

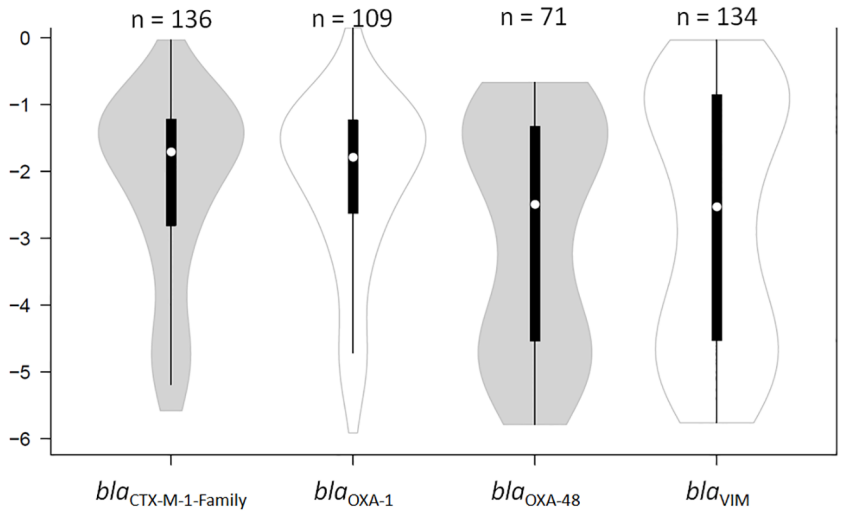

FIGURE 1
Violin plot showing the distribution of the relative loads of the samples that were positive by qPCR for *bla*$_{\text{CTX-M-1-Family}}$, *bla*$_{\text{OXA-1}}$, *bla*$_{\text{OXA-48}}$, and *bla*$_{\text{VIM}}$. The results are expressed in an inverse logarithmic scale where 0 is 100% of the bacterial population, -1 is 10%, -2 is 1%, and so on until -6 which is 0.0001% of the bacterial population, and our detection limit. "n" stands for the number of samples that were positive for the respective gene of antibiotic resistance.

The consumption of carbapenems, non-carbapenem β-lactams, and glycopeptides was significantly associated with testing negative for *bla*$_{\text{CTX-M-1-Family}}$ and *bla*$_{\text{OXA-1}}$ ($P < 0.05$). Consumption of aminoglycosides and Trimethoprim/Sulfamethoxazole (TMX) was also significantly associated with testing negative for *bla*$_{\text{OXA-48}}$ ($P < 0.05$). Additionally, the consumption of TMX was significantly associated with lower median RL values for *bla*$_{\text{OXA-48}}$ (-1.82 (1.5%) versus -4.45 (0.004%); $P < 0.05$). No statistically significant associations were determined for the rest of the antibiotic classes and the other antibiotic resistance genes.

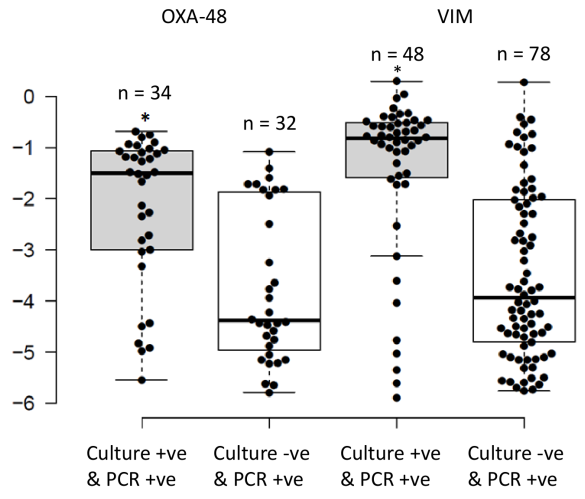

FIGURE 2
Distribution of the relative loads of the samples that were positive by routine cultures and PCR for OXA-48 and VIM, compared to those that were only positive by PCR. The results are expressed in an inverse logarithmic scale where 0 is 100% of the bacterial population, -1 is 10%, -2 is 1%, and so on until -6 which is 0.0001% of the bacterial population, and our detection limit. *Implies statistically higher relative intestinal loads for samples that were positive by PCR and routine cultures as opposed to being positive by PCR alone (P<0.05).

3.4 Intestinal dominance by bacteria harboring β-lactamase genes and extra-intestinal spread

The RLs determined for the four genes tested for were compared to incidents where extra-intestinal isolates were collected within 14 days of rectal swab collection. Thirty-three extra-intestinal β-lactam resistant isolates have been registered in the hospital information system from 18 patients included in the study. Fourteen isolates were obtained during the two weeks before the collection of the rectal swab, seven on the same day, and twelve during the two weeks after the collection of the rectal swabs. These incidents were at least 2 weeks apart when collected from the same patient in order to exclude ongoing infections caused by the same isolate. Twenty of the extra-intestinal isolates were related to infections while the remaining thirteen were considered colonisations, as registered by the attending physician at the time (Table 3). In 28 of these episodes (84.85%), the patients received antibiotics up to 30 days before extra-intestinal detection of MDROs. It was possible to compare the extra-intestinal isolates to the intestinal ones in only 21 of these cases (13 of them were infections) since in the remaining cases, no growth was reported through routine culture from the corresponding rectal swab. In 16 of these 21 (76.2%) cases the same organism was detected in both the rectal swabs and the extra-intestinal site. Clonality analyses through RAPD comparing these isolates was only possible for 9 incidents (where the isolates were stored in the hospital's bacterial collection), and in 8 of them (88.9%) the same clone was detected. In terms of the β-lactam resistance genes, in out 27 of the 33 isolates (81.8%), the same gene was detected in the intestinal (detected

through qPCR) and extra-intestinal sites (registered in the hospital's database).

The intestinal RLs of the antibiotic resistance genes collected within 2 weeks (average = 2 days; median = same day) from the extra-intestinal episode had median RLs of -1.36 (4.4%) for $bla_{\text{CTX-M-1-Family}}$, -1.48 (3.5%) for $bla_{\text{OXA-1}}$, -1.05 (8.9%) for $bla_{\text{OXA-48}}$, and -1.97 (1.1%) for bla_{VIM}. The RLs of $bla_{\text{CTX-M-1-Family}}$ and $bla_{\text{OXA-48}}$ were significantly higher in the samples close to an episode of extra-intestinal spread than in samples that were not associated to extra-intestinal episodes (-1.36 (4.4%) and -1.05 (8.9%) versus -1.85 (1.4%) and -3.25 (0.06%), respectively; $P < 0.05$; Figure 3). No statistical significance was detected for bla_{VIM}. There were 11 extra-intestinal samples that corresponded with reporting of a culture-negative rectal swab. Seven of these samples corresponded with infections (bacteremia, peritonitis, and lower respiratory tract infections), and in all of them except for one, the same gene was detected in the rectal swab through PCR compared to the gene reported in the extra-intestinal isolate. In the seventh sample, no antibiotic resistant gene was detected in the rectal swab and an ESBL-producing organism was reported to cause ventilator associated pneumonia. Also among these 11 samples, 7 corresponded with the patient receiving antibiotics and the rest did not correspond with antibiotic consumption during the 30 days before sample collection. In the 4 remaining episodes, nothing was detected by PCR in the rectal swabs and all 4 episodes were registered as asymptomatic bacteruria.

ROC analysis (Youden method) of the capacity of the RLs to identify samples close to an extra-intestinal spread episode determined a cut-off value of 6.5% for organisms harbouring $bla_{\text{OXA-48}}$ (area under the curve = 0.89, sensitivity = 0.89, specificity = 0.87; $P < 0.05$; Figure 4C). In none of the other three genes the intestinal RL could identify samples close to extra-intestinal spread episodes (Figure 4A, B, D).

3.5 Microbiome diversity and relative intestinal loads

Metagenomic analyses (*16SrDNA*) were done with the same rectal swab suspensions used for qPCR in a subset of forty selected samples (S1 to S40) (Figure 5). Figure 5B shows the same samples but where only *Klebsiella* spp. (red) and *Pseudomonas* spp. (green) are highlighted. These two organisms were chosen since, according to the local epidemiology at HULP, were the most likely organisms to harbour the genes tested for in our study. The observed number of genera, α-diversity (calculated according to the Shannon method), and percent relative loads (%RLs) of the four genes tested for in these samples are shown in Supplementary Table 2.

Comparing the positive samples to the negative ones, a higher diversity among the negative samples was observed (median of 31 genera versus 15 genera; $P>0.05$). Moreover, looking at the percentage of *Klebsiella* spp. and *Pseudomonas* spp. (Figure 5B), it is evident that all but 4 samples that were positive for at least one of the tested genes were dominated by one or both of these organisms, while in all but 2 samples that were negative for these genes these organisms were almost absent. Of the 4 positive samples that showed an exception, S1 was dominated by *Enterococcus* spp., S7 and S24 were relatively diverse, and S21 showed dominance by

TABLE 2 Distribution of samples in light of antibiotic consumption in the 30 days prior to the collection of the rectal swab.

Antibiotic Consumption up to 30 Days Before Sample Collection		
Patients With no Antibiotics Received		21
Patients that Received Antibiotics		69
Samples Collected with no Antibiotics Received		105
Samples Collected from Patients that Received Antibiotics		277
Number of Antibiotics Received (by Class)		Number of Rectal Swabs
1		72
2		40
3 or more		165
Antibiotics Received	Number of Rectal Swabs	Median Days Received
Non-Carbapenem β-Lactams	217	3 (range: 1 – 38)
Glycopeptides	160	5 (range: 1 – 29)
Carbapenems	124	6 (range: 1 – 29)
Aminoglycosides	104	2 (range: 1 – 27)
Trimethoprim/Sulfamethoxazole	83	3 (range: 1 – 25)
Others	390	3 (range: 1 – 30)

[1]The other antibiotics received are macrolides, fluoroquinolones, linezolid, and the antifungals fluconazole, metronidazole, micafungin, and voriconazole.

TABLE 3 Extra-intestinal detection of isolates resistant to β-lactams.

Extra-Intestinal β-Lactam Resistant Isolates	
Extra-intestinal β-lactam resistant isolates	33
Bacteraemias	5
Surgical wound infections	3
Ventillator-associated pneumonias	3
Conjuctivitis	2
Pneumonias	2
Pyelonephritis	1
Sepsis	1
Surgery-related peritonitis	1
Pericatheter skin infection	1
Traqueobronchitis	1
Colinisations	13
Asymptomatic bacteruria	5
Broncheal aspirate	5
Skin	2
Pharyngeal swab	1

Acinetobacter spp. It is also interesting to note that the negative samples S38 and S39 were dominated by *Enterococcus* spp. and S40 was dominated by *Acinetobacter* spp. For samples S21 and S24, ESBL- and OXA-48-producing *K. pneumoniae* were registered in the hospital's information system database, respectively. For samples S1, S38, S39, and S40, no record of a β-lactam resistant organism in the rectal swabs was registered in the hospital's database system.

4 Discussion

In this study, we analyzed the intestinal RLs of the four genes of β-lactamases that are endemic at our hospital ($bla_{\text{CTX-M-1-Family}}$, $bla_{\text{OXA-1}}$, $bla_{\text{OXA-48}}$, and bla_{VIM}) using a previously validated qPCR assay (Dahdouh et al., 2022). The %RLs of $bla_{\text{CTX-M-1-Family}}$ and $bla_{\text{OXA-1}}$, which are commonly found on the same plasmid (Livermore et al., 2019), for the most part had values that ranged between 1% (-1) and 10% (-2) of the total bacterial population. However, those of $bla_{\text{OXA-48}}$ and bla_{VIM} showed a bi-modal distribution where they were either very high or very low, with relatively few samples in between (Figure 1). This can have very important implications for intestinal colonizations with carbapenemase-producing organisms since they can be present at low RLs, which routine cultures are more prone to miss (Figure 2), but can quickly dominate the intestine and rise to high RLs with an increased probability of spreading into extra-intestinal sights and cause infections (Figure 3). Moreover, the bi-modal distribution could be related to the different pharmacokinetic/pharmacodynamic properties of antibiotics that affect these genes where they could be present in the gut in sub-inhibitory concentrations and allow these organisms to persist in low RLs (Sadgrove and Jones, 2019), a phenomenon that is not as observed for ESBL-producers. These latter organisms were, for the most part, colonizing the intestines at high RLs (Figure 1). This might be due to carbapenems, non-carbapenem β-lactams, and glycopeptides inhibiting the growth of ESBL carriers even at low amounts, as

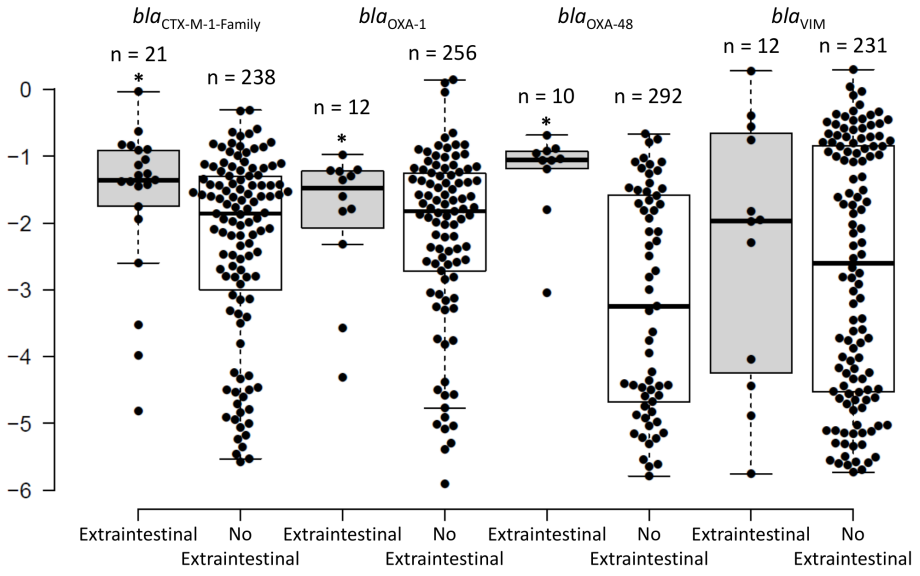

FIGURE 3
The distribution of the intestinal relative loads of the $bla_{\text{CTX-M-1-Family}}$, $bla_{\text{OXA-1}}$, $bla_{\text{OXA-48}}$, and bla_{VIM} genes within 2 weeks of extra-intestinal isolation of an organism harbouring the same gene, as compared to the intestinal relative loads that do not correspond to extra-intestinal isolation of an organism harbouring these genes. * signifies statistically higher relative loads for the swabs corresponding with an extra-intestinal isolate compared to those that do not.

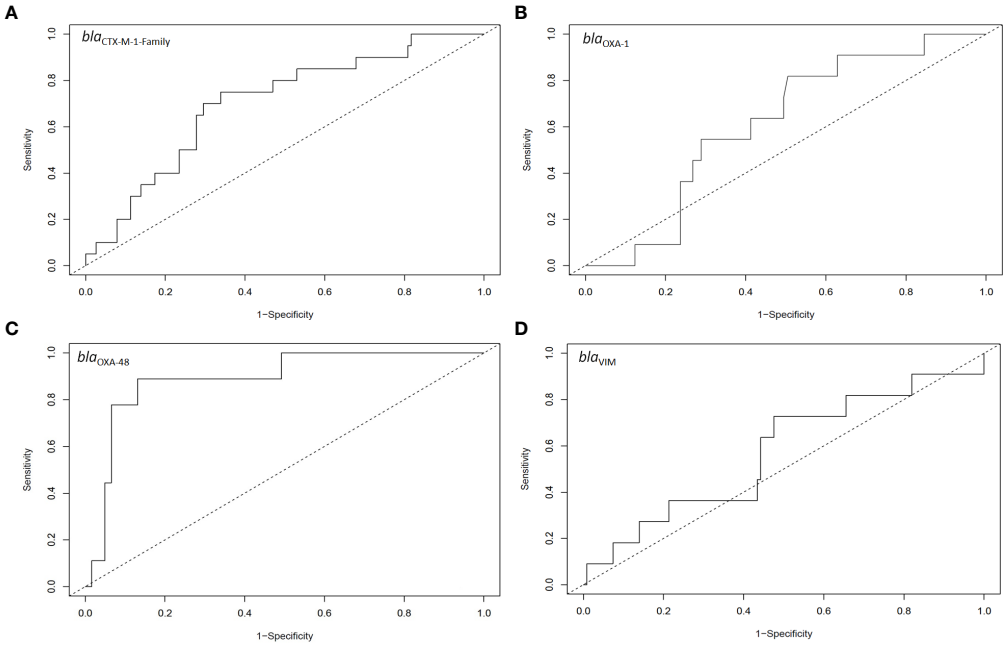

FIGURE 4
ROC analysis for the relative intestinal loads of **(A)** $bla_{CTX\text{-}M\text{-}1\text{-}Family}$, **(B)** $bla_{OXA\text{-}1}$, **(C)** $bla_{OXA\text{-}48}$, and **(D)** bla_{VIM} for samples that had extra-intestinal isolates harbouring the relative genes as compared to those that did not have extra-intestinal isolates harbouring these genes. The number of samples included in these analyses are the same as those in Figure 3.

seen through the associations between testing negative for the ESBL genes and consumption of these antibiotics, making it unlikely that these organisms colonize at low RLs. This could also explain why they are almost constantly encountered at high RLs since these, or other antibiotics, can kill off the bacterial community and allow these ESBL producers to survive and dominate the intestines if they acquire additional mechanisms of antibiotic resistance that were not tested for in this study.

The data we obtained in this study from a heterogeneous pediatric population is somewhat different from that obtained for adults, where the %RLs of $bla_{OXA\text{-}48}$ were mostly above 10% of the bacterial population (Lázaro-Perona et al., 2020). They were also different from those determined for pediatric liver transplant patients that receive prolonged and repeated treatments with antibiotics (Dahdouh et al., 2022). Nevertheless, in all three studies, the consumption of antibiotics was associated with intestinal RLs, where in adults the consumption of non-β-lactams and carbapenems were associated with high RLs for $bla_{OXA\text{-}48}$ (Lázaro-Perona et al., 2020), and additionally to $bla_{CTX\text{-}M\text{-}1\text{-}Family}$ and $bla_{OXA\text{-}1}$ for pediatric liver transplanted patients (Dahdouh et al., 2022). In contrast, this current study showed that the consumption of β-lactams and glycopeptides is associated with a lower incidence of detecting $bla_{CTX\text{-}M\text{-}1\text{-}Family}$ and $bla_{OXA\text{-}1}$, and the consumption of aminoglycosides and TMX with a lower incidence of detecting $bla_{OXA\text{-}48}$ in the critically ill pediatric patient population. The main reason for this difference between these studies is likely due to the highly heterogeneous nature of the patient population of this current study where different developmental stages, underlying conditions, co-morbidities, and treatments received with their specific pharmacokinetic/pharmacodynamic properties can make it difficult to obtain clear conclusions (Sadgrove and Jones, 2019; Ramirez et al., 2020; Shah et al., 2021). It might also be related to the short hospital stays for a significant number of included patients were the MDROs might not have had the chance to colonize their intestines. Nevertheless, this can have important implications for choosing the right antibiotics that can help in clearing an infection, as well as decrease the intestinal RL of MDROs. Further studies will be required to determine which antibiotics can achieve this optimum equilibrium between curing the patients and lowering the extent, or even eliminating, intestinal colonization by MDROs.

Despite the different effects that were observed in relation to antibiotic consumption, all three studies performed at our lab (including this one), and studies performed by other groups (Sun et al., 2021; Migliorini et al., 2022; Pérez-Nadales et al., 2022) demonstrated a relationship between high intestinal RLs and increased risk of extra-intestinal spread and subsequent infections by MDROs. Our study additionally shows intestinal dominance of the gut microbiome by a few organisms among the samples that were positive for antibiotic resistance genes in 26 out of 29 samples. Nevertheless, our method missed intestinal dominance in 5 samples that were negative for all the tested genes (Figure 5), most likely due to them harboring antibiotic resistance genes or mechanisms that were not tested for. This highlights another limitation of this current study and the need to develop more inclusive assays in case this approach is to be adapted to the routine practice. However, through further development and fine-tuning, our approach can prove to be valuable in being able to predict the effect of different treatments on intestinal dominance, make it possible to track this dominance over time, and take preventive measures that can stop

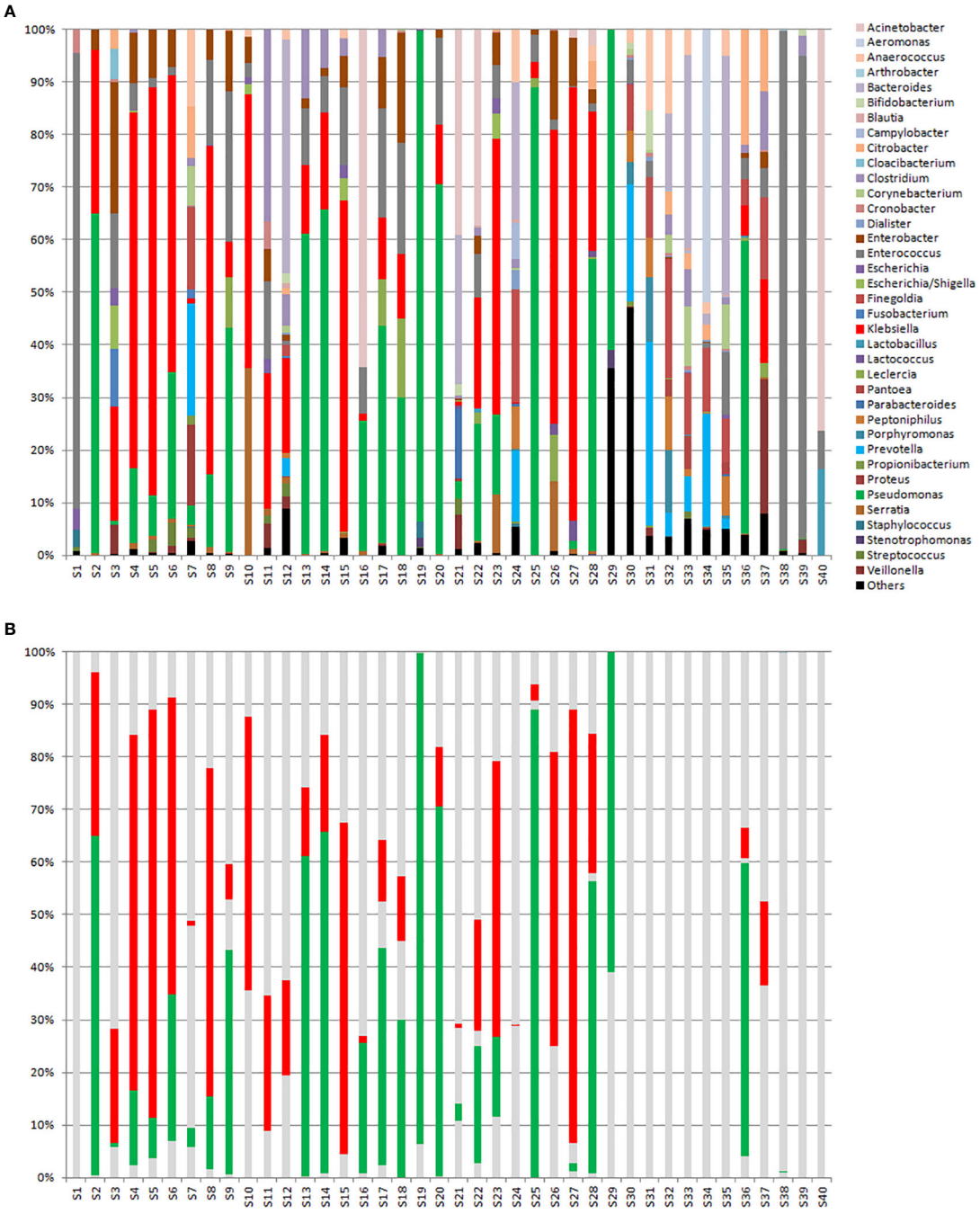

FIGURE 5
(A) *16sDNA* sequencing results for samples S1 to S29 that were ordered according to decreasing relative intestinal loads to one or several of the genes tested for, and samples S30 to S40 that were negative to all genes tested for. **(B)** The same samples shown in Part A but where only *Klebsiella* spp. (in red) and *Pseudomonas* spp. (in green) are highlighted.

the extra-intestinal dissemination of MDROs, especially since they are capable of causing infections. This is also interesting since, through this approach, very small RLs of MDROs (that are otherwise missed) can be detected and frequent sampling can trace a rise in RLs, allowing for clinical interventions before these organisms dominate the intestinal microbiome. Moreover, this approach can be combined with the local epidemiology at any hospital, making it adaptable and expandable for its applications where it can be directed towards the most common local genes of antibiotic resistance, opportunistic pathogens, and even dominant clones. Further studies will be directed at determining the clinical impact of this approach, especially in light of the patients' clinical progression over time and in light of all the other clinical factors.

Taken together, our data suggests that using qPCR for the determination of the intestinal loads of resistance genes is more accurate than relying on routine cultures in critically ill pediatric patients. It also shows a link between lower frequencies of $bla_{\text{CTX-M-1-Family}}$ and $bla_{\text{OXA-1}}$ and the consumption of non-β-lactams and

carbapenems, and lower frequencies of $bla_{\text{OXA-48}}$ and the consumption of TMX and aminoglycosides. Finally, we showed a link between intestinal dominance determined by our assay, and extra-intestinal spread of MDROs, making this tool a valuable one that can be used to track the extent of colonization in critically ill pediatric patients.

Data availability statement

All the data generated or analyzed during this study are included in this article and its supplementary material files. The obtained sequences were deposited in Genbank under the Bioproject with the accession number PRJNA911601. Further enquiries can be directed to the corresponding author.

Ethics statement

The studies involving human participants were reviewed and approved by Comite Etico de Investigacion Clinica del Hospital Universitario La Paz (PI-3428). Written informed consent from the participants' legal guardian/next of kin was not required to participate in this study in accordance with the national legislation and the institutional requirements.

Author contributions

ED performed the lab work described in this article and drafted the manuscript. FM-R, EC-B, CS, and LE-G tracked the patients involved in the outbreak, collected the clinical data, and participated in acquiring the samples. GR-C identified the rectal swabs included in the study and performed the bacterial cultures. FL-P performed part of the whole-genome sequencing and clonality analyses. MC-M performed data analyses and recovered part of the data from the hospital's information system database. MA-G performed part of the PCRs and clonality analyses. ED and JM designed the project. JM supervised the project. All authors contributed to the article and approved the submitted version.

Funding

This work has been possible thanks to funding allocated to ED from the European Union's Horizon 2020 research and innovation programme under the Marie Skłodowska-Curie Individual Fellowship grant agreement No. 796084 (qMAR). After qMAR termination, ED has been funded from the Agencia Estatal de Investigación of the Spanish Ministry of Science and Innovation in the form of a Juan de la Cierva – Incorporación grant number IJC2019-038832-I. Follow-up work has been allowed by support provided by Fondo de Investigaciones Sanitarias, Instituto de Salud Carlos III, grants PI16/01209 and PI19/01356 to JM. Co-financed by European Development Regional Fund "A way to achieve Europe". The funders had no role in study design, data collection and analysis, decision to publish, or preparation of the manuscript.

Conflict of interest

The authors declare that the research was conducted in the absence of any commercial or financial relationships that could be construed as a potential conflict of interest.

Publisher's note

Supplementary material

The Supplementary Material for this article can be found online at: https://www.frontiersin.org/articles/10.3389/fcimb.2023.1180714/full#supplementary-material

References

Dahdouh, E., Fernández-Tomé, L., Cendejas-Bueno, E., Ruiz-Carrascoso, G., Schüffelmann, C., Alós-Díez, M., et al. (2022). Intestinal dominance by multidrug-resistant bacteria in pediatric liver transplant patients. *Microbiol. Spectr.* 8, e0284222. doi: 10.1128/spectrum.02842-22

Dahdouh, E., Lázaro-Perona, F., Ruiz-Carrascoso, G., Sánchez García, L., Saenz de Pipaón, M., and Mingorance, J. (2021). Intestinal dominance by *Serratia marcescens* and *Serratia ureilytica* among neonates in the setting of an outbreak. *Microorganisms* 9 (11), 2271. doi: 10.3390/microorganisms9112271

Gaufin, T., Tobin, N. H., and Aldrovandi, G. M. (2018). The importance of the microbiome in pediatrics and pediatric infectious diseases. *Curr. Opin. Pediatr.* 30 (1), 117–124. doi: 10.1097/MOP.0000000000000576

Hsueh, P. R., Teng, L. J., Yang, P. C., Chen, Y. C., Ho, S. W., and Luh, K. T. (1998). Persistence of a multidrug-resistant *Pseudomonas aeruginosa* clone in an intensive care burn unit. *J. Clin. Microbiol.* 36, 1347–1351. doi: 10.1128/JCM.36.5.1347-1351.1998

Lázaro-Perona, F., Rodríguez-Tejedor, M., Ruiz-Carrascoso, G., Díaz-Pollán, B., Loeches, B., Ramos-Ramos, J. C., et al. (2020). Intestinal loads of OXA-48-producing *Klebsiella pneumoniae* in colonized patients determined from surveillance rectal swabs. *Clin. Microbiol. Infect* 27(8):1169.e7–1169.e12. doi: 10.1016/j.cmi.2020.09.054

Lerner, A., Adler, A., Abu-Hanna, J., Cohen Percia, S., Kazma Matalon, M., and Carmeli, Y. (2015). Spread of KPC-producing carbapenem-resistant Enterobacteriaceae: the importance of super-spreaders and rectal KPC concentration. *Clin. Microbiol. Infect.* 21 (5), 470.e1–470.e7. doi: 10.1016/j.cmi.2014.12.015

Livak, K. J., and Schmittgen, T. D. (2001). Analysis of relative gene expression data using real-time quantitative PCR and the 2(-delta delta C(T)) method. *Methods* 25 (4), 402–408. doi: 10.1006/meth.2001.1262

Livermore, D. M., Day, M., Cleary, P., Hopkins, K. L., Toleman, M. A., Wareham, D. W., et al. (2019). OXA-1 β-lactamase and non-susceptibility to penicillin/β-lactamase inhibitor combinations among ESBL-producing *Escherichia coli*. *J. Antimicrob. Chemother.* 74 (2), 326–333. doi: 10.1093/jac/dky453

Migliorini, L. B., Leaden, L., de Sales, R. O., Correa, N. P., Marins, M. M., Koga, P. C. M., et al. (2022). The gastrointestinal load of carbapenem-resistant enterobacteriacea is associated with the transition from colonization to infection by *Klebsiella pneumoniae* isolates harboring the bla_{KPC} gene. *Front. Cell Infect. Microbiol.* 12. doi: 10.3389/fcimb.2022.928578

Pérez-Blanco, V., Redondo-Bravo, L., Ruíz-Carrascoso, G., Paño-Pardo, J. R., Gómez-Gil, R., Robustillo-Rodela, A., et al. (2018). Epidemiology and control measures of an OXA-48-producing *Enterobacteriaceae* hospital-wide oligoclonal outbreak. *Epidemiol. Infect.* 146 (5), 656–662. doi: 10.1017/S0950268818000249

Pérez-Nadales, E., Natera, A. M., Recio-Rufián, M., Guzmán-Puche, J., Cano, Á., Frutos-Adame, A., et al. (2022). Proof-of-concept study to quantify changes in intestinal loads of KPC-producing Klebsiella pneumoniae in colonized patients following selective digestive decontamination with oral gentamicin. *J Glob Antimicrob Resist* S2213-7165 (22):16–22. doi: 10.1016/j.jgar.2022.04.010

Ramirez, J., Guarner, F., Bustos Fernandez, L., Maruy, A., Sdepanian, V. L., and Cohen, H. (2020). Antibiotics as major disruptors of gut microbiota. *Front. Cell Infect. Microbiol.* 10. doi: 10.3389/fcimb.2020.572912

Sadgrove, N. J., and Jones, G. L. (2019). From Petri dish to patient: bioavailability estimation and mechanism of action for antimicrobial and immunomodulatory natural products. *Front. Microbiol.* 10. doi: 10.3389/fmicb.2019.02470

Shah, T., Baloch, Z., Shah, Z., Cui, X., and Xia, X. (2021). The intestinal microbiota: impacts of antibiotics therapy, colonization resistance, and diseases. *Int. J. Mol. Sci.* 22 (12), 6597. doi: 10.3390/ijms22126597

Sim, C. K., Kashaf, S. S., Stacy, A., Proctor, D. M., Almeida, A., Bouladoux, N., et al. (2022). A mouse model of occult intestinal colonization demonstrating antibiotic-induced outgrowth of carbapenem-resistant *Enterobacteriaceae*. *Microbiome* 10 (1), 43. doi: 10.1186/s40168-021-01207-6

Sun, Y., Patel, A., SantaLucia, J., Roberts, E., Zhao, L., Kaye, K., et al. (2021). Measurement of *Klebsiella* intestinal colonization density to assess infection risk. *mSphere* 6 (3), e0050021. doi: 10.1128/mSphere.00500-21

Weinstein, R. A. (2012). Intensive care unit environments and the fecal patina: a simple problem? *Crit. Care Med.* 40 (4), 1333–1334. doi: 10.1097/CCM.0b013e318241012f

Willmann, M., Vehreschild, M. J. G. T., Biehl, L. M., Vogel, W., Dörfel, D., Hamprecht, A., et al. (2019). Distinct impact of antibiotics on the gut microbiome and resistome: a longitudinal multicenter cohort study. *BMC Biol.* 17 (1), 76. doi: 10.1186/s12915-019-0692-y

Young, V. B. (2017). The role of the microbiome in human health and disease: an introduction for clinicians. *BMJ* 356, j831. doi: 10.1136/bmj.j831

frontiers | Frontiers in Cellular and Infection Microbiology

TYPE Original Research
PUBLISHED 01 August 2023
DOI 10.3389/fcimb.2023.1229473

OPEN ACCESS

EDITED BY
Luis Esau Lopez Jacome,
Instituto Nacional de Rehabilitación,
Mexico

REVIEWED BY
Julio Guerrero Castro,
Umeå University, Sweden
Benjamin Vega-Baray,
National Autonomous University of Mexico,
Mexico

*CORRESPONDENCE
Mai M. Zafer
maizafer@acu.edu.eg

†These authors have contributed equally to this work

RECEIVED 26 May 2023
ACCEPTED 10 July 2023
PUBLISHED 01 August 2023

CITATION
Zafer MM, Hussein AFA, Al-Agamy MH, Radwan HH and Hamed SM (2023) Retained colistin susceptibility in clinical *Acinetobacter baumannii* isolates with multiple mutations in *pmrCAB* and *lpxACD* operons. *Front. Cell. Infect. Microbiol.* 13:1229473. doi: 10.3389/fcimb.2023.1229473

Retained colistin susceptibility in clinical *Acinetobacter baumannii* isolates with multiple mutations in *pmrCAB* and *lpxACD* operons

Mai M. Zafer[1*†], Amira F. A. Hussein[2,3], Mohamed H. Al-Agamy[4,5], Hesham H. Radwan[4] and Samira M. Hamed[6†]

[1]Department of Microbiology and Immunology, Faculty of Pharmacy, Ahram Canadian University, Cairo, Egypt, [2]Clinical and Chemical Pathology Department, Faculty of Medicine, Cairo University, Cairo, Egypt, [3]Faculty of Applied Health Science, Galala University, Cairo, Egypt, [4]Department of Pharmaceutics, College of Pharmacy, King Saud University, Riyadh, Saudi Arabia, [5]Department of Microbiology and Immunology, Faculty of Pharmacy, Al-Azhar University, Cairo, Egypt, [6]Department of Microbiology and Immunology, Faculty of Pharmacy, October University for Modern Sciences and Arts (MSA), 6th of October, Giza, Egypt

The progressive increase in the resistance rates to first- and second-line antibiotics has forced the reuse of colistin as last-line treatment for *Acinetobacter baumannii* infections, but the emergence of colistin-resistant strains is not uncommon. This has been long linked to acquired chromosomal mutations in the operons *pmrCAB* and *lpxACD*. Hence, such mutations are routinely screened in colistin-resistant strains by most studies. The current study was designed to explore the possible existence of *pmrCAB* and *lpxACD* mutations in colistin-susceptible isolates. For this purpose, the whole genome sequences of eighteen multi-/extensively drug resistant *A. baumannii* were generated by Illumina sequencing and screened for missense mutations of the operons *pmrCAB* and *lpxACD*. Most of the isolates belonged to global clones (GCs) including GC1 (n=2), GC2 (n=7), GC7 (n=2), GC9 (n=3), and GC11 (n=1). The minimum inhibitory concentrations (MICs) of colistin were determined by the broth microdilution assay. Seventeen isolates were fully susceptible to colistin with MICs ranging from (≤0.125 to 0.5 µg/ml). Interestingly, all colistin-susceptible isolates carried missense mutations in *pmrCAB* and *lpxACD* operons with reference to *A. baumannii* ATCC 19606. Overall, 34 mutations were found. Most substitutions were detected in *pmrC* (n=20) while no mutations were found in *pmrA* or *lpxA*. Notably, the mutation pattern of the two operons was almost conserved among the isolates that belonged to the same sequence type (ST) or GC. This was also confirmed by expanding the analysis to include *A. baumannii* genomes deposited in public databases. Here, we demonstrated the possible existence of missense mutations in *pmrCAB* and *lpxACD* operons in colistin-susceptible isolates, shedding light on the importance of interpreting mutations with reference to colistin-susceptible isolates of the same ST/GC to avoid the misleading impact of the ST/GC-related polymorphism. In turn, this may lead to misinterpretation of mutations and, hence, overlooking the real players in colistin resistance that are yet to be identified.

KEYWORDS

healthcare-associated infections, *Acinetobacter baumannii*, extensive drug resistance, colistin resistance, whole-genome sequencing, *pmrCAB*, *lpxACD*, mutation

1 Introduction

The continual occurrence of mutations in non-susceptible pathogenic strains and the associated determinants of antimicrobial resistance within hospitals, countries, and across the world are currently the greatest threats to international Public Health (Shelenkov et al., 2021). The wide use of antibiotics in immunocompromised patients at intensive care units and the absence of antibiotic stewardship programs in hospital settings have led to the occurrence of pathogens that are multiple drug-resistant (MDR) and the rise of extensively drug-resistant (XDR) strains. Therefore, clinicians were forced to depend on colistin as the last treatment option to combat these infections (Seleim et al., 2022). *A. baumannii*, a particularly problematic pathogen poses a significant threat to public health, by causing severe and invasive infections that are associated with high mortality rates in immunocompromised individuals and patients receiving intensive care. MDR and/or XDR *A. baumannii* have been reported to cause a significant degree of infections in Egypt during recent years (Ghaith et al., 2017; Al-Hassan et al., 2019). However, the direness of the situation is often masked in Egypt and other developing countries because of the lack of surveillance systems that can be attributed to restricted financial resources. Epidemiological surveillance is one significant tactic to assess and combat the burden exerted by problematic MDR pathogens in hospital settings. Overcoming antibiotic resistance is a critical challenge in the treatment of *Acinetobacter* infections (Wong et al., 2017), especially in view of the rise in carbapenem resistance among this species. Carbapenem resistance is generally associated with MDR and XDR phenotypes, which have been frequently demonstrated in *Acinetobacter* (Infectious Diseases Society Of, A 2012). Due to this problematic carbapenem-resistant *A. baumannii* (CRAB) clinical isolates, numerous Egyptian hospitals have reintroduced polymyxin use for therapy. Polymyxins E or colistin, the last therapeutic option for MDR Gram-negative pathogen infections, is widely used for the treatment of CRAB infections (Chamoun et al., 2021). Mechanistically, the interaction between the cationic non-ribosomal lipopeptides of colistin, and the lipid A component of lipopolysaccharide (LPS) in the outer membrane of the cell envelope destabilizes the latter. This subsequently allows the uptake of polymyxins into the periplasm and increases permeability by disrupting both outer and inner membrane integrity (Moffatt et al., 2019). Acquired colistin resistance develops primarily via drug target alteration. Substitutions or mobile genetic element insertion or deletion in the genes involved in the biosynthesis of lipid A, may result in structural or functional modifications in the lipid A moiety (Chamoun et al., 2021). Two key mechanisms for chromosomally mediated colistin resistance have been identified. The first involves LPS lipid A phosphoester group modifications, subsequent to *pmrCAB* operon mutations, which alter the affinity of lipid A to polymyxins by reducing its net negative charge. The operon *pmrCAB* comprises the *pmrC* gene that encodes a phosphoEthanolamine (pEtN) transferase, in addition to *pmrA* and *pmrB*, which encode the two component system (TCS), *PmrA/PmrB*. Overexpression of *pmrC* is induced by mutations in TCS (mainly *pmrA*) leading to colistin resistance via pEtN-mediated modification of lipid A [8,9]. Discrete genetic events are required for an adequate colistin resistance level in *A. baumannii*, which are up-regulation of *pmrAB*, *pmrB* point mutations, which leads to *pmrC* overexpression, and further addition of pEtN to lipid A (Beceiro et al., 2011). The second mechanism essentially involves termination of lipid A production due to various nucleotide substitutions, deletions, and insertions in one of its biosynthesis genes (*lpxA*, *lpxC*, and *lpxD*) that leads to frameshift mutations or produce truncated proteins that damage lipid A biosynthesis (Olaitan et al., 2014; Moffatt et al., 2019). In colistin-resistant isolates, there are non-synonymous mutations in the *lpxC* (P30L or S, N287D) and *lpxD* (E117K) genes that were previously reported from different origins (Oikonomou et al., 2015). Both colistin-susceptible and colistin-resistant isolates were found to carry the amino acid substitutions N287D (*lpxC*) and E117K (*lpxD*). It was also reported the possibility of these alterations in amino acids together with a mutation in the *pmrCAB* operon could result in synergistic effect that causes colistin resistance (Nurtop et al., 2019; Jovcic et al., 2021; Usjak et al., 2022). Several studies have focused on investigating the determinants of antibiotic resistance in colistin-resistant *A. baumannii* isolates. In this study, we investigated *pmrCAB* and *lpxACD* mutations in *A. baumannii* strains with retained susceptibility to colistin. Additionally, we made a comparative analysis of mutation patterns in colistin-susceptible isolates from distinct sequence types (STs).

2 Materials and methods

2.1 Bacterial strains

A total of 18 clinical isolates of *A. baumannii* were collected from the chemical and clinical pathology department at the Kasr Al-Ainy Hospital, Cairo University, Egypt, in the period from July to October 2020. All the isolates were obtained from patients at intensive care unit (ICU) and neonatal intensive care unit (NICU). The isolates were collected from blood, wound and sputum of adults and neonates. These were cultured on MacConkey agar medium (Oxoid, Altrincham, Cheshire, UK). Isolates were identified using Gram staining and culture morphology and were further confirmed using the VITEK 2 compact system (bioMérieux, Marcy l'Etoile, France) and amplification of $bla_{\text{OXA-51-like}}$ genes using the Polymerase Chain Reaction (Turton et al., 2006).

Ethics approval and consent to participate: This work has been carried out in accordance with the relevant guidelines. The study was approved by the local ethical committee of the Department of Clinical and Chemical Pathology, Faculty of Medicine, Cairo University. All the collected isolates were recovered for routine investigations and no extra isolates were collected for the purpose of the study. Informed consent was not necessary as there was no direct contact with patients.

2.2 Antibiotic susceptibility testing

This test was performed on Mueller–Hinton agar (Oxoid, Altrincham, Cheshire, UK) using the standard disk diffusion method as per the Clinical and Laboratory Standards Institute

guidelines (CLSI, 2020). A panel of 12 antibiotic disks, namely amikacin, cefepime, cefotaxime, cefoxitin, ceftriaxone, imipenem, levofloxacin, meropenem, piperacillin/tazobactam, tigecycline, and trimethoprim/sulfamethoxazole (Oxoid, Altrincham, Cheshire, UK) were used for the susceptibility profiling of the isolates. Minimum inhibitory concentrations (MICs) for colistin susceptibility were determined via the broth microdilution test. The results of the antimicrobial susceptibility tests were interpreted according to CLSI (2020) for all tested antimicrobial agents except tigecycline and colistin for which the breakpoints of the European Committee on Antimicrobial Susceptibility Testing (EUCAST, 2023) were used. As there is no tigecycline susceptibility breakpoints for *Acinetobacter* spp., we used the breakpoints specified for the *Enterobacterales*. While the CLSI (2020) has abolished the classification of *Acinetobacter* spp. as colistin-susceptible retaining only the intermediate (MIC ≤ 2) and resistant (MIC ≥ 4) categories, *Acinetobacter* spp. isolates having colistin MIC ≤ 2 are still categorized as colistin-susceptible by the EUCAST (2023). *Pseudomonas aeruginosa* ATCC 27853 and *Escherichia coli* ATCC 25922 were used as quality control strains.

2.3 Whole-genome sequencing (WGS), multilocus sequence typing (MLST), and analysis of colistin resistance genes

Draft genomes of the isolates were previously generated by us (Hamed et al., 2022) via Illumina MiSeq sequencing (Illumina Inc., San Diego, CA, USA). Extraction of DNA and library preparation were performed as previously described (Hamed et al., 2022). Illumina reads were assessed for quality using FastQC (Andrews, 2010) and low-quality reads were trimmed using Trimmomatic v0.32 (Bolger et al., 2014). SPAdes 3.14.1 was used for the de novo assembly of the trimmed reads (Bankevich et al., 2012). QUAST v5.0.2 (Gurevich et al., 2013) was used for generating the assembly metrics. Annotation of the draft genomes was achieved using the NCBI Prokaryotic Genome Annotation Pipeline (Tatusova et al., 2016). For plasmid assembly, we used PlasmidSPAdes (Antipov et al., 2016) and visualized the assembly graphs on bandage (Wick et al., 2015). The isolates were additionally analyzed for multilocus sequence types (MLST) using PubMLST server (https://pubmlst.org/abaumannii/). The phylogenetic relationships among each other, and with other international strains was analyzed using, CSI phylogeny 1.4 online tool (https://cge.cbs.dtu.dk/services/CSIPhylogeny/). Clonal complexes (CC) and global clones (GCs) were inferred via goeBURST analysis using the Phyloviz software version 2.0 (Ribeiro-Goncalves et al., 2016).

Our previous study focused on colistin resistance mechanisms in a colistin-resistant isolate, M19. In contrast, herein, we analyzed genes previously linked to colistin resistance in the colistin-susceptible isolates. The annotated files were visualized using the SnapGene v5.1.3.1, available at http://www.snapgene.com. Mutations were determined by pairwise alignment against the respective *A. baumannii* ATCC 19606 gene sequences using the Basic Local Alignment Search Tool (BLAST) available at https://blast.ncbi.nlm.nih.gov/Blast.cgi. Other colistin resistance genes were screened by the Comprehensive Antibiotic Resistance Database (CARD) server (https://card.mcmaster.ca/analyze/rgi) (Alcock et al., 2020).

2.4 Comparative analysis of *pmrCAB* and *lpxACD* operons in other *A. baumannii* genomes deposited in the BV-BRC database

To confirm that the mutation pattern found in our colistin-susceptible isolates is partly due to ST-related polymorphism, we compared the *pmrCAB* and *lpxACD* operons carried by our strains to strains sequenced in other studies. For this purpose, the public genome sequences of *A. baumannii* strains having the same STs and the closest genome sequences to our isolates were obtained from the Bacterial and Viral Bioinformatics Resource Center (BV-BRC), available at: https://www.bv-brc.org/, using the similar genome finder tool. Using the same platform, we extracted the predicted amino acid sequences of *pmrCAB* and *lpxACD* protein products. Multiple sequence alignments were done using Clustal Omega version 1.2.4 (https://www.ebi.ac.uk/Tools/msa/clustalo/) and visualized using MView version 1.63, available at: https://www.ebi.ac.uk/Tools/msa/mview/.

2.5 Zeta potential measurements

The zeta potential (ZP) of bacterial suspensions containing 1×10^9 CFU/mL was measured after 10-fold dilution. The zeta cells were filled with bacterial cell suspensions, and the electrophoretic mobility (EPM) of the cells was recorded at 150 V and 25°C using a ZP analyzer (Malvern Zeta sizer Nano ZS, Malvern, Worcestershire, UK). To ensure reproducibility of measurements, a minimum of three runs per sample were conducted as described before (Soon et al., 2011).

2.6 Statistical analysis

Statistical analysis of the ZP values was performed with GraphPad Prism 8 software (GraphPad Software, San Diego, CA, USA). Comparison of the ZP of the isolates within each GC was done by the Student's t-test and one-way analysis of variance (ANOVA), where appropriate. Pairwise comparisons were done using Tukey's multiple comparisons test. P values less than 0.05 were considered statistically significant.

3 Results

A total of 18 cultures that grew MDR/XDR *A. baumannii* were included in the study. Most patients were female and varied between neonates and older females. All the isolates were collected from ICU and NICU patients, and most cultures were obtained from patients with the greatest proportion of samples

recovered from blood and wounds. Amplification of the $bla_{\text{OXA-51-like}}$ gene confirmed that the collected isolates were *A. baumannii*. Most of the isolates belonged to GCs as shown in Figure 1.

3.1 Antimicrobial resistance profiles

All the isolates analyzed demonstrated high rates of resistance toward the tested antibiotics, with the exception of polymyxin and tigecycline, to which they were highly susceptible. Further, all isolates were CRAB (imipenem- and meropenem-resistant) and a total of five isolates were found to be amikacin-susceptible. Colistin susceptibility was tested by the broth microdilution method, and the MIC values obtained are shown in Figure 1. All the isolates were colistin-susceptible, except for M19, with an MIC ≥128 µg/ml (Figure 1).

3.2 Sequence analysis of genes related to colistin resistance

The assembled data of the WGS analysis of the isolates revealed the absence of mobile plasmid-mediated colistin resistance genes (*mcr1-10*). Several non-synonymous mutations were found in *pmrB*, *pmrC*, *lpx*C, and *lpx*D in the 18 isolates irrespective of their susceptibility to colistin (Figure 2).

3.2.1 Amino acid substitutions in PmrCAB

While no mutations were found in *pmrA* among the 18 isolates, at least 20 amino acid substitutions were detected in PmrC. These included L2M, A28S, Q37T, V58l, T76N, V100l, V118F, l131V, V151A, F166L, L218F, R230Q, Q232H, N300D, l342T, A370S, V486l, H499R, K514N, and K531T (Figure 2). These amino acid substitutions were observed in colistin-susceptible isolates and were associated with colistin MICs that ranged from ≤0.125 µg/ml to 0.5 µg/ml. M19, the only colistin-resistant isolate with an MIC ≥128 µg/ml, harbored three mutations in *pmrC*. Of these two mutations (N300D and A370S) were also found in the colistin-susceptible strain M10 that is phylogenetically related to M19, while the third mutation (V486I) could not be determined. Notably, N300D was shared by all isolates. At least six mutations were ST/GC-specific. These included V58I that was shared by all GC2 isolates, Q232H that was carried by the two isolates that belonged to ST113$^{\text{Pas}}$/GC7. In addition, I342T, H499R, V461I, and K531T were specific for the Pasteur STs ST85, ST19, ST164, and GC2, respectively. The mutation I131V was shared between the isolates that belonged to the STs ST113 $^{\text{Pas}}$, ST85$^{\text{Pas}}$, and ST19$^{\text{Pas}}$, while A370S was shared between ST164$^{\text{Pas}}$ isolates and GC2 isolates.

Eight missense mutations, namely H89L, Q110K, A138T, G143C, F146C, P360Q, N440H, and A444V were detected in *pmrB*. Of these, H89L was detected only in M19, while N440H was found in all isolates. Two mutations were ST/GC-specific. These included P360Q that is specific for ST19$^{\text{Pas}}$/GC1 isolates and A444V specific for GC2 isolates.

3.2.2 Amino acid substitutions in LpxCD

Only one missense mutation was found in the gene *lpxC* and was predicted to be associated with the amino acid alteration N287D. The mutation was detected in all isolates except M09 in which the complete sequence of the gene could not be determined. Further, five amino acid substitutions in *lpxD*, namely A12V, E18G, V63I, E117K, and G166S were detected. No unique mutations were found in the colistin-resistant isolate M19 compared to the colistin-susceptible isolates.

The mutation E117K was specific for GC2 isolates, while G166S was found in the two isolates that belonged to ST113$^{\text{Pas}}$. The mutation V63I was shared between two Pasteur STs namely ST113 and ST164. Correlations between ST and colistin MIC in the context of the detected mutations in the isolates analyzed are illustrated in Figure 1.

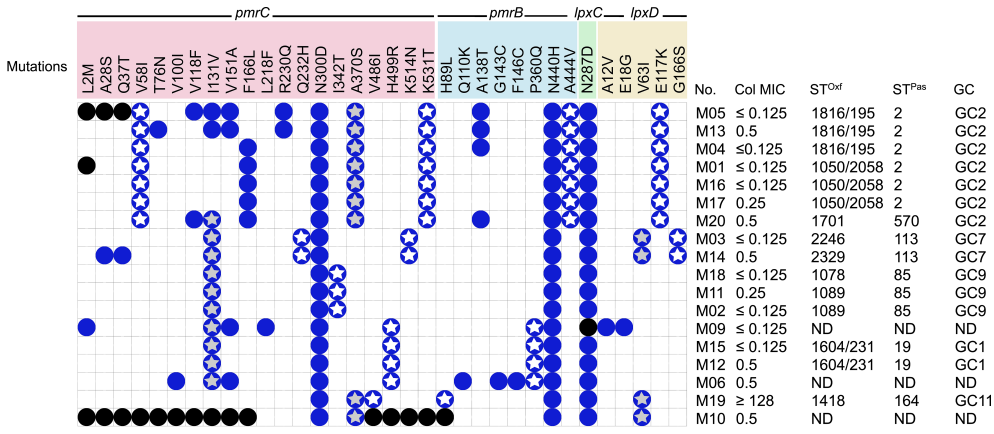

FIGURE 1
Distribution of *pmrCAB* and *lpxACD* mutations in the tested isolates and correlation to STs/GCs and colistin MIC. No missense mutations were identified in *pmrA* or *lpxA* in any of the tested isolates. Blue circles denote the presence of mutations; black circles means that the mutation could not be determined due to incomplete gene sequence; white stars denote ST-specific mutations; grey stars denote mutations shared between more than one ST; GC, global clone; MIC, minimum inhibitory concentration in µg/ml; ST$^{\text{Pas}}$, sequence type according to Pasteur scheme; ST$^{\text{Oxf}}$, sequence type according to Oxford scheme.

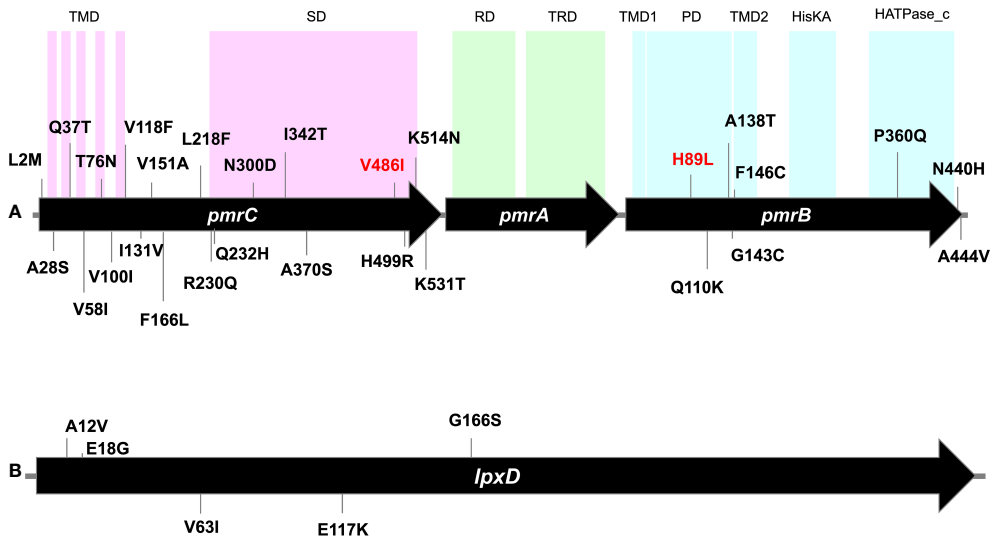

FIGURE 2
Gene maps showing point mutations identified in *pmrCAB* operon **(A)** and *lpxD* gene **(B)** carried by the tested isolates. Numbers denote codons affected by mutations. Mutations written in red are the unique mutations detected in the colistin-resistant isolate M19 but could not be determined in its phylogenetically related isolate M10. Mutations of *lpxC* were not shown as only one mutation (N278D) was carried by all isolates. TMD, transmembrane domain; SD, Sulfate domain; RD, receiver domain; TRD, transcriptional regulatory domain; PD, periplasmic domain; HisKA, histidine kinase A domain; HATPase_c, histidine kinase-like ATPase. Domain locations were adapted from Gerson et al. (2020) and Ko et al. (2017).

3.2.3 Other colistin resistance determinants

Genes encoding EptA (ethanolamine phosphotransferase), a homolog of PmrC, were identified in 10 of the 18 isolates. These were most commonly carried by the GC2 isolates (M01, M04, M05, M13, M16, M17, and M20), and less frequently in the GC9 isolates (M02 and M11). Only a single GC1 isolate (M12) harbored an EptA-coding gene. The EptA-coding genes carried by M01, M12, M13, M05, and M20 demonstrated similarity to *eptA-2* (GenBank accession: KC700023). Notably, none of the EptA-coding genes were preceded by an IS*Aba1* element that is known to drive *eptA* overexpression, which provides a PmrAB-independent mechanism for colistin resistance. The isolates M02 and M11 carried the EptA-coding genes on a 116,047 bp plasmid that showed 99.96% similarity to a plasmid carried by *A. baumannii*, ACN21 (GenBank accession: CP038645.1) (Figure 3). The genetic environment of EptA-coding genes in other strains could not be identified.

Further, an examination of IS*Aba*125 insertion into the H-NS family transcriptional regulator-coding gene, previously linked to high-level colistin resistance (Deveson Lucas et al., 2018) revealed its absence in the colistin-resistant (M19) as well as the colistin-susceptible isolates.

3.3 Comparison of *pmrCAB* and *lpxACD* sequences to closely-related global strains

In order to confirm the association between *pmrCAB* and *lpxACD* mutations and the STs/GCs rather than the phenotypic resistance to colistin, we made a large-scale mutation analysis on more isolates retrieved from the BV-BRC database. The operon sequences of our isolates were compared to global strains with the same STs. The multiple sequence alignments of the predicted amino acid sequences of PmrC, PmrB, LpxC, and LpxD are shown in Supplementary Figures 1-19. Our analysis confirmed the ST/GC specificity of all mutations described in our isolates carrying the same ST/GC. Some rare exceptions in which the wildtype genes were retained were also evident.

This expanded analysis also showed that the *pmrC* mutation V486I that was uniquely found in the colistin-resistant isolate M19 and could not be determined in the phylogenetically-related isolate M10 (Figure 2) was likely a ST-related polymorphism. This was evidenced by the existence of this mutation in all strains that belonged to the same ST. In contrast, the *pmrB* mutation H89L was only detected in M19 and three other foreign strains included in our analysis (151, 198, and GML-KP48-AB-TR). Unfortunately, the colistin susceptibility of the three strains was not available. Hence, further analysis is required to investigate the exact role of this mutation in colistin resistance.

Furthermore, we searched the metadata of the global strains included in the current study for colistin susceptibility. While the susceptibility profiles were not available for the majority of the strains, colistin susceptibility was reported for 33 strains. Only two strains namely, MS14413 (ST^{Pas} 2) and Ab-NDM-1 (ST^{Pas} 85), were reported to be colistin-resistant. In addition to the ST/GC-related polymorphism reported in the current study, MS14413 carried a unique mutation in *pmrB* that was associated by the amino acid alteration T232I. Similarly, only one unique mutation was found in Ab-NDM-1. This was found in *pmrB* gene and was associated by the amino acid alteration T187P.

3.4 Zeta potential alteration

A negative ZP was obtained for all tested isolates. The colistin-susceptible isolates revealed ZP values ranging from -20.8 ± 0.666 to

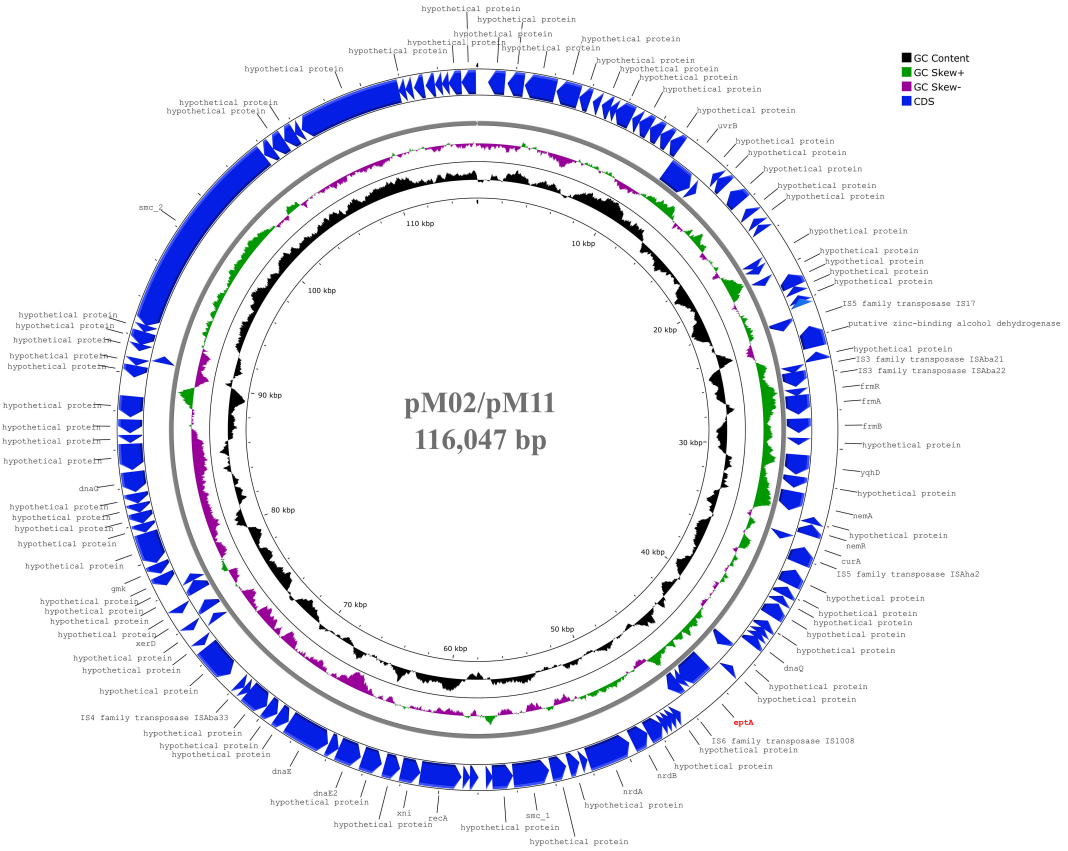

FIGURE 3
Circular map of 116,047 bp plasmid carried by M02 and M11 harbouring *eptA* gene. The plasmid showed highest similarity to another plasmid carried by *A. baumannii* strain ACN21 (GenBank: CP038645.1). The gene *eptA* was labelled in red and was not preceded by IS*Aba1* previously reported as essential for overexpression. The map was generated using the Proksee web server (https://proksee.ca/).

-8.70 ± 0.627 mV. The ZP value of colistin-resistant cells (M19) was considerably less negative than that of the colistin-susceptible strains (-5.11 ± 0.77), while its phylogenetically-related colistin-susceptible isolate M10 had a less negative ZP (-3.71 ± 0.676) than all other colistin-susceptible strains and the resistant isolate M19. The ZP values of *A. baumannii* cells of all strains are shown in Figure 4.

Student's *t*-test and One-way ANOVA were used for comparing the ZP values of all isolates within each GC/ST, while comparisons of the groups of isolates that belonged to different ST/GC were analyzed by one-way ANOVA. The difference between the ZP values of the isolates within each ST/GC was statistically significant (P-values <0.001). Additionally, a statistically significant difference was found between the ZP values of the isolates that belonged to different STs/GCs (P-value <0.0001) but pairwise comparisons showed that this significant difference exists only between GC11 isolates and others (P-values are shown in Supplementary Figure 20).

To investigate the relationship between the ZP and colistin resistance, pairwise comparisons were done between the ZP of individual isolates using the colistin-resistant strain M19 as a control. Significant difference was found between the ZP value of M19 and all other isolates except the phylogenetically-related colistin-susceptible isolate M10. P-values of the Tukey's multiple comparison test are shown in Supplementary Figure 21.

4 Discussion

Treatment failure in *A. baumannii* is very common due to lack of understating the exact mechanisms of resistance to antibiotics together with the absence of novel therapies. In recent years, the alarming increase in the rates of CRAB strains in Egyptian hospitals have forced the reuse of colistin for treating these pathogens. Colistin is the antibiotic of choice for treating CRAB infections in healthcare facilities, a significant challenge to infection control in nosocomial settings. Elucidating the exact mechanisms that mediate and control colistin resistance is thus crucial to preserve its efficacy. To explore the relationship between chromosomally-mediated mechanisms of colistin resistance and the colistin resistance phenotype, we investigated 18 clinical isolates of *A. baumannii* collected from ICU and NICU patients by WGS. All of the isolates were previously characterized for MLST according to Pasteur and Oxford scheme. Some isolates were assigned two Oxford STs due to carrying two copies of *gdhB* locus, as described before (Gaiarsa et al., 2019). Most of the isolates belonged to high-risk GCs

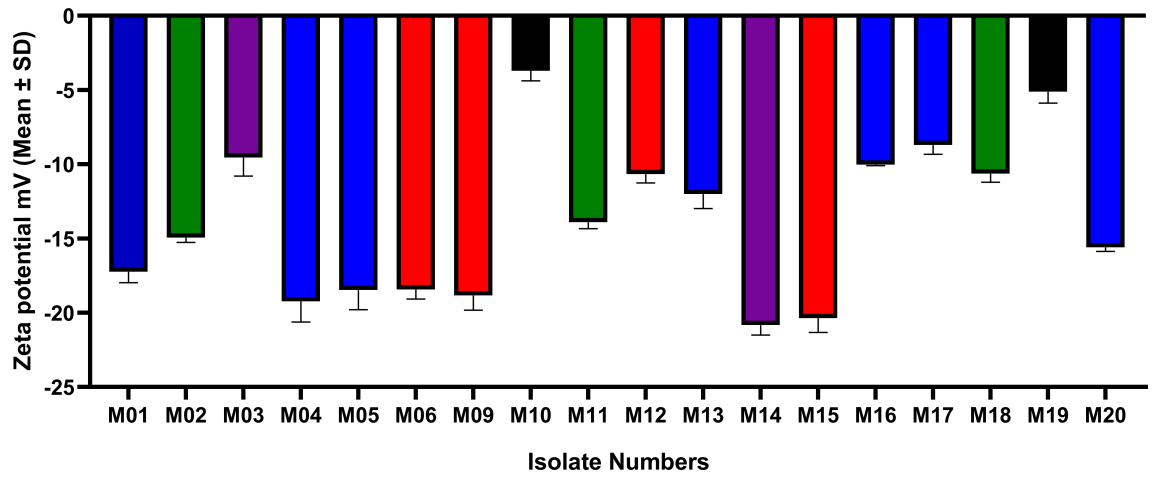

FIGURE 4
ZP values (mean±SD) of colistin-susceptible and resistant *A. baumannii* cells. Same colors refer to phylogenetically related isolates. M01, M04, M05, M13, M16, M17, and M20 all belong to GC2. M02, M11 and M18 has the same ST^{Pas}85 and belong to GC9. M03 and M14 have the same ST^{Pas}113 and belong to GC7. M06, M09, M12 and M15 belong to GC1. M10 is clonally related to M19 ST^{Pas}164 (GC11).

including GC1, GC2, GC7, GC9, and the most recently described clone, GC11 (Hansen et al., 2023).

Given the importance of studying resistance mechanisms in distinct strains, genetic investigation was carried out in colistin-susceptible strains. Detecting the MIC of colistin using the broth microdilution method is the only reliable method and remains the gold standard for assessing colistin resistance in *A. baumannii* approved by both the CLSI and by the EUCAST (CLSI, 2020; EUCAST, 2021). Of the 18 isolates analyzed, only a single strain, M19, demonstrated colistin resistance with an MIC ≥128 µg/ml. This percent of resistance was much lower than that was recently reported in Egypt in a study conducted on 17 A. *baumannii* isolates in which nine of them were colistin-resistant (Fam et al., 2020). It is noteworthy to mention that high rates of resistance toward different antibiotics were detected among our studied collection, and this could be attributed to the fact that high resistance patterns are usually observed in critically ill hospitalized patients due to existence of comorbidities and the overuse of antibiotics.

The plasmid-mediated colistin resistance determinants *mcr* genes were not detected in our studied isolates. This goes in line with most of studies conducted on colistin-resistant *A. baumannii* isolates. Moreover, the studies that reported the existence of *mcr* genes failed to sequence any *mcr* variants (Khoshnood et al., 2020; Snyman et al., 2020). Instead, *pmrAB* mutations appears to be the driving mechanism of colistin resistance in *A. baumannii* in most of published reports (Seleim et al., 2022). A total of 34 point mutations were identified in our strains (Figure 2) within the *pmrCAB* and *lpx*ACD operons. The association of colistin resistance in *A. baumannii* with mutations in the putative two-component regulatory system PmrAB was first reported in 2009 (Adams et al., 2009). Although previous studies have reported mutations in the response regulator-coding gene *pmrA* (Arroyo et al., 2011; Lesho et al., 2013), we observed none. Colistin resistance is primarily a consequence of mutations in the *pmrCAB* operon, especially in the *pmrB* region (Nurtop et al., 2019), and we observed the highest number of mutations in the *pmrC* region. Sequence analysis revealed eight amino acid substitutions in PmrB and 20 amino acid substitutions in PmrC, all of which were detected in colistin-susceptible isolates, except for the single colistin-resistant strain, M19. Thus, it may be inferred that not all amino acid substitutions result in elevated colistin MICs. Seleim et al. (2022) reported that the *pmrC* expression level could not differentiate between colistin-resistant and colistin-susceptible isolates, and they observed that the correlation between *pmrC* expression levels and colistin MICs was not significant (Seleim et al., 2022). Additionally, this was also reported by Gerson et al. (2020). Thus, it is therefore concluded that colistin resistance mechanisms in *A. baumannii* are much more complicated than believed. The resistant strain M19 harbored unique and distinct mutations in *pmrC* and *pmrB*, and none in *pmrA*. These included three substitutions in PmrC, including N300D, A370S, and V486I, and two substitutions, namely H89L and N440H in PmrB. Notably, V486I and H89L were only observed in this strain. The H89L substitution in PmrB (Nurtop et al., 2019) and the V486I substitution in PmrC (Srisakul et al., 2022) have been previously reported in colistin-resistant *A. baumannii* isolates. While found here in colistin-susceptible isolates that belonged to three STs, some *pmrC* mutations (I131V and H499R) and *pmrB* mutations (P360Q) were previously linked to resistance to colistin (Arroyo et al., 2011; Misic et al., 2018). In agreement with our findings, N440H and A444V mutations of *pmrB* were previously predicted not to affect colistin susceptibility (Thi Khanh Nhu et al., 2016). To completely understand lipid A modification and the resulting colistin-susceptible phenotype, the effects exerted by *pmrCAB* mutations on the expression of *pmrC* require further investigation.

A total of six diverse LpxCD amino acid substitutions in colistin-susceptible *A. baumannii* strains were evident. The colistin-resistant isolate M19 harbored the mutation N287D in *lpx*C that was also present in the colistin-susceptible isolates. A previous study reported that mutations in *lpx*D or *pmr*B alone may

suffice to induce colistin resistance, thus suggesting synergism between the effects of mutations within these genes in promoting the same (Nurtop et al., 2019). The diverse range of amino acid substitutions reported in this study, some of which have been previously described, suggest that the exact colistin resistance mechanisms in *A. baumannii* requires extensive investigation. Interestingly, conserved mutation patterns were mostly found in *A. baumannii* strains that belonged to the same ST/GC, particularly those inferred by the Pasteur scheme, regardless of their susceptibility to colistin. This was further confirmed by an expanded analysis in which more strains with the same STs as those identified here were included in the mutation analysis. Hence, we here emphasize the importance of carefully analyzing colistin resistance-related mutations with reference to a colistin-susceptible strain that belongs to the same ST as the one under investigation. Otherwise, the mechanisms underlying colistin resistance may be incorrectly inferred and the real contributors to colistin resistance may be overlooked. We found many studies that investigated *pmrCAB* and *lpxACD* mutations with reference to *A. baumannii* ATCC 19606 and ATCC 17978 that may lead to overestimation of mutation-related resistance and overlooking the real mechanism of resistance (Mavroidi et al., 2015; Haeili et al., 2018; Nurtop et al., 2019; Jovcic et al., 2021; Eze et al., 2022; Usjak et al., 2022; Kabic et al., 2023).

As the susceptibility profiles of the global strains included in our study were revised, only two strains with confirmed colistin resistance were identified (MS14413 and Ab-NDM-1). Interestingly, the only unique mutations identified in the two strains were found in *pmrB*, confirming the crucial role of this gene in driving colistin resistance. Notably, other mutations identified by the authors as a contributor to colistin resistance in Ab-NDM-1 were the *pmrC* mutations I115V, N284D, and I326T (Fernandez-Cuenca et al., 2020). These correspond to the mutations I131V, N300D, and I342T (according to the numbering of *A. baumannii* ATC 19606, GenBank CP059040) identified here as polymorphism. This further emphasizes the importance of the data presented here for the correct interpretation of *pmrCAB* and *lpxACD* mutations.

The bacterial surface charge has frequently been described in terms of ZP, which is the potential at the shear plane of the electrical double layer surrounding a cell in solution (Soon et al., 2011). Our results showed that the colistin-resistant cells display less negative ZP than the colistin-susceptible cells. The less negative ZP exhibited by the colistin-resistant isolate M19 in comparison to that of the colistin-susceptible cells has been previously explained to be a consequence of alterations in the structure and composition of the outer membrane (Soon et al., 2011). Colistin-resistant cells were previously reported to have more propensity for clumping in small clusters compared to colistin-susceptible cells (Soon et al., 2009). This was justified by the higher colloid aggregate stability within the particle carrying a lower magnitude of charge due to reduced electrostatic repulsion (Klodzinska et al., 2010). Lipid A phosphates esterification with 2-aminoethanol or 4-amino-4-deoxy-L-arabinose resulting in charge shielding has been reported before in colistin-resistant *E. coli* (Gatzeva-Topalova et al., 2005) and *Pseudomonas aeruginosa* (Gooderham and Hancock, 2009). Unexpectedly, M10, a colistin-susceptible isolate, exhibited the lowest negative ZP among all the isolates. Notably, this isolate is phylogenetically related to M19 (the colistin-resistant isolate) as described previously (Hamed et al., 2022), and thus the aberrant zeta potential may either be a consequence of cell membrane alterations or a reflection of ST-related polymorphism. Statistical analysis of the ZP values of all isolates revealed a significant difference between the ZP values of the isolates that belonged to the same ST/GC. This contradicts our hypothesis that the isolates that belong to the same ST/GC may have similar ZP values. More studies are recommended to better understand the relationship between STs and the ZP of *A. baumannii*.

The existence of the alternative pEtN transferase named ethanolamine phosphotransferase A-1 (EptA) in *A. baumannii* was previously demonstrated by Lesho et al. (2013). The authors described two PmrC homologs designated EptA-1 and EptA-2 that were localized outside the *pmrABC* operon. The same study has also reported the overexpression of *eptA*-1 and *eptA*-2 in the colistin-resistant isolates. Another study conducted on a pair of MDR *A. baumannii* by Deveson Lucas et al. (2018) indicated that overexpression of the "orphan" *eptA* in a pre-colistin-treatment *A. baumannii* strain resulted in increased colistin resistance (Deveson Lucas et al., 2018). This finding provides evidence for *eptA* encoding a functional pEtN transferase that mediates colistin resistance (Deveson Lucas et al., 2018). In our collection, EptA-coding genes were harbored by the GC2 isolates (M01, M04, M05, M13, M16, M17, and M20), two GC9 isolates (M02, M11) and a single GC1 isolate, M12. None of the *eptA* genes identified here was preceded by IS*Aba1* insertion. This confirms the assumption made by Potron et al. (2019) that overexpression of *eptA* genes, and subsequently colistin resistance is a consequence of an upstream insertion of an IS*Aba1* element (Potron et al., 2019).

The insertion of IS*Aba125* within a gene encoding an H-NS family transcriptional regulator was previously linked to *eptA* overexpression and colistin resistance (Deveson Lucas et al., 2018). This was not found in any of our isolates.

5 Conclusion

Our study reinforces the need for extensive investigations for the elucidation of the exact mechanisms that contribute to colistin resistance in *A. baumannii*, which consequently influences possible therapeutic options. Colistin resistance mechanisms in *A. baumannii* are complex and not easily understood. Multiple mutations in *pmrCAB* and *lpx*ACD are unlikely to result in increased colistin resistance. The evaluation of mutations with reference to colistin-susceptible isolates of the same ST/GC is essential to avoid misinterpretation of ST/GC-related polymorphisms. Evidence was provided by expanding our analysis to include *A. baumannii* strains with the same STs as our isolates retrieved from a public database. Further, large scale studies including more colistin-resistant and colistin-susceptible strains are recommended to better establish the relationship between the ZP and colistin resistance and to confirm, with statistical evidence, the ST-related polymorphism of *pmrCAB* and *lpx*ACD operons that may exist in both colistin-susceptible and colistin-resistant strains.

Data availability statement

The datasets presented in this study can be found in online repositories. The names of the repository/repositories and accession number(s) can be found in the article/Supplementary Material.

Author contributions

Conceptualization, MZ, AH, MA, HR, and SH. Methodology, MZ, AH, and SH. Software, SH. Writing—original draft preparation, MZ. Writing—review and editing, MZ, AH, MA, HR, and SH. Visualization, SH. Funding acquisition, MA. All authors have read and agreed to the published version of the manuscript.

Funding

This research was funded by the Deanship of Scientific Research at King Saud University, grant number RGP-038.

Acknowledgments

The authors would like to thank the chemical and clinical pathology department, Faculty of Medicine, Cairo University. The authors extend their appreciation to Prince Naif Health Research Center, Investigator support Unit for the language editing service provided.

Conflict of interest

The authors declare that the research was conducted in the absence of any commercial or financial relationships that could be construed as a potential conflict of interest.

Publisher's note

All claims expressed in this article are solely those of the authors and do not necessarily represent those of their affiliated organizations, or those of the publisher, the editors and the reviewers. Any product that may be evaluated in this article, or claim that may be made by its manufacturer, is not guaranteed or endorsed by the publisher.

Supplementary material

The Supplementary Material for this article can be found online at: https://www.frontiersin.org/articles/10.3389/fcimb.2023.1229473/full#supplementary-material

References

Adams, M. D., Nickel, G. C., Bajaksouzian, S., Lavender, H., Murthy, A. R., Jacobs, M. R., et al. (2009). Resistance to colistin in Acinetobacter baumannii associated with mutations in the PmrAB two-component system. *Antimicrob. Agents Chemother.* 53, 3628–3634. doi: 10.1128/AAC.00284-09

Alcock, B. P., Raphenya, A. R., Lau, T. T. Y., Tsang, K. K., Bouchard, M., Edalatmand, A., et al. (2020). CARD 2020: antibiotic resistome surveillance with the comprehensive antibiotic resistance database. *Nucleic Acids Res.* 48, D517–D525. doi: 10.1093/nar/gkz935

Al-Hassan, L., Zafer, M. M., and El-Mahallawy, H. (2019). Multiple sequence types responsible for healthcare-associated *Acinetobacter baumannii* dissemination in a single centre in Egypt. *BMC Infect. Dis.* 19, 829. doi: 10.1186/s12879-019-4433-1

Andrews, S. (2010)FastQC: a quality control tool for high throughput sequence data. Available at: http://www.bioinformatics.babraham.ac.uk/projects/fastqc.

Antipov, D., Hartwick, N., Shen, M., Raiko, M., Lapidus, A., and Pevzner, P. A. (2016). plasmidSPAdes: assembling plasmids from whole genome sequencing data. *Bioinformatics* 32, 3380–3387. doi: 10.1093/bioinformatics/btw493

Arroyo, L. A., Herrera, C. M., Fernandez, L., Hankins, J. V., Trent, M. S., and Hancock, R. E. (2011). The pmrCAB operon mediates polymyxin resistance in Acinetobacter baumannii ATCC 17978 and clinical isolates through phosphoethanolamine modification of lipid A. *Antimicrob. Agents Chemother.* 55, 3743–3751. doi: 10.1128/AAC.00256-11

Bankevich, A., Nurk, S., Antipov, D., Gurevich, A. A., Dvorkin, M., Kulikov, A. S., et al. (2012). SPAdes: a new genome assembly algorithm and its applications to single-cell sequencing. *J. Comput. Biol.* 19, 455–477. doi: 10.1089/cmb.2012.0021

Beceiro, A., Llobet, E., Aranda, J., Bengoechea, J. A., Doumith, M., Hornsey, M., et al. (2011). Phosphoethanolamine modification of lipid A in colistin-resistant variants of *Acinetobacter baumannii* mediated by the PmrAB two-component regulatory system. *Antimicrob. Agents Chemother.* 55, 3370–3379. doi: 10.1128/AAC.00079-11

Bolger, A. M., Lohse, M., and Usadel, B. (2014). Trimmomatic: a flexible trimmer for Illumina sequence data. *Bioinformatics* 30, 2114–2120. doi: 10.1093/bioinformatics/btu170

Chamoun, S., Welander, J., Martis-Thiele, M. M., Ntzouni, M., Claesson, C., Vikstrom, E., et al. (2021). Colistin dependence in extensively drug-resistant acinetobacter baumannii strain is associated with ISAjo2 and ISAba13 insertions and multiple cellular responses. *Int. J. Mol. Sci.* 22, 576. doi: 10.3390/ijms22020576

CLSI (2020). *Performance standards for antimicrobial susceptibility testing. 30th edition* (Wayne, PA: Clinical and Laboratory Standards Institute).

Deveson Lucas, D., Crane, B., Wright, A., Han, M. L., Moffatt, J., Bulach, D., et al. (2018). Emergence of high-level colistin resistance in an acinetobacter baumannii clinical isolate mediated by inactivation of the global regulator H-NS. *Antimicrob. Agents Chemother.* 62, e02442. doi: 10.1128/AAC.02442-17

EUCAST. (2021) *The European Committee on Antimicrobial Susceptibility Testing. Breakpoint tables for interpretation of MICs and zone diameters.* Available at: http://www.eucast.org.

EUCAST. (2023) *The European Committee on Antimicrobial Susceptibility Testing. Breakpoint tables for interpretation of MICs and zone diameters.* Available at: http://www.eucast.org.

Eze, E. C., Falgenhauer, L., and El Zowalaty, M. E. (2022). Draft genome sequences of extensively drug resistant and pandrug resistant *Acinetobacter baumannii* strains isolated from hospital wastewater in South Africa. *J. Glob Antimicrob. Resist.* 31, 286–291. doi: 10.1016/j.jgar.2022.08.024

Fam, N. S., Gamal, D., Mohamed, S. H., Wasfy, R. M., Soliman, M. S., El-Kholy, A. A., et al. (2020). Molecular characterization of carbapenem/colistin-resistant Acinetobacter baumannii clinical isolates from Egypt by whole-genome sequencing. *Infect. Drug Resist.* 13, 4487–4493. doi: 10.2147/IDR.S288865

Fernandez-Cuenca, F., Perez-Palacios, P., Galan-Sanchez, F., Lopez-Cerero, L., Lopez-Hernandez, I., Lopez Rojas, R., et al. (2020). First identification of bla(NDM-1) carbapenemase in bla(OXA-94)-producing *Acinetobacter baumannii* ST85 in Spain. *Enferm Infecc Microbiol. Clin. (Engl Ed)* 38, 11–15. doi: 10.1016/j.eimc.2019.03.008

Gaiarsa, S., Batisti Biffignandi, G., Esposito, E. P., Castelli, M., Jolley, K. A., Brisse, S., et al. (2019). Comparative analysis of the two *Acinetobacter baumannii* multilocus sequence typing (MLST) schemes. *Front. Microbiol.* 10. doi: 10.3389/fmicb.2019.00930

Gatzeva-Topalova, P. Z., May, A. P., and Sousa, M. C. (2005). Crystal structure and mechanism of the Escherichia coli ArnA (PmrI) transformylase domain. An enzyme for lipid A modification with 4-amino-4-deoxy-L-arabinose and polymyxin resistance. *Biochemistry* 44, 5328–5338. doi: 10.1021/bi047384g

Gerson, S., Lucassen, K., Wille, J., Nodari, C. S., Stefanik, D., Nowak, J., et al. (2020). Diversity of amino acid substitutions in PmrCAB associated with colistin resistance in clinical isolates of *Acinetobacter baumannii*. *Int. J. Antimicrob. Agents* 55, 105862. doi: 10.1016/j.ijantimicag.2019.105862

Ghaith, D. M., Zafer, M. M., Al-Agamy, M. H., Alyamani, E. J., Booq, R. Y., and Almoazzamy, O. (2017). The emergence of a novel sequence type of MDR *Acinetobacter baumannii* from the intensive care unit of an Egyptian tertiary care hospital. *Ann. Clin. Microbiol. Antimicrob.* 16, 34. doi: 10.1186/s12941-017-0208-y

Gooderham, W. J., and Hancock, R. E. (2009). Regulation of virulence and antibiotic resistance by two-component regulatory systems in Pseudomonas aeruginosa. *FEMS Microbiol. Rev.* 33, 279–294. doi: 10.1111/j.1574-6976.2008.00135.x

Gurevich, A., Saveliev, V., Vyahhi, N., and Tesler, G. (2013). QUAST: quality assessment tool for genome assemblies. *Bioinformatics* 29, 1072–1075. doi: 10.1093/bioinformatics/btt086

Haeili, M., Kafshdouz, M., and Feizabadi, M. M. (2018). Molecular mechanisms of colistin resistance among pandrug-resistant isolates of *Acinetobacter baumannii* with high case-fatality rate in intensive care unit patients. *Microb. Drug Resist.* 24, 1271–1276. doi: 10.1089/mdr.2017.0397

Hamed, S. M., Hussein, A. F. A., Al-Agamy, M. H., Radwan, H. H., and Zafer, M. M. (2022). Genetic configuration of genomic resistance islands in *Acinetobacter baumannii* clinical isolates from Egypt. *Front. Microbiol.* 13. doi: 10.3389/fmicb.2022.878912

Hansen, F., Porsbo, L. J., Frandsen, T. H., Kaygisiz, A. N. S., Roer, L., Henius, A. E., et al. (2023). Characterisation of carbapenemase-producing *Acinetobacter baumannii* isolates from danish patients 2014-2021: detection of a new international clone - IC11. *Int. J. Antimicrob. Agents* 62, 106866. doi: 10.1016/j.ijantimicag.2023.106866

Infectious Diseases Society Of, A (2012). White paper: recommendations on the conduct of superiority and organism-specific clinical trials of antibacterial agents for the treatment of infections caused by drug-resistant bacterial pathogens. *Clin. Infect. Dis.* 55, 1031–1046. doi: 10.1093/cid/cis688

Jovcic, B., Novovic, K., Dekic, S., and Hrenovic, J. (2021). Colistin resistance in environmental isolates of *Acinetobacter baumannii*. *Microb. Drug Resist.* 27, 328–336. doi: 10.1089/mdr.2020.0188

Kabic, J., Novovic, K., Kekic, D., Trudic, A., Opavski, N., Dimkic, I., et al. (2023). Comparative genomics and molecular epidemiology of colistin-resistant *Acinetobacter baumannii*. *Comput. Struct. Biotechnol. J.* 21, 574–585. doi: 10.1016/j.csbj.2022.12.045

Khoshnood, S., Savari, M., Abbasi Montazeri, E., and Farajzadeh Sheikh, A. (2020). Survey on genetic diversity, biofilm formation, and detection of colistin resistance genes in clinical isolates of *Acinetobacter baumannii*. *Infect. Drug Resist.* 13, 1547–1558. doi: 10.2147/IDR.S253440

Klodzinska, E., Szumski, M., Dziubakiewicz, E., Hrynkiewicz, K., Skwarek, E., Janusz, W., et al. (2010). Effect of zeta potential value on bacterial behavior during electrophoretic separation. *Electrophoresis* 31, 1590–1596. doi: 10.1002/elps.200900559

Ko, K. S., Choi, Y., and Lee, J.-Y. (2017). Old drug, new findings: colistin resistance and dependence of *Acinetobacter baumannii*. *Precis Future Med.* 1, 159–167. doi: 10.23838/pfm.2017.00184

Lesho, E., Yoon, E. J., Mcgann, P., Snesrud, E., Kwak, Y., Milillo, M., et al. (2013). Emergence of colistin-resistance in extremely drug-resistant Acinetobacter baumannii containing a novel pmrCAB operon during colistin therapy of wound infections. *J. Infect. Dis.* 208, 1142–1151. doi: 10.1093/infdis/jit293

Mavroidi, A., Likousi, S., Palla, E., Katsiari, M., Roussou, Z., Maguina, A., et al. (2015). Molecular identification of tigecycline- and colistin-resistant carbapenemase-producing *Acinetobacter baumannii* from a Greek hospital from 2011 to 2013. *J. Med. Microbiol.* 64, 993–997. doi: 10.1099/jmm.0.000127

Misic, D., Asanin, J., Spergser, J., Szostak, M., and Loncaric, I. (2018). OXA-72-mediated carbapenem resistance in sequence type 1 multidrug (Colistin)-resistant *Acinetobacter baumannii* associated with urinary tract infection in a dog from serbia. *Antimicrob. Agents Chemother.* 62, e00219. doi: 10.1128/AAC.00219-18

Moffatt, J. H., Harper, M., and Boyce, J. D. (2019). Mechanisms of polymyxin resistance. *Adv. Exp. Med. Biol.* 1145, 55–71. doi: 10.1007/978-3-030-16373-0_5

Nurtop, E., Bayindir Bilman, F., Menekse, S., Kurt Azap, O., Gonen, M., Ergonul, O., et al. (2019). Promoters of colistin resistance in *Acinetobacter baumannii* infections. *Microb. Drug Resist.* 25, 997–1002. doi: 10.1089/mdr.2018.0396

Oikonomou, O., Sarrou, S., Papagiannitsis, C. C., Georgiadou, S., Mantzarlis, K., Zakynthinos, E., et al. (2015). Rapid dissemination of colistin and carbapenem resistant Acinetobacter baumannii in Central Greece: mechanisms of resistance, molecular identification and epidemiological data. *BMC Infect. Dis.* 15, 559. doi: 10.1186/s12879-015-1297-x

Olaitan, A. O., Morand, S., and Rolain, J. M. (2014). Mechanisms of polymyxin resistance: acquired and intrinsic resistance in bacteria. *Front. Microbiol.* 5. doi: 10.3389/fmicb.2014.00643

Potron, A., Vuillemenot, J. B., Puja, H., Triponney, P., Bour, M., Valot, B., et al. (2019). ISAba1-dependent overexpression of EptA in clinical strains of *Acinetobacter baumannii* resistant to colistin. *J. Antimicrob. Chemother.* 74, 2544–2550. doi: 10.1093/jac/dkz241

Ribeiro-Goncalves, B., Francisco, A. P., Vaz, C., Ramirez, M., and Carrico, J. A. (2016). PHYLOViZ Online: web-based tool for visualization, phylogenetic inference, analysis and sharing of minimum spanning trees. *Nucleic Acids Res.* 44, W246–W251. doi: 10.1093/nar/gkw359

Seleim, S. M., Mostafa, M. S., Ouda, N. H., and Shash, R. Y. (2022). The role of PmrCAB genes in colistin-resistant *Acinetobacter baumannii*. *Sci. Rep.* 12, 20951. doi: 10.1038/s41598-022-25226-x

Shelenkov, A., Petrova, L., Zamyatin, M., Mikhaylova, Y., and Akimkin, V. (2021). Diversity of international high-risk clones of acinetobacter baumannii revealed in a russian multidisciplinary medical center during 2017-2019. *Antibiotics (Basel)* 10, 1009. doi: 10.3390/antibiotics10081009

Snyman, Y., Whitelaw, A. C., Reuter, S., Dramowski, A., Maloba, M. R. B., and Newton-Foot, M. (2020). Clonal expansion of colistin-resistant *Acinetobacter baumannii* isolates in Cape Town, South Africa. *Int. J. Infect. Dis.* 91, 94–100. doi: 10.1016/j.ijid.2019.11.021

Soon, R. L., Nation, R. L., Cockram, S., Moffatt, J. H., Harper, M., Adler, B., et al. (2011). Different surface charge of colistin-susceptible and -resistant *Acinetobacter baumannii* cells measured with zeta potential as a function of growth phase and colistin treatment. *J. Antimicrob. Chemother.* 66, 126–133. doi: 10.1093/jac/dkq422

Soon, R. L., Nation, R. L., Hartley, P. G., Larson, I., and Li, J. (2009). Atomic force microscopy investigation of the morphology and topography of colistin-heteroresistant *Acinetobacter baumannii* strains as a function of growth phase and in response to colistin treatment. *Antimicrob. Agents Chemother.* 53, 4979–4986. doi: 10.1128/AAC.00497-09

Srisakul, S., Wannigama, D. L., Higgins, P. G., Hurst, C., Abe, S., Hongsing, P., et al. (2022). Overcoming addition of phosphoethanolamine to lipid A mediated colistin resistance in Acinetobacter baumannii clinical isolates with colistin-sulbactam combination therapy. *Sci. Rep.* 12, 11390. doi: 10.1038/s41598-022-15386-1

Tatusova, T., Dicuccio, M., Badretdin, A., Chetvernin, V., Nawrocki, E. P., Zaslavsky, L., et al. (2016). NCBI prokaryotic genome annotation pipeline. *Nucleic Acids Res.* 44, 6614–6624. doi: 10.1093/nar/gkw569

Thi Khanh Nhu, N., Riordan, D. W., Do Hoang Nhu, T., Thanh, D. P., Thwaites, G., Huong Lan, N. P., et al. (2016). The induction and identification of novel Colistin resistance mutations in *Acinetobacter baumannii* and their implications. *Sci. Rep.* 6, 28291. doi: 10.1038/srep28291

Turton, J. F., Woodford, N., Glover, J., Yarde, S., Kaufmann, M. E., and Pitt, T. L. (2006). Identification of Acinetobacter baumannii by detection of the blaOXA-51-like carbapenemase gene intrinsic to this species. *J. Clin. Microbiol.* 44, 2974–2976. doi: 10.1128/JCM.01021-06

Usjak, D., Novovic, K., Filipic, B., Kojic, M., Filipovic, N., Stevanovic, M. M., et al. (2022). *In vitro* colistin susceptibility of pandrug-resistant Ac. baumannii is restored in the presence of selenium nanoparticles. *J. Appl. Microbiol.* 133, 1197–1206. doi: 10.1111/jam.15638

Wick, R. R., Schultz, M. B., Zobel, J., and Holt, K. E. (2015). Bandage: interactive visualization of *de novo* genome assemblies. *Bioinformatics* 31, 3350–3352. doi: 10.1093/bioinformatics/btv383

Wong, D., Nielsen, T. B., Bonomo, R. A., Pantapalangkoor, P., Luna, B., and Spellberg, B. (2017). Clinical and pathophysiological overview of acinetobacter infections: a century of challenges. *Clin. Microbiol. Rev.* 30, 409–447. doi: 10.1128/CMR.00058-16

frontiers | Frontiers in Cellular and Infection Microbiology

TYPE Original Research
PUBLISHED 11 August 2023
DOI 10.3389/fcimb.2023.1229194

OPEN ACCESS

EDITED BY
Elvira Garza González,
Autonomous University of Nuevo León, Mexico

REVIEWED BY
Ulises Garza-Ramos,
National Institute of Public Health, Mexico
Ibrahim Bitar,
Charles University, Czechia
Chang-Wei Lei,
Sichuan University, China

*CORRESPONDENCE
Luhua Zhang
zhluhua@swmu.edu.cn
Wei Zeng
mercedes600@126.com

RECEIVED 26 May 2023
ACCEPTED 24 July 2023
PUBLISHED 11 August 2023

CITATION
Li Y, Yin M, Fang C, Fu Y, Dai X, Zeng W and Zhang L (2023) Genetic analysis of resistance and virulence characteristics of clinical multidrug-resistant *Proteus mirabilis* isolates. *Front. Cell. Infect. Microbiol.* 13:1229194. doi: 10.3389/fcimb.2023.1229194

Genetic analysis of resistance and virulence characteristics of clinical multidrug-resistant *Proteus mirabilis* isolates

Ying Li[1], Ming Yin[1], Chengju Fang[1], Yu Fu[1], Xiaoyi Dai[1], Wei Zeng[2]* and Luhua Zhang[1]*

[1]The School of Basic Medical Science and Public Center of Experimental Technology, Southwest Medical University, Luzhou, Sichuan, China, [2]Department of Clinical Laboratory, The Hejiang People's hospital, Luzhou, Sichuan, China

Objective: *Proteus mirabilis* is the one of most important pathogens of catheter-associated urinary tract infections. The emergence of multidrug-resistant (MDR) *P. mirabilis* severely limits antibiotic treatments, which poses a public health risk. This study aims to investigate the resistance characteristics and virulence potential for a collection of *P. mirabilis* clinical isolates.

Methods and results: Antibiotic susceptibility testing revealed fourteen MDR strains, which showed high resistance to most β-lactams and trimethoprim/sulfamethoxazole, and a lesser extent to quinolones. All the MDR strains were sensitive to carbapenems (except imipenem), ceftazidime, and amikacin, and most of them were also sensitive to aminoglycosides. The obtained MDR isolates were sequenced using an Illumina HiSeq. The core genome-based phylogenetic tree reveals the high genetic diversity of these MDR *P. mirabilis* isolates and highlights the possibility of clonal spread of them across China. Mobile genetic elements SXT/R391 ICEs were commonly (10/14) detected in these MDR *P. mirabilis* strains, whereas the presence of resistance island *Pm*GRI1 and plasmid was sporadic. All ICEs except for ICE*Pmi*Chn31006 carried abundant antimicrobial resistance genes (ARGs) in the HS4 region, including the extended-spectrum β-lactamase (ESBL) gene $bla_{CTX\text{-}M\text{-}65}$. ICE*Pmi*Chn31006 contained the sole ARG $bla_{CMY\text{-}2}$ and was nearly identical to the global epidemic ICEPmiJpn1. The findings highlight the important roles of ICEs in mediating the spread of ARGs in *P. mirabilis* strains. Additionally, these MDR *P. mirabilis* strains have great virulence potential as they exhibited significant virulence-related phenotypes including strong crystalline biofilm, hemolysis, urease production, and robust swarming motility, and harbored abundant virulence genes.

Conclusion: In conclusion, the prevalence of MDR *P. mirabilis* with high virulence potential poses an urgent threat to public health. Intensive monitoring is needed to reduce the incidence of infections by MDR *P. mirabilis*.

KEYWORDS

***Proteus mirabilis*, ICE, blaCTX-M-65, PmGRI1, virulence**

1 Introduction

Proteus mirabilis, a Gram-negative rod-shaped bacterium belonging to the Morganellaceae family of the order Enterobacterales, is well-known for its urease production and characteristic bull's-eye-pattern swarming motility on agar plates (Hamilton et al., 2018). While the bacterium can cause a variety of human infections, it is most noted as a pathogen of catheter-associated urinary tract infections (CAUTIs) (Schaffer et al., 2015). These CAUTIs frequently progress to bacteremia due to *P. mirabilis*, which carries a high mortality rate (Schaffer et al., 2015; Armbruster et al., 2018). *P. mirabilis* possesses a diverse set of virulence factors relevant to CAUTIs, such as motility, the production of urease, hemolysins, biofilm formation, adhesin, and fimbriae-mediated adherence (Armbruster et al., 2018). Once established in the catheterized urinary tract, *P. mirabilis* usually causes chronic infection and blockage that are extremely difficult to eliminate (Wasfi et al., 2020).

Owing to the flagella-mediated motility, *P. mirabilis* can easily contact uroepithelial cells, thereby promoting internalization and cytotoxicity, and facilitate transmission of the infection upward into the bladder and kidneys (Armbruster et al., 2018). *P. mirabilis* can simultaneously express multiple types of fimbriae, and several of them are implicated in virulence, such as the best characterized mannose-resistant *Proteus*-like (MR/P) fimbriae encoded by the *mrp* operon (*mrpABCDEFGHJ*) (Pearson and Mobley, 2008). Urease is a nickel-metalloenzyme that acts by hydrolyzing urea into ammonia and carbon dioxide, which is implicated in the development of infection-induced stone formation (Rutherford, 2014). CAUTIs generally stem from the formation of unusual crystalline biofilm structures on catheter surfaces (Schaffer et al., 2015). *P. mirabilis* is a biofilm former on the surface of living or abiotic surfaces and is capable to form crystalline biofilm in the urinary environment with the help of urease and adhesive proteins, such as MR/P fimbriae (Armbruster et al., 2018). The formation of extensive crystalline biofilms can occlude the urine flow through the catheter, which frequently leads to the reflux of infected urine to the kidneys and causes pyelonephritis, septicemia, and shock (Holling et al., 2014).

Proteus species possess intrinsic resistance to colistin, nitrofurantoin, tigecycline, and tetracycline (Girlich et al., 2020). In recent years, multidrug-resistant (MDR) *P. mirabilis* isolates are becoming increasingly common (Falagas and Karageorgopoulos, 2008; Li et al., 2022). They have been frequently described with multiple acquired antimicrobial resistance genes (ARGs) encoding extended-spectrum β-lactamases (ESBLs), such as CTX-M-65 (Lei et al., 2018b), and carbapenemases such as KPC-2 and NDM-1(Hua et al., 2020; He et al., 2021), and show co-resistance to fluoroquinolones, aminoglycosides, and sulfamethoxazole-trimethoprim (Korytny et al., 2016; Lei et al., 2018b; Shaaban et al., 2022). The prevalence of MDR *P. mirabilis* isolates and their ongoing acquisition of ARGs pose challenges to clinical treatments.

Mobile genetic elements, including plasmids, and resistance genomic islands such as integrative and conjugative elements (ICEs), play a central role in the acquisition and spread of ARGs in *P. mirabilis* (Lei et al., 2016; Li et al., 2021; Ma et al., 2021). ICE is a distinct region of a bacterial chromosome that is self-transmissible by conjugation (Partridge et al., 2018). Especially, the SXT/R391 family of ICEs constitutes a diverse group of mobile elements that carry multidrug resistance genes in *Proteus*. SXT/R391 ICEs are characterized by a conserved integrase that mediates the integration into the 5′ end of the chromosomal *prfC* gene by site-specific recombination (Wozniak et al., 2009). SXT/R391 ICEs share a conserved backbone consisting of 52 nearly identical core genes (Li et al., 2016a; Sato et al., 2020), and also contain variable DNA regions, dubbed hotspots (HS1 to HS5) and variable regions (VRI-VRV) that carry genes for antimicrobial resistance, such as bla_{CMY-2} (Lei et al., 2016), *tet*(X6) (He et al., 2020), and bla_{NDM-1} (Kong et al., 2020). SXT/R391 ICEs in *P. mirabilis* also carried multi-resistance gene *cfr* and tigecycline resistance gene cluster *tmexCD3-toprJ1* (Ma et al., 2022).

The present study was conducted to investigate the prevalence, resistance gene profiles, and virulence determinants for clinical *P. mirabilis* isolates from a county hospital in the Sichuan province of China. Also, virulence characteristics including motility, urease production, hemolytic activity, and biofilm formation were determined to better understand the potential risk of these MDR *P. mirabilis* isolates.

2 Materials and methods

2.1 Bacterial isolates

32 *P. mirabilis* strains were isolated from different clinical samples of patients at the Hejiang County People's Hospital, in Luzhou City, Sichuan Province of China, from January to December 2021. Written informed consent from the patients was exempted from this study since the present study only focused on bacteria, and the strains were isolated as a part of the routine hospital laboratory procedures. Isolates were initially identified with both the VITEK 2 system (BioMérieux, Marcy-l'Étoile, France) and 16S rRNA gene sequencing analysis (Lane, 1991).

2.2 Antimicrobial susceptibility testing

The minimum inhibitory concentrations (MICs) of 23 antimicrobial agents, including ampicillin, amikacin, ampicillin/sulbactam, azlocillin, aztreonam, cefazolin, cefepime, cefoxitin, cefixime, cefotetan, ceftazidime, ceftriaxone, ciprofloxacin, ertapenem, gentamicin, imipenem, meropenem, levofloxacin, nitrofurantoin, mezlocillin, piperacillin/tazobactam, tobramycin, and trimethoprim-sulfamethoxazole were automatically performed by the VITEK 2 system. MICs of ceftazidime, cefotaxime, and meropenem were manually confirmed using the broth microdilution method, and the susceptibility testing for ceftazidime was also performed by Kirby Bauer disk diffusion method, with *Escherichia coli* strain ATCC 25922 as the quality control. The results of antibiotic susceptibility testing were interpreted by the breakpoints defined by the Clinical and

Laboratory Standards Institute standards for Enterobacterales (CLSI, M100) (CLSI, 2023). MDR strains were defined as non-susceptibility to three or more of the following antibiotic groups: β-lactam-β-lactam inhibitor combinations, cephalosporins, aminoglycosides, fluoroquinolones or trimethoprim-sulfamethoxazole (Korytny et al., 2016).

2.3 Genomic sequencing and bioinformatic analysis

Fourteen MDR *P. mirabilis* were selected for genomic DNA extraction using the QIAamp DNA Mini Kit (Qiagen, Hilden, Germany) following the manufacturer's guidelines. Whole genome sequencing was performed on the HiSeq 2000 (Illumina, San Diego, CA, USA) Sequencer with a 150 bp paired-end library and 200 × coverage by the Beijing Tsingke Bioinformatics Technology Co. Ltd. The raw reads were trimmed using Trimmomatic v0.38 before being assembled into draft genomes using SPAdes v3.12.0 program (Bankevich et al., 2012; Bolger et al., 2014). Annotation was carried out using Prokka (Seemann, 2014). Genome-based species identification was performed by average nucleotide identity (ANI) analysis. The ANI value between genome sequences of these clinical isolates and that of reference strain *P. mirabilis* HI4320 (Accession no. NC_010554) was calculated with JSpeciesWS (Richter et al., 2016). 96% is the cut-off for defining a bacterial species. Plasmid incompatibility types, antibiotic resistance genes (ARGs), and insertion elements (ISs) were predicted using PlasmidFinder (Carattoli and Hasman, 2020), ResFinder (Bortolaia et al., 2020), and ISfinder (Siguier et al., 2006). The detection of SXT/R391 ICE in the whole genome sequences was performed using the conserved integrase gene (int_{SXT}). The contigs of SXT/R391 ICE were extracted and assembled against the reference ICE of FZP3105 from our previous study (Li et al., 2022), and gaps between contigs were closed by PCR and Sanger sequencing. The contigs of *Pm*GRI1 were extracted and assembled against the reference *Pm*GRI1-CYPM1 (GenBank accession CP012674). Linear sequence alignment was carried out using BLAST and visualized with Easyfig 2.2.3(Sullivan et al., 2011).

2.4 Phylogenetic analysis

The genome sequences of other representative *Proteus* isolates in China were retrieved from the GenBank. Genetic relationship of different *Proteus* isolates was assessed based on single nucleotide polymorphisms (SNPs) in their core genomes, as previously described with minor modification (Li et al., 2022). Briefly, the GFF3 files generated by Prokka were piped into Roary to create a core genome alignment. SNPs were extracted using snp-sites v2.3.2 (Kwok and Hitchins, 2015). A maximum-likelihood phylogenetic tree was constructed based on the SNPs using FastTree version 2.1.10 under the GTRGAMMA model with 1000 bootstrap iterations (Price et al., 2010).

2.5 Transferability assay

Conjugation experiments were carried out using broth-based method with the *E. coli* strain J53 (sodium azide-resistant) or EC600 (rifampicin-resistant) as the recipient, as described previously with minor modification (Li et al., 2022). After the donor and recipient strains were grown to exponential stage (the optical density at 600 nm reaches ~0.5), mix them at a ratio of 1:1 before incubation at 37° C for 24 h. Transconjugants were selected on Luria-Bertani (LB) agar plates containing 4 μg/ml cefotaxime plus 150 μg/ml sodium azide (for J53) or 200 μg/ml rifampicin (for EC600). The presence of SXT/R391 ICE was confirmed by PCR using the primers targeting int_{SXT} (Sato et al., 2020).

2.6 Measurement of virulence

2.6.1 Crystalline biofilm assay

Broth cultures of *P. mirabilis* (OD600~0.4) were diluted 1/100 into fresh LB broth containing 50% filter sterilized human urine prepared from a pool of urine from several healthy volunteers. 200 μl diluted bacterial cultures were incubated statically in sterile 96-well microtiter plates (Costar 3599, Corning, NY, USA) for 24 h at 37°C. The culture supernatant was then removed and the biofilm production was quantified by the crystal violet staining method as described previously(Li et al., 2016b). Negative control wells contained only LB broth and human urine. The average OD595 values were calculated for sextuplicate, and the tests were repeated three times. The cut-off value (ODc) was defined as 3 SD above the mean OD595 of the negative control. If OD595≤ODc, absence of biofilm; if ODc≤OD595 ≤ 2×ODc, weak biofilm producer; if 2×ODc≤OD595 ≤ 4×ODc, moderate biofilm producer; if 4×ODc≤OD595, strong biofilm producer(Qu et al., 2022).

2.6.2 Urease, hemolysis, and motility assays

The urease quantification assay was performed as described previously (Durgadevi et al., 2019a). Briefly, overnight culture of *P. mirabilis* was mixed with LB broth containing filter sterilized urea (20 g/L) in the ratio of 1:100. After incubation for 24 h at 37°C, the color change (orange to pink) was observed by adding 0.02% phenol red reagent (pH indicator). The hemolytic ability of *P. mirabilis* strains was determined by culturing on a 10% sheep blood plate for 24 h at 37 °C. For motility assays, 1 μl of culture was point inoculated onto the surface center of the solid LB agar plates. After incubation for 24 h at 37 °C in a lid-side-up position, motility was measured as the diameter across which *P. mirabilis* grew (Durgadevi et al., 2019b).

2.7 Virulence genes analysis

The presence of genes related to bacterial virulence factors including fimbriae (*mrpA*, *ucaA*, *pmfA*, *pmpA*), hemolysin (*hpmAB*), Urease (*ureC*), biofilm formation (*pst*, *rcsD*), autotransporters (*pta*, *aipA*), proteases (*zapA*), and siderophore

(*nrpR*) were identified using the Virulence Factors of Pathogenic Bacteria Database (VFDB) (Chen et al., 2005). The identification of flagella genes (*flhA*, *fliF*, *fliG*, *fliP*, *fliL*, *flgN*, *flaD*) was performed in a pairwise BLASTn alignment.

3 Results and discussion

3.1 Sources and antimicrobial susceptibility profiles of MDR *P. mirabilis* strains

Among the 32 P. *mirabilis* strains, 14 (43.8%) of them were identified as MDR, which were recovered from sputum (n=7, 50%), urine (n=4, 28.6%), stool (n=1, 7.1%), ascites (n=1, 7.1%), and wound secretion (n=1, 7.1%). Results of the antimicrobial susceptibility test indicated that all the MDR strains were resistant to ampicillin, azlocillin, cefazolin, cefixime, mezlocillin, ampicillin/sulbactam, and trimethoprim/sulfamethoxazole, in addition to their intrinsic resistance profiles (Table 1). They also showed high resistance rates (>70.0%) to ceftriaxone (n =12, 85.7%), and a lesser extent to cefotetan (n =8, 57.1%), ciprofloxacin (n=8, 57.1%), and levofloxacin (n=8, 57.1%). Four isolates (28.6%) were resistant to piperacillin/tazobactam. Resistance to antimicrobial agents, including cefepime, cefoxitin, aztreonam, gentamicin, and tobramycin was rarely (n<3) detected. All the MDR strains were sensitive to meropenem (MIC ≤ 1), ertapenem (MIC ≤ 0.5), ceftazidime (MIC ≤ 1), and amikacin (MIC ≤ 2). The Kirby Bauer test confirmed the sensitivity of these strains to ceftazidime. Consistent with the observation that *P. mirabilis* possesses intrinsic decreased susceptibility to imipenem (but not meropenem and ertapenem), 92.9% of MDR strains (n=13) were resistant to imipenem in this study, which was thought to be caused by weak affinity with penicillin-binding proteins or porin loss (Girlich et al., 2020).

3.2 Genotypic resistance of MDR *P. mirabilis* strains

We sequenced the genomes of all 14 MDR isolates on the Illumina platform. The genomes vary from 3,964,688 bp to 4,212,070 bp, with an average GC content of 38.80% to 39.09% (Table S1). The genomic analysis identified the presence of 35 different ARGs in the 14 MDR *P. mirabilis* strains, and 11 (78.6%) of them carried at least 15 ARGs (Table 1). Three different ESBLs genes, $bla_{\text{CTX-M-65}}$, $bla_{\text{CTX-M-63}}$, and $bla_{\text{CMY-2}}$, were detected. Among them, $bla_{\text{CTX-M-65}}$, which has been identified in many *P. mirabilis* strains from humans and animals in China (Li et al., 2022; Qu et al., 2022), also represents the most prevalent one in this study. All the strains except for HJP18031 carried abundant aminoglycosides resistance genes, with *aac(3)-IV* (n=11), *aph(4)-Ia* (n=11), *aph(6)-Id* (n=8), and *aph(3")-Ib* (n=8) being the most prevalent. Of the detected quinolone resistance genes, *aac(6')-Ib-cr* (n=10, 71.4%) is the most common, followed by *qnrD1* (n=8, 57.1%), and *qnrS1* was only detected in one isolate. Furthermore, we found that genotypic and phenotypic resistance in these strains often does not match. Almost all the $bla_{\text{CTX-M-65}}$-harboring isolates (except for HJP22016) remain sensitive to aztreonam. Also, the presence of *aac(6')-Ib-cr* did not lead to quinolone resistance in several strains, such as HJP21048, HJP31010, and HJP31030. These findings suggest that the functions of these ARGs may be regulated by some unknown mechanisms in *P. mirabilis* strains (Li et al., 2022).

3.3 Genomic phylogeny of MDR *P. mirabilis* strains

To understand the genetic relationship of 14 MDR *P. mirabilis* strains in this study with other isolates from different geographic locations in China (Table S2), a core genome-based phylogenetic tree was constructed, which revealed five distinct groups (Figure 1). The tested strains are diffusely distributed in the tree, suggesting the genetic diversity of them. HJP21048 and HJP31006 are present in the subclade II that is distant from other tested strains, suggesting a different origin of them. In subclade IV, four strains HJP26021, HJP31010, HJP31030, and HJP01027 are tightly clustered, and they share identical core genomes (SNP=0) as well as resistance phenotypes, showing the clonal nature of them. Notably, HJP26021, HJP31010, and HJP01027 were subsequent isolates from the sputum of a single patient a few days apart, whereas HJP31030 was from another patient in the same inpatient ward but a different room, indicating the clone spread of this MDR strain. In subclade V, strains from this study cluster with several isolates from animals and humans from different locations in China. Especially, HJP17012 and HJP05004 are closely related (105 SNPs), and tightly cluster together with several clinical isolates and animal-derived strains. These findings suggest the possibility of circulation and clonal spread of these MDR *P. mirabilis* strains across different regions of China.

3.4 Genetic features of ARG-bearing plasmids in MDR *P. mirabilis* strains

Only two types of plasmids, IncQ1 and Col3M, were identified in these *P. mirabilis* strains and eight of them harbor the 2,683-bp Col3M plasmid, which encodes a quinolone resistance protein QnrD1 and a hypothetical protein. BLASTn analysis showed that the Col3M plasmid is very common in *P. mirabilis* strains of different origins. Two IncQ1-type replication genes were detected in HJP05004 and HJP16012, respectively. In HJP05004, the IncQ1 plasmid pCTX-M_HJP05004 is 40,486 bp in size and has no other known ARGs except $bla_{\text{CTX-M-63}}$ (Figure 2A). It consists of a 38-kb backbone comprising genes for replication (*repA*), maintenance (*topB*), and conjugation (*vir* genes). The sole acquired resistance gene region was identified downstream of *dnaA* (encoding the chromosomal replication initiation ATPase DnaA), wherein $bla_{\text{CTX-M-63}}$ was present in an IS*Ecp1*-$bla_{\text{CTX-M-63}}$ transposition unit. The insertion sequence IS*Ecp1* is known to mobilize adjacent sequences, including $bla_{\text{CTX-M}}$ genes, by using its own left inverted repeat (IRL) in conjunction with alternative sequences resembling its right inverted repeat (IRR) (Zong et al., 2010). BLASTn revealed that pCTX-M_HJP05004 is partly similar (71%

10.3389/fcimb.2023.1229194

TABLE 1 Clinical information and genomic characterization of 14 MDR *P. mirabilis* isolates.

Strain	Specimen	Age (Year) /Gender[a]	Antimicrobial resistance genes	Resistance phenotype[b]	Plasmid replicons	Genomic islands
HJP21048	Wound secretion	72/M	*aac(6')-Ib-cr*, *aph(3')-Ia*, *aadA2b*, *arr-3*, *bleO*, *cat*, *catB3*, *fosA3*, *ere*(A), *tet*(C), *tet*(J), bla_{OXA-1}, *qnrD1*, *sul1*, *dfrA32*	AMP, AZL, SAM, CZO, CEF, CTT, IPM, MEZ, NIT, SXT	Col3M	ICE
HJP21049	Ascites	93/F	*aac(6')-Ib-cr*, *aph(4)-Ia*, *aadA2b*, *aac(3)-IV*, *arr-3*, *dfrA32*, *bleO*, bla_{OXA-1}, $bla_{CTX-M-65}$, *fosA3*, *qnrD1*, *catB3*, *floR*, *ere*(A), *tet*(C), *tet*(J), *sul1*, *sul2*	AMP, AZL, SAM, CZO, CEF, CRO, CIP, IPM, LVX, MEZ, NIT, SXT	Col3M	ICE
HJP16012	Stool	72/M	*aac(3)-IIa*, *aph(6)-Id*, *aph(3'')-Ib*, *aph(3')-Ia*, *aadA5*, *mph*(A), *catA1*, *cat*, *dfrA17*, *tet*(J), bla_{TEM-1B}, *sul1*, *sul2*	AMP, AZL, SAM, CZO, CEF, CTT, CIP, IPM, LVX, MEZ, NIT, SXT	IncQ1	
HJP22021	Urine	71/M	*aac(6')-Ib-cr*, *aadA1*, *aph(4)-Ia*, *aac(3)-IV*, *dfrA1*, *arr-3*, bla_{OXA-1}, $bla_{CTX-M-65}$, *cat*, *floR*, *catA1*, *catB3*, *tet*(J), *fosA3*, *sul1*, *sul2*	AMP, AZL, SAM, CZO, CEF, CTT, CRO, CIP, IPM, LVX, MEZ, NIT, TZP, SXT		*Pm*GRI1
HJP05004	Urine	53/M	*aac(6')-Ib-cr*, *aadA1*, *aac(3)-IV*, *aph(6)-Id*, *aadA5*, *aph(3'')-Ib*, *aph(4)-Ia*, *aadA2b*, *aph(3')-Ia*, *aac(3)-IId*, bla_{OXA-1}, $bla_{CTX-M-63}$, bla_{TEM-1B}, *arr-3*, *catA1*, *catB3*, *cat*, *cmlA1*, *floR*, *dfrA17*, *dfrA1*, *tet*(J), *sul1*, *sul2*	AMP, AZL, SAM, CZO, CEF, CTT, CRO, CIP, GEN, IPM, LVX, MEZ, NIT, SXT	IncQ1	*Pm*GRI1
HJP18031	Sputum	89/M	*catA1*, *cat*, *floR*, *qnrS1*, *tet*(J)	AMP, AZL, SAM, CZO, CEF, CTT, CRO, CIP, IPM, LVX, MEZ, NIT, TOB, SXT		
HJP17012	Sputum	75/M	*aph(3')-VIa*, *aadA1*, *aph(3'')-Ib*, *aph(6)-Id*, *aadA2b*, *aac(6')-Ib-cr*, *aph(4)-Ia*, *aac(3)-IV*, *arr-3*, bla_{OXA-1}, $bla_{CTX-M-65}$, bla_{TEM-1B}, *tet*(J), *floR*, *fosA3*, *cmlA1*, *cat*, *catB3*, *catA1*, *dfrA1*, *sul1*, *sul2*, *sul3*	AMP, AZL, SAM, CZO, CEF, CTT, FEP, CRO, CIP, IPM, LVX, MEZ, NIT, TZP, SXT		ICE, *Pm*GRI1
HJP20004	Sputum	81/M	*aac(6')-Ib-cr*, *aph(6)-Id*, *aph(3'')-Ib*, *aadA2b*, *aph(4)-Ia*, *aac(3)-IV*, *aph(3')-Ia*, *aadA1*, *dfrA1*, *dfrA32*, *ere*(A), *tet*(J), *tet*(C), *arr-3*, bla_{OXA-1}, $bla_{CTX-M-65}$, *cat*, *catA1*, *catB3*, *floR*, *sul1*, *sul2*	AMP, AZL, SAM, CZO, CEF, CRO, CIP, IPM, MEZ, NIT, SXT		ICE, *Pm*GRI1
HJP31006	Vaginal secretion	28/F	*aph(4)-Ia*, *aadA2*, *aac(3)-IV*, *aph(3')-Ia*, *bleO*, bla_{CMY-2}, *dfrA12*, *qnrD1*, *tet*(J), *floR*, *cat*, *sul2*	AMP, AZL, SAM, CZO, CEF, CTT, CIP, IPM, LVX, MEZ, NIT, TZP, SXT	Col3M	ICE
HJP22016	Urine	57/F	*aadA2b*, *aph(4)-Ia*, *aac(3)-IV*, $bla_{CTX-M-65}$, *ere*(A), *fosA3*, *qnrD1*, *dfrA32*, *dfrA1*, *cat*, *floR*, *catB3*, *tet*(J), *tet*(C), *sul2*	AMP, AZL, SAM, ATM, CZO, CEF, CTT, FEP, CRO, IPM, LVX, MEZ, NIT, TZP, SXT	Col3M	ICE, *Pm*GRI1
HJP26021	Sputum	78/M	*aph(3'')-Ib*, *aac(3)-IV*, *aadA2b*, *aph(6)-Id*, *aac(6')-Ib-cr*, *aph(4)-Ia*, *aph(3')-VIa*, *arr-3*, bla_{OXA-1}, $bla_{CTX-M-65}$, *catB3*, *cat*, *dfrA32*, *ere*(A), *floR*, *fosA3*, *qnrD1*, *tet*(C), *tet*(J), *sul1*, *sul2*	AMP, AZL, SAM, CZO, CEF, CRO, IPM, MEZ, NIT, SXT	Col3M	ICE
HJP31010	Sputum	78/M	*aph(3'')-Ib*, *aph(4)-Ia*, *aadA2b*, *aac(3)-IV*, *aph(3')-VIa*, *aph(6)-Id*, *aac(6')-Ib-cr*, *arr-3*, bla_{OXA-1}, $bla_{CTX-M-65}$, *catB3*, *cat*, *dfrA32*, *ere*(A), *floR*, *fosA3*, *qnrD1*, *tet*(C), *tet*(J), *sul1*, *sul2*	AMP, AZL, SAM, CZO, CEF, CRO, IPM, MEZ, NIT, SXT	Col3M	ICE
HJP31030	Urine	80/M	*aph(3'')-Ib*, *aac(3)-IV*, *aadA2b*, *aph(6)-Id*, *aph(3')-VIa*, *aph(4)-Ia*, *aac(6')-Ib-cr*, *arr-3*, bla_{OXA-1}, $bla_{CTX-M-65}$, *catB3*, *cat*, *dfrA32*, *ere(A)*, *floR*, *fosA3*, *qnrD1*, *tet*(C), *tet*(J), *sul1*, *sul2*	AMP, AZL, SAM, CZO, CEF, CRO, MEZ, NIT, SXT	Col3M	ICE
HJP01027	Sputum	78/M	*aac(6')-Ib-cr*, *aph(4)-Ia*, *aph(3'')-Ib*, *aadA2b*, *aph(3')-VIa*, *aac(3)-IV*, *aph(6)-Id*, *arr-3*, bla_{OXA-1}, $bla_{CTX-M-65}$, *catB3*, *cat*, *dfrA32*, *ere*(A), *floR*, *fosA3*, *qnrD1*, *tet*(C), *tet*(J), *sul1*, *sul2*	AMP, AZL, SAM, CZO, CEF, CRO, IPM, MEZ, NIT, SXT	Col3M	ICE

[a]Gender: M, male; F, female.

[b]AMP, ampicillin; ATM, aztreonam; AZL, azlocillin; CIP, ciprofloxacin; CRO, ceftriaxone; CTT, cefotetan; CEF, cefixime; CZO, cefazolin; FEP, cefepime; FOX, cefoxitin; GEN, gentamicin; IPM, imipenem; LVX, levofloxacin; MEZ, mezlocillin; NIT, nitrofurantoin; SAM, ampicillin/sulbactam; SXT, trimethoprim/sulfamethoxazole; TOB, tobramycin; TZP, piperacillin/tazobactam.

10.3389/fcimb.2023.1229194

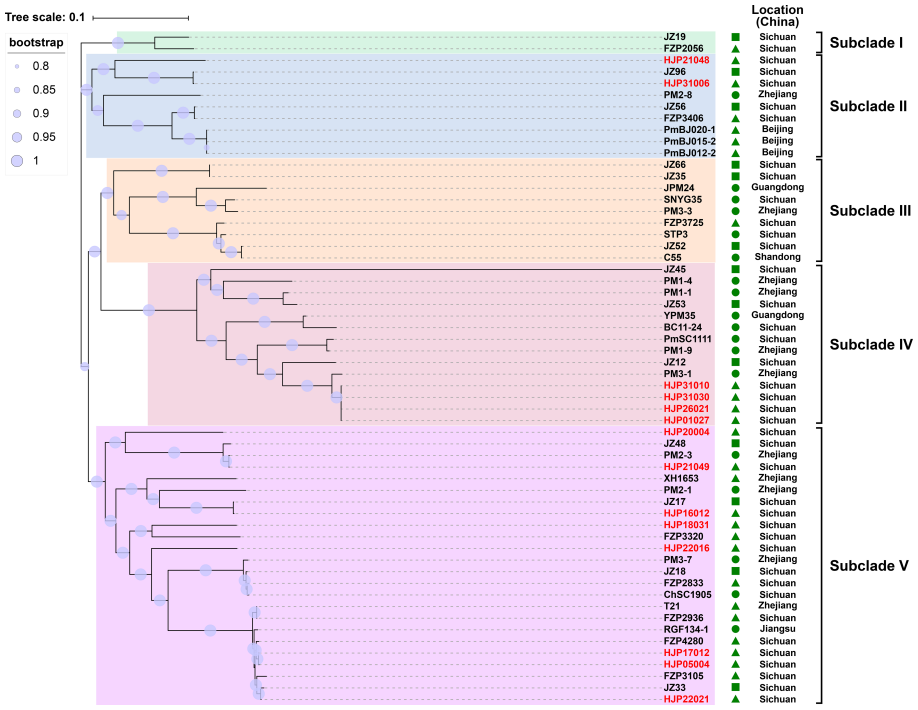

FIGURE 1
Phylogenetic analysis of MDR *P. mirabilis* strains. The phylogenetic tree was constructed based on the SNPs in their core genome with the maximum-likelihood method in FastTree. Strains identified in this study are highlighted in red. The host of the isolate is indicated by triangles (animals), squares (food) or circles (humans). The tree scale indicates substitutions per site.

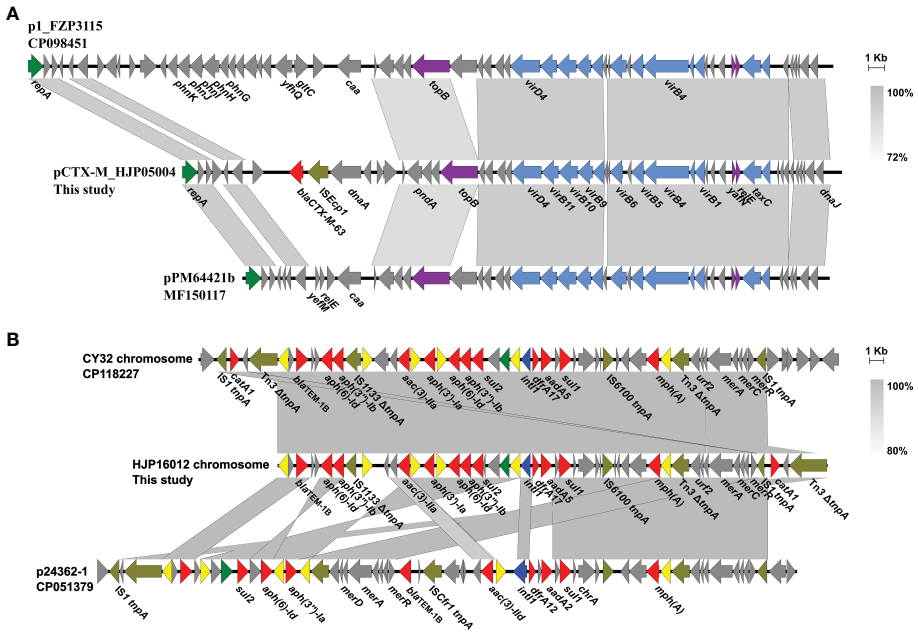

FIGURE 2
Genetic organization of plasmids or plasmid-derived region in MDR *P. mirabilis* strains. **(A)** Comparison of pCTX-M_HJP05004 with p1_FZP3115. Genes are denoted by arrows. $bla_{CTX\text{-}M\text{-}63}$, *ISEcp1*, *repA*, conjugation genes, and maintenance genes are highlighted in red, olive, green, blue, and purple, respectively. Regions of >73% identity are indicated by grey shading. **(B)** Organization of the plasmid-derived region on the chromosome of HJP16012, and comparisons to related regions. Genes are denoted by arrows. ARGs, replication genes, integrase genes, *IS26*, and other transposase genes are highlighted in red, green, blue, yellow, and olive, respectively. Regions of > 80% identity are indicated by grey shading. Δ represents truncated genes.

coverage, >97.1% nucleotide identity) to p1_FZP3115 (CP098451, *P. mirabilis*, patient) from China, and pPM64421b (MF150117, *P. mirabilis*, unknown) from Brazil, indicating global spread of this type of plasmid.

On the chromosome of HJP16012, thirteen ARGs conferring resistance to aminoglycosides (*aadA5*, *aph(6)-Id*, *aph(3")-Ib*, *aph (3')-Ia*, *aac(3)-IIa*, *aph(6)-Id*, *aph(3")-Ib*), β-lactam (bla_{TEM-1B}), macrolide (*mph*(A)), amphenicol (*catA1*), sulphonamides (*sul1*, *sul2*), and trimethoprim (*dfrA17*) are clustered in a 39, 086-bp MDR region, wherein an IncQ1-type replication gene *repA* is present. The MDR region showed high similarity (98% coverage, 99.56% identity) to the one found in a *P. mirabilis* strain CY32 (CP118227, chicken, China), and was partly similar (85% coverage, 99.87% identity) to the plasmid p24362-1 (CP051379) recovering from a *Salmonella enterica* strain from swine in the USA. The result reveals that the MDR regions on the chromosomes of *P. mirabilis* HJP16012 and CY32 seem to be derived from a p24362-1-like plasmid. Further sequence analysis showed that two copies of IS*1* flanked the MDR region in CY32 and HJP16012 (Figure 2B), suggesting a possible role of IS*1*-mediated composite transposon in the integration process (Partridge et al., 2018).

3.5 The resistance genomic islands in MDR *P. mirabilis* strains

In recent years, five *Salmonella* genomic island 1 (SGI1)-relative elements, including SGI1(Ahmed et al., 2006), *Proteus* genomic island 1 (PGI1)(Siebor and Neuwirth, 2014), *Proteus* genomic island 2 (PGI2)(Lei et al., 2018a), GI*Pmi*1(Siebor et al., 2018), and *Pm*GRI1(Lei et al., 2020) have been identified in *P. mirabilis* strains. The presence of SGI-relative elements in our *P. mirabilis* isolates was screened by searching the integrase gene of SGI1 (KM234279), PGI1(KJ411925), PGI2 (MG201402), GI*Pmi*1 (MF490433), and *Pm*GRI1(MW699445) from the whole sequenced genomes. As a result, five (35.71%, 5/14) strains contained the *Pm*GRI1 integrase gene (Table 1). No other integrase genes of SGI1-relative elements were detected in these strains.

*Pm*GRI1 is a multidrug-resistant GI that has been found in several *P. mirabilis* isolates of animal and human origins from different locations in China (Ma et al., 2021; Li et al., 2022). Based on the genome data, the complete sequences of *Pm*GRI1 in strain HJP17012 (*Pm*GRI1-17012) was successfully assembled. *Pm*GRI1-17012 is 40,678 bp in size, and *catA1* is the only known and complete antimicrobial resistance gene (Figure 3). BLASTn analysis showed that the configuration of *Pm*GRI1-17012 is identical to that of *Pm*GRI1-CYPM1 (CP012674), which was recovered from a clinical *P. mirabilis* strain from Taiwan, China, in 2012. Due to possible complex structures or high numbers of transposases and ISs, the complete sequences of *Pm*GRI1 in HJP05004, HJP22021, and HJP20004 were fragmented in two or more contigs. *Pm*GRI1-05004 and *Pm*GRI1-20004 are also possible variants of *Pm*GRI1-CYPM1 as revealed by the existing assembly. *Pm*GRI1-22021 seems to have a more complex genetic structure, with a number of genes, including several ARGs, being inserted upstream and downstream of *tnpA* of Tn21, respectively (Figure 3). Altogether, the presence of *Pm*GRI1 in the tested strains reconfirmed its prevalence in *P. mirabilis* in China, highlighting that *Pm*GRI1 may serve as an important vehicle in capturing and spreading ARGs.

In addition, we detected the presence of SXT/R391 ICEs by targeting the conserved integrase gene (int_{SXT}) and found that ten out of the fourteen (71.4%, 10/14) MDR *P. mirabilis* strains were

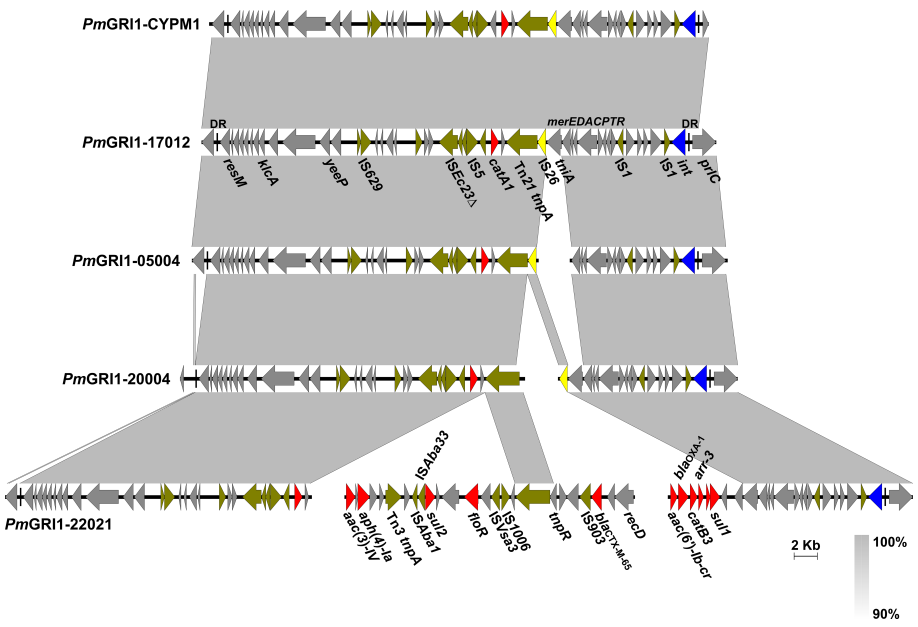

FIGURE 3
Comparative analysis of the *Pm*GRI1 in MDR *P. mirabilis* strains. Genes are denoted by arrows and the direction of transcription is indicated by the arrowheads. ARGs, integrase genes, *IS26*, and other transposase genes are highlighted in red, blue, yellow, and olive, respectively. Regions of >90% identity are indicated by grey shading. Δ represents truncated genes.

positive for the int_{SXT} gene (> 96% identity to that of SXT, AY055428, Table 1). The complete sequences of seven SXT/R391 ICEs were successfully assembled, ranging in size from 91,092 bp to 131,933 bp. Among them, ICE*Pmi*Chn26021, ICE*Pmi*Chn31010, ICE*Pmi*Chn31030, and ICE*Pmi*Chn01027 are almost identical, mainly differing by an insertion or deletion of the *aph(6)-Id* gene (an aminoglycosides resistance gene). BLASTn analysis showed that ICE*Pmi*Chn21049 is similar (94% coverage, 99.96% nucleotide identity) to ICE*Pmi*Chn-HERJC4 (MZ221994) recovering from *P. mirabilis* strain HERJC4 from chicken in China. ICE*Pmi*Chn20004 is closely related (99% coverage, >99.9% identity) to several ICEs of human and animal origins from different locations in China, such as those in *P. mirabilis* strain PM8762 (CP092652, patient, 2021), and *P. mirabilis* strain HBNNC12 (MZ277865, cow, 2018). ICE*Pmi*Chn31006 is nearly identical (99% query coverage, 99.95% identity) to the element ICEPmiJpn1 initially described in Japan (Harada et al., 2010) and was later detected in other parts of the world (Sato et al., 2020), confirming the global spread of this element. The four clonally related ICEs, ICE*Pmi*Chn26021, ICE*Pmi*Chn31010, ICE*Pmi*Chn31030, and ICE*Pmi*Chn01027, showed the highest similarity (94% coverage, 99.95% nucleotide identity) to ICE*Pmi*Chn3105 (Accession no. CP098444), while HJP31010 (or HJP31030, or HJP01027, or HJP26021) is genetically distant from FZP3105 according to the species tree (Figure 1). The results suggest the cryptic dissemination and independent acquisition of MDR ICEs in *P. mirabilis* strains.

3.6 Genetic features of ICEs in MDR *P. mirabilis* strains

Genetic analysis revealed that these ICEs shared a common backbone structure with most SXT/R391 ICEs (Figure 4). Additionally, all ICEs except for ICE*Pmi*Chn31006 contained four hotspots (HS1, HS2, HS4, HS5) and one variable region (VR) III. Their HS4 (*traN-s063*) regions contain 15 to 19 ARGs (encoding for β-lactam, aminoglycoside, fluoroquinolone, fosfomycin, tetracycline, macrolide, sulphonamide, trimethoprim, and rifamycin resistance) that are clustered together in an IS*Ppu12*-mediated composite transposon (Figure 4). The MDR HS4 regions identified in this study are highly similar to each other, with IS*26*-mediated excision/replacement upstream of *tet*(A) and IS*CR2*-mediated insertion of ARGs downstream of *floR* representing two major modular differences of them (Figure S1). These HS4 regions are also similar to that in ICE*Pmi*ChnHBSZC16 (MZ277866, *P. mirabilis*, animal, China), ICE*Eco*ChnXH1815 (CP069386, *E. coli*, patient, China), and ICE*Kpn*ChnQD23 (CP042858, *Klebsiella pneumoniae*, patient, China), suggesting that ICEs may sever as an important vehicle in mediating the accumulation and dissemination of ARGs across bacterial species from different sources. ICE*Pmi*Chn31006 carries no VRIII and MDR HS4, but an HS3 region, with inserted genes encoding a pair of methylcytosine-specific restriction enzyme *mcrBC*. The sole ARG bla_{CMY-2} (encoding β-lactam resistance) in ICE*Pmi*Chn31006 is present in the HS5 region and locates downstream of the truncated IS*Ecp1*, the element assumed to be involved in mobilization and expression of bla_{CMY-2} (Figure 4) (Harada et al., 2010). To determine the transfer ability of these ICEs, we selected four ICE-carrying strains (HJP21049, HJP17012, HJP31006, and HJP26021) for the conjugation experiments. However, no transconjugants were obtained after repeated attempts, despite that conjugative genes were complete. The unsuccessful conjugation might result from the exceptionally low transferability that is below detectable limits.

It has been known that SXT/R391 ICEs have the potential to be transferred and thus are important agents in the dissemination of antimicrobial resistance. SXT/R391 ICEs are commonly detected in

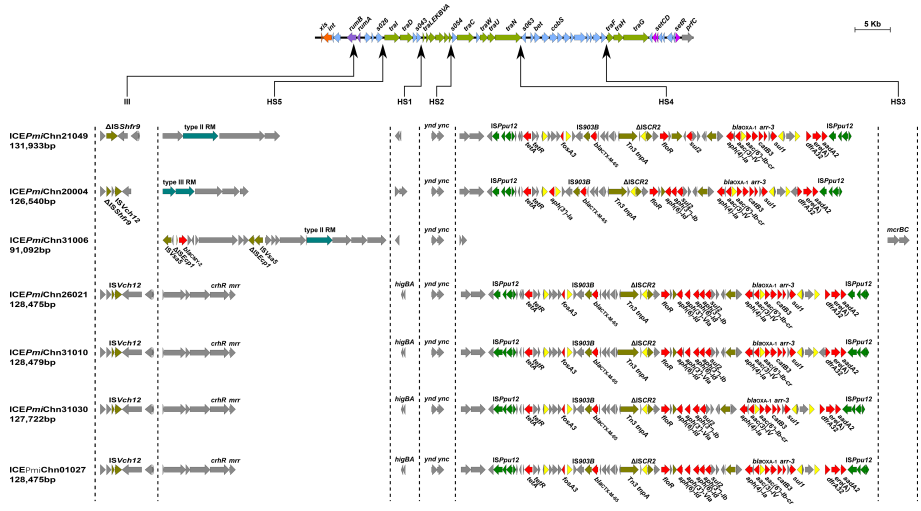

FIGURE 4
Genetic features of the ICEs in MDR *P. mirabilis* strains. The upper line shows the backbone of SXT/R391 ICEs with conserved core genes. Genes are denoted by arrows and those involved in site-specific excision and integration (*xis* and *int*), DNA repair (*rumAB*), conjugative transfer (*tra*), and regulation (*setCDR*) are highlighted in orange, purple, green, and amaranth. Under the backbone, hotspots (HS1-HS5), and variable regions (II-IV) are shown, with thin arrows indicating the sites of their insertion. Other genes in the insertion regions are indicated by light blue arrows. Δ represents truncated genes.

Proteus, as the vehicle of various resistance genes, including several clinically important ARGs, such as $bla_{CTX\text{-}M\text{-}65}$ (Li et al., 2022), $bla_{NDM\text{-}1}$ (He et al., 2021), and *tet*(X6) (Peng et al., 2020). The findings in this study demonstrates highly genetic plasticity in the MDR HS4 region of ICEs carried by *Proteus* strains and further highlights them as a public health threat that requires continuous monitoring.

3.7 Virulence characteristics of MDR *P. mirabilis* strains

All the tested strains produce strong crystalline biofilm in the urine environment and all of them, except for HJP16012, are urease producers (Figures S2, S3). The hemolysis was observed in seven strains, including HJP21049, HJP05004, HJP17012, HJP20004, HJP26021, HJP16012, and HJP31030 (Figure S4). In addition, different degrees of swarming migration on agar surfaces, with diameter lengths of 42 to 80 mm, were observed in these strains (Figure S5). Whether motility is positively correlated with bacterial virulence needs further verification.

The fimbriae of *P. mirabilis* are essential virulence factors in UTIs (Schaffer et al., 2015). In this study, all the MDR *P. mirabilis* strains contained *mrpA* encoding the MR/P fimbriae, which is known to contribute to biofilm formation and virulence. 85.71% (12/14) strains contained the *pmpA* (encoding the *P. mirabilis* P-like fimbria) and 71.42% (10/14) of them contained the uroepithelial cell adhesin (UCA) fimbriae gene *ucaA*, while only two strains (14.29%) had the *Proteus mirabilis* fimbria (PMF) gene *pmfA* (Figure 5). CAUTI is generally initiated by biofilm formation on the urinary catheter (Schaffer et al., 2015). Several factors contribute to *P. mirabilis* biofilm formation *in vitro*, including but not limited to urease, MR/P fimbriae, Pst (phosphate transporter), and RcsD (flagellar regulation) (Schaffer et al., 2015). In addition to *mrpA* as mentioned above, all of the tested strains also contained *ureC* (encoding the urease), *pst*, and *rcsD* (Figure 5). This result provides a possible explanation for the strains' strong biofilms. It is known that flagella are essential for swimming and swarming motility, which is an important characteristic feature of *P. mirabilis* uropathogenesis (Belas and Suvanasuthi, 2005). Some flagella genes, including *flhA* (encoding the flagellar assembly protein), *fliF* (encoding the flagellar MS-ring protein), *fliG* (encoding the flagellar motor switch protein), *fliP* (encoding the flagellar biosynthetic protein), *fliL* (encoding the flagellar basal body-associated protein), and *flgN* (encoding the flagella filament assembly) were identified in all the tested strains. *flaD* (encoding the flagellar capping protein) was absent in HJP05004, HJP17012, and HJP18031, whose swarming abilities, however, were not affected at all, suggesting that *flaD* maybe not very necessary for swarming motility. As previously reported (Cestari et al., 2013), *hpmAB* (encoding the hemolysin HpmA and its secretion protein HpmB) is highly conserved across the tested *P. mirabilis* isolates, whereas only seven of them exhibited hemolytic activity, suggesting an unknown regulatory mechanism is involved. Besides, 78.57% (11/14) of these *P. mirabilis* strains contained the siderophore synthase gene *nrpR*, which is important for colonizing the urinary tract (Schaffer et al., 2015). It was determined that non-fimbrial adhesins AipA (adhesion and invasion autotransporter) and Pta (*Proteus* toxic agglutinin) are required for invading and colonizing of *P. mirabilis* in the bladder (Armbruster et al., 2018). All of the tested strains carried *pta*, and four (28.57%) of them had *aipA* (Figure 5). Taken together, these results demonstrate a number of virulence genes associated with bacterial pathogenicity in these MDR *P. mirabilis* strains, revealing the virulence potential of them.

4 Conclusion

In conclusion, this study revealed that ESBL genes are commonly detected in MDR *P. mirabilis* isolates in this hospital, whereas carbapenemase genes are rare. SXT/R391 ICEs, followed by SG1-relative GIs (*Pm*GRI1 in our case) represent major vehicles in mediating the dissemination of ARGs in *P. mirabilis* isolates. Plasmids also contribute to the resistance spread but to a lesser extent. Worryingly, the revelation of virulence-related phenotypes and the presence of abundant virulence genes in these MDR *P. mirabilis* strains pose an urgent threat to public health. Therefore, to better deal with infections caused by this species, close surveillance of the prevalence of MDR strains and related mobile elements from clinical is urgently recommended.

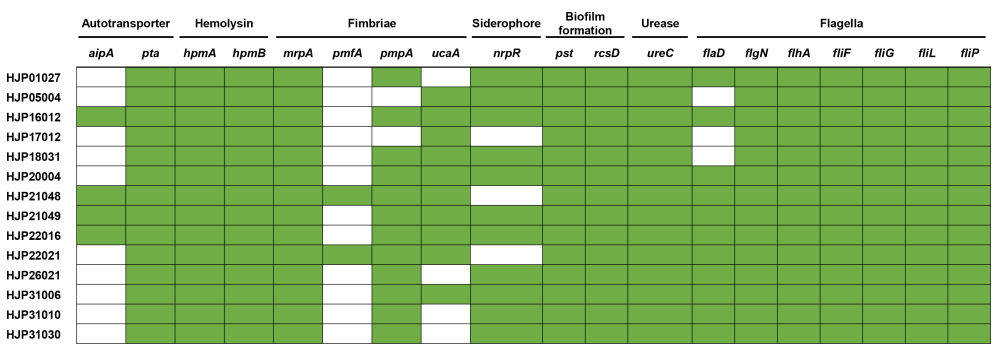

FIGURE 5
Heatmap of genes related to major bacterial virulence factors. These virulence-associated genes among the isolates are denoted by filled squares (green) for presence and empty squares for absence.

Data availability statement

The datasets presented in this study can be found in online repositories. The names of the repository/repositories and accession number(s) can be found in the article/Supplementary Material.

Author contributions

YL: conceptualization, formal analysis and writing-original draft. MY, CF and YF: methodology, resources and formal analysis. XD: software. WZ: resources, writing-review and editing. LZ: conceptualization, writing-review and editing, and supervision. All authors contributed to the article and approved the submitted version.

Funding

This work was supported by the Scientific and technological project in Sichuan Province (2022JDRC0144), Project supported by the Joint Funds of the People's Hospital of Hejiang and Southwest Medical University Natural Science Foundation (2021HJXNYD09 and 2021HJXNYD07). The funders had no role in study design, data collection and interpretation, or the decision to submit the work for publication.

Conflict of interest

The authors declare that the research was conducted in the absence of any commercial or financial relationships that could be construed as a potential conflict of interest.

Publisher's note

Supplementary material

The Supplementary Material for this article can be found online at: https://www.frontiersin.org/articles/10.3389/fcimb.2023.1229194/full#supplementary-material

References

Ahmed, A. M., Hussein, A. I. A., and Shimamoto, T. (2006). *Proteus mirabilis* clinical isolate harbouring a new variant of *Salmonella* genomic island 1 containing the multiple antibiotic resistance region. *J. Antimicrobial Chemother* 59 (2), 184–190. doi: 10.1093/jac/dkl471

Armbruster, C. E., Mobley, H. L. T., and Pearson, M. M. (2018). Pathogenesis of *Proteus mirabilis* infection. *EcoSal Plus* 8 (1). doi: 10.1128/ecosalplus.ESP-0009-2017

Bankevich, A., Nurk, S., Antipov, D., Gurevich, A. A., Dvorkin, M., Kulikov, A. S., et al. (2012). SPAdes: a new genome assembly algorithm and its applications to single-cell sequencing. *J. Comput. Biol.* 19 (5), 455–477. doi: 10.1089/cmb.2012.0021

Belas, R., and Suvanasuthi, R. (2005). The ability of *Proteus mirabilis* to sense surfaces and regulate virulence gene expression involves FliL, a flagellar basal body protein. *J. Bacteriol* 187 (19), 6789–6803. doi: 10.1128/JB.187.19.6789-6803.2005

Bolger, A. M., Lohse, M., and Usadel, B. (2014). Trimmomatic: a flexible trimmer for Illumina sequence data. *Bioinformatics* 30 (15), 2114–2120. doi: 10.1093/bioinformatics/btu170

Bortolaia, V., Kaas, R. S., Ruppe, E., Roberts, M. C., Schwarz, S., Cattoir, V., et al. (2020). ResFinder 4.0 for predictions of phenotypes from genotypes. *J. Antimicrob. Chemother.* 75 (12), 3491–3500. doi: 10.1093/jac/dkaa345

Carattoli, A., and Hasman, H. (2020). PlasmidFinder and in silico pMLST: identification and typing of plasmid replicons in whole-genome sequencing (WGS). *Methods Mol. Biol.* 2075, 285–294. doi: 10.1007/978-1-4939-9877-7_20

Cestari, S. E., Ludovico, M. S., Martins, F. H., da Rocha, S. P. D., Elias, W. P., and Pelayo, J. S. (2013). Molecular detection of HpmA and HlyA hemolysin of uropathogenic *Proteus mirabilis*. *Curr. Microbiol.* 67 (6), 703–707. doi: 10.1007/s00284-013-0423-5

Chen, L., Yang, J., Yu, J., Yao, Z., Sun, L., Shen, Y., et al. (2005). VFDB: a reference database for bacterial virulence factors. *Nucleic Acids Res.* 33 (Database issue), D325–D328. doi: 10.1093/nar/gki008

CLSI (2023). "Performance Standards for Antimicrobial Susceptibility Testing," in *CLSI supplement M100, 33th ed* (Wayne, PA, USA: Clinical and Laboratory Standards Institute).

Durgadevi, R., Abirami, G., Alexpandi, R., Nandhini, K., Kumar, P., Prakash, S., et al. (2019a). Explication of the potential of 2-hydroxy-4-methoxybenzaldehyde in hampering uropathogenic *Proteus mirabilis* crystalline biofilm and virulence. *Front. Microbiol.* 10. doi: 10.3389/fmicb.2019.02804

Durgadevi, R., Veera Ravi, A., Alexpandi, R., Krishnan Swetha, T., Abirami, G., Vishnu, S., et al. (2019b). Virulence targeted inhibitory effect of linalool against the exclusive uropathogen *Proteus mirabilis*. *Biofouling* 35 (5), 508–525. doi: 10.1080/08927014.2019.1619704

Falagas, M. E., and Karageorgopoulos, D. E. (2008). Pandrug resistance (PDR), extensive drug resistance (XDR), and multidrug resistance (MDR) among Gram-negative bacilli: need for international harmonization in terminology. *Clin. Infect. Dis.* 46 (7), 1121–1122. doi: 10.1086/528867

Girlich, D., Bonnin, R. A., Dortet, L., and Naas, T. (2020). Genetics of acquired antibiotic resistance genes in *Proteus* spp. *Front. Microbiol.* 11. doi: 10.3389/fmicb.2020.00256

Hamilton, A. L., Kamm, M. A., Ng, S. C., and Morrison, M. (2018). *Proteus* spp. as putative gastrointestinal pathogens. *Clin. Microbiol. Rev.* 31 (3), e00085-17. doi: 10.1128/CMR.00085-17

Harada, S., Ishii, Y., Saga, T., Tateda, K., and Yamaguchi, K. (2010). Chromosomally encoded bla_{CMY-2} located on a novel SXT/R391-related integrating conjugative element in a *Proteus mirabilis* clinical isolate. *Antimicrob. Agents Chemother.* 54 (9), 3545–3550. doi: 10.1128/AAC.00111-10

He, J., Sun, L., Zhang, L., Leptihn, S., Yu, Y., and Hua, X. (2021). A Novel SXT/R391 Integrative and Conjugative Element Carries Two Copies of the bla_{NDM-1} Gene in *Proteus mirabilis*. *mSphere* 6 (4), e0058821. doi: 10.1128/mSphere.00588-21

He, D., Wang, L., Zhao, S., Liu, L., Liu, J., Hu, G., et al. (2020). A novel tigecycline resistance gene, *tet*(X6), on an SXT/R391 integrative and conjugative element in a *Proteus genomospecies* 6 isolate of retail meat origin. *J. Antimicrob. Chemother.* 75 (5), 1159–1164. doi: 10.1093/jac/dkaa012

Holling, N., Lednor, D., Tsang, S., Bissell, A., Campbell, L., Nzakizwanayo, J., et al. (2014). Elucidating the genetic basis of crystalline biofilm formation in *Proteus mirabilis*. *Infect. Immun.* 82 (4), 1616–1626. doi: 10.1128/IAI.01652-13

Hua, X., Zhang, L., Moran, R. A., Xu, Q., Sun, L., van Schaik, W., et al. (2020). Cointegration as a mechanism for the evolution of a KPC-producing multidrug resistance plasmid in *Proteus mirabilis*. *Emerg. Microbes Infect.* 9 (1), 1206–1218. doi: 10.1080/22221751.2020.1773322

Kong, L.-H., Xiang, R., Wang, Y.-L., Wu, S.-K., Lei, C.-W., Kang, Z.-Z., et al. (2020). Integration of the bla_{NDM-1} carbapenemase gene into a novel SXT/R391 integrative and conjugative element in *Proteus vulgaris*. *J. Antimicrobial Chemother* 75 (6), 1439–1442. doi: 10.1093/jac/dkaa068

Korytny, A., Riesenberg, K., Saidel-Odes, L., Schlaeffer, F., and Borer, A. (2016). Bloodstream infections caused by multi-drug resistant *Proteus mirabilis*: Epidemiology, risk factors and impact of multi-drug resistance. *Infect. Dis. (Lond)* 48 (6), 428–431. doi: 10.3109/23744235.2015.1129551

Kwok, C. T., and Hitchins, M. P. (2015). Allele quantification pyrosequencing(R) at designated SNP sites to detect allelic expression imbalance and loss-of-heterozygosity. *Methods Mol. Biol.* 1315, 153–171. doi: 10.1007/978-1-4939-2715-9_12

Lane, D. J. (1991). 16S/23S rRNA sequencing. *Nucleic Acid techniques bacterial systematics*, 115–175.

Lei, C. W., Chen, Y. P., Kang, Z. Z., Kong, L. H., and Wang, H. N. (2018b). Characterization of a Novel SXT/R391 Integrative and Conjugative Element Carrying cfr, $bla_{CTX-M-65}$, *fosA3*, and *aac(6′)-Ib-cr* in *Proteus mirabilis*. *Antimicrob. Agents Chemother.* 62 (9), e00849-18. doi: 10.1128/AAC.00849-18

Lei, C.-W., Chen, Y.-P., Kong, L.-H., Zeng, J.-X., Wang, Y.-X., Zhang, A.-Y., et al. (2018a). PGI2 is a novel SGI1-relative multidrug-resistant genomic island characterized in *Proteus mirabilis*. *Antimicrobial Agents chemother* 62 (5), e00019–e00018. doi: 10.1128/AAC.00019-18

Lei, C. W., Yao, T. G., Yan, J., Li, B. Y., Wang, X. C., Zhang, Y., et al. (2020). Identification of *Proteus* genomic island 2 variants in two clonal *Proteus mirabilis* isolates with coexistence of a novel genomic resistance island *Pm*GRI1. *J. Antimicrob. Chemother.* 75 (9), 2503–2507. doi: 10.1093/jac/dkaa215

Lei, C. W., Zhang, A. Y., Wang, H. N., Liu, B. H., Yang, L. Q., and Yang, Y. Q. (2016). Characterization of SXT/R391 integrative and conjugative elements in *Proteus mirabilis* isolates from food-producing animals in China. *Antimicrob. Agents Chemother.* 60 (3), 1935–1938. doi: 10.1128/AAC.02852-15

Li, Y., Cao, S., Zhang, L., Lau, G. W., Wen, Y., Wu, R., et al. (2016b). A tolC-like protein of *Actinobacillus pleuropneumoniae* is involved in antibiotic resistance and biofilm formation. *Front. Microbiol.* 7. doi: 10.3389/fmicb.2016.01618

Li, X., Du, Y., Du, P., Dai, H., Fang, Y., Li, Z., et al. (2016a). SXT/R391 integrative and conjugative elements in *Proteus* species reveal abundant genetic diversity and multidrug resistance. *Sci. Rep.* 6, 37372. doi: 10.1038/srep37372

Li, Y., Liu, Q., Qiu, Y., Fang, C., Zhou, Y., She, J., et al. (2022). Genomic characteristics of clinical multidrug-resistant *Proteus* isolates from a tertiary care hospital in southwest China. *Front. Microbiol.* 13. doi: 10.3389/fmicb.2022.977356

Li, Y., Qiu, Y., She, J., Wang, X., Dai, X., and Zhang, L. (2021). Genomic Characterization of a *Proteus* sp. Strain of Animal Origin Co-Carrying bla_{NDM-1} and *lnu* (G). *Antibiotics* 10 (11), 1411. doi: 10.3390/antibiotics10111411

Ma, W. Q., Han, Y. Y., Zhou, L., Peng, W. Q., Mao, L. Y., Yang, X., et al. (2022). Contamination of *Proteus mirabilis* harbouring various clinically important antimicrobial resistance genes in retail meat and aquatic products from food markets in China. *Front. Microbiol.* 13. doi: 10.3389/fmicb.2022.1086800

Ma, B., Wang, X., Lei, C., Tang, Y., He, J., Gao, Y., et al. (2021). Identification of three novel *pm*GRI1 genomic resistance islands and one multidrug resistant hybrid structure of tn7-like transposon and *pm*GRI1 in *Proteus mirabilis*. *Antibiotics (Basel)* 10 (10), 1268. doi: 10.3390/antibiotics10101268

Partridge, S. R., Kwong, S. M., Firth, N., and Jensen, S. O. (2018). Mobile genetic elements associated with antimicrobial resistance. *Clin. Microbiol. Rev.* 31 (4), e00088-17. doi: 10.1128/CMR.00088-17

Pearson, M. M., and Mobley, H. L. (2008). Repression of motility during fimbrial expression: identification of 14 *mrpJ* gene paralogues in *Proteus mirabilis*. *Mol. Microbiol.* 69 (2), 548–558. doi: 10.1111/j.1365-2958.2008.06307.x

Peng, K., Li, R., He, T., Liu, Y., and Wang, Z. (2020). Characterization of a porcine *Proteus cibarius* strain co-harbouring *tet*(X6) and *cfr*. *J. Antimicrob. Chemother.* 75 (6), 1652–1654. doi: 10.1093/jac/dkaa047

Price, M. N., Dehal, P. S., and Arkin, A. P. (2010). FastTree 2–approximately maximum-likelihood trees for large alignments. *PloS One* 5 (3), e9490. doi: 10.1371/journal.pone.0009490

Qu, X., Zhou, J., Huang, H., Wang, W., Xiao, Y., Tang, B., et al. (2022). Genomic investigation of *Proteus mirabilis* isolates recovered from pig farms in Zhejiang province, China. *Front. Microbiol.* 13. doi: 10.3389/fmicb.2022.952982

Richter, M., Rosselló-Móra, R., Oliver Glöckner, F., and Peplies, J. (2016). JSpeciesWS: a web server for prokaryotic species circumscription based on pairwise genome comparison. *Bioinformatics* 32 (6), 929–931. doi: 10.1093/bioinformatics/btv681

Rutherford, J. C. (2014). The emerging role of urease as a general microbial virulence factor. *PloS Pathog.* 10 (5), e1004062. doi: 10.1371/journal.ppat.1004062

Sato, J. L., Fonseca, M. R. B., Cerdeira, L. T., Tognim, M. C. B., Sincero, T. C. M., Noronha do Amaral, M. C., et al. (2020). Genomic analysis of SXT/R391 integrative conjugative elements from *Proteus mirabilis* isolated in Brazil. *Front. Microbiol.* 11. doi: 10.3389/fmicb.2020.571472

Schaffer, J. N., Pearson, M. M., Mulvey, M. A., Stapleton, A. E., and Klumpp, D. J. (2015). *Proteus mirabilis* and urinary tract infections. *Microbiol. Spectr.* 3 (5). doi: 10.1128/microbiolspec.UTI-0017-2013

Seemann, T. (2014). Prokka: rapid prokaryotic genome annotation. *Bioinformatics* 30 (14), 2068–2069. doi: 10.1093/bioinformatics/btu153

Shaaban, M., Elshaer, S. L., and Abd El-Rahman, O. A. (2022). Prevalence of extended-spectrum beta-lactamases, AmpC, and carbapenemases in *Proteus mirabilis* clinical isolates. *BMC Microbiol.* 22 (1), 247. doi: 10.1186/s12866-022-02662-3

Siebor, E., de Curraize, C., and Neuwirth, C. (2018). Genomic context of resistance genes within a French clinical MDR *Proteus mirabilis*: identification of the novel genomic resistance island GIPmi1. *J. Antimicrob. Chemother.* 73 (7), 1808–1811. doi: 10.1093/jac/dky126

Siebor, E., and Neuwirth, C. (2014). *Proteus* genomic island 1 (PGI1), a new resistance genomic island from two *Proteus mirabilis* French clinical isolates. *J. Antimicrobial Chemother* 69 (12), 3216–3220. doi: 10.1093/jac/dku314

Siguier, P., Perochon, J., Lestrade, L., Mahillon, J., and Chandler, M. (2006). ISfinder: the reference centre for bacterial insertion sequences. *Nucleic Acids Res.* 34 (Database issue), D32–D36. doi: 10.1093/nar/gkj014

Sullivan, M. J., Petty, N. K., and Beatson, S. A. (2011). Easyfig: a genome comparison visualizer. *Bioinformatics* 27 (7), 1009–1010. doi: 10.1093/bioinformatics/btr039

Wasfi, R., Hamed, S. M., Amer, M. A., and Fahmy, L. I. (2020). *Proteus mirabilis* biofilm: development and therapeutic strategies. *Front. Cell Infect. Microbiol.* 10. doi: 10.3389/fcimb.2020.00414

Wozniak, R. A., Fouts, D. E., Spagnoletti, M., Colombo, M. M., Ceccarelli, D., Garriss, G., et al. (2009). Comparative ICE genomics: insights into the evolution of the SXT/R391 family of ICEs. *PloS Genet.* 5 (12), e1000786. doi: 10.1371/journal.pgen.1000786

Zong, Z., Partridge, S. R., and Iredell, J. R. (2010). IS*Ecp1*-mediated transposition and homologous recombination can explain the context of $bla_{(CTX-M-62)}$ linked to *qnrB2*. *Antimicrob. Agents Chemother.* 54 (7), 3039–3042. doi: 10.1128/AAC.00041-10

frontiers | Frontiers in Cellular and Infection Microbiology

TYPE Original Research
PUBLISHED 25 August 2023
DOI 10.3389/fcimb.2023.1227063

OPEN ACCESS

EDITED BY
Luis Esau Lopez Jacome,
Instituto Nacional de Rehabilitación, Mexico

REVIEWED BY
Ulises Garza-Ramos,
National Institute of Public Health, Mexico
Jossue Mizael Ortiz-Álvarez,
National Council of Science and Technology (CONACYT), Mexico

*CORRESPONDENCE
Junjie Ying
652868133@qq.com
Tianhong Ma
15990312207@163.com

†These authors have contributed equally to this work

RECEIVED 22 May 2023
ACCEPTED 31 July 2023
PUBLISHED 25 August 2023

CITATION
Tian C, Song J, Ren L, Huang D, Wang S, Fu L, Zhao Y, Bai Y, Fan X, Ma T and Ying J (2023) Complete genetic characterization of carbapenem-resistant *Acinetobacter johnsonii*, co-producing NDM-1, OXA-58, and PER-1 in a patient source. *Front. Cell. Infect. Microbiol.* 13:1227063. doi: 10.3389/fcimb.2023.1227063

Complete genetic characterization of carbapenem-resistant *Acinetobacter johnsonii*, co-producing NDM-1, OXA-58, and PER-1 in a patient source

Chongmei Tian[1†], Jianqin Song[2†], Lingzhi Ren[3], Delian Huang[4], Siwei Wang[5], Liping Fu[1], Yaping Zhao[1], Yongfeng Bai[6], Xueyu Fan[6], Tianhong Ma[7*] and Junjie Ying[8*]

[1]Department of Pharmacy, Shaoxing Hospital of Traditional Chinese Medicine Affiliated to Zhejiang Chinese Medical University, Shaoxing, Zhejiang, China, [2]Department of Traditional Chinese Medicine, Hangzhou Linping District Hospital of Integrated Chinese and Western Medicine, Hangzhou, China, [3]Department of Clinical Laboratory, The People's Hospital of Zhangqiu Area, Jinan, China, [4]School of Medical Technology and Information Engineering, Zhejiang Chinese Medical University, Hangzhou, China, [5]Core Facility, The Quzhou Affiliated Hospital of Wenzhou Medical University, Quzhou People's Hospital, Quzhou, China, [6]Department of Clinical Laboratory, The Quzhou Affiliated Hospital of Wenzhou Medical University, Quzhou People's Hospital, Quzhou, China, [7]Department of Pharmacy, Jiaxing Hospital of Traditional Chinese Medicine, Jiaxing, China, [8]Department of Urology, The Quzhou Affiliated Hospital of Wenzhou Medical University, Quzhou People's Hospital, Quzhou, China

The emergence of carbapenemase-producing *Acinetobacter* spp. has been widely reported and become a global threat. However, carbapenem-resistant *A. johnsonii* strains are relatively rare and without comprehensive genetic structure analysis, especially for isolates collected from human specimen. Here, one *A. johnsonii* AYTCM strain, co-producing NDM-1, OXA-58, and PER-1 enzymes, was isolated from sputum in China in 2018. Antimicrobial susceptibility testing showed that it was resistant to meropenem, imipenem, ceftazidime, ciprofloxacin, and cefoperazone/sulbactam. Whole-genome sequencing and bioinformatic analysis revealed that it possessed 11 plasmids. bla_{OXA-58} and bla_{PER-1} genes were located in the pAYTCM-1 plasmid. Especially, a complex class 1 integron consisted of a 5′ conserved segment (5′ CS) and 3′ CS, which was found to carry sul1, arr-3, qnrVC6, *and* bla_{PER-1} cassettes. Moreover, the bla_{NDM-1} gene was located in 41,087 conjugative plasmids and was quite stable even after 70 passages under antibiotics-free conditions. In addition, six prophage regions were identified. Tracking of closely related plasmids in the public database showed that pAYTCM-1 was similar to pXBB1-9, pOXA23_010062, pOXA58_010030, and pAcsw19-2 plasmids, which were collected from the strains of sewage in China. Concerning the pAYTCM-3 plasmids, results showed that strains were collected from different sources and their hosts were isolated from various countries, such as China, USA, Japan, Brazil, and Mexico, suggesting that a wide spread occurred all over the world. In conclusion, early surveillance is warranted to avoid the extensive spread of this high-risk clone in the healthcare setting.

KEYWORDS

***Acinetobacter johnsonii*, carbapenem resistance, NDM-1, OXA-58, PER-1, integron**

Introduction

Acinetobacter spp. are ubiquitous in nature and are usually identified in the hospital environment, and some of these species have been reported in a variety of nosocomial infections (Wong et al., 2017). The most common species to cause infections is *A. baumannii*, followed by *A. calcoaceticus* and *A. lwoffii*. However, *A. johnsonii*, a kind of potentially opportunistic pathogen in *Acinetobacter* spp., generally distributed in natural or nosocomial environments, such as agricultural soil (Wang et al., 2019; Jia et al., 2021).

Carbapenems are the main antimicrobial agents for the treatment of infections with multidrug-resistant *Acinetobacter* spp., including *A. johnsonii* (Tang et al., 2020). However, the problem of carbapenem resistance is being increasingly reported, which has contributed to a huge challenge for clinicians (Bonnin et al., 2014). The carbapenem resistance mechanism was usually mediated via enzymatic inactivation (such as carbapenemases), efflux pump overexpression, and target site modification (i.e., altered penicillin-binding proteins) (Mohd Rani et al., 2017; Castanheira et al., 2023). Upon previous studies, more than 210 β-lactamases have been identified in *Acinetobacter* spp. with class D β-lactamases being the most widespread carbapenemase (Mohd Rani et al., 2017), including OXA-23, OXA-24, and OXA-58 (Liu et al., 2021). Moreover, several insertion sequence (IS) elements such as IS*Aba1* and IS*Aba3* could increase the expression of class D β-lactamase genes (including $bla_{\text{OXA-58}}$-like and $bla_{\text{OXA-23}}$-like genes) when they were found upstream of these IS elements (Mohd Rani et al., 2017).

Considering the increasing resistance to carbapenems and almost all other antimicrobial agents, *Acinetobacter* spp. are important resistant microorganisms with a global public health threat, which are associated with severe nosocomial infections including pneumonia, urinary tract, bloodstream, and wound infections (Gonzalez-Villoria and Valverde-Garduno, 2016). However, limited knowledge concerning the carbapenem resistance was known in *A. johnsonii* strains. Until now, researchers only reported some genome sequences and described the features of *A. johnsonii* strains which are isolated from the environment, especially in hospital sewage (Feng et al., 2016; Zong et al., 2020). However, little is known about this species which was collected from a patient source in the hospital. Here, we investigated the genetic characteristics of one carbapenem-resistant *A. johnsonii*, co-producing NDM-1, OXA-58, and PER-1 in a patient's sputum in 2018 in China. To the best of our knowledge, this is the first comprehensive description of one carbapenem-resistant *A. johnsonii* from a patient source.

Materials and methods

Bacterial isolation and identification of the *A. johnsonii* AYTCM strain

A flowchart is shown in Figure S1 (Behzadi and Gajdacs, 2021). *A. johnsonii* AYTCM strain was isolated from sputum in China in 2018. Isolate identification was conducted using matrix-assisted laser desorption ionization-time of flight mass spectrometry (MALDI-TOF MS, Bruker Daltonik GmbH, Bremen, Germany) and further confirmed by PCR and 16S rRNA (GenBank ID: NR_164627.1) gene-based sequencing with specific primers 27F (5′-agagtttgatcctggctcag-3′) and 1492R (5′-ggttaccttgttacgactt-3′) (Zong et al., 2020).

Minimum inhibitory concentration measurement

Antimicrobial susceptibility testing (AST) was performed by the broth microdilution method and interpreted based on the recommendations of Clinical and Laboratory Standards Institute (CLSI) 2021 guidelines and European Committee on Antimicrobial Susceptibility Testing (EUCAST) 2021 breakpoint tables for tigecycline. The antimicrobial agents used in this study were shown as follows: ceftazidime (CAZ), cefoperazone/sulbactam (CFS), imipenem (IPM), meropenem (MEM), ciprofloxacin (CIP), amikacin (AMI), colistin (COL), tigecycline (TGC), and cefiderocol (CFDC). *Escherichia coli* ATCC 25922 served as the quality control strain.

Mating experiments

To determine whether the plasmids carrying $bla_{\text{NDM-1}}$, $bla_{\text{OXA-58}}$, and $bla_{\text{PER-1}}$ were transferable, conjugation experiments using *E. coli* J53 (sodium azide resistant) as the recipient strain were carried out using the filter mating method (Yang et al., 2021). Transconjugants were screened on Mueller–Hinton (MH) agar plates containing sodium azide (100 mg/L) and meropenem (2 mg/L). The identity of putative transconjugants was confirmed via PCR and MALDI-TOF MS.

Stability experiments of plasmids carrying $bla_{\text{NDM-1}}$, $bla_{\text{OXA-58}}$, or $bla_{\text{PER-1}}$ genes

A. johnsonii AYTCM strain was grown overnight at 37°C in 2 mL of Luria broth (LB) without antibiotics, followed by serial passage of 2-μL overnight culture into the 2-mL LB (1:1,000) each day, with a yield 10 generations, lasting for 7 days (Tian et al., 2022). On the last day, samples were collected and streaked onto antibiotic-free MHA plates. Colonies were selected randomly, and the presence of $bla_{\text{NDM-1}}$, $bla_{\text{OXA-58}}$, or $bla_{\text{PER-1}}$ genes was confirmed by PCR with specific primers.

Whole-genome sequencing, assembly, quality control, and annotation

Genomic DNA was extracted from *A. johnsonii* AYTCM strain using Qiagen Mini Kit (Qiagen, Germany) and Gentra® Puregene® Yeast/Bact. Kit (Qiagen, Germany) for Illumina and Nanopore sequencing, respectively. For trimming, quality control, and quality assessment of raw reads, fastp v 0.20.1 was used (Chen

et al., 2018). *De novo* assembly of the reads of Illumina and MinION was constructed using Unicycler v0.4.8 (Wick et al., 2017). The assembly sequence was assessed via QUAST v 5.0.2 (Gurevich et al., 2013). Genome sequence annotation was conducted using the National Center for Biotechnology Information (NCBI) Prokaryotic Genome Annotation Pipeline (PGAP) (http://www.ncbi.nlm.nih.gov/genome/annotation_prok/) and the Rapid Annotation of microbial genomes using Subsystems Technology (RAST) server (Overbeek et al., 2014; Tatusova et al., 2016). Annotation function was further compared with *A. johnsonii* C6 (accession no. FUUY00000000) and MB44 (accession no. LBMO00000000) strains (Tian et al., 2016; Kaas et al., 2017).

Bioinformatics analysis

Antimicrobial resistance genes were identified using the ABRicate program (https://github.com/tseemann/abricate) based on the ResFinder database (http://genomicepidemiology.org/) (Zankari et al., 2012). Bacterial virulence factors were identified using the virulence factor database (VFDB, http://www.mgc.ac.cn/VFs/) (Liu et al., 2022a). Average nucleotide identity (ANI) analysis with *A. johnsonii* C6 (accession no. FUUY00000000) and MB44 (accession no. LBMO00000000) strains was conducted using an ANI calculator (http://enve-omics.ce.gatech.edu/ani/index) (Luis and Konstantinos, 2016), and genome-based phylogenetic reconstruction with *A. johnsonii*, *A. baumannii*, *A. pittii*, and *A. seifertii* strains was further performed using the BacWGSTdb server (Marquez-Ortiz et al., 2017; Feng et al., 2021). Insertion sequences (ISs) were identified with ISfinder (Siguier et al., 2006). Conjugation transfer elements, including the origin site of DNA transfer (*oriT*), type IV secretion system (T4SS), type IV coupling protein (T4CP), and relaxase-related encoding genes, were predicted using *oriT*finder with default parameter settings (Li et al., 2018). PHAge Search Tool (PHAST) was utilized for the prediction of bacteriophages (Zhou et al., 2011). Typing of plasmids was performed based on a previous description (Lam et al., 2023). The plasmid structure was visualized using DNAPlotter (https://www.sanger.ac.uk/tool/dnaplotter/) (Carver et al., 2009). Plasmid comparisons were conducted using the Circoletto tool (http://tools.bat.infspire.org/circoletto/) (Darzentas, 2010). Similar plasmids in *Acinetobacter* spp., *Providencia rettgeri*, and *Klebsiella pneumoniae* were tracked using the BacWGSTdb server (Marquez-Ortiz et al., 2017; Feng et al., 2021).

Results

Genome annotations and subsystem categories

Genome was annotated using PGAP and RAST. Based on PGAP annotation, there are 3,980 genes in total, of which 3,731 are protein-coding genes, 136 are pseudo genes, and the remaining 113 are predicted RNA-coding genes. Compared with the PGAP server, 4,182 genes, including 109 RNA-coding genes, belonged to 293 subsystems when annotated using RAST. The statistics of the subsystem is shown (Figure 1). Most of them belonged to metabolism (427), amino acids and derivatives (252), and carbohydrates (130). Additionally, 14 CDS were sorted into "Phages, transposable elements, plasmids" and only 2 and 1 CDS belonged to "cell division and cell cycle" and "dormancy and sporulation," respectively. Functional comparison showed that most subsystems were metabolism among three *A. johnsonii* strains. However, a huge difference was found in "Phages, Prophages, Transposable elements, Plasmids". There are two CDS that belonged to "Phages, Prophages, Transposable elements, Plasmids" in *A. johnsonii* C6 and MB44 strains. However, 14 subsystems of this function were identified in *A. johnsonii* AYTCM strain.

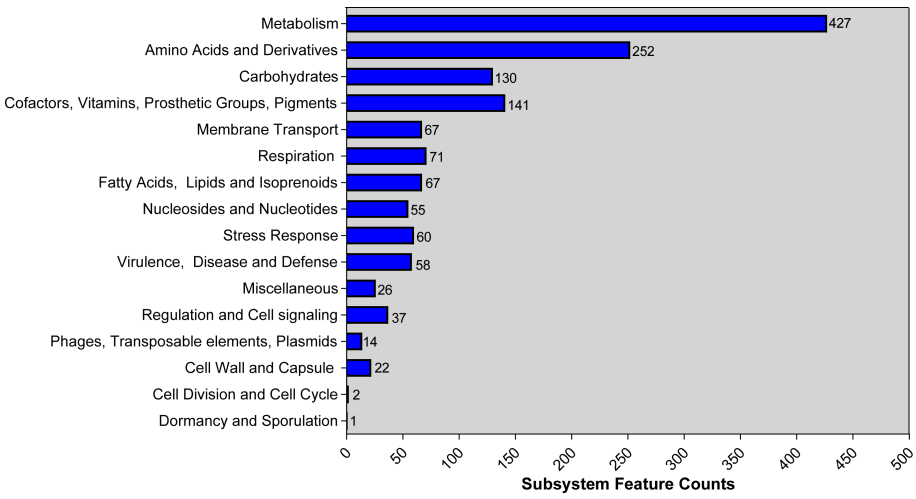

FIGURE 1
RAST annotation of *A. johnsonii* AYTCM strain. The number of each subsystem category is shown on the right of column.

MICs, antimicrobial resistance, and virulence profiles

Antimicrobial susceptibility testing revealed that *A. johnsonii* AYTCM strain possessed a multidrug-resistant (MDR) profile and the meropenem and imipenem MICs are all >128 mg/L. Furthermore, it exhibited resistance to ceftazidime (>128 mg/L), ciprofloxacin (>32 mg/L), and cefoperazone/sulbactam (128 mg/L) but still remained susceptible to tigecycline (1 mg/L) and cefiderocol (<0.03 mg/L). The MICs of colistin and amikacin are 2 mg/L and 32 mg/L, respectively, which were defined as intermediate.

Analysis of the genome of *A. johnsonii* AYTCM strain revealed that, in addition to co-harboring chromosomal $bla_{\text{OXA-652}}$ and *aadA27*, a series of other antibiotic resistance genes were identified, including $bla_{\text{OXA-58}}$, $bla_{\text{NDM-1}}$, $bla_{\text{PER-1}}$, msr*(E)*, mph *(E)*, aac(3)-IId, aph(3′)-VIa, sul1, arr-3, qnrVC6, *ble-MBL*, *aph (3′)-VI, tet*(39), *sul2*, and bla_{MCA} (Table 1). However, only two virulence factors, two-component regulatory system *bfmRS* involved in Csu expression and *lpxC*-encoding lipopolysaccharide (LPS), were found in AYTCM strain.

ANI, core-genome phylogeny, lipooligosaccharide outer core, and capsular polysaccharide (KL)

According to the ANI analysis, the result showed that 95.82% two-way ANI between *A. johnsonii* AYTCM and *A. johnsonii* C6 and 95.86% ANI were found between *A. johnsonii* AYTCM and *A. johnsonii* MB44 and only 79.89% two-way ANI between *A. johnsonii* AYTCM and *A. baumannii* ATCC 17978. Core-genome phylogeny analysis showed a close genetic relationship among *A. johnsonii* AYTCM, C6, and MB44 strains. However, a huge diversity was observed among *A. baumannii*, *A. pittii*, and other *A. seifertii* strains based on the phylogenetic tree (Figure S2A). Similar results of SNP difference are shown in Figure S2B.

Kaptive revealed that AYTCM strain contains OC locus 1c (OCL-1c), matching the 92.01% nucleotide identity. The K locus in *A. johnsonii* AYTCM strain is KL19, to which it matches with an overall nucleotide identity of 72.75%.

Transfer ability and stability of plasmids in the *A. johnsonii* AYTCM strain

Mating assays were performed to explore the transfer ability of $bla_{\text{NDM-1}}$, $bla_{\text{OXA-58}}$, and $bla_{\text{PER-1}}$ genes; results showed that only $bla_{\text{NDM-1}}$ could transfer to the recipient strain. The stability assays revealed that all three resistance genes were quite stable even after 70 passages under antibiotics-free conditions.

Genome characterization of the chromosome and 11 plasmids

Hybrid assembly of the short and long reads generated a 3,567,832-bp size circular chromosome with a GC content of 41.60% (Table 1). One intrinsic resistance gene, $bla_{\text{OXA-652}}$, was identified in the chromosome. Of note, *A. johnsonii* AYTCM strain carries 11 plasmids, namely, pAYTCM-1 to pAYTCM-11, with sizes between 2,356 bp and 378,197 bp and GC contents ranging from 34.38% to 42.44% (Table 1). Apart from pAYTCM-2, pAYTCM-5, pAYTCM-9, pAYTCM-10, and pAYTCM-11, various kinds of resistance genes were found in other plasmids. Analysis of *rep* genes showed that only pAYTCM-7 possessed one identified name with Aci1.

TABLE 1 Molecular characterization of the genome of *A. johnsonii* AYTCM strain.

Genome	Replicon	Size (bp)	GC content	Resistance genes	Accession numbers
Chromosome	ND	3,567,832	41.60%	$bla_{\text{OXA-652}}$, *aadA27*	CP121776
pAYTCM-1	ND	378,197	39.93%	$bla_{\text{OXA-58}}$, msr*(E)*, mph*(E)*, aac(3)-IId, aph(3′)-VIa, sul1, arr-3, qnrVC6, $bla_{\text{PER-1}}$	CP121777
pAYTCM-2	ND	44,599	36.89%	ND	CP121778
pAYTCM-3	ND	41,087	38.32%	$bla_{\text{NDM-1}}$, *ble-MBL*, *aph(3′)-VI*	CP121779
pAYTCM-4	ND	22,357	35.15%	msr*(E)*, mph*(E)*	CP121780
pAYTCM-5	ND	13,499	35.78%	ND	CP121781
pAYTCM-6	ND	8,636	35.47%	*tet*(39)	CP121782
pAYTCM-7	Aci1	7,579	38.88%	*sul2*	CP121783
pAYTCM-8	ND	6,289	34.38%	bla_{MCA}	CP121784
pAYTCM-9	ND	6,147	37.17%	ND	CP121785
pAYTCM-10	ND	4,135	42.44%	ND	CP121786
pAYTCM-11	ND	2,356	36.54%	ND	CP121787

ND, not detected.

10.3389/fcimb.2023.1227063

Genetic context characterization of pAYTCM-1 multidrug-resistant plasmid

pAYTCM-1 is a huge 378,197-bp multidrug-resistant plasmid with an average GC content of 39.93%. It comprises different regions, including type IV secretion system (T4SS) region, class 1 integron region, and mercury resistance region (Figure 2A). bla_{OXA-58} and bla_{PER-1} genes were located in the pAYTCM-1 plasmid. Concerning the genetic context of bla_{OXA-58}, three intact and one truncated IS*Ajo2* were located upstream or downstream. 9-bp TSD sequences were observed in the upstream and downstream of IS*Ajo2* genetic elements. Nevertheless, the TSD sequences were all different (Figure 2B). Importantly, a complex class 1 integron complex consisted of a 5′ conserved segment (5′ CS) and 3′ CS, which was found to carry sul1, arr-3, qnrVC6, *and* bla_{PER-1} cassettes (Figure 2C). Of note, 10 XerC and XerD-like binding sites (p*dif* sites) were found in the pAYTCM-1 plasmid (Table 2). In addition, no *oriT* was identified in the pAYTCM-1 plasmid and no transconjugants were obtained via conjugation. Moreover, results of the Circoletto tool showed that there were many similar segments

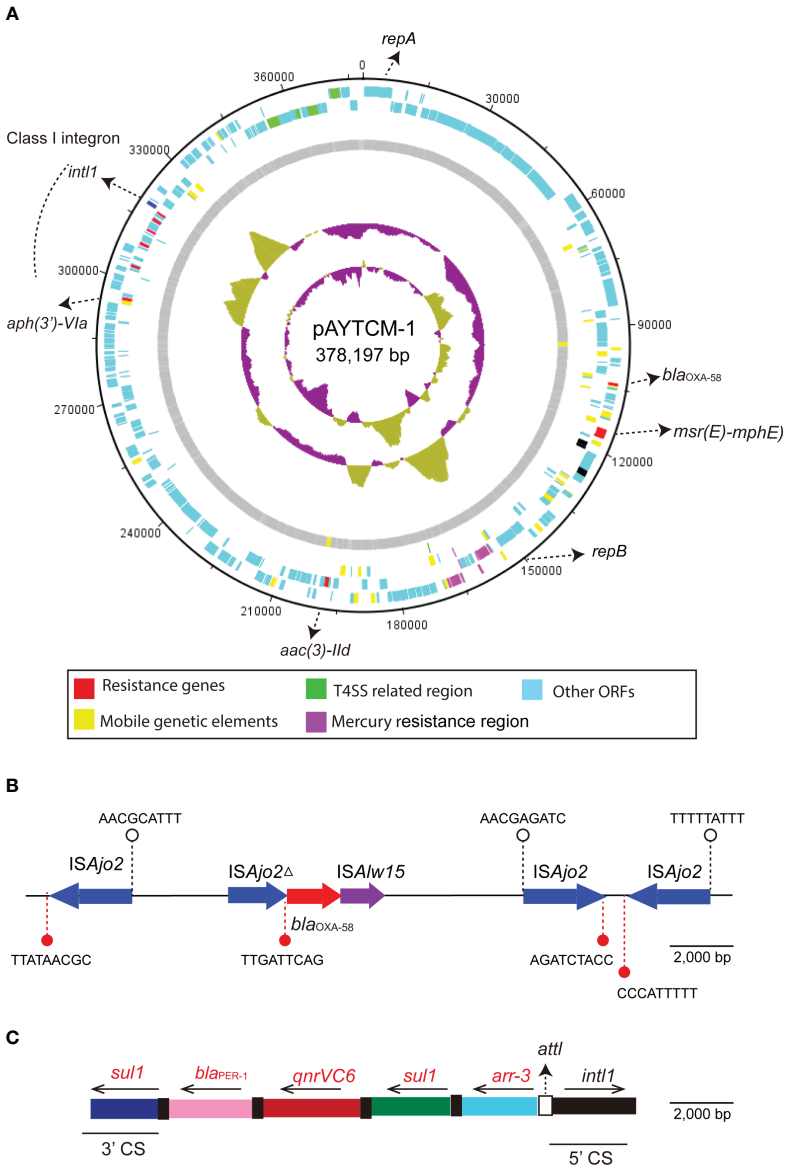

FIGURE 2
Circular map and genetic environment of the pAYTCM-1 plasmid. **(A)** Circular map of the pAYTCM-1 plasmid. Different filled boxes indicate various open reading frames (ORFs). The GC content and GC skew are shown in the inner rings. Resistance genes (red filled boxes), mobile genetic elements (yellow filled boxes), T4SS region (green filled boxes), and mercury resistance region (purple filled boxes). Light blue represents other ORFs. **(B)** Genetic environment of the bla_{OXA-58} gene. The red filled arrow indicates the position of the bla_{OXA-58} gene. Blue filled arrows indicate IS*Ajo2* and IS*Ajo2Δ*. Purple filled arrow indicates IS*Alw15*. Arrows' directions indicate the ORF directions. 9-bp target site duplications (TSD) are shown upstream and downstream of IS*Ajo2* and IS*Ajo2Δ* using white or red filled circles, respectively. **(C)** Structure of the class 1 integron containing bla_{PER-1}. *intI1* is shown as a black filled box. attI is shown as a white filled box. The 5′ conserved segment (5′ CS) and 3′ CS of class 1 integron are labeled. The various kinds of resistance genes were shown as different colors with the names labeled above with the orientation indicated by thin black arrows.

10.3389/fcimb.2023.1227063

TABLE 2 *pdif* sites of the pAYTCM-1 plasmid.

Name	Start	End	Left arm	Center	Right arm	Site
pdif1	97,630	97,657	ATTTCGTATAA	GGTGTA	TTATGTTAATT	C|D
pdif2	99,839	99,866	GATTCGTATAA	GGTGTA	TTATGTTAATT	D|C
pdif3	101,969	101,996	ATTTAACATAA	TGGCTG	TTATACGAAAC	C|D
pdif4	106,222	106,249	ATTTTGTATAA	GGTGTA	TTATGTTAATT	D|C
pdif5	107,789	107,816	ATTTAACATAA	TGGGCG	TTATACGAAAA	C|D
pdif6	108,640	108,667	ACTTCGCATAA	CGCCCA	TTATGTTAATT	D|C
pdif7	109,282	109,309	ACTTAACATAA	TGGCGG	TTATACGAAAT	C|D
pdif8	110,501	110,528	ATTTAACATAA	TGGCTG	TTATGCGAACG	D|C
pdif9	117,181	117,208	ATTTAACATAA	AATTTC	TTATGTGAAGT	C|D
pdif10	260,147	260,174	AATCTAGATAA	TTAGCA	ATATACGATAT	D|C

between pAYTCM-1 and pXBB1-9 (GenBank accession number: CP010351) plasmids (Figure 3). Genetic structure comparison revealed that 98% coverage and 99.91% identity were identified between pAYTCM-1 and pXBB1-9 plasmids, which was found in the *A. johnsonii* XBB1 isolate from a hospital sewage in 2010 in Chengdu, western China.

Genetic features of bla_{NDM-1}-carrying plasmid pAYTCM-3

The bla_{NDM-1} carbapenem gene was located in 41,087 plasmids with the GC content of 38.32%. Genetic context analysis revealed that bla_{NDM-1} was IS*Aba14-aph(3′)-VI*-IS*Aba125-bla*$_{NDM-1}$-*ble*-

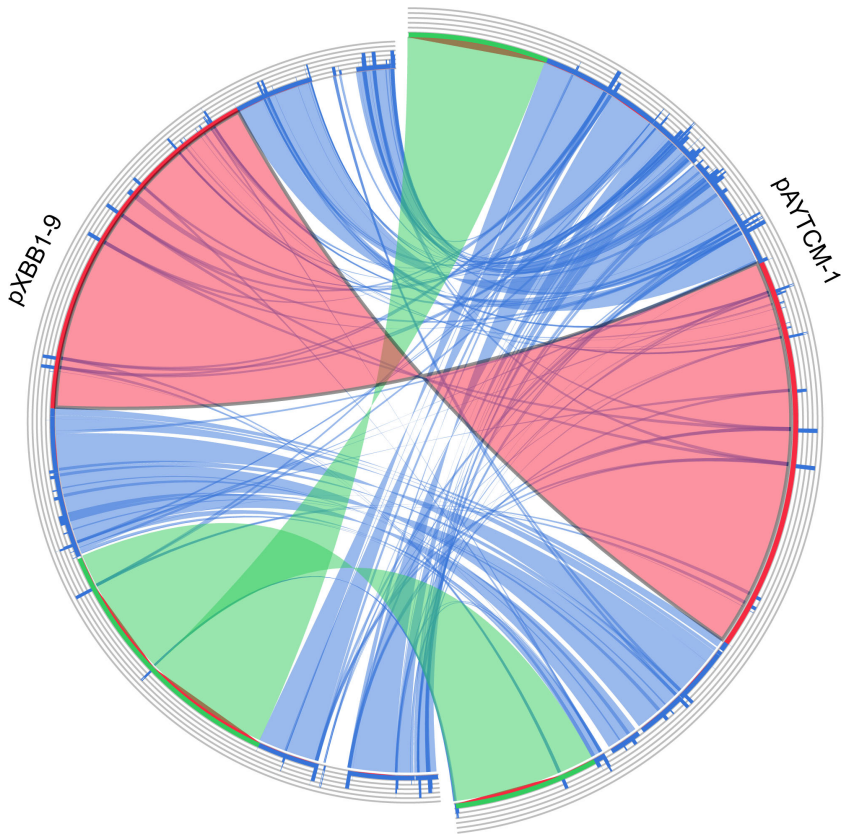

FIGURE 3
Plasmid comparison with pXBB1-9 using Circoletto. Ribbons represent the alignments produced by BLAST, their width the alignment length, and the colors the alignment bitscore in four quartiles: blue for the first 25% of the maximum bitscore, green for the next 25%, orange for the third, and finally red for the top bitscores of between 75% and 100%.

10.3389/fcimb.2023.1227063

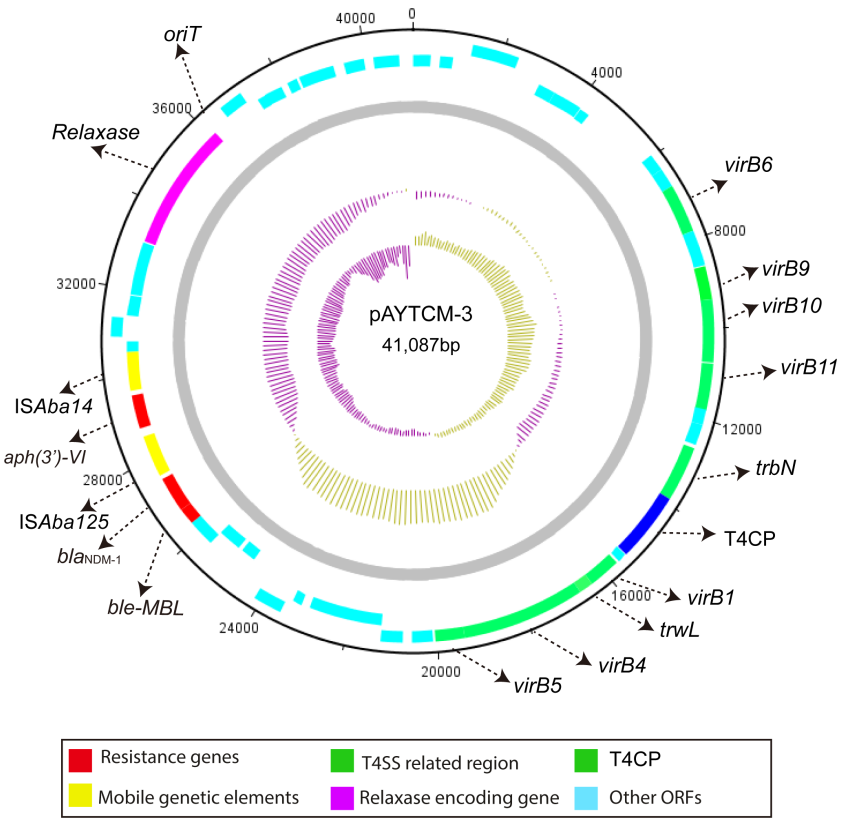

FIGURE 4
Circular map of pAYTCM-3. Different filled boxes indicate various open reading frames (ORFs). The GC content and GC skew are shown in the inner rings. Resistance genes are shown as a red filled box. Mobile genetic elements are shown as a yellow filled box. The T4SS region and T4CP are indicated as a green filled box. The relaxase-encoding gene is shown in the purple filled box. Light blue represents other ORFs. Moreover, the position of *oriT* was also labeled.

MBL (Figure 4). Moreover, a T4SS region, T4CP, a gene encoding relaxase, and a 38-bp *oriT* region (AGGGATTCATAAG GGAATTATTCCCTTATGTGGGGCTT) were identified. pAYTCM-3 could transfer to *E. coli* J53 via conjugation.

Prophage regions in the chromosome

Prophage regions were predicted by the PHASTER tool; results showed two intact, two questionable, and two incomplete regions in the chromosome (Figure 5A). Based on the PHASTER tool, regions 4 and 5 were predicted to be intact due to the score of >90. In addition, regions 1 and 6 were classified as questionable due to the scores of 70–90. However, regions 2 and 3 were shown as incomplete due to the low scores. Gene functions of the two intact and two questionable prophage regions are shown, including attachment, phage integration, and cell lysis (Figure 5B).

Track and characteristics of closely related plasmids in the public database

To track the closely related plasmids from different countries, a wide search was performed via the BacWGSTdb server. Data showed that pAYTCM-1 was similar to pXBB1-9, pOXA23_010062, pOXA58_010030, and pAcsw19-2 plasmids (Table 3). Their sizes are all >300 kb, and they were collected from the strains of sewage in China. However, the species were various, including *A. johnsonii*, *A. wuhouensis*, and *A. defluvii*.

Concerning the closely related plasmids of pAYTCM-3, results showed that hosts, also carrying the bla_{NDM-1}-related plasmid, were collected from several different sources, including feces, blood, sputum, pus, sewage, and hospital environment, from 2005 to 2023. These bla_{NDM-1}-harboring plasmids were all collected in *Acinetobacter* spp. and not in *P. rettgeri* and *K. pneumoniae*. Their hosts were isolated from various countries, such as China, USA, Japan, Brazil, and Mexico.

Discussion

Emergence of carbapenemase-producing *Acinetobacter* spp. has become dominant in several countries, and it is being increasingly considered a quite important nosocomial pathogen and poses a huge challenge to the healthcare setting (Mohd Rani et al., 2017). Class D β-lactamases (mainly OXA-23), commonly named as OXA, are responsible for carbapenem resistance in *Acinetobacter* spp. species (Zong et al., 2020). However, the reports of other β-

10.3389/fcimb.2023.1227063

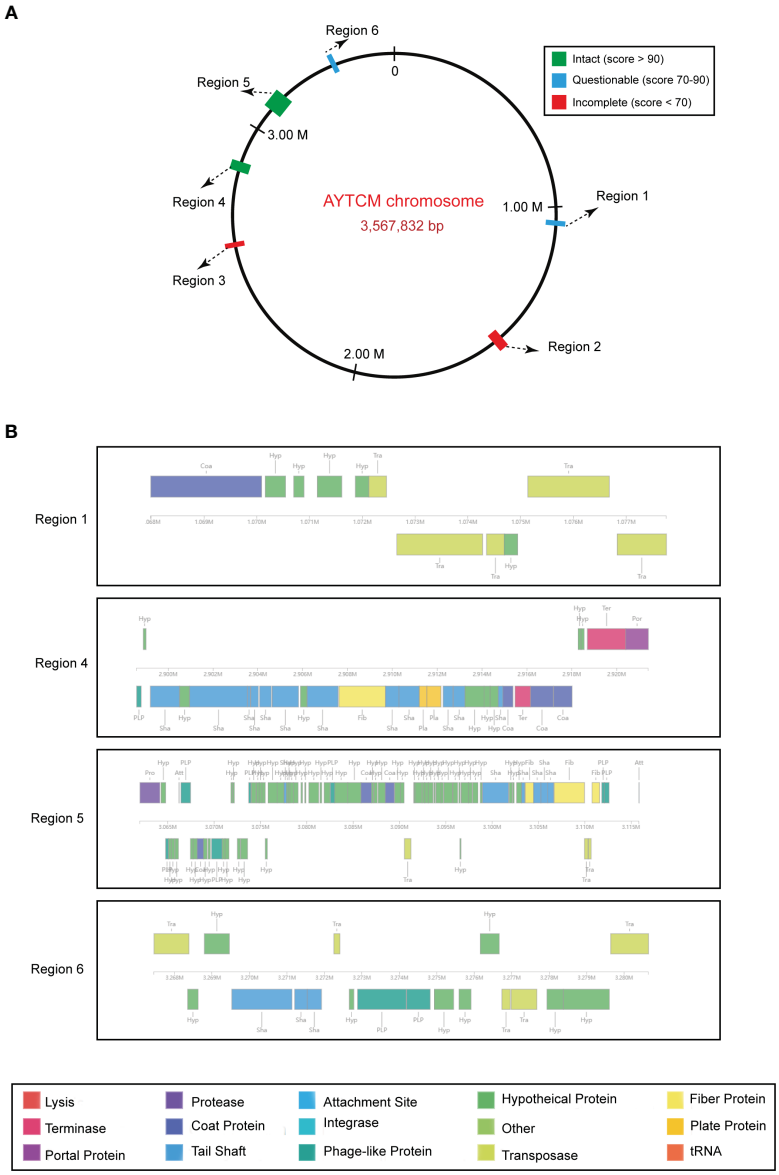

FIGURE 5
Predicted prophage regions within the *A johnsonii* AYTCM chromosome. **(A)** Six prophage regions positions in the chromosome. Green filled boxes mean the intact prophage regions (score > 90), filled boxes mean the questionable prophage regions (score 70–90), filled boxes mean the incomplete prophage regions (score < 70). **(B)** Structure of two intact and two questionable prophage regions. Genes are colored based on predicted functions.

lactamases (e.g., NDM-1) are relatively rare, especially for those with a high resistance level. In this work, NDM-1 and OXA-58 were found in our strain, which leads to a high-level carbapenem resistance. To promote better understanding regarding the genomic features of our *A. johnsonii* strain, whole-genome sequencing and further RAST software were used to classify the different CDS into subsystems based on their function. Consistent with other *A. pittii* strains, the majority of the CDS belong to the function of "Metabolism" (Chapartegui-Gonzalez et al., 2022).

Mobile genetic elements (MGEs), including ISs, integrons, and transposons, play a particularly important role in the movement and dissemination of resistance genes (Gorbunova et al., 2021). Concerning the acquisition of the bla_{OXA-58} gene, many copies of IS*Ajo2* were identified in the pAYTCM-1 plasmid and located upstream and downstream of bla_{OXA-58}. Nevertheless, considering the various 9-bp TSD sequences of IS*Ajo2*, we failed to find direct evidence to conclude that bla_{OXA-58} was embedded into the plasmid via different IS*Ajo2*. Interestingly, XerC/XerD-like recombinase sites (p*dif* sites) were considered as a new approach for the transfer of carbapenem resistance genes, such as bla_{OXA-24}, bla_{OXA-72}, and bla_{OXA-58} (Merino et al., 2010; Kuo et al., 2016; Liu et al., 2021). Here, 10 p*dif* sites were identified in the pAYTCM-1

TABLE 3 Track of similar plasmids using the BacWGSTdb database.

Plasmid name	Accession number	Size (bp)	Species	Host	Source	Country	Year	Antimicrobial resistance genes
pXBB1-9	NZ_CP010351.1	398,857	*A. johnsonii*	–	Sewage	China	2010	*arr-3*, *aac(3)-IId*, *aac(6')-Ib*, *aph(3'')-Ib*, *aph(3')*-VIa, *aph(6)-Id*, bla_{OXA-58}, bla_{PER-1}, *mph*(E), *msr*(E), *sul1*, *tet*(Y)
pOXA23_010062	NZ_CP033130.1	311,749	*A. wuhouensis*	–	Sewage	China	2015	*aac(3)-IId*, *aph(3')*-VIa, bla_{OXA-23}, bla_{OXA-58}, *mph*(E), *msr*(E)
pOXA58_010030	NZ_CP029396.2	355,358	*A. defluvii*	–	sewage	China	2015	*arr-3*, *aac(6')-Ib3*, *aph(3')*-VIa, bla_{OXA-58}, *mph*(E), *msr*(E), *sul1*, *sul2*
pAcsw19-2	NZ_CP043309.1	351,885	*A. johnsonii*	–	sewage	China	2019	*aph(3')-VIa*, bla_{NDM-1}, bla_{OXA-58}, *mph*(E), *msr*(E)
pNDM-JN01	KM210086.1	41,084	*A. lwoffii*	Homo sapiens	Feces	China	2023	*aph(3')-VI*, bla_{NDM-14}
pAB17	MT002974.1	41,087	*A. baumannii*	Homo sapiens	–	Brazil	2023	*aph(3')-VI*, bla_{NDM-1}
unnamed2	NZ_CP027532.1	41,087	*A. baumannii*	–	–	USA	2018	*aph(3')-VI*, bla_{NDM-1}
p4TQ-NDM	NZ_CP045130.1	41,086	*A. indicus*	Cow	Feces	China	2017	*aph(3')-VI*, bla_{NDM-1}
pNDM-AP	KJ003839.1	39,364	*A. pittii*	Homo sapiens	Blood	China	–	*aph(3')-VI*, bla_{NDM-1}
pSU1805NDM	LC483156.1	41,022	*A. pittii*	–	Hospital environment	Japan	–	*aph(3')-VI*, bla_{NDM-1}
pIEC38057	MK053934.1	41,085	*A. nosocomialis*	–	Blood	Brazil	2016	*aph(3')-VI*, bla_{NDM-1}
pNDM-0285	NZ_CP026127.1	39,359	*A. baumannii*	–	–	USA	2016	*aph(3')-VI*, bla_{NDM-1}
p18TQ-NDM	NZ_CP045133.1	40,439	*A. indicus*	Cow	Feces	China	2017	*aph(3')-VI*, bla_{NDM-1}
p23TQ-NDM	NZ_CP045197.1	41,393	*A. indicus*	Cows	Feces	China	2017	*aph(3')-VI*, bla_{NDM-1}
pNDM-AB	NC_020818.1	47,098	*A. baumannii*	Pig	Lung	China	–	*aph(3')-VI*, bla_{NDM-1}, *mph*(E), *msr*(E)
pXM1	AMXH01000087.1	47,274	*A. pittii*	Homo sapiens	Sputum	China	2010	*aph(3')-VI*, bla_{NDM-1}
pNDM-BJ01	NC_019268.1	47,274	*A. lwoffii*	–	–	China	2011	*aph(3')-VI*, bla_{NDM-1}
pNDM-BJ02	NC_019281.1	46,165	*A. lwoffii*	–	–	China	2011	*aph(3')-VI*, bla_{NDM-1}
p6200-47.274kb	NZ_CP010399.1	47,274	*A. baumannii*	Homo sapiens	Bodily fluid	Colombia	2012	*aph(3')-VI*, bla_{NDM-1}
pAbNDM-1	NC_019985.2	48,368	*A. baumannii*	–	–	China	–	*aph(3')-VI*, bla_{NDM-1}
p6411-9.012kb	NZ_CP010370.2	47,274	*A. nosocomialis*	Homo sapiens	Excreted bodily substance	Colombia	2012	*aph(3')-VI*, bla_{NDM-1}
pAhaeAN54e	NZ_CP041229.1	45,460	*A. haemolyticus*	Homo sapiens	Peritoneal dialysis fluid	Mexico	2016	*aph(3')-VI*, bla_{NDM-1}
pNDM-Iz4b	NC_025000.1	46,570	*A. lwoffii*	Homo sapiens	–	China	–	*aph(3')-VI*, bla_{NDM-1}
pNDM1_060092	NZ_CP035935.1	48,560	*A. cumulans*	–	Sewage	China	2018	*aph(3')-VI*, bla_{NDM-1}
pNDM-40-1	NC_023322.1	45,826	*A. bereziniae*	Homo sapiens	Pus	India	2005	*aph(3')-VI*, bla_{NDM-1}
pNDM1_010005	NZ_CP032132.1	39,357	*A. chinensis*	–	Sewage	China	2015	*aph(3')-VI*, bla_{NDM-1}

"-" means unknown.

plasmid. Furthermore, we observed that the bla_{OXA-58} gene was flanked by two p*dif* sites. Consequently, the bla_{OXA-58} gene might have been introduced by p*dif* site-mediated specific recombination. This is consistent with previous research (Feng et al., 2016). Moreover, considering the high coverage and identity with pXBB1-9 (Feng et al., 2016), we deduced that the pAYTCM-1 plasmid may come from a hospital environment-related *A. johnsonii* isolate XBB1 strain and underwent slight evolution. Another finding in this study is that bla_{PER-1} was also located in the pAYTCM-1 plasmid. Liu et al. reported that the production of PER-1 in *A. baumannii* is the key mechanism of cefiderocol resistance (Liu et al., 2022b). However, the MIC of cefiderocol was low and considered as susceptible in our *A. johnsonii* AYTCM strain. We inferred that the resistance in *A. baumannii* was caused by species specificity.

In our previous study, we reported that bla_{NDM-1} was located in the chromosome, which was mediated by two IS*Aba125*-based Tn*125* composite transposons, highlighting the importance of Tn*125*-mediated transfer of bla_{NDM-1} resistance determinants (Tian et al., 2022). However, we could not find the composite Tn*125* transposon in the *A. johnsonii* AYTCM strain due to that only one copy of IS*Aba125* was identified. In addition, two studies from Krahn et al. and Abouelfetouh et al. showed that prophages may play a key role in the carbapenem resistance genes, such as bla_{NDM-1} and bla_{OXA-23} (Krahn et al., 2016; Abouelfetouh et al., 2022). In addition, a study demonstrated the presence of resistance genes (including *mcr-1* and *vanA*) in the phage fraction and its role on the acquisition and transfer of these resistance genes (Pires et al., 2023). However, the bla_{NDM-1} gene is not part of any of the prophages. Hence, the relationship of these prophages and the bla_{NDM-1} gene should be further confirmed through induced experiments. Concerning the bla_{NDM-1}-harboring plasmids, we discovered that they were located in diverse sources and hosts and in various countries. These data indicated that a wide spread of bla_{NDM-1}-bearing plasmids has occurred all over the world. However, these plasmids usually transferred among different *Acinetobacter* species. Concerning the various resistance plasmids in *A. johnsonii* AYTCM strain, it is revealed that our strain has great potential to capture plasmids that contribute to its resistance. Since our strain is of patient origin, there may be a great possibility that this strain will emerge and further spread between patients and the environment in the hospital. More importantly, Lam et al. reported that the Aci1 plasmid usually was found in extensively and pan-resistant *A. baumannii* isolates which belong to global clones GC1 and GC2 (Lam et al., 2023). Here, the Aci1 plasmid has been identified in *A. johnsonii* strain, further suggesting that the Aci1 plasmid has transferred among various *Acinetobacter* species.

Apart from resistance determinants, virulence factors should also be paid attention in bacteria. However, the low content of virulence factors in *A. johnsonii* AYTCM strain is in clear contrast to the high number of resistance genes. Thus, in the surveillance of *A. johnsonii*, researchers should probably pay more attention to the antimicrobial resistance when compared with virulence. This is a different aspect from the hypervirulent carbapenem-resistant *K. pneumoniae* (Pu et al., 2023).

Conclusion

This study is the first comprehensive description for the complete genome characteristics of a carbapenem-resistant *A. johnsonii*, co-producing NDM-1, OXA-58, and PER-1 from a patient source. The *A. johnsonii* isolate AYTCM carried 11 plasmids, which revealed great genome plasticity for this species, which possesses huge potential to capture resistance plasmids. Moreover, the Aci1 plasmid has been identified in *A. johnsonii* strain using the current plasmid typing system. However, other eight plasmids failed to type. Therefore, the *rep* genes for the plasmid typing system need to be further explored. Early surveillance of this kind of carbapenem-resistant isolate is warranted to avoid the extensive spread of this high-risk clone in the healthcare setting.

Data availability statement

The original contributions presented in the study are publicly available. This data can be found here: https://www.ncbi.nlm.nih.gov/; PRJNA953498.

Ethics statement

This study was approved by the local Ethics Committees of the Hospital with a waiver of informed consent since this study mainly focused on bacterial genome and the retrospective nature of the study.

Author contributions

CT and JS designed the experiments, analyzed the data, and wrote the initial manuscript. CT, LR, DH, SW, LF, YZ, and YB performed the majority of the experiments. JS collected the bacteria. XF, TM, and JY supervised this study and reviewed and edited the paper. All authors read and approved the final version of the manuscript.

Funding

This work was supported by the Medical Health Science and Technology Project of Zhejiang Provincial Health Commission (2023KY1270, 2022RC278); Natural Science Foundation of Zhejiang Province (LQ19H160002), Quzhou technology projects, China (2019K36); and Zhejiang Province Traditional Chinese Medicine Science and Technology Project (2023ZL729).

Conflict of interest

The authors declare that the research was conducted in the absence of any commercial or financial relationships that could be construed as a potential conflict of interest.

Publisher's note

All claims expressed in this article are solely those of the authors and do not necessarily represent those of their affiliated organizations, or those of the publisher, the editors and the reviewers. Any product that may be evaluated in this article, or claim that may be made by its manufacturer, is not guaranteed or endorsed by the publisher.

Supplementary material

The Supplementary Material for this article can be found online at: https://www.frontiersin.org/articles/10.3389/fcimb.2023.1227063/full#supplementary-material

References

Abouelfetouh, A., Mattock, J., Turner, D., Li, E., and Evans, B. A. (2022). Diversity of carbapenem-resistant Acinetobacter baumannii and bacteriophage-mediated spread of the Oxa23 carbapenemase. *Microb. Genom* 8. doi: 10.1099/mgen.0.000752

Behzadi, P., and Gajdacs, M. (2021). Writing a strong scientific paper in medicine and the biomedical sciences: a checklist and recommendations for early career researchers. *Biol. Futur.* 72, 395–407. doi: 10.1007/s42977-021-00095-z

Bonnin, R. A., Docobo-Perez, F., Poirel, L., Villegas, M. V., and Nordmann, P. (2014). Emergence of OXA-72-producing Acinetobacter pittii clinical isolates. *Int. J. Antimicrob. Agents* 43, 195–196. doi: 10.1016/j.ijantimicag.2013.10.005

Carver, T., Thomson, N., Bleasby, A., Berriman, M., and Parkhill, J. (2009). DNAPlotter: circular and linear interactive genome visualization. *Bioinformatics* 25, 119–120. doi: 10.1093/bioinformatics/btn578

Castanheira, M., Mendes, R. E., and Gales, A. C. (2023). Global epidemiology and mechanisms of resistance of Acinetobacter baumannii-calcoaceticus complex. *Clin. Infect. Dis.* 76, S166–S178. doi: 10.1093/cid/ciad109

Chapartegui-Gonzalez, I., Lazaro-Diez, M., and Ramos-Vivas, J. (2022). Genetic resistance determinants in clinical Acinetobacter pittii genomes. *Antibiotics (Basel)* 11. doi: 10.3390/antibiotics11050676

Chen, S., Zhou, Y., Chen, Y., and Gu, J. (2018). fastp: an ultra-fast all-in-one FASTQ preprocessor. *Bioinformatics* 34, i884–i890. doi: 10.1093/bioinformatics/bty560

Darzentas, N. (2010). Circoletto: visualizing sequence similarity with Circos. *Bioinformatics* 26, 2620–2621. doi: 10.1093/bioinformatics/btq484

Feng, Y., Yang, P., Wang, X., and Zong, Z. (2016). Characterization of Acinetobacter johnsonii isolate XBB1 carrying nine plasmids and encoding NDM-1, OXA-58 and PER-1 by genome sequencing. *J. Antimicrob. Chemother.* 71, 71–75. doi: 10.1093/jac/dkv324

Feng, Y., Zou, S., Chen, H., Yu, Y., and Ruan, Z. (2021). BacWGSTdb 2.0: a one-stop repository for bacterial whole-genome sequence typing and source tracking. *Nucleic Acids Res.* 49, D644–D650.

Gonzalez-Villoria, A. M., and Valverde-Garduno, V. (2016). Antibiotic-resistant Acinetobacter baumannii increasing success remains a challenge as a nosocomial pathogen. *J. Pathog.* 2016, 7318075. doi: 10.1155/2016/7318075

Gorbunova, V., Seluanov, A., Mita, P., Mckerrow, W., Fenyo, D., Boeke, J. D., et al. (2021). The role of retrotransposable elements in ageing and age-associated diseases. *Nature* 596, 43–53. doi: 10.1038/s41586-021-03542-y

Gurevich, A., Saveliev, V., Vyahhi, N., and Tesler, G. (2013). QUAST: quality assessment tool for genome assemblies. *Bioinformatics* 29, 1072–1075. doi: 10.1093/bioinformatics/btt086

Jia, J., Guan, Y., Li, X., Fan, X., Zhu, Z., Xing, H., et al. (2021). Phenotype profiles and adaptive preference of Acinetobacter johnsonii isolated from Ba River with different environmental backgrounds. *Environ. Res.* 196, 110913. doi: 10.1016/j.envres.2021.110913

Kaas, R. S., Mordhorst, H., Leekitcharoenphon, P., Dyring Jensen, J., Haagensen, J., Molin, S., et al. (2017). Draft genome sequence of Acinetobacter johnsonii C6, an environmental isolate engaging in interspecific metabolic interactions. *Genome Announc* 5. doi: 10.1128/genomeA.00155-17

Krahn, T., Wibberg, D., Maus, I., Winkler, A., Bontron, S., Sczyrba, A., et al. (2016). Intraspecies Transfer of the Chromosomal Acinetobacter baumannii blaNDM-1 Carbapenemase Gene. *Antimicrob. Agents Chemother.* 60, 3032–3040. doi: 10.1128/AAC.00124-16

Kuo, H. Y., Hsu, P. J., Chen, J. Y., Liao, P. C., Lu, C. W., Chen, C. H., et al. (2016). Clonal spread of blaOXA-72-carrying Acinetobacter baumannii sequence type 512 in Taiwan. *Int. J. Antimicrob. Agents* 48, 111–113. doi: 10.1016/j.ijantimicag.2016.04.020

Lam, M. M. C., Koong, J., Holt, K. E., Hall, R. M., and Hamidian, M. (2023). Detection and Typing of Plasmids in Acinetobacter baumannii Using rep Genes Encoding Replication Initiation Proteins. *Microbiol. Spectr.* 11, e0247822. doi: 10.1128/spectrum.02478-22

Li, X., Xie, Y., Liu, M., Tai, C., Sun, J., Deng, Z., et al. (2018). oriTfinder: a web-based tool for the identification of origin of transfers in DNA sequences of bacterial mobile genetic elements. *Nucleic Acids Res.* 46, W229–W234. doi: 10.1093/nar/gky352

Liu, X., Lei, T., Yang, Y., Zhang, L., Liu, H., Leptihn, S., et al. (2022b). Structural basis of PER-1-mediated cefiderocol resistance and synergistic inhibition of PER-1 by cefiderocol in combination with Avibactam or Durlobactam in Acinetobacter baumannii. *Antimicrob. Agents Chemother.* 66, e0082822. doi: 10.1128/aac.00828-22

Liu, H., Moran, R. A., Chen, Y., Doughty, E. L., Hua, X., Jiang, Y., et al. (2021). Transferable Acinetobacter baumannii plasmid pDETAB2 encodes OXA-58 and NDM-1 and represents a new class of antibiotic resistance plasmids. *J. Antimicrob. Chemother.* 76, 1130–1134. doi: 10.1093/jac/dkab005

Liu, B., Zheng, D., Zhou, S., Chen, L., and Yang, J. (2022a). VFDB 2022: a general classification scheme for bacterial virulence factors. *Nucleic Acids Res.* 50, D912–D917. doi: 10.1093/nar/gkab1107

Luis, M. R., and Konstantinos, T. K. (2016). The enveomics collection: A toolbox for specialized analyses of microbial genomes and metagenomes. *PeerJ. Prepr* 4, e1900v1.

Marquez-Ortiz, R. A., Haggerty, L., Olarte, N., Duarte, C., Garza-Ramos, U., Silva-Sanchez, J., et al. (2017). Genomic epidemiology of NDM-1-encoding plasmids in Latin American clinical isolates reveals insights into the evolution of multidrug resistance. *Genome Biol. Evol.* 9, 1725–1741. doi: 10.1093/gbe/evx115

Merino, M., Acosta, J., Poza, M., Sanz, F., Beceiro, A., Chaves, F., et al. (2010). OXA-24 carbapenemase gene flanked by XerC/XerD-like recombination sites in different plasmids from different Acinetobacter species isolated during a nosocomial outbreak. *Antimicrob. Agents Chemother.* 54, 2724–2727. doi: 10.1128/AAC.01674-09

Mohd Rani, F., Ni, A. R., Ismail, S., Alattraqchi, A. G., Cleary, D. W., Clarke, S. C., et al. (2017). Acinetobacter spp. Infections in Malaysia: A review of antimicrobial resistance trends, mechanisms and epidemiology. *Front. Microbiol.* 8 2479. doi: 10.3389/fmicb.2017.02479

Overbeek, R., Olson, R., Pusch, G. D., Olsen, G. J., Davis, J. J., Disz, T., et al. (2014). The SEED and the Rapid Annotation of microbial genomes using Subsystems Technology (RAST). *Nucleic Acids Res.* 42, D206–D214. doi: 10.1093/nar/gkt1226

Pires, J., Santos, R., and Monteiro, S. (2023). Antibiotic resistance genes in bacteriophages from wastewater treatment plant and hospital wastewaters. *Sci. Total Environ.* 892, 164708. doi: 10.1016/j.scitotenv.2023.164708

Pu, D., Zhao, J., Lu, B., Zhang, Y., Wu, Y., Li, Z., et al. (2023). Within-host resistance evolution of a fatal ST11 hypervirulent carbapenem-resistant Klebsiella pneumoniae. *Int. J. Antimicrob. Agents* 61, 106747. doi: 10.1016/j.ijantimicag.2023.106747

Siguier, P., Perochon, J., Lestrade, L., Mahillon, J., and Chandler, M. (2006). ISfinder: the reference centre for bacterial insertion sequences. *Nucleic Acids Res.* 34, D32–D36. doi: 10.1093/nar/gkj014

Tang, L., Shen, W., Zhang, Z., Zhang, J., Wang, G., Xiang, L., et al. (2020). Whole-Genome Analysis of Two Copies of bla (NDM-1) Gene Carrying Acinetobacter johnsonii Strain Acsw19 Isolated from Sichuan, China. *Infect. Drug Resist.* 13, 855–865. doi: 10.2147/IDR.S236200

Tatusova, T., Dicuccio, M., Badretdin, A., Chetvernin, V., Nawrocki, E. P., Zaslavsky, L., et al. (2016). NCBI prokaryotic genome annotation pipeline. *Nucleic Acids Res.* 44, 6614–6624. doi: 10.1093/nar/gkw569

Tian, S., Ali, M., Xie, L., and Li, L. (2016). Draft Genome Sequence of Acinetobacter johnsonii MB44, Exhibiting Nematicidal Activity against Caenorhabditis elegans. *Genome Announc* 4. doi: 10.1128/genomeA.01772-15

Tian, C., Xing, M., Fu, L., Zhao, Y., Fan, X., and Wang, S. (2022). Emergence of uncommon KL38-OCL6-ST220 carbapenem-resistant Acinetobacter pittii strain, co-producing chromosomal NDM-1 and OXA-820 carbapenemases. *Front. Cell Infect. Microbiol.* 12, 943735. doi: 10.3389/fcimb.2022.943735

Wang, W., Chen, X., Yan, H., Hu, J., and Liu, X. (2019). Complete genome sequence of the cyprodinil-degrading bacterium Acinetobacter johnsonii LXL_C1. *Microb. Pathog.* 127, 246–249. doi: 10.1016/j.micpath.2018.11.016

Wick, R. R., Judd, L. M., Gorrie, C. L., and Holt, K. E. (2017). Unicycler: Resolving bacterial genome assemblies from short and long sequencing reads. *PloS Comput. Biol.* 13, e1005595. doi: 10.1371/journal.pcbi.1005595

Wong, D., Nielsen, T. B., Bonomo, R. A., Pantapalangkoor, P., Luna, B., and Spellberg, B. (2017). Clinical and pathophysiological overview of Acinetobacter infections: a century of challenges. *Clin. Microbiol. Rev.* 30, 409–447. doi: 10.1128/CMR.00058-16

Yang, X., Dong, N., Liu, X., Yang, C., Ye, L., Chan, E. W., et al. (2021). Co-conjugation of virulence plasmid and KPC plasmid in a clinical Klebsiella pneumoniae strain. *Front. Microbiol.* 12, 739461. doi: 10.3389/fmicb.2021.739461

Zankari, E., Hasman, H., Cosentino, S., Vestergaard, M., Rasmussen, S., Lund, O., et al. (2012). Identification of acquired antimicrobial resistance genes. *J. Antimicrob. Chemother.* 67, 2640–2644. doi: 10.1093/jac/dks261

Zhou, Y., Liang, Y., Lynch, K. H., Dennis, J. J., and Wishart, D. S. (2011). PHAST: a fast phage search tool. *Nucleic Acids Res.* 39, W347–W352. doi: 10.1093/nar/gkr485

Zong, G., Zhong, C., Fu, J., Zhang, Y., Zhang, P., Zhang, W., et al. (2020). The carbapenem resistance gene bla(OXA-23) is disseminated by a conjugative plasmid containing the novel transposon Tn6681 in Acinetobacter johnsonii M19. *Antimicrob. Resist. Infect. Control* 9, 182.

frontiers | Frontiers in Cellular and Infection Microbiology

TYPE Original Research
PUBLISHED 29 August 2023
DOI 10.3389/fcimb.2023.1240580

OPEN ACCESS

EDITED BY
Elvira Garza González,
Autonomous University of Nuevo León, Mexico

REVIEWED BY
Xin Lu,
Chinese Center For Disease Control and Prevention, China
Jianmin Zhang,
South China Agricultural University, China

*CORRESPONDENCE
Ruichao Li
rchl88@yzu.edu.cn
Xiaorong Yang
yangyangxr@163.com

†These authors have contributed equally to this work

RECEIVED 15 June 2023
ACCEPTED 14 August 2023
PUBLISHED 29 August 2023

CITATION
Sun X, Zhang L, Meng J, Peng K, Huang W, Lei G, Wang Z, Li R and Yang X (2023) The characteristics of *mcr*-bearing plasmids in clinical *Salmonella enterica* in Sichuan, China, 2014 to 2017.
Front. Cell. Infect. Microbiol. 13:1240580.
doi: 10.3389/fcimb.2023.1240580

The characteristics of *mcr*-bearing plasmids in clinical *Salmonella enterica* in Sichuan, China, 2014 to 2017

Xinran Sun[1,2†], Lin Zhang[3†], Jiantong Meng[4†], Kai Peng[1,2], Weifeng Huang[3], Gaopeng Lei[3], Zhiqiang Wang[1,2], Ruichao Li[1,2*] and Xiaorong Yang[3*]

[1]Jiangsu Co-Innovation Center for Prevention and Control of Important Animal Infectious Diseases and Zoonoses, College of Veterinary Medicine, Yangzhou University, Yangzhou, China, [2]Institute of Comparative Medicine, Yangzhou University, Yangzhou, China, [3]Center for Disease Control and Prevention of Sichuan Province, Chengdu, Sichuan, China, [4]Center for Disease Control and Prevention of Chengdu City, Chengdu, China

Salmonella is one of the most important zoonotic pathogens and a major cause of foodborne illnesses, posing a serious global public health hazard. The emergence of plasmid-mediated *mcr* genes in *Salmonella* has greatly reduced the clinical choice of salmonellosis treatment. The aim of this study was to investigate the plasmid characteristics of *mcr*-positive Salmonella identified from patients in Sichuan, China during 2014 to 2017 by whole genomes sequencing. In this study, a total of 12 *mcr*-positive isolates (1.15%, ; *mcr*-1, n=10; *mcr*-3, n=2) were identified from 1046 Salmonella isolates using PCR. Further characterization of these isolates was performed through antimicrobial susceptibility testing, conjugation assays, whole genome sequencing, and bioinformatics analysis. The *mcr-1* gene in these isolates were carried by three types of typical *mcr-1*-bearing plasmids widely distributed in Enterobacteriaceae (IncX4, IncI2 and IncHI2). Of note, two mcr-1-harboring IncHI2 plasmids were integrated into chromosomes by insertion sequences. Two *mcr-3*-bearing plasmids were IncC and IncFIB broad-host-range plasmids respectively. Genetic context analysis found that *mcr-1* was mainly located in Tn*6330* or truncated Tn*6300*, and *mcr-3* shared a common genetic structure *tnpA-mcr-3-dgkA-ISKpn40*. Overall, we found that *mcr* gene in clinical *Salmonella* were commonly carried by broad-host plasmids and have potential to transfer into other bacteria by these plasmids. Continuous surveillance of MDR *Salmonella* in humans and investigation the underlying transmission mechanisms of ARGs are vital to curb the current severe AMR concern.

KEYWORDS

***Salmonella* enterica, colistin resistance, *mcr*, plasmid, genomics**

1 Introduction

Colistin is a polypeptide antimicrobial with a narrow antibacterial spectrum that is largely effective against Gram-negative bacteria and has long been used in clinical medicine and animal husbandry (Landman et al., 2008; Biswas et al., 2012). In livestock industry, it was allowed and widely used for non-therapeutic usage, such as growth promotion, in many countries (Li et al., 2006). In clinical practice, it was commonly used as a non-preferred treatment for multidrug-resistant (MDR) Gram-negative bacteria due to its toxicity to human previously (Conway et al., 1997). However, the emergence of carbapenem-resistant Enterobacteriaceae (CRE) had limited the clinical treatment options. The World Health Organization (WHO) listed colistin as the highest priority critically important antibiotic fighting against CRE. The emergence of plasmid-medicated colistin resistance gene, *mcr-1*, in animal *Escherichia coli* in 2015 fundamentally changed the administration practice of colistin (Liu et al., 2016). Several countries have banned the use of colistin as an animal growth promoter (Wang et al., 2020). However, the current global prevalence of the mobile colistin resistance gene *mcr-1* and its variants are still a serious concern (Wang et al., 2017; Sun et al., 2018). To date, ten different *mcr* variants (*mcr-1* to *mcr-10*) have been identified in different bacteria isolated from animals, foods, humans, and the environment (Hussein et al., 2021). The majority of them were found in plasmids, suggesting that *mcr* variants could be transmitted across intraspecific and interspecific bacteria. The *mcr-1* gene was shown to be more prevalent in bacteria from animal sources than that from patients with nosocomial illnesses (Huang et al., 2017; Tian et al., 2017). This phenomenon may be related to the different exposure of colistin in different settings.

Salmonella is a group of gram-negative bacteria found in the intestinal tract of humans and animals as well as in the environment that can cause gastrointestinal diseases and fever called salmonellosis (Lin et al., 1995; Holschbach and Peek, 2018). Recently, a global systematic meta-analysis estimated that approximately 15% of patients with non-typhoidal *Salmonella* invasive disease die (Marchello et al., 2022). In some developing countries, infections caused by *Salmonella* are endemic and represent a serious public health hazard (Abd El-Ghany, 2020). Most healthy people infected by *Salmonella* can recover without specific treatment and do not require treatments of antimicrobials. However, young children and people with weakened immune systems may have an increased risk of developing bacteremia, meningitis and osteomyelitis (Marchello et al., 2022). Although *mcr* genes have seriously spread in Enterobacteriaceae, colistin resistance *Salmonella* were significantly less than *E. coli* and *Klebsiella pneumoniae*. Nonetheless, colistin resistance has emerged in clinical *Salmonella* in many countries, and *mcr-1* and *mcr-3* were the most common variants (Portes et al., 2022). The public health risk caused by colistin-resistant *Salmonella* has increasingly arisen. However, there are few systematic investigations of the plasmid characteristics in *mcr*-positive clinical *Salmonella* (Shen et al., 2021; Portes et al., 2022). In this study, we comprehensively investigated the characteristics of *mcr*-bearing plasmids in clinical *Salmonella* isolates isolated from Sichuan province during 2014 to 2017.

2 Materials and methods

2.1 Bacterial isolates

The clinical *Salmonella* isolates were collected from different hospitals in Sichuan province, China between 2014 and 2017. The *Salmonella* isolates were recovered from patients following the previous methods (Xia et al., 2009). The *mcr*-positive isolates were screened by the multiplex PCR method and confirmed by Sanger sequencing (Rebelo et al., 2018). All *mcr*-positive isolates were stored at -80°C in LB broth containing 20% glycerol for further investigation.

2.2 Antimicrobial susceptibility testing and conjugation assay

The MICs (minimum inhibitory concentrations) of *mcr*-positive isolates against different antimicrobials, including kanamycin, ciprofloxacin, meropenem, ampicillin, colistin, enrofloxacin, tetracycline and ceftiofur, were tested using broth microdilution as per Clinical and Laboratory Standards Institute (CLSI) standards (CLSI, 2020). *E. coli* ATCC25922 was used for quality control. In order to test the transferability of *mcr* genes, conjugation experiments were performed using *E. coli* C600 (Rif^R) as recipients. Briefly, the donor and recipient strains were grown in LB broth until they reached the logarithmic growth phase, then mixed at the ratio of 1:1 and cultured overnight on LB agar plates. The transconjugants were screened on LB agar plates with rifampin (300 mg/L) and colistin (2 mg/L), and validated using PCR targeting the *mcr* genes and 16S rDNA gene sequencing.

2.3 Genomic DNA extraction and whole genome sequencing

In order to decipher the genetic structure features of *mcr* genes in these *Salmonella* isolates. We first extracted their genomic DNA using FastPure Bacteria DNA Isolation Mini Kit (Vazyme™, China) according to the instructions of the manufacturer. The purity and concentration of genomic DNA were evaluated using the Titertek-Berthold Colibri (Berthold™, Germany) and the Qubit® Fluorometer (Thermo Fisher™, US) respectively. Then, extracted genomic DNA was sequenced using both short-read and long-read sequencing methods. Short-read DNA sequencing was conducted on the BGISEQ-50 platform with the SE50 strategy. The long-read sequencing was performed on ONT (Oxford Nanopore Technologies) MinION platform using the SQK-LSK109 library preparation kit in R9.4 flow cells.

2.4 Genome assembly and genomic feature analysis

The complete genomic sequences of *mcr*-positive *Salmonella* isolates were obtained using Unicycler (Wick et al., 2017) with hybrid assemble strategy based on short- and long-read data. An online fully-automated service, RAST was used to annotate the complete genomes (https://rast.nmpdr.org/). Antimicrobial resistance genes (ARGs), insertion sequences (ISs) and plasmid replicon genes were detected using abricate tool (https://github.com/tseemann/abricate) based on NCBI AMRFinderPlus, ISFinder and PlasmidFinder databases. The plasmid data were downloaded from NCBI RefSeq database (https://ftp.ncbi.nlm.nih.gov/genomes/refseq/plasmid/). The *Salmonella* serovars were identified using SISTR (Yoshida et al., 2016). The multi-locus sequence type (MLST) was analyzed using an mlst tool (https://github.com/tseemann/mlst). BRIG v.0.95 and Easyfig v.2.2.3 were used to generate plasmid comparison maps (Alikhan et al., 2011; Sullivan et al., 2011).

3 Results

3.1 Identification of *mcr*-positive *S. enterica* and antimicrobial susceptibility testing

In total, 12 *mcr*-positive isolates (ten *mcr-1* and two *mcr-3*) were detected from 1046 clinical *Salmonella* isolates using PCR. The prevalence and basic genomic features have been identified in our previous study (Li et al., 2022). For the 12 *mcr*-positive *S. enterica*, five isolates each year were detected in 2016 and 2017. The remaining two isolates were found in 2014. No *mcr*-positive isolates were detected in 2015. Antimicrobial susceptibility testing showed that the 12 *mcr*-positive *S. enterica* isolates were all resistant to colistin but sensitive to meropenem. In addition, the majority of them were resistant to ampicillin, tetracycline, aztreonam and kanamycin, whereas they were almost all sensitive to ciprofloxacin and enrofloxacin (Table 1). The majority of 12 *mcr*-positive *S. enterica* isolates showed multidrug resistance against three or more types of antimicrobials, designated as MDR isolates. According to the conjugation assay, the colistin resistance phenotype of the 12 *S. enterica* isolates could be transferred into *E. coli* C600. Antimicrobial susceptibility testing showed that all transconjugants were resistant to colistin. In addition, majority of transconjugants displayed resistance to other antimicrobials (Table 1). This indicated that the resistance genes in donor *S. enterica* were probable carried by conjugative MDR plasmids.

3.2 Genetic context of *mcr-1* and *mcr-3*

The genetic contexts of *mcr-1* in the ten *mcr-1* positive *Salmonella* isolates were classified as five types (Figure 1). The genetic structures of *mcr-1* in IncX4 plasmids were identical. No mobile elements were detected around the *mcr-1* gene in IncX4 plasmids. In IncHI2 plasmids, four different *mcr-1* genetic structures were found. Apart from plasmid pSC2017167-mcr-256k, we found an IS*Apl1* in the upstream of *mcr-1* in the other IncHI2 plasmids. In addition, we detected a reversed IS*Apl1* in the downstream of *mcr-1* in plasmid pSC2017297-mcr-249k. IS*Apl1* was an important element associated with the rapid dissemination of *mcr-1*, which is usually located in both upstream and downstream of *mcr-1* forming an IS*Apl1-mcr-1-pap2*-IS*Apl1* (Tn*6330*) transposon (Snesrud et al., 2018). Another study demonstrated that *mcr-1* genetic structures with only one IS*Apl1* or with IS*Apl1* absent were formed by deletion of IS*Apl1* from the ancestral Tn*6330* (Snesrud et al., 2018). We detected truncated Tn*6330* in many *mcr-1*-bearing plasmids, suggesting that the genetic structures of *mcr-1* in these plasmids have evolved for a long time.

The genetic structures of *mcr-3* in plasmids pSC2016091-mcr-116k and pSC2016290-mcr-147k were similar and shared a common core structure *tnpA-mcr-3-dgkA*-IS*Kpn40* (Figure 1). In plasmid pSC2016091-mcr-116k, we found a truncated IS*26* present upstream and an intact IS*26* present downstream of *mcr-3*. Only an intact IS*26* present upstream of *mcr-3* was detected in plasmid pSC2016290-mcr-147k. Similar to the mobilization of *mcr-1* medicated by Tn*6330*, the mobility of *mcr-3* is usually associated with a composite transposon structure IS*Kpn40-mcr-3.1-dgkA*-IS*Kpn40* (He et al., 2020). Apart from IS*Kpn40*, the highly mobilized IS*26* around *mcr-3* deserves our attention, as it may facilitate the horizontal translocation of *mcr-3*.

3.3 Distribution of *mcr*-bearing plasmids in *S. enterica* isolates

Long-read nanopore sequencing and short-read Illumina sequencing were performed on the 12 *S. enterica* isolates. The complete chromosomes and plasmids of these isolates were obtained using a hybrid assembly strategy and single-read analysis, as described in our previous study (Li et al., 2018). According to the assembly results, we found two chromosomally integrated IncHI2 plasmids from isolates SC2016025 and SC2016090 as a similar phenomenon previously reported (Figures 2A, D) (Chang et al., 2022). Similar *mcr-1*-bearing IncHI2/HI2A plasmids were found in other *mcr-1* positive isolates from our investigation including SC2017030, SC2017100, SC2017297 and SC2017167. Moreover, these *mcr-1*-bearing IncHI2/HI2A plasmids were also found in NCBI nr database by BLASTn analysis (Figure 2A). Almost identical *mcr-1* bearing plasmids were simultaneously detected in different genus, different geographical locations, different sources of isolates, implying that such plasmids play a crucial role in the horizontal transmission of *mcr-1*.

Comparative analysis found that there are some structure differences in these *mcr-1*-bearing IncHI2/HI2A plasmids from different isolates. A replicon gene of IncN plasmids was absent in plasmids pSC2017100-mcr-218k, pSC2017297-mcr-249k and pSC2017030-mcr-251k. In plasmid pSC2017100-mcr-218k, a region encoding multiple resistance genes containing *cmlA1*, *floR*

TABLE 1 The basic information and MICs (mg/L) of *mcr*-positive isolates and their transconjugants in this study.

Isolates	Gene	Serovar	STs[a]	Antimicrobials[b]							
				KAN	CIP	MEM	AMP	CL	ENR	TET	CFF
SC2014107	*mcr-1*	Orion	684	8	≤0.25	≤0.25	8	8	≤0.25	4	≤0.25
SC2014238	*mcr-1*	Meleagridis	463	4	≤0.25	≤0.25	>128	4	≤0.25	8	>128
SC2016025	*mcr-1*	I 4,[5],12:i:-	34	128	4	≤0.25	>128	8	2	128	>128
SC2016042	*mcr-1*	I 4,[5],12:i:-	34	8	≤0.25	≤0.25	>128	8	≤0.25	128	8
SC2016090	*mcr-1*	I 4,[5],12:i:-	34	8	≤0.25	≤0.25	>128	4	2	64	>128
SC2016091	*mcr-3*	I 4,[5],12:i:-	34	8	≤0.25	≤0.25	>128	8	≤0.25	128	>128
SC2016290	*mcr-3*	I 4,[5],12:i:-	34	4	≤0.25	≤0.25	>128	8	≤0.25	32	>128
SC2017030	*mcr-1*	I 4,[5],12:i:-	34	>128	≤0.25	≤0.25	>128	8	≤0.25	64	>128
SC2017057	*mcr-1*	I 4,[5],12:i:-	34	>128	≤0.25	≤0.25	>128	1	≤0.25	16	128
SC2017100	*mcr-1*	I 4,[5],12:i:-	34	2	0.5	≤0.25	>128	4	≤0.25	32	>128
SC2017167	*mcr-1*	I 4,[5],12:i:-	34	>128	≤0.25	≤0.25	>128	4	≤0.25	64	>128
SC2017297	*mcr-1*	I 4,[5],12:i:-	34	>128	≤0.25	≤0.25	>128	8	1	32	>128
cSC2014107	*mcr-1*	/	/	1	≤0.25	≤0.25	8	2	1	0.5	≤0.25
cSC2014238	*mcr-1*	/	/	1	≤0.25	≤0.25	32	2	0.5	0.5	0.5
cSC2016025	*mcr-1*	/	/	4	0.5	≤0.25	>128	2	1	32	128
cSC2016042	*mcr-1*	/	/	2	≤0.25	≤0.25	32	2	0.5	0.5	0.5
cSC2016090	*mcr-1*	/	/	4	≤0.25	≤0.25	>128	2	1	0.5	16
cSC2016091	*mcr-3*	/	/	1	≤0.25	≤0.25	>128	2	1	≤0.25	>128
cSC2016290	*mcr-3*	/	/	1	≤0.25	≤0.25	>128	2	0.5	4	>128
cSC2017030	*mcr-1*	/	/	>128	≤0.25	≤0.25	>128	2	0.5	32	32
cSC2017057	*mcr-1*	/	/	8	≤0.25	≤0.25	>128	2	0.5	32	64
cSC2017100	*mcr-1*	/	/	2	≤0.25	≤0.25	>128	2	0.5	0.5	16
cSC2017167	*mcr-1*	/	/	>128	≤0.25	≤0.25	>128	2	0.5	0.5	16
cSC2017297	*mcr-1*	/	/	>128	≤0.25	≤0.25	>128	1	0.5	16	64

[a]STs indicate sequence types.
[b]KAN, kanamycin; CIP, ciprofloxacin; MEM, meropenem; AMP, ampicillin; CL, colistin; ENR, enrofloxacin; TET, tetracycline; CFF, ceftiofur.

and *sul2* was lost (Figure 2A). The evolution of this type of plasmids in different isolates may result in their structural changing. IncHI2/HI2A plasmids with *mcr-1* are commonly detected in *E. coli* (Lu et al., 2020). This type of *mcr-1* positive plasmid has recently been found frequently in *Salmonella* (Vazquez et al., 2021), indicating that the *mcr-1* gene has the ability to transfer to other species of bacteria with their assistance. We should pay more attention to monitor the spread of such *mcr-1*-bearing plasmids.

We identified three *mcr-1*-bearing IncX4 plasmids in isolates SC2014238, SC2016042 and SC2017057. The three IncX4 plasmids shared 100% identity and 100% coverage with each other. In addition, there are many IncX4 plasmids from other genus of bacteria that are identical to the three plasmids (Figure 2B). Like IncHI2/HI2A plasmids, IncX4 plasmids were also a common plasmid type carrying *mcr-1*, because they are self-transferable with high conjugation frequencies (Sun et al., 2017). Apart from IncHI2/HI2A and IncX4 plasmids, an IncI2 plasmid harboring *mcr-1* with 62kb in length was identified in isolate SC2014107 (Figure 2C). The IncI2 plasmids have recently been noticed due to they are usually associated with the transmission of ESBLs genes and *mcr-1* (Wong et al., 2015). A previous investigation showed that IncI2 plasmids were the most common type of *mcr-1*-carrying plasmids (Ricker et al., 2022). In addition, we found many *mcr-1*-bearing IncI2 plasmids from different bacteria in nr database (Figure 2C), indicating that the IncI2 plasmids were broad-host-range plasmids.

Apart from *mcr-1*, another *mcr* variant *mcr-3* was detected in isolates SC2016090 and SC2016091. Whole genome analysis of the two isolates found that the *mcr-3* gene was located on plasmids. In isolate SC2016090, *mcr-3* was carried by an IncC plasmid pSC2016290-mcr-147k with a size 147kb. Besides, the plasmid also carried $bla_{\text{CTX-M-55}}$, $bla_{\text{TEM-1B}}$, *catA2*, *aph(6)-Id*, *tet*(A) and *floR*. We noticed that a few of such *mcr-3*-bearing plasmids have been detected in other *Salmonella* isolates (Figure 3A). Of note, the

plasmid pSC2016290-mcr-147k showed a partial backbone similar to an *E. coli* plasmid pECAZ155_KPC carrying the carbapenemase gene bla_{KPC-2}. This phenomenon implied that the plasmid pSC2016290-mcr-147k could integrate into other plasmids, causing the *mcr-3* gene to spread to other bacteria. Another *mcr-3*-bearing plasmid found in isolate SC2016091 was an IncFIB type plasmid pSC2019091-mcr3-116k with 116kb. Coincidently, the plasmid also carried ESBL gene $bla_{CTX-M-55}$ (Figure 3B). Furthermore, the IncFIB plasmids belonged to a type of broad host plasmids, and there are numerous plasmids from various bacteria sharing a backbone comparable to the IncFIB plasmid.

3.4 Prevalence characteristics and structures of *mcr*-positive plasmids

In order to further investigate the prevalence and plasmid backbone structures of *mcr*-positive plasmids, all plasmid data in the RefSeq database were downloaded and utilized for comparative analysis of plasmid backbone structures. Through BLASTn analysis, a total of 136 complete plasmids encoding *mcr* were identified among over twenty-seven thousand plasmids in database. The plasmid replicon types of plasmids were further determined using the plasmidfinder database. The major of *mcr-1* variants identified in both the database and this study was found in plasmids of replicon types IncX4 (34/122), IncI2 (49/122), and IncHI2/HI2A (31/122), and all plasmids of those types carried only *mcr-1*, suggesting those plasmids has a strong correlation with *mcr-1* horizontal transfer. Additionally, eleven plasmids encoding *mcr-3* identified in the database and this study, belonging to four different replicon types, including IncFII (5/11), IncC (4/11), IncI1 (1/11), IncFII/FIB (1/11). Furthermore, the plasmids carrying *mcr-8*, with replicon types IncFII (1/4), IncFII/FIA (2/4) and IncFII/FIB (1/4), and eight additional plasmids carrying *mcr-10* was determined to be of replicon type IncFII/FIB (5/8), IncFII (1/8), IncFII/FIA (1/8) and IncFII (1/8).

The main hosts of *mcr*-positive plasmids in the RefSeq database were identified as *Salmonella enterica* (18/136) and *Escherichia coli* (96/136).

The plasmids from both the database and this study were merged for further investigations. Among these plasmids, those belonging to replicon types IncX4 and IncI2 were most abundant, often in the size range of approximately 30kb and 60kb, respectively, followed by IncHI2A/HI2 type plasmids mainly distributed between 220kb to 270kb in length (Figure 4). Alignment of plasmid backbone structures revealed that, aside from IncFII/FIB replicon type *mcr*-positive plasmids, those with the same plasmid replicon types displayed similar backbone structures (Supplement Figure 1). These plasmids with similar structures were found in different host bacteria especially *Escherichia coli*, indicating the horizontal transmission of *mcr*-positive plasmids carrying different *mcr* variants among different hosts.

3.5 Genetic characteristics of multidrug resistant chromosomally integrated plasmid

To investigate the formation mechanism of the integrated plasmid, we employed third-generation DNA sequencing to obtain accurate genome structures of strain SC2016090. The chromosome of SC2016090 was 5,247,576-bp in length, exhibited a GC content of 51.9% and comprised 4,927 predicted coding

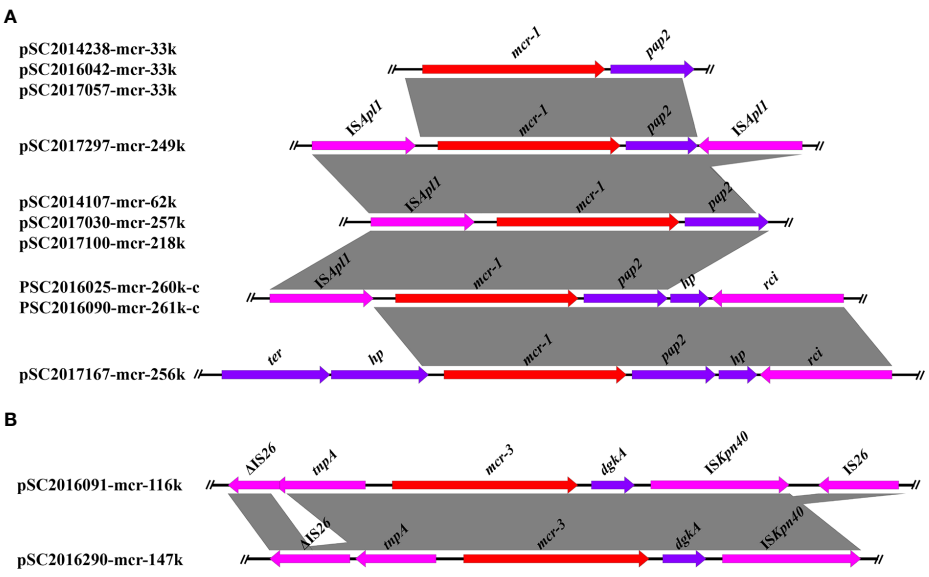

FIGURE 1
Linear comparison of the core genetic contexts of *mcr* genes investigated in this study. **(A)** The genetic context of *mcr-1* in plasmids and chromosomal plasmids. PSC2016025-mcr-260k-c and PSC2016090-mcr-261k-c were two chromosomally integrated plasmids. **(B)** The genetic structure of *mcr-3* in plasmids pSC2016091-mcr-116k and pSC2016290-mcr-147.

10.3389/fcimb.2023.1240580

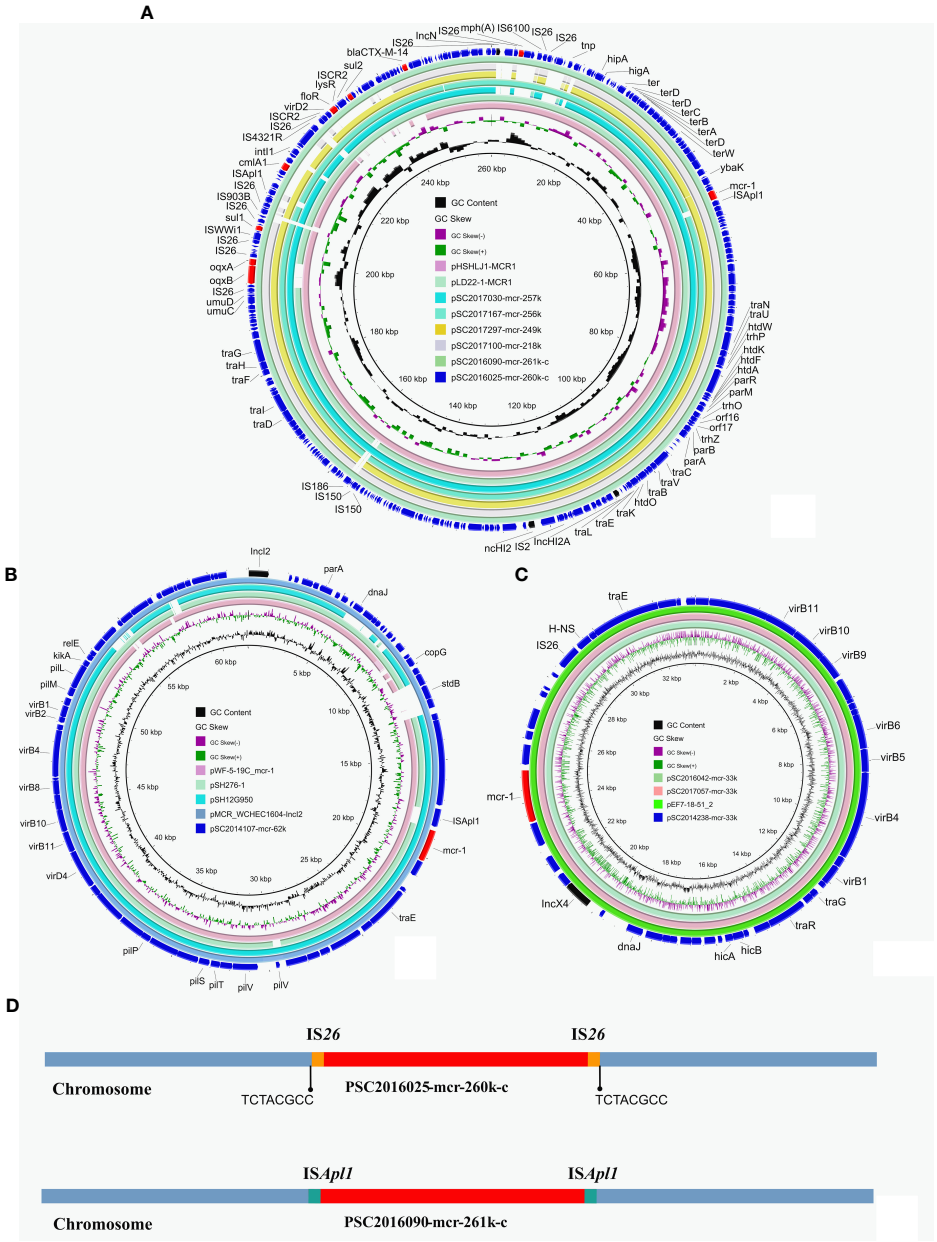

FIGURE 2
Structure analysis of *mcr-1*-bearing plasmids in *Salmonella* isolates. **(A)** Comparative analysis of *mcr-1*-carrying IncHI2 plasmids and chromosomally integrated plasmids in this study with *other* similar plasmids including pLD22-1-MCR1 (CP047877.1) and pHSHLJ1-MCR1 (KX856066.1). **(B)** Four identical *mcr-1*-bearing IncX4 plasmids including three identified in this study and plasmid pEF7-18-51_2 (CP063489.1) from NCBI database. **(C)** Circular comparative analysis of pSC2014107-mcr-62k with four closely related plasmids including pMCR_WCHEC1604-IncI2 (KY829117.1), pSH12G950 (MH522410.1), pSH276-1 (MG299140.1) and pWF-5-19C_mcr-1 (KX505142.1). Resistance genes and plasmid replicon genes in these plasmids were highlighted in red arrows and black arrows respectively. **(D)** The integration sites of chromosomal plasmids PSC2016025-mcr-260k-c and PSC2016090-mcr-261k-c.

sequences (CDSs). Comparative analysis using BLASTn revealed that the chromosome of SC2016090 showed remarkable similarity (93% coverage, 99.97% identity) to the chromosome of *Salmonella enterica* strain ST101 (CP050731.1), isolated from a diarrheal patient in Shanghai. However, the SC2016090 chromosome contained an extra 261,335 bp DNA fragment with 46.8% GC content (Figure 5) that was not present in the ST101 chromosome. Further investigation revealed that this extra fragment encompassed 249 CDSs and displayed 99% identity with plasmids pMCR_NDM (CP049111.1) and pSI_16E242 (ON960347.1), with coverage of 95% and 99%, respectively. Notably, within the extra DNA fragment of strain SC2016090, several others resistance genes, including $bla_{CTX\text{-}M}$, *sul3*, *aadA2*, and *fosA* were detected, IncHI2 replicon was also coding in the extra DNA fragment. Furthermore, a comprehensive analysis

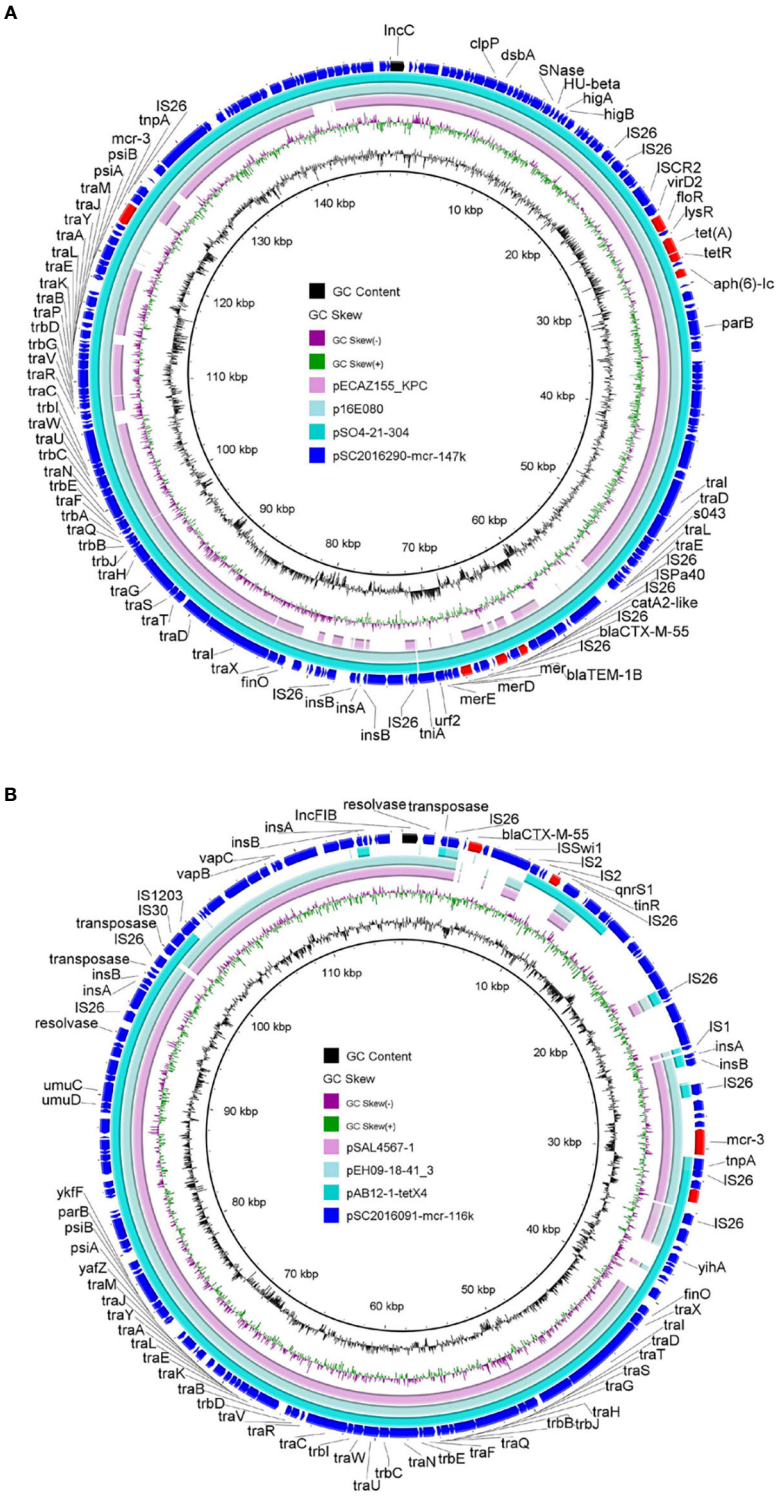

FIGURE 3
Structure analysis of *mcr-3*-bearing plasmids. **(A)** Comparative analysis of plasmid pSC2016290-mcr-147k with plasmids pSO4-21-304 (AP014634.1), p16E080 (MN647788.1) and pECAZ155_KPC (CP019001.1). **(B)** Structure analysis of plasmid pSC2016091-mcr-116k with other similar plasmids including pAB12-1-tetX4 (MZ054177.1), pEH09-18-41_3 (CP063506.1) and pSAL4567-1 (AP023307.1).

of the extra DNA fragment unveiled the presence of numerous mosaic genetic elements, including the clustered Tn*26*. Interestingly, we found the CDS for a D-serine transporter (DsdX, QIU08742.1) was truncated by insertion of the extra DNA fragment. Additionally, the presence of the IS*Apl1* in both areas of the fragment's ends and the reverse repeating base sequence located on both sides of the extra plasmid segment, suggested the involvement of IS*Apl1* in the insertion of the integrated plasmid (Figure 5).

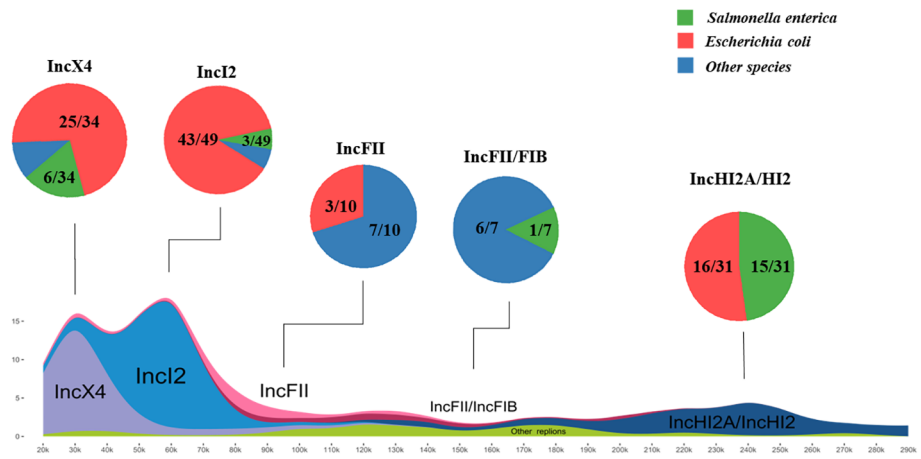

FIGURE 4
Host distribution and structural characteristics of *mcr*-positive plasmids The investigation of *mcr*-plasmids from RefSeq database *via* BLASTn comparison. A total of 136 complete plasmids encoding *mcr* were identified. *Salmonella enterica* and *Escherichia coli* are the Major hosts of positive plasmids. IncX4 and IncI2 plasmids as most abundant (approx. 30kb or 60kb), followed by IncHI2A/HI2 (220kb-270kb). The frequent detection of *mcr* in various plasmid backbones and bacterial isolates highlights the widespread distribution and prevalence of this resistance mechanism.

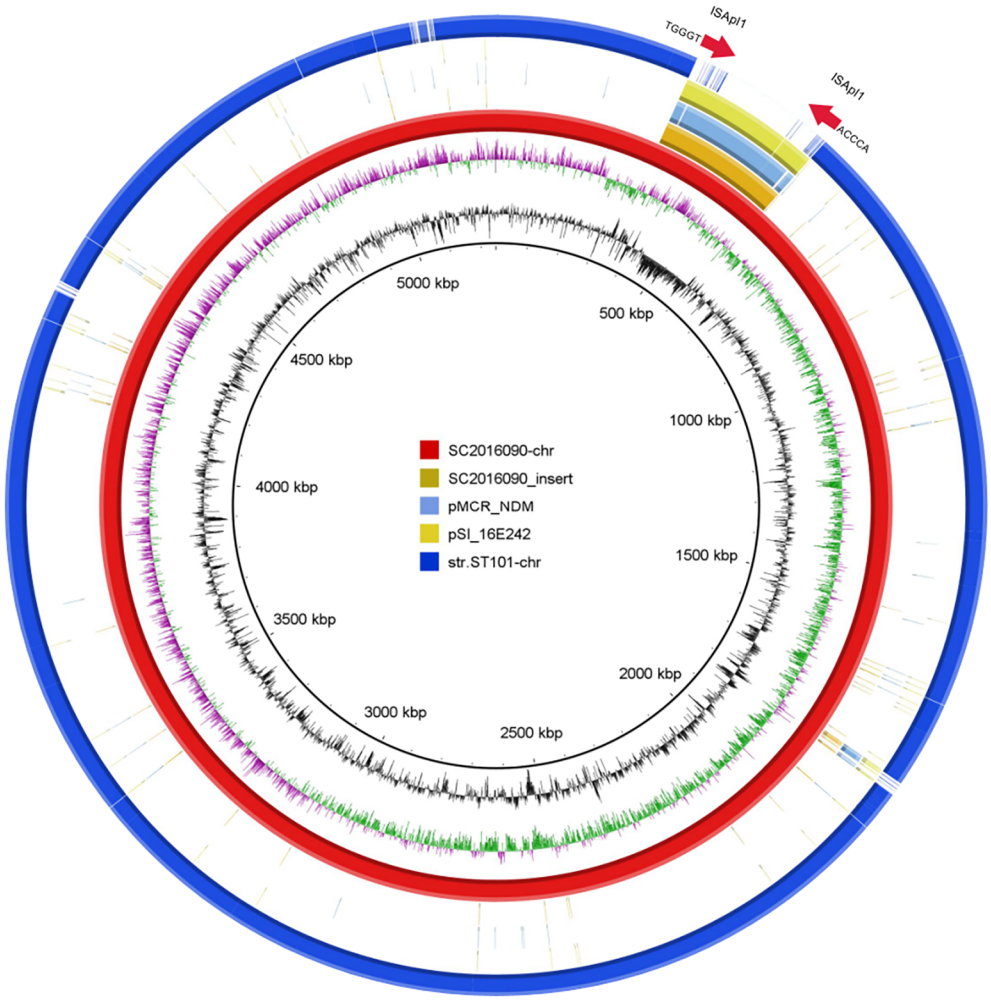

FIGURE 5
The presence of the IS*Apl1* gene and structure analysis of multidrug-resistant chromosomally integrated plasmid. BLASTn revealed high homology (93% coverage and 99.97% identity) between SC2016090 and *Salmonella enterica* strain ST101 chromosomes (CP050731.1). The extra fragment showed 99% identity with plasmids pMCR_NDM (CP049111.1) and pSI_16E242 (ON960347.1), with respective coverage of 95% and 99%. The presence of the IS*Apl1* transposase and reverse repeating base sequence was detected at both ends of the fragment.

4 Discussion

Although colistin was not the first-line antibiotic for the treatment of *Salmonella* infections, emergence of colistin resistant *Salmonella* in clinical posed a great threaten to human health. To date, many studies have proved that colistin resistance genes *mcr* have spread in *Salmonella* of animal and human sources (Lu et al., 2019; Yang et al., 2022). This alarmed that colistin resistant *Salmonella* should not be neglected. Plasmids play an important role in the dissemination of *mcr* in many bacteria, including *Salmonella*. Understanding the *mcr*-bearing plasmids characteristics of *Salmonella* is important to prevent the diffusion of *mcr* in *Salmonella*. In this study, we comprehensively investigated the characteristics of *mcr*-bearing plasmids in 1046 clinical *S. enterica* isolates collected in Sichuan province from 2014 to 2017. We found that *mcr-1* was predominated *mcr* variant in clinical *Salmonella*. Three different types of *mcr-1*-bearing plasmids (IncHI2/IncHI2A, IncX4 and IncI2) were found in the 10 *mcr-1* positive *Salmonella* isolates. Of note, the three types of plasmids were commonly detected in *E. coli* (Sun et al., 2017; Lu et al., 2020), implying that *mcr-1* in *Salmonella* was probably came from *E. coli*. Apart from *mcr-1*, we also detected two *mcr-3* positive *Salmonella* isolates. The *mcr-3* gene in the two *Salmonella* isolates were carried by two different types of plasmids (IncC and IncFIB). It is worth noting that the *mcr-3*-bearing plasmids detected in *Salmonella* were also broad-host plasmids. In addition, both *mcr-1*- and *mcr-3*-harboring plasmids in our study could be transferred into *E. coli* by conjugation assay, indicating that *mcr* genes in clinical *Salmonella* isolates might spread into other bacteria.

According to our investigation, we found majority of *mcr*-positive *Salmonella* isolates belonged to *S.* 4 [5],,12:i:-. Previous study showed that MDR phenotype of *S.* 4,[5],12:i:- was determined by IncHI2 plasmids they carried (Mu et al., 2022). We also found a high detection rate of IncHI2 plasmids in *mcr-1* positive clinical *S.* 4,[5],12:i:-. This alerted us to pay more attention to monitor the spread of IncHI plasmids in different ecological niche.

In summary, the prevalence of *mcr* genes was low in clinical *Salmonella* in Sichuan, China. The *mcr-1* was more prevalence than *mcr-3*. The propagation of *mcr* genes in *Salmonella* was mainly mediated by plasmids. The *mcr*-bearing plasmids detected in clinical *Salmonella* could transfer among different Enterobacteriaceae bacteria. Continuous surveillance of *mcr*-bearing *Salmonella* in different settings as the One Health approach should be performed to curb the potential risk caused by MDR *Salmonella*.

Data availability statement

The datasets presented in this study can be found in online repositories. The names of the repository/repositories and accession number(s) can be found in the article/Supplementary Material.

Ethics statement

The manuscript presents research on animals that do not require ethical approval for their study.

Author contributions

XY, RL, and ZW contributed to conception and design of the study. XS, LZ, JM performed the experiments and organized the data. KP and WH conducted the sequencing and bioinformatics analysis. WH and GL did data curation and visualization. XS and KP wrote the first draft of the manuscript. RL and XY reviewed and edited the manuscript. All authors contributed to the article and approved the submitted version.

Funding

This work was supported by the Key Research and Development Program of Sichuan Province (Major Science and Technology Projects) (2022ZDZX0017) and the Priority Academic Program Development of Jiangsu Higher Education Institutions (PAPD).

Conflict of interest

The authors declare that the research was conducted in the absence of any commercial or financial relationships that could be construed as a potential conflict of interest.

Publisher's note

Supplementary material

The Supplementary Material for this article can be found online at: https://www.frontiersin.org/articles/10.3389/fcimb.2023.1240580/full#supplementary-material

References

Abd El-Ghany, W. A. (2020). Salmonellosis: a food borne zoonotic and public health disease in Egypt. *J. Infect. Dev. Ctries* 14, 674–678. doi: 10.3855/jidc.12739

Alikhan, N. F., Petty, N. K., Ben Zakour, N. L., and Beatson, S. A. (2011). BLAST Ring Image Generator (BRIG): simple prokaryote genome comparisons. *BMC Genomics* 12, 402. doi: 10.1186/1471-2164-12-402

Biswas, S., Brunel, J. M., Dubus, J. C., Reynaud-Gaubert, M., and Rolain, J. M. (2012). Colistin: an update on the antibiotic of the 21st century. *Expert Rev. Anti Infect. Ther.* 10, 917–934. doi: 10.1586/eri.12.78

Chang, M. X., Zhang, J., Zhang, J. F., Ding, X. M., Lu, Y., Zhang, J., et al. (2022). Formation, transmission, and dynamic evolution of a multidrug-resistant chromosomally integrated plasmid in salmonella spp. *Front. Microbiol.* 13, 846954. doi: 10.3389/fmicb.2022.846954

CLSI (2020). "Performance Standards for antimicrobial susceptibility Testing," in *CLSI supplement M100, 30th ed* (Wayne, PA: Clinical and Laboratory Standards Institute).

Conway, S. P., Pond, M. N., Watson, A., Etherington, C., Robey, H. L., and Goldman, M. H. (1997). Intravenous colistin sulphomethate in acute respiratory exacerbations in adult patients with cystic fibrosis. *Thorax* 52, 987–993. doi: 10.1136/thx.52.11.987

He, Y. Z., Long, T. F., Chen, C. P., He, B., Li, X. P., Schuyler, J., et al. (2020). ISKpn40-Mediated Mobilization of the Colistin Resistance Gene mcr-3.11 in Escherichia coli. *Antimicrob. Agents Chemother.* 64. doi: 10.1128/AAC.00851-20

Holschbach, C. L., and Peek, S. F. (2018). Salmonella in dairy cattle. *Vet. Clin. North Am. Food Anim. Pract.* 34, 133–154. doi: 10.1016/j.cvfa.2017.10.005

Huang, X., Yu, L., Chen, X., Zhi, C., Yao, X., Liu, Y., et al. (2017). High prevalence of colistin resistance and mcr-1 gene in Escherichia coli isolated from food animals in china. *Front. Microbiol.* 8, 562. doi: 10.3389/fmicb.2017.00562

Hussein, N. H., Al-Kadmy, I. M. S., Taha, B. M., and Hussein, J. D. (2021). Mobilized colistin resistance (mcr) genes from 1 to 10: a comprehensive review. *Mol. Biol. Rep.* 48, 2897–2907. doi: 10.1007/s11033-021-06307-y

Landman, D., Georgescu, C., Martin, D. A., and Quale, J. (2008). Polymyxins revisited. *Clin. Microbiol. Rev.* 21, 449–465. doi: 10.1128/CMR.00006-08

Li, J., Nation, R. L., Turnidge, J. D., Milne, R. W., Coulthard, K., Rayner, C. R., et al. (2006). Colistin: the re-emerging antibiotic for multidrug-resistant Gram-negative bacterial infections. *Lancet Infect. Dis.* 6, 589–601. doi: 10.1016/S1473-3099(06)70580-1

Li, R., Peng, K., Huang, W., Sun, X., Huang, Y., Lei, G., et al. (2022). The genomic epidemiology of mcr-positive Salmonella enterica in clinical patients from 2014 to 2017 in Sichuan, China and global epidemiological features. *J. Infect* 85(6), 702–769. doi: 10.1016/j.jinf.2022.08.042

Li, R., Xie, M., Dong, N., Lin, D., Yang, X., Wong, M. H. Y., et al. (2018). Efficient generation of complete sequences of MDR-encoding plasmids by rapid assembly of MinION barcoding sequencing data. *Gigascience* 7, 1–9. doi: 10.1093/gigascience/gix132

Lin, J., Lee, I. S., Frey, J., Slonczewski, J. L., and Foster, J. W. (1995). Comparative analysis of extreme acid survival in Salmonella typhimurium, Shigella flexneri, and Escherichia coli. *J. Bacteriol* 177, 4097–4104. doi: 10.1128/jb.177.14.4097-4104.1995

Liu, Y. Y., Wang, Y., Walsh, T. R., Yi, L. X., Zhang, R., Spencer, J., et al. (2016). Emergence of plasmid-mediated colistin resistance mechanism MCR-1 in animals and human beings in China: a microbiological and molecular biological study. *Lancet Infect. Dis.* 16, 161–168. doi: 10.1016/S1473-3099(15)00424-7

Lu, X., Xiao, X., Liu, Y., Huang, S., Li, R., and Wang, Z. (2020). Widespread Prevalence of Plasmid-Mediated Colistin Resistance Gene mcr-1 in Escherichia coli from Pere David's Deer in China. *mSphere* 5(6), e01221-20. doi: 10.1128/mSphere.01221-20

Lu, X., Zeng, M., Xu, J., Zhou, H., Gu, B., Li, Z., et al. (2019). Epidemiologic and genomic insights on mcr-1-harbouring Salmonella from diarrhoeal outpatients in Shanghai, China, 2006-2016. *Ebiomedicine* 42, 133–144. doi: 10.1016/j.ebiom.2019.03.006

Marchello, C. S., Birkhold, M., Crump, J. A.iN.T.S.c.c. Vacc-i (2022). Complications and mortality of non-typhoidal salmonella invasive disease: a global systematic review and meta-analysis. *Lancet Infect. Dis.* 22, 692–705. doi: 10.1016/S1473-3099(21)00615-0

Mu, Y., Li, R., Du, P., Zhang, P., Li, Y., Cui, S., et al. (2022). Genomic epidemiology of ST34 monophasic salmonella enterica serovar typhimurium from clinical patients from 2008 to 2017 in Henan, China. *Engineering* 15(8), 34–44. doi: 10.1016/j.eng.2022.05.006

Portes, A. B., Rodrigues, G., Leitao, M. P., Ferrari, R., Conte Junior, C. A., and Panzenhagen, P. (2022). Global distribution of plasmid-mediated colistin resistance mcr gene in Salmonella: a systematic review. *J. Appl. Microbiol.* 132, 872–889. doi: 10.1111/jam.15282

Rebelo, A. R., Bortolaia, V., Kjeldgaard, J. S., Pedersen, S. K., Leekitcharoenphon, P., Hansen, I. M., et al. (2018). Multiplex PCR for detection of plasmid-mediated colistin resistance determinants, mcr-1, mcr-2, mcr-3, mcr-4 and mcr-5 for surveillance purposes. *Euro Surveill* 23(6), 17–00672. doi: 10.2807/1560-7917.ES.2018.23.6.17-00672

Ricker, N., Chalmers, G., Whalen, E., Allen, H. K., and Meinersmann, R. J. (2022). Genomic changes within a subset of IncI2 plasmids associated with dissemination of mcr-1 genes and other important antimicrobial resistance determinants. *Antibiotics (Basel)* 11. doi: 10.3390/antibiotics11020181

Shen, C., Ma, F., Deng, S., Zhong, L. L., El-Sayed Ahmed, M. A. E., Zhang, G., et al. (2021). Prevalence, genomic characteristics, and transmission dynamics of mcr-1-positive Salmonella enterica Typhimurium from patients with infectious diarrhea. *Int. J. Med. Microbiol.* 311, 151501. doi: 10.1016/j.ijmm.2021.151501

Snesrud, E., McGann, P., and Chandler, M. (2018). The birth and demise of the ISApl1-mcr-1-ISApl1 composite transposon: the vehicle for transferable colistin resistance. *mBio* 9. doi: 10.1128/mBio.02381-17

Sullivan, M. J., Petty, N. K., and Beatson, S. A. (2011). Easyfig: a genome comparison visualizer. *Bioinformatics* 27, 1009–1010. doi: 10.1093/bioinformatics/btr039

Sun, J., Fang, L. X., Wu, Z., Deng, H., Yang, R. S., Li, X. P., et al. (2017). Genetic analysis of the incX4 plasmids: Implications for a unique pattern in the mcr-1 acquisition. *Sci. Rep.* 7, 424. doi: 10.1038/s41598-017-00095-x

Sun, J., Zhang, H., Liu, Y. H., and Feng, Y. (2018). Towards understanding MCR-like colistin resistance. *Trends Microbiol.* 26, 794–808. doi: 10.1016/j.tim.2018.02.006

Tian, G. B., Doi, Y., Shen, J., Walsh, T. R., Wang, Y., Zhang, R., et al. (2017). MCR-1-producing Klebsiella pneumoniae outbreak in China. *Lancet Infect. Dis.* 17, 577. doi: 10.1016/S1473-3099(17)30266-9

Vazquez, X., Garcia, V., Fernandez, J., Bances, M., de Toro, M., Ladero, V., et al. (2021). Colistin resistance in monophasic isolates of salmonella enterica ST34 collected from meat-derived products in Spain, with or without CMY-2 co-production. *Front. Microbiol.* 12, 735364. doi: 10.3389/fmicb.2021.735364

Wang, Y., Tian, G. B., Zhang, R., Shen, Y., Tyrrell, J. M., Huang, X., et al. (2017). Prevalence, risk factors, outcomes, and molecular epidemiology of mcr-1-positive Enterobacteriaceae in patients and healthy adults from China: an epidemiological and clinical study. *Lancet Infect. Dis.* 17, 390–399. doi: 10.1016/S1473-3099(16)30527-8

Wang, Y., Xu, C., Zhang, R., Chen, Y., Shen, Y., Hu, F., et al. (2020). Changes in colistin resistance and mcr-1 abundance in Escherichia coli of animal and human origins following the ban of colistin-positive additives in China: an epidemiological comparative study. *Lancet Infect. Dis.* 20, 1161–1171. doi: 10.1016/S1473-3099(20)30149-3

Wick, R. R., Judd, L. M., Gorrie, C. L., and Holt, K. E. (2017). Unicycler: Resolving bacterial genome assemblies from short and long sequencing reads. *PLoS Comput. Biol.* 13, e1005595. doi: 10.1371/journal.pcbi.1005595

Wong, M. H., Liu, L., Yan, M., Chan, E. W., and Chen, S. (2015). Dissemination of IncI2 Plasmids That Harbor the blaCTX-M Element among Clinical Salmonella Isolates. *Antimicrob. Agents Chemother.* 59, 5026–5028. doi: 10.1128/AAC.00775-15

Xia, S., Hendriksen, R. S., Xie, Z., Huang, L., Zhang, J., Guo, W., et al. (2009). Molecular characterization and antimicrobial susceptibility of Salmonella isolates from infections in humans in Henan Province, China. *J. Clin. Microbiol.* 47, 401–409. doi: 10.1128/JCM.01099-08

Yang, C., Chen, K., Ye, L., Heng, H., Chan, E. W. C., and Chen, S. (2022). Genetic and drug susceptibility profiles of mcr-1-bearing foodborne Salmonella strains collected in Shenzhen, China during the period 2014-2017. *Microbiol. Res.* 265, 127211. doi: 10.1016/j.micres.2022.127211

Yoshida, C. E., Kruczkiewicz, P., Laing, C. R., Lingohr, E. J., Gannon, V. P., Nash, J. H., et al. (2016). The salmonella in silico typing resource (SISTR): an open web-accessible tool for rapidly typing and subtyping draft salmonella genome assemblies. *PLoS One* 11, e0147101. doi: 10.1371/journal.pone.0147101

frontiers | Frontiers in Cellular and Infection Microbiology

TYPE Original Research
PUBLISHED 07 September 2023
DOI 10.3389/fcimb.2023.1236777

OPEN ACCESS

EDITED BY
Elvira Garza González,
Autonomous University of Nuevo León, Mexico

REVIEWED BY
Marja-Liisa Hänninen,
University of Helsinki, Finland
Leonardo Gabriel Panunzi,
CEA Saclay, France

*CORRESPONDENCE
Tengfei Zhang
tfzhang23@163.com
Qingping Luo
qingping0523@163.com

†These authors have contributed equally to this work

RECEIVED 08 June 2023
ACCEPTED 18 August 2023
PUBLISHED 07 September 2023

CITATION
Xiao J, Cheng Y, Zhang W, Lu Q, Guo Y, Hu Q, Wen G, Shao H, Luo Q and Zhang T (2023) Genetic characteristics, antimicrobial susceptibility, and virulence genes distribution of *Campylobacter* isolated from local dual-purpose chickens in central China.
Front. Cell. Infect. Microbiol. 13:1236777.
doi: 10.3389/fcimb.2023.1236777

Genetic characteristics, antimicrobial susceptibility, and virulence genes distribution of *Campylobacter* isolated from local dual-purpose chickens in central China

Jia Xiao[1†], Yiluo Cheng[1†], Wenting Zhang[1,2], Qin Lu[1,2], Yunqing Guo[1,2], Qiao Hu[1,2], Guoyuan Wen[1,2], Huabin Shao[1,2], Qingping Luo[1,2,3*] and Tengfei Zhang[1,2*]

[1]Key Laboratory of Prevention and Control Agents for Animal Bacteriosis (Ministry of Agriculture and Rural Affairs), Institute of Animal Husbandry and Veterinary, Hubei Academy of Agricultural Sciences, Wuhan, China, [2]Hubei Provincial Key Laboratory of Animal Pathogenic Microbiology, Institute of Animal Husbandry and Veterinary, Hubei Academy of Agricultural Sciences, Wuhan, China, [3]Institute of Animal Husbandry and Veterinary, Hubei Academy of Agricultural Sciences, Hubei Hongshan Laboratory, Wuhan, China

Food-borne antibiotic-resistant *Campylobacter* poses a serious threat to public health. To understand the prevalence and genetic characteristics of *Campylobacter* in Chinese local dual-purpose (meat and eggs) chickens, the genomes of 30 *Campylobacter* isolates, including 13 *C. jejuni* and 17 *C. coli* from Jianghan-chickens in central China, were sequenced and tested for antibiotic susceptibility. The results showed that CC-354 and CC-828 were the dominant clonal complexes of *C. jejuni* and *C. coli*, respectively, and a phylogenetic analysis showed that three unclassified multilocus sequence types of *C. coli* were more closely genetically related to *C. jejuni* than to other *C. coli* in this study. Of the six antibiotics tested, the highest resistance rates were to ciprofloxacin and tetracycline (100%), followed by lincomycin (63.3%), erythromycin (30.0%), amikacin (26.7%), and cefotaxime (20.0%). The antibiotic resistance rate of *C. coli* was higher than that of *C. jejuni*. The GyrA T86I mutation and 15 acquired resistance genes were detected with whole-genome sequencing (WGS). Among those, the GyrA T86I mutation and *tet(O)* were most prevalent (both 96.7%), followed by the *blaOXA*-type gene (90.0%), *ant(6)-Ia* (26.7%), *aac(6')-aph(3'')* (23.3%), *erm*(B) (13.3%), and other genes (3.3%). The ciprofloxacin and tetracycline resistance phenotypes correlated strongly with the GyrA T86I mutation and *tet(O)*/*tet(L)*, respectively, but for other antibiotics, the correlation between genes and resistance phenotypes were weak, indicating that there may be resistance mechanisms other than the resistance genes detected in this study. Virulence gene analysis showed that several genes related to adhesion, colonization, and invasion (including *cadF*, *porA*, *ciaB*, and *jlpA*) and cytolethal distending toxin (*cdtABC*) were only present in *C. jejuni*. Overall, this study extends our knowledge of the epidemiology and antibiotic resistance of *Campylobacter* in local Chinese dual-purpose chickens.

KEYWORDS

***Campylobacter*, antibiotic resistance, whole-genome sequencing, antibiotic-resistance gene, virulence factor**

1 Introduction

According to the report of the World Health Organization (WHO), food-borne diseases, ranging from diarrhea to cancer, are a major cause of human morbidity and mortality and affect one in 10 people worldwide every year (WHO, 2022). Campylobacteriosis is one of the most frequently reported food-borne diseases throughout the world (EFSA BIOHAZ Panel [EFSA Panel on Biological Hazards] et al., 2020). The acute infectious diarrhea caused by *Campylobacter* is mainly treated with antibiotics, such as fluoroquinolones and macrolides (Pham et al., 2016). However, the use of antibiotics in both human treatments and animal breeding hisolated from poultry meat samples.as caused antimicrobial resistance in *Campylobacter* to become an increasingly serious problem, and has posed a serious threat to public health over the past two decades (Luangtongkum et al., 2009). In 2017, fluoroquinolone-resistant *Campylobacter* was listed as one of the six high-priority antimicrobial-resistant pathogens by WHO (Romanescu et al., 2023). In China, bacterial antibiotic resistance monitoring data show that *Campylobacter* has maintained a high level of resistance to ciprofloxacin (> 90%) in various regions, (Li et al., 2016; Wang et al., 2016; Ju et al., 2018).

Poultry is the most important natural host of *Campylobacter*. In the European Union, the average prevalence of *Campylobacter* in birds and contaminated broiler carcasses is 71.2% and 75.8%, respectively (Soro et al., 2020), and more than 90% of commercial laying hens are colonized with *Campylobacter* (Jones et al., 2016). The breed of chicken is directly related to *Campylobacter* infection. Brena (Brena, 2013) reported that chickens reared indoors under higher welfare standards with decreased stocking density, the prevalence of *Campylobacter* was lower in a slower-growing breed (Hubbard JA57) than in a standard fast-growing breed (Ross 308). However, Humphrey et al. (Humphrey et al., 2014) demonstrated no intrinsic difference in the susceptibility of broiler breeds to *C. jejuni* under their experimental conditions.

China has many indigenous poultry resources, and many local chickens are dual-purpose (meat–egg) producers, with a longer growth cycle than broiler chickens. In general, traditional commercial broilers, such as AA broiler, Ross 308, are slaughtered in about 42 days (Fortuoso et al., 2019). However, some of the Chinese local chickens, such as Jianghan-chickens, usually start laying eggs at 140-150 days and then are slaughtered as food around 300 days. The life cycle of this type of production differs from that of commercial chickens, which may make the ecology (including antibiotic resistance) of *Campylobacter* different in production cycle. Previous studies have reported that under the same breeding conditions, the Huainan partridge chicken had a lower rate of *Campylobacter* infection than Heihua chickens or Ni-ke hon chickens, but a higher rate than AA+ chickens (Huang et al., 2009). Bai et al. (Bai et al., 2021) found that the isolation rate of *Campylobacter* was lower in slaughterhouses processing yellow feather broilers (14.2%) than in those processing white feather broilers or turkeys (from 26.3 to 100%). However, there are still few data on the prevalence of *Campylobacter* in local chickens in China.

The prevalence of antibiotic-resistant *Campylobacter* in poultry also cannot be ignored. Bacteria usually acquire antimicrobial resistance (AMR) by two main pathways. One involves chromosomal mutations at the target sites of antibiotic action, such as the point mutation in the *gyrA* gene that causes resistance to fluoroquinolone antibiotics (Iovine, 2013). The second involves the horizontal gene transfer of mobile genetic elements that contain resistance genes (Aksomaitiene et al., 2021). In the past few years, antibiotic-resistant *Campylobacter* in chicken house environment, eggshell, carcasses, poultry production, and the processing chain have been reported in many countries (Modirrousta et al., 2016; Tang et al., 2020b; Habib et al., 2023). Although several studies have detected antimicrobial-resistant *Campylobacter* in dual-purpose chickens (Foster-Nyarko et al., 2021; Metreveli et al., 2022; Rangaraju et al., 2022), Jianghan-chicken is a unique resource, which distributed in Central China. At present, the research on Jianghan-chicken is mainly focused on the eradication of *Salmonella* pullorum and avian leukosis, the overall resistance and virulence of *Campylobacter* in this chicken are unclear. Notably, the prevalence of *Campylobacter*, the generation and spread of its antibiotic resistance, and the complexity of its pathogenesis are probably related to the diversity of the *Campylobacter* genome. Many virulence genes have undergone expansion or contraction in specific lineages, resulting in differences in the content of virulence genes and ultimately leading to the specificity of their pathogenicity (Zhong et al., 2022). Fortunately, DNA sequencing technologies provide efficient methods with which to understand the antibiotic-resistance and pathogenic mechanisms of *Campylobacter*.

In this study, we investigated the genetic diversity, antibiotic resistance, and the distributions of the resistance and virulence genes of *Campylobacter* in local dual-purpose Jianghan-chickens in four regions of central China. We also used whole-genome sequencing (WGS) to evaluate the genetic diversity of *Campylobacter* and the phenotypic and genetic determinants associated with its intrinsic resistance. This data from this study extends our understanding of the prevalence and genomic characteristics of food-borne *Campylobacter* in local chickens in China.

2 Materials and methods

2.1 Bacterial isolates and culture conditions

In this study, 30 *Campylobacter* isolates were isolated from 312 samples collected from eight chicken farms breeding local dual-purpose (meat–egg) chickens in four regions of central China in 2022 (Supplementary Table 1). Freshly collected cloacal swabs were stored in Cary–Blair Modified Transport Medium (Amresco, Englewood, USA) and transported to the laboratory at 4°C for *Campylobacter* isolation. The samples were pre-enriched in Bolton broth containing *Campylobacter* growth supplement (Oxoid, Basingstoke, UK) and *Campylobacter* Bolton broth selective supplement (Oxoid), and cultured at 42°C for 24 h under microaerobic conditions (5% O_2, 10% CO_2, and 85% N_2). Subsequently, 100 µl cultures were inoculated on modified charcoal cefoperazone deoxycholate agar (mCCDA, Oxoid) plates

containing *Campylobacter* CCDA selective supplements at 42°C under microaerobic condition for 48 h. Suspected positive colonies were identified with Gram staining and 16S rDNA PCR (Linton et al., 1997). All isolates were identified with PCR targeting the *C. jejuni*-specific *hipO* gene and the *C. coli*-specific *asp* gene (Lawson et al., 1998).

2.2 Antimicrobial sensitivity testing

All isolates were tested for antimicrobial susceptibility to ciprofloxacin, tetracycline, cefotaxime, amikacin, erythromycin, and lincomycin with the disk diffusion method on Mueller Hinton Agar (Oxoid), according to the Clinical and Laboratory Standards Institute (CLSI) guidelines (Igwaran and Okoh, 2020). When the isolates were resistant to at least three different types of antibiotics, they were considered multidrug resistant (MDR). *Escherichia coli* ATCC 25922 was used as a quality control strain.

2.3 Whole-genome sequencing and analysis

The genomic DNA of the *Campylobacter* species was extracted with the TIANamp Bacteria DNA Kit (Tiangen, Beijing, China). The purity and concentration of the genomic DNA were determined by NanoDrop™ One sectrophotometer (Thermo Fisher Scientific, Waltham, MA, USA). Genomic DNA (5 μg; $OD_{260/280}$ = 1.8–2.0) was used for library construction. The Illumina NovaSeq 6000 sequencing platform (MajorBio Co., Shanghai, China) was used to sequence those libraries with a 2 × 150-bp read length. The raw reads obtained after sequencing were filtered with the fastp software (version 0.19.6) (Chen et al., 2018) and clean reads were obtained after the adapter sequences and low-quality sequences (Q < 20) were removed. The clean reads were then assembled with SOAPdenovo version 2.04 (Luo et al., 2012). The assembled contigs were uploaded to PubMLST (https://pubmlst.org/Campylobacter/) to determine their multilocus sequence types (STs) and clonal complexes (CCs). The phylogenetic tree and SNP count matrix heat map based on SNP analysis was obtained by using the online tool "multiple genome analysis" provided by BacWGSTdb 2.0 (http://bacdb.cn/BacWGSTdb/). RM1221_CP000025, which had abundant studies on its genome (Parker et al., 2006; Neal-McKinney et al., 2021; St. Charles et al., 2022), was selected as reference genome in BacWGSTdb tool and the construction of the phylogenetic tree in this tool relies on Neighbor-Joining (NJ) algorithm (Feng et al., 2021). The virulence genes were predicted based on the Virulence Factor Database (VFDB; http://www.mgc.ac.cn/VFs/). The tool ResFinder v.4.1 was used to detect acquired AMR genes and point mutations in specific genes conferring AMR; 90% minimum percentage identity and 60% minimum length coverage were used as the selection criteria. The sequence of the regulatory region of the *cmeABC* promoter (CmeR-Box) which is a 16-base inverted repeat sequence [TGTAATA (or T) TTTATTACA] (Cheng et al., 2020) and the amino acid sequence of CmeR were obtained by comparing the sequence alignment through BLAST (https://blast.ncbi.nlm.nih.gov/Blast.cgi). RAST Server (Rapid Annotation using Subsystem Technology) was used for Genome annotation of the assembled genome of multi-drug resistant *Campylobacter spp*, and the annotation scheme was ClassicRAST (http://rast.theseed.org/FIG/rast.cgi). Antibiotic resistance gene were also analyzed by Mobile Element Finder (https://cge.food.dtu.dk/services/MobileElementFinder/), and SnapGene® 2.3.2 was used to visualize gene arrangement.

2.4 Correlation analysis of susceptibility phenotypes and genotypes

The possible link between the *Campylobacter* resistance phenotype and the genotype predicted with WGS was analyzed by manually comparing the susceptibility test results (resistance or susceptibility) with the presence of known corresponding resistance genes and/or specific mutations. The percentage correlation between the resistance phenotype and genotype was calculated as the sum of true positives and true negatives divided by all the isolates tested. The positive predictive value was calculated by dividing the true positives by the sum of the true positives and false negatives, and the negative predictive value was calculated by dividing the true negatives by the sum of the true negatives and false positives. Sensitivity was calculated by dividing the true positives by the sum of the true positives and false positives, and specificity was calculated by dividing the true negatives by the sum of the true negatives and false negatives (Hodges et al., 2021).

3 Results

3.1 Genetic diversity analysis

Among the 30 *Campylobacter* isolates (13 C. *jejuni* and 17 C. *coli*) sequenced, nine sequence types (STs) in five clonal complexes (CC) based on multilocus sequence typing (MLST) were identified. Three *C. coli* and one *C. jejuni* isolates were not assigned an ST. ST8724 and ST2328 were not defined as a CC (Figure 1; Supplementary Table 2). The dominant ST for *C. jejuni* was ST354 (53.8%, 7/13), and the other isolates belonged to ST7469, ST8724, ST43, ST3924, or ST2328 (each 7.6%, 1/13). CC-354 was the dominant CC among the *C. jejuni* isolates. Among the *C. coli* isolates, ST825 was the most frequent ST (52.9%, 9/17), followed by ST872 (23.5%, 4/17) and ST1586 (5.9%, 1/17), and all of these assigned STs belonged to CC-828.

SNP analysis was further carried out, and we found that there was a certain genetic diversity among these isolates, and these differences involved SNP differences vary greatly, from a few to thousands (Supplementary Figure 1). All the isolates can be cluster to four main branches of the phylogenetic tree (Figure 1). Branches 1 and 2 contained the major clonal complex CC-828 of *C. coli*, and branch 3 contained the main clonal complex (CC-354) of *C. jejuni*. Interestingly,

10.3389/fcimb.2023.1236777

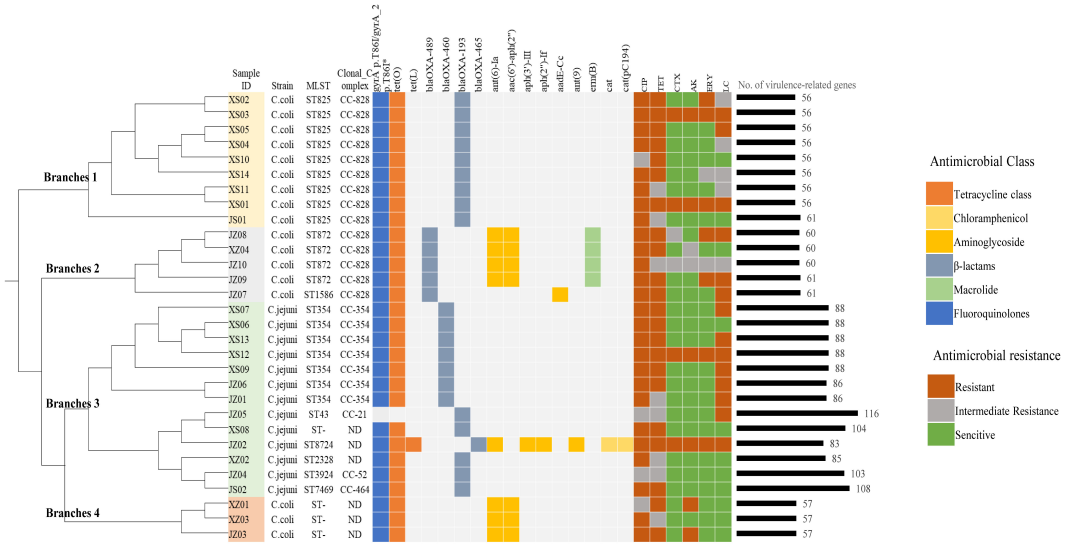

FIGURE 1
Genetic relationships, antimicrobial-resistance phenotypes, and the distributions of resistance- and virulence-related genes determined in this study. The phylogenetic tree was constructed based on genomic single-nucleotide polymorphisms, and the reference genome was RM1221_CP000025. The genetic determinants of antibiotic resistance are grouped according to their corresponding antibiotic categories and are color coded. The isolates were divided into 4 branches of the tree and distinguished by different colors: yellow (branch 1), gray (branch 2), green (branch 3), red (branch 4). CIP, ciprofloxacin; TET, tetracycline; CTX, cefotaxime; AK, amikacin; ERY, erythromycin; LC, lincomycin. *Point mutation.

branch 4, which contained the three *C. coli* isolates with unassigned STs, clustered with the larger branch containing *C. jejuni*.

3.2 Antimicrobial susceptibility

All the isolates were tested for susceptibility to six antibiotics. As shown in Table 1, all showed resistance to ciprofloxacin and tetracycline (100% in both *C. jejuni* and *C. coli*). More than half the isolates were resistant to lincomycin (61.5% of *C. jejuni* and 64.7% of *C. coli*). The resistance rates of *Campylobacter* to erythromycin, amikacin, and cefotaxime were 30.0%, 26.7%, and 20.0%, respectively. The resistance rate of *C. coli* to erythromycin was 41.2%, which was more than twice that of *C. jejuni* (15.4%). The data showed similar trends for amikacin (35.3% in *C. coli* and 15.4% in *C. jejuni*). Among the 30 isolates, 22 were resistant to three or more classes of antimicrobial agents, and the most prevalent pattern of MDR was resistance to ciprofloxacin, tetracycline, and lincomycin (45.5%, 10/22) (Figure 1).

3.3 Antibiotic resistance genes and resistance mutations

In this study, a C257T chromosomal point mutation in the *gyrA* gene, which conferring the Thr-86-Ile substitution, and 15 acquired resistance genes were identified by genome-wide analysis. Figure 1 and Supplementary Table 3 show the distributions of the genetic determinants of resistance detected in each isolate with WGS.

Of all the isolates tested, 96.7% (29/30) carried the *gyrA* gene point mutation (C257T) along with a ciprofloxacin resistance phenotype. The correlation analysis of resistance phenotype and genotype showed that the *gyrA* C257T mutation correlated strongly with ciprofloxacin resistance (100% in *C. coli* and 92.3% in *C. jejuni*) (Table 2).

TABLE 1 Resistance rates of tested *Campylobacter* isolates to six antibiotics.

Antibiotic category	Antimicrobial Agent[a]	*C. jejuni* (n=13)		*C. coli* (n=17)		Total (n=30)	
		No. of resistant isolates[b]	Resistance rates (%)	No. of resistant isolates[b]	Resistance rates (%)	No. of resistant isolates[b]	Resistance rates (%)
Fluoroquinolones	CIP	13	100.0%	17	100.0%	30	100.0%
Tetracycline class	TET	13	100.0%	17	100.0%	30	100.0%
β-lactams	CTX	2	15.4%	4	23.5%	6	20.0%
Aminoglycosides	AK	2	15.4%	6	35.3%	8	26.7%
Macrolides	ERY	2	15.4%	7	41.2%	9	30.0%
Lincosamides	LC	8	61.5%	11	64.7%	19	63.3%

[a]CIP, Ciprofloxacin; TET, Tetracycline; CTX, Cefotaxime; AK, Amikacin; ERY, Erythromycin; LC, Lincomycin. [b]Resistant isolates contain resistance and intermediate resistance.

TABLE 2 Correlation analysis of antibiotic resistance phenotype and antibiotic resistance determinants.

Antibiotic class	Antibiotic(s) tested by AST	Strains	Phenotype	No. of isolates	Resistance gene(s) or mutation(s) corresponding to resistance phenotype	No. with AMR gene present	Correlation between genotype and phenotype	Positive predictive values	Negative predictive value	Sensitivity	Specificity
Fluoroquinolones	CIP	*C. coli*	R/IR	17	GyrA_2p.T86I	17	100.0%	100.0%	–	100.0%	–
			S	0		0					
		C. jejuni	R/IR	13	GyrA T86I	12	92.3%	92.3%	–	100.0%	0.0%
			S	0		0					
Tetracycline class	TE	*C. coli*	R/IR	17	tet(O)	17	100.0%	100.0%	–	100.0%	–
			S	0		0					
		C. jejuni	R/IR	13	tet(O); tet(L)	12	92.3%	92.3%	–	100.0%	0.0%
			S	0		0					
β-lactams	CTX	*C. coli*	R/IR	4	blaOXA-489; blaOXA-193	4	41.2%	100.0%	23.1%	28.6%	100.0%
			S	13		10					
		C. jejuni	R/IR	2	blaOXA-465; blaOXA-460; blaOXA-193;	2	15.4%	100.0%	0.0%	15.4%	–
			S	11		11					
Aminoglycosides	AK	*C. coli*	R/IR	6	ant(6)-Ia; aac(6')-aph (2''); aadE-Cc	4	64.7%	66.7%	63.6%	50.0%	77.8%
			S	11		4					
		C. jejuni	R/IR	2	aph(2'')-If; aph(3')-III; ant(6)-Ia;ant(9)	1	92.3%	50.0%	100.0%	100.0%	91.7%
			S	11		0					
Macrolides	ERY	*C. coli*	R/IR	7	erm(B)	3	70.6%	42.9%	90.0%	75.0%	69.2%
			S	10		1					
		C. jejuni	R/IR	2	–	0	84.6%	0.0%	100.0%	–	84.6%
			S	11		0					
Lincosamides	LC	*C. coli*	R/IR	11	erm(B)	3	47.1%	27.3%	83.3%	75.0%	38.5%
			S	6		1					
		C. jejuni	R/IR	8	–	0	38.5%	0.0%	100.0%	–	38.5%
			S	5		0					

R, resistance; IR, intermediate resistance; S, sensitive.

10.3389/fcimb.2023.1236777

10.3389/fcimb.2023.1236777

Most of the isolates (96.7%, 29/30) contained the *tet(O)* gene, and one *C. jejuni* strain carried *tet(L)* (3.3%, 1/30). All isolates showed tetracycline resistance. The correlation between the tetracycline resistance phenotype and the resistance gene *tet*(*O*) or *tet*(*L*) was 100% in *C. coli* and 92.3% in *C. jejuni*.

The *blaOXA*-type β-lactamase-encoding gene was identified in 27 strains (90%, 27/30). And 22.2% (6/27) of isolates were resistant to cefotaxime.

Six aminoglycoside antibiotic resistance genes were detected in our isolates: *ant(6)-Ia* (26.7%, 8/30), *aac(6')-aph(3'')* (23.3%, 7/30), *aph(3')-III* (3.3%, 1/30), *aph(2'')-If* (3.3%, 1/30), *ant(9)* (3.3%, 1/30), and *aadE-Cc* (3.3%, 1/30). In this study, these genes mainly occurred in pairs, such as *ant(6)-Ia* and *aac(6')-aph(3'')*, in *C. coli* (23.3%, 7/30). These resistance gene combinations did not correlate strongly with the amikacin resistance phenotypic in *C. coli* (64.7%), but did correlate strongly with it in *C. jejuni* (92.3%).

The erythromycin and lincomycin resistance gene *erm*(B) was only identified in four *C. coli* isolates (13.3%, 4/30). The correlation between *erm*(B) and the erythromycin or lincomycin resistance phenotype was not strong (70.6% or 47.1%, respectively, in *C. coli*; and 84.6% or 38.5%, respectively, in *C. jejuni*). Further analysis of the isolates for point mutations in 23S rRNA revealed eight mutations in total (Supplementary Table 4), although neither the A2075G nor A2074C/G mutation, which reportedly cause erythromycin resistance, was detected.

3.4 CmeR-Box polymorphisms

A CmeR-Box polymorphism analysis of all isolates (Table 3) detected six CmeR-Box variants in 28 isolates. Among these, point substitutions were most common (96.4%), involving 17 *C. coli* and 10 *C. jejuni* isolates, whereas only one *C. jejuni* isolate (3.6%) had a point deletion, and no point insertion was detected in the CmeR-Box.

3.5 Genetic environment analysis of antibiotic resistance gene clusters in an MDR *C. jejuni* isolate

We analyzed the genetic environments of the resistance genes in *C. jejuni* JZ02, which was resistant to all of six antibiotics tested. Two antibiotic resistance gene clusters were detected (Figure 2). Gene cluster 1 contained the *tet(O)*, *tet(L)*, and *cat* (pC194) genes (Figure 2A). A transposase was encoded upstream from the *tet(L)* gene, and a 39-bp repeat and another transposase gene that shared 100% identity with IS1216 family transposase gene, were detected between *tet (O)* and *cat* (pC194). Moreover, a transposon encoding the protein TnpV was detected upstream from the *tet(O)* gene. Gene cluster 2 consisted of the *ant (9)*, *aph(3')-III*, *aph(2'')-If*, and *cat* genes (Figure 2B). However, no mobile genetic elements or repetitive sequences were detected in this gene cluster, although a box element and several hypothetical proteins with sequences similar to those of some Gram-positive bacteria were found.

TABLE 3 CmeR-Box polymorphisms in *C. jejuni* and *C. coli* isolates.

	CmeR-Box polymorphisms[a]	No. of isolates	% of isolates
C. jejuni	TGTAATAAAAATTATA	6	20.0%
	TGTAATAAATATTATA	3	10.0%
	TGTGATAAAAATTACA	1	3.3%
	TGTAATAAA-ATTACA	1	3.3%
	TGTAATAAAAATTACA	2	6.7%
C. coli	TGTAATAAATATTACA	16	53.3%
	TGTAATAAATATTGCA	1	3.3%

[a]underline means point substitution, "-" means point deletion.

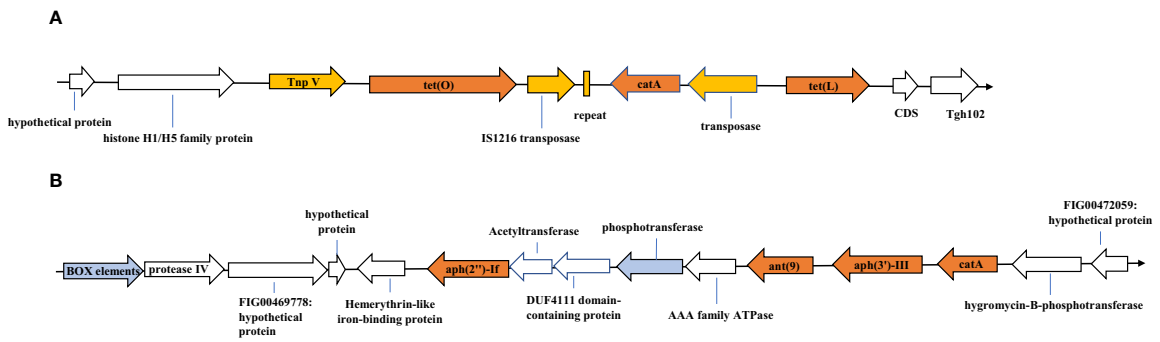

FIGURE 2
Resistance gene clusters identified in Campylobacter jejuni strain JZ02. **(A)** Tetracycline resistance gene cluster; **(B)** Aminoglycosides resistance gene cluster. SnapGene® 2.3.2 made this figure.

3.6 Virulence gene detection

Based on the VFDB, 126 virulence-related genes, involving adhesion, invasion, motility, toxins, and the type IV secretion system, were identified (Supplementary Table 5). We observed more virulence-related genes in *C. jejuni* (83–116 per isolate) than in *C. coli* (56–61 per isolate), and among them, isolates *C. jejuni* JZ05 (CC-21) and JS02 (CC-464) had the most virulence-related genes (Figure 1). Most of the genes only detected in *C. jejuni* were related to motility and adhesion, including *cadF*, *htrB*, *pebA*, *ciaB*, *jlpA*, and *cheA*, and genes encoding cytolethal distending toxin (*cdtABC*) were also only detected in *C. jejuni*. Type IV secretion system genes, including *virB11*, *virB10*, *virB9*, *virB8*, *virB4*, and *virD4*, were detected in one *C. jejuni* isolate (3.3%), and *wlaN* was only found in two *C. jejuni* isolates (6.7%) (Table 4). *Campylobacter* isolates in most branches (branch 1, 2, 4) of the phylogenetic tree had similar numbers of virulence genes, and the categories of these genes were not quite different. Interestingly, in branch 3, the type and abundance of virulence genes vary greatly from different ST types, and most of the different genes are related to capsular synthesis and immune regulation. Some isolates with more virulence-related genes were distributed in a sub-branch of branch 3.

4 Discussion

Campylobacter is the main bacterial pathogen causing human diarrhea worldwide, and its increasing prevalence and antibiotic resistance have caused great concern globally in recent years, in both human and veterinary clinics. Poultry is the main host of *Campylobacter*, but the prevalence of the pathogen varies across different species and different regions. For instance, an investigation in southeastern Italy showed that the prevalence of *C. jejuni* was higher in broilers than in laying hens (45.7% and 21.1%, respectively) (Parisi et al., 2007). In Europe, the prevalence of broiler flocks colonized with *Campylobacter* ranged from 18% to > 90% in different countries (Newell and Fearnley, 2003). Meat–egg dual-purpose local chickens may differ from commercial varieties because their breeding modes and breeding cycles differ, and they may pose a potential risk of *Campylobacter* transmission to both meat and eggs (Ahmed et al., 2021). Therefore, we investigated the phylogenetic relationships, virulence genes, antibiotic resistance, and genetic bases of the resistance phenotypes of *Campylobacter* isolates collected from local meat–egg dual-purpose chicken in China.

In this study, we identified two main prevalent *Campylobacter* species, *C. jejuni* and *C. coli*, and found strong genetic diversity in

TABLE 4 Frequencies of parts of predicted virulence-related factors in the genomes of 30 *Campylobacter* isolates.

VF class	Related genes	*C. jejuni* (n=13)		*C. coli* (n=17)		Total (n=30)	
		NO.of isolate	% of isolates	NO.of isolate	% of isolates	NO.of isolate	% of isolates
Adherence	*cadF*	13	100.00%	0	0.00%	13	43.30%
	porA	5	38.50%	0	0.00%	5	16.70%
	pebA	13	100.00%	0	0.00%	13	43.30%
	jlpA	13	100.00%	0	0.00%	13	43.30%
Immune modulation	*htrB*	13	100.00%	0	0.00%	13	43.30%
	wlaN	2	15.40%	0	0.00%	2	6.70%
	Cj1135	13	100.00%	0	0.00%	13	43.30%
	kpsD/M	13	100.00%	17	100.00%	30	100.00%
	neuA1	2	15.40%	0	0.00%	2	6.70%
	kpsF	13	100.00%	14	82.40%	27	90.00%
	cheA	13	100.00%	0	0.00%	13	43.30%
Type IV secretion system	*virB10/virB11/virB4/virB8/virB9/virD4*	1	7.70%	0	0.00%	1	3.30%
Toxin	*cdtA*	12	92.30%	0	0.00%	12	40.00%
	cdtB	13	100.00%	0	0.00%	13	43.30%
	cdtC	13	100.00%	0	0.00%	13	43.30%
Motility	*flgB*	13	100.00%	17	100.00%	30	100.00%
	flhB	13	100.00%	17	100.00%	30	100.00%
	flaA	10	76.90%	6	35.30%	16	53.30%
Invasion	*ciaB*	13	100.00%	0	0.00%	13	43.30%

the *Campylobacter* strains transmitted in these chickens. The National Center for Biotechnology Information (NCBI) database indicated that CC-354 strains occur mainly in the United States and the United Kingdom, whereas they are quite dispersed in other countries (Yu et al., 2020). A previous study showed that CC-353 and CC-464 are the dominant CCs of *C. jejuni* in central China, and CC-354 was the dominant population of *C. jejuni* detected in the present study. CC-21 is also the most frequently reported *C. jejuni* genotype in diarrhea patients in China (Zhang et al., 2020b), and in Zhang et al.'s study (Zhang et al., 2020a), CC-21 was also the dominant *Campylobacter* CC in chickens in southeastern China. However, in the present study, only one strain belonging to CC-21 was isolated, suggesting that the diversity of *C. jejuni* may vary by region and sample source, and that the epidemic patterns of *Campylobacter* may differ in local meat–egg dual-purpose chickens. Three ST types, ST1586, ST872, and ST828, were found in the *C. coli* isolates, which belong to the same clonal complex, CC-828. This was expected because CC-828 is the dominant population of *C. coli*, and a large number of past studies have reported its prevalence around the world (Zhang et al., 2016; Di Giannatale et al., 2019; Gomes et al., 2019). Based on principal component analysis (PCA) on the evolutionary distances of core gene families, Snipen et al. reported that *Campylobacter* has a mixed evolutionary pattern characterized by genomes (Snipen et al., 2012). It is noteworthy that the three *C. coli* strains with undefined STs detected in this study clustered with *C. jejuni* on the same large branch of a phylogenetic tree based on a genomic SNP analysis, suggesting that their genetic relationship was close. Previous studies have shown that an bidirectional increase in the rate of recombination between *C. jejuni* and *C. coli* has led to the gradual convergence of the two species (Sheppard et al., 2008).

Antibiotic resistance has become one of the most important factors threatening human public health globally (Mancuso et al., 2021). It is noteworthy that 73.3% of *Campylobacter* isolates were multidrug resistant in the present study. The resistance rates of *Campylobacter* to ciprofloxacin and tetracycline in China are high, and studies have reported rates of 90%–100% in broilers (Ma et al., 2014; Li et al., 2016; Wang et al., 2021). In the present study, there were similar high resistance rates to ciprofloxacin and tetracycline in both *C. jejuni* and *C. coli*. In the past, fluoroquinolones have been widely used in the edible animal industry, especially in poultry production, although tetracyclines are also commonly used to treat and prevent bacterial diseases in poultry in China. This may explain the high resistance rates to these two antibiotics in *Campylobacter*. In the early 1980s, the development and introduction of the third-generation extended-spectrum cephalosporin cefotaxime provided a new treatment for patients infected with Gram-negative bacilli (Hawkey, 2008). Here, we detected a relatively low rate of cefotaxime resistance (20.0%). Although it is not approved for use in food animals in China (Dai et al., 2008), we detected a high rate of amikacin resistance in *Campylobacter* (26.7%). Nor did the proportion of erythromycin-resistant isolates in our study differ greatly from that reported in previous studies (30.0% and 25.2%, respectively) (Cheng et al., 2020). However, the erythromycin resistance rate of *C. jejuni* was lower than in previous studies (15.4% and 30.1%, respectively), whereas the rate in *C. coli* was higher (41.2% and 18.3%, respectively) (Cheng et al., 2020). We detected high rates of resistance to lincomycin in both *C. jejuni* and *C. coli*, which may be related to the antibiotics commonly used in the areas from which the isolates were collected. The resistance of *C. coli* to antibiotics other than tetracycline and ciprofloxacin was greater than that of *C. jejuni*. These findings are consistent with the results of Tang et al. (Tang et al., 2020a), who reported that the prevalence of antibiotic resistance in chicken-derived *C. coli* was higher than in chicken-derived *C. jejuni*. In general, there is a worrying trend that, although the addition of antibiotics to feed supplements was banned in China in 2020, it has not reduced antibiotic resistance. On the contrary, some antibiotic resistance rates are still rising in some regions (Cheng et al., 2020).

Previous studies have shown that there is a strong correlation between the presence of AMR determinants detected with WGS and phenotypic antibiotic resistance (Rokney et al., 2020; Habib et al., 2023). However, it is known that *Campylobacter* also has many resistance mechanisms other than resistance gene-mediated, such as changes in membrane permeability, modification of the antibiotic efflux pumps, etc. (Iovine, 2013). The determinants of drug resistance do not always confer resistance phenotypes, and single resistance determinant may correlate weakly with certain antibiotics (Šoprek et al., 2022). In this study, we found that the overall correlation between the 16 antibiotic resistance determinants detected with ResFinder v.4.1 and phenotypic resistance was not strong, and that there were huge differences between the different antibiotics. This suggests that current research into the resistance mechanisms of *Campylobacter* remains to be improved, and that simply analyzing bacterial resistance in terms of the antibiotic resistance determinants predicted with WGS does not provide an accurate assessment.

In the present study, phenotypic resistance to ciprofloxacin and tetracycline correlated well with the presence of the *gyrA* gene point mutation (C257T) and the *tet(O)* or *tet(L)* gene, respectively, confirming that they are the main factors conferring resistance to the corresponding antimicrobial agents. CTX-M type β-lactamases usually are the cause of drug resistance of Gram-negative bacteria to cephalosporin such as cefotaxime, but CTX-M was not found in resistant strains in this study. In our isolates, 90% isolates of our study contained *blaOXA*-type β-lactamase-encoding gene. Indeed, most *Campylobacter* strains contain the *bla-OXA* gene encoding β-lactamase that confers resistance to carbapenems, but not to cephalosporin (Hadiyan et al., 2022). Research has already shown that different β-lactamases have different hydrolysis profiles (Poirel et al., 2011) and that the expression of β-lactamase directly affects the resistance of strains to β-lactam antibiotics (Casagrande Proietti et al., 2020). This may also explain why strains containing the *bla-OXA* gene but with a β-lactam-sensitive phenotype have been found in several other studies (Griggs et al., 2009; Zeng et al., 2014; Hadiyan et al., 2022). Our study

further confirmed that the presence of *bla-OXA* gene is not related to the resistance of cephalosporin drugs.

The prevalence of aminoglycoside-resistance-related determinants was low in the isolates tested, but these determinants showed relatively high diversity. A previous study demonstrated that the combined action of the *aph(3')-III*, *aac(6')-aph(2'')*, and *ant(6)-Ia* genes conferred resistance to aminoglycoside antibiotics on *Campylobacter* (Zhang et al., 2022), which was confirmed in our study. However, even with the synergistic effect of *ant(6)-Ia* and *aac (6')-aph(3'')*, the correlation between each gene and amikacin resistance was still low. Moreover, a *C. coli* isolate containing *aadE-Cc* showed a sensitive phenotype. This finding is consistent with a report by Painset et al. (Painset et al., 2020), who also observed *Campylobacter* strains carrying the *aadE-Cc* gene that were not resistant to some aminoglycoside antibiotics. There may be some unknown mechanism that inactivate these genes in *Campylobacter*.

Erythromycin and lincomycin have similar resistance mechanisms (Zhao et al., 2016; Wang et al., 2022). In the present study, the correlation between *erm*(B) and resistance to those two antibiotics was not strong. Therefore, we analyzed the sequence of 23S rRNA, and found no A2075G mutation.

Since most of the strains in this study have multi-drug resistance, we analyzed the genetic environment of the resistance gene of JZ02 (resistant to six antibiotics), and try to know how this strain obtained the antibiotic resistance gene. As is known that *Campylobacter* can acquire exogenous DNA through natural transformation (Wang and Taylor, 1990). The spread of antibiotic resistance genes in *Campylobacter* isolates from humans, animals, and the environment has previously been reported (Asuming-Bediako et al., 2019). The tetracycline resistance gene *tet(O)* is believed to have originated in Gram-positive cocci (Zilhao et al., 1988), and the tetracycline resistance mediated by this gene is mainly spread via the horizontal transfer of resistance genes on conjugated plasmids (Wardak et al., 2007). Although we found that resistance gene *tet(O)* was located on chromosome of isolate JZ02, some tranposase-encoding sequences were detected near *tet(O)*. The presence of these transposases implies that the antibiotic-resistance genes were co-transferred with some mobile genetic elements into the genomes of related strains. Although no relevant mobile elements were found in cluster 2, several genes, such as *ant(9)* and *aph(2'')-If*, which encode aminoglycoside-modifying enzymes, are similar to those of some Gram-positive bacteria, indicating that they may have derived from Gram-positive bacteria in the environment or animal intestines (Fabre et al., 2018).

The ability of *Campylobacter* to cause human diseases is considered multifactorial, and several genes are closely related to its virulence, including *ciaB* and *cdtABC* (Lopes et al., 2021). An analysis of the virulence-related genes of our isolates showed that *C. jejuni* carried more virulence-related genes than *C. coli*, which is consistent with the study of Lapierre et al. (Lapierre et al., 2016), and most of these genes were involved in motility (*flaA*), adhesion (*cadF*, *cheA*, *jlpA* et al), and invasion (*ciaB*). It is noteworthy that in this study, CC-21 and CC-464 had the most virulence-related genes and these two clonal complexes are also common among the clinical isolates of *Campylobacter* (Zhang et al., 2020a; Zhang et al., 2020b; Zang et al., 2021). Then we found that the additional genes they carried were mainly involved in immune modulation like bacterial capsule biosynthesis, especially by sugar and aminotransferase enzymes (kfiD, glf, Cj1426c, Cj1432c, Cj1434c, Cj1435c, Cj1436c, Cj1437c) while these genes do not be harbored in other complexes(Supplementary Table 5; Supplementary Figure 2). Although a high prevalence of virulence-associated genes (*ciaB* and *flaA*) has been already reported in *Campylobacter* strains infecting children with moderate to severe diarrhea (Quetz et al., 2012), these genes were only detected in *C. jejuni* in the present study. This may explain why *C. jejuni* colonizes its host more readily than *C. coli* and is responsible for more food-borne bacterial infection events (Moffatt et al., 2019; Callahan Sean et al., 2021; Schirone and Visciano, 2021). Virulence genes related to the type IV secretion system were only found in one strain of *C. jejuni*, and these genes are less prevalent in Asia and Europe (Panzenhagen et al., 2021). We also detected the *wlaN* gene, which is involved in Guillain–Barre syndrome in two *C. jejuni* isolates (Guirado et al., 2020).

In conclusion, in this study, we have demonstrated the genetic diversity and antimicrobial susceptibility of *Campylobacter* isolated from local dual-purpose chickens in China, and analyzed their resistance- and virulence-related genes. It thus provides important data on the epidemiological characteristics of *Campylobacter* in this food source.

Data availability statement

The datasets presented in this study can be found in online repositories. The names of the repository/repositories and accession number(s) can be found in the article/Supplementary Material.

Ethics statement

The studies involving animals were reviewed and approved by the Ethics Committee of Institute of Animal Husbandry and Veterinary, Hubei Academy of Agricultural Sciences (Wuhan, China).

Author contributions

JX, YC, QingL, and TZ conceived and designed the experiments. JX, YC, QinL, and YG performed the experiments. GW, WZ, and QH analyzed the data. JX, HS, and TZ wrote the manuscript. All authors contributed to the article and approved the submitted version.

Funding

This work was supported by grants from the National Key Research and Development Plan of China (2022YFD1800400),

the China Agriculture Research System (CARS-41), the Key Projects of Hubei Natural Science Foundation (2021CFA019), and the Key Research and Development Program of Hubei Province (2022BBA0055).

Conflict of interest

The authors declare that the research was conducted in the absence of any commercial or financial relationships that could be construed as a potential conflict of interest.

Publisher's note

All claims expressed in this article are solely those of the authors and do not necessarily represent those of their affiliated organizations, or those of the publisher, the editors and the reviewers. Any product that may be evaluated in this article, or claim that may be made by its manufacturer, is not guaranteed or endorsed by the publisher.

Supplementary material

The Supplementary Material for this article can be found online at: https://www.frontiersin.org/articles/10.3389/fcimb.2023.1236777/full#supplementary-material

SUPPLEMENTARY FIGURE S1
Matrix of SNP pair counts among 30 isolates. Number of SNP was calculated by comparing the genome sequences to the reference (RM1221) genome. Background colors represent different number of pairwise SNPs.

SUPPLEMENTARY FIGURE S2
Distribution of virulence-related genes of 30 isolates.

References

Ahmed, T., Ameer, H. A., and Javed, S. (2021). Pakistan's backyard poultry farming initiative: Impact analysis from a public health perspective. *Trop. Anim. Health Production* 53 (2), 210. doi: 10.1007/s11250-021-02659-6

Aksomaitiene, J., Novoslavskij, A., Kudirkiene, E., Gabinaitiene, A., and Malakauskas, M. (2021). Whole genome sequence-based prediction of resistance determinants in high-level multidrug-resistant campylobacter jejuni isolates in Lithuania. *Microorganisms* 9 (1), 66. doi: 10.3390/microorganisms9010066

Asuming-Bediako, N., Parry-Hanson Kunadu, A., Abraham, S., and Habib, I. (2019). Campylobacter at the human–food interface: The african perspective. *Pathogens* 8 (2), 87. doi: 10.3390/pathogens8020087

Bai, J., Chen, Z., Luo, K., Zeng, F., Qu, X., Zhang, H., et al. (2021). Highly prevalent multidrug-resistant campylobacter spp. Isolated from a yellow-feathered broiler slaughterhouse in South China. *Front. Microbiol.* 12, 682741. doi: 10.3389/fmicb.2021.682741

Brena, M. C. (2013). Effect of different poultry production methods on Campylobacter incidence and transmission in the broiler meat food chain. (University of Liverpool). Available at: https://livrepository.liverpool.ac.uk/18837/1/BrenaMar_Nov2013_18837.pdf

Callahan Sean, M., Dolislager Carolina, G., and Johnson Jeremiah, G. (2021). The host cellular immune response to infection by campylobacter Spp. and its role in disease. *Infection Immun.* 89 (8), e0011621. doi: 10.1128/iai.00116-21

Casagrande Proietti, P., Guelfi, G., Bellucci, S., De Luca, S., Di Gregorio, S., Pieramati, C., et al. (2020). Beta-lactam resistance in Campylobacter coli and Campylobacter jejuni chicken isolates and the association between blaOXA-61 gene expression and the action of β-lactamase inhibitors. *Vet.* 241, 108553. doi: 10.1016/j.vetmic.2019.108553

Chen, S., Zhou, Y., Chen, Y., and Gu, J. (2018). fastp: an ultra-fast all-in-one FASTQ preprocessor. *Bioinformatics* 34 (17), i884–i890. doi: 10.1093/bioinformatics/bty560

Cheng, Y., Zhang, W., Lu, Q., Wen, G., Zhao, Z., Luo, Q., et al. (2020). Point deletion or insertion in CmeR-Box, A2075G substitution in 23S rRNA, and presence of erm(B) are key factors of erythromycin resistance in campylobacter jejuni and campylobacter coli isolated from central China. *Front. Microbiol.* 11, 203. doi: 10.3389/fmicb.2020.00203

Dai, L., Lu, L.-M., Wu, C.-M., Li, B.-B., Huang, S.-Y., Wang, S.-C., et al. (2008). Characterization of antimicrobial resistance among Escherichia coli isolates from chickens in China between 2001 and 2006. *FEMS Microbiol. Lett.* 286 (2), 178–183. doi: 10.1111/j.1574-6968.2008.01272.x

Di Giannatale, E., Calistri, P., Di Donato, G., Decastelli, L., Goffredo, E., Adriano, D., et al. (2019). Thermotolerant Campylobacter spp. in chicken and bovine meat in Italy: Prevalence, level of contamination and molecular characterization of isolates. *PLoS One* 14 (12), e0225957. doi: 10.1371/journal.pone.0225957

EFSA BIOHAZ Panel (EFSA Panel on Biological Hazards) Koutsoumanis, K., Allende, A., Alvarez-Ordóñez, A., Bolton, D., Bover-Cid, S., et al (2020). Update and review of control options for Campylobacter in broilers at primary production. *EFSA J.* 18 (4), e06090. doi: 10.2903/j.efsa.2020.6090

Fabre, A., Oleastro, M., Nunes, A., Santos, A., Sifré, E., Ducournau, A., et al. (2018). Whole-genome sequence analysis of multidrug-resistant campylobacter isolates: A focus on aminoglycoside resistance determinants. *J. Clin. Microbiol.* 56 (9), e00390–e00318. doi: 10.1128/JCM.00390-18

Feng, Y., Zou, S., Chen, H., Yu, Y., and Ruan, Z. (2021). BacWGSTdb 2.0: a one-stop repository for bacterial whole-genome sequence typing and source tracking. *Nucleic Acids Res.* 49 (D1), D644–D650. doi: 10.1093/nar/gkaa821

Fortuoso, B. F., dos Reis, JoãoH., Gebert, R. R., Barreta, M., Griss, L. G., Casagrande, R. A., et al. (2019). Glycerol monolaurate in the diet of broiler chickens replacing conventional antimicrobials: Impact on health, performance and meat quality. *Microbial Pathogenesis* 129, 161–167. doi: 10.1016/j.micpath.2019.02.005

Foster-Nyarko, E., Alikhan, N. F., Ravi, A., Thomson, N. M., Jarju, S., Kwambana-Adams, B. A., et al. (2021). Genomic diversity of Escherichia coli isolates from backyard chickens and Guinea fowl in the Gambia. *Microb. Genom.* 7 (1), mgen000484. doi: 10.1099/mgen.0.000484

Gomes, C. N., Frazão, M. R., Passaglia, J., Duque, S. S., Medeiros, M. I.C., and Falcão, J. P. (2019). Molecular epidemiology and resistance profile of campylobacter jejuni and campylobacter coli strains isolated from different sources in Brazil. *Microbial Drug Resistance* 26 (12), 1516–1525. doi: 10.1089/mdr.2019.0266

Griggs, D. J., Peake, L., Johnson, M. M., Ghori, S., Mott, A., et al. (2009). β-lactamase-mediated β-lactam resistance in campylobacter species: Prevalence of cj0299 (blaOXA-61) and evidence for a novel β-lactamase in C. jejuni. *Antimicrob. Agents Chemother.* 53 (8), 3357–3364. doi: 10.1128/aac.01655-08

Guirado, P., Paytubi, S., Miró, E., Iglesias-Torrens, Y., Navarro, F., Cerdà-Cuéllar, M., et al. (2020). Differential Distribution of the wlaN and cgtB Genes, Associated with Guillain-Barré Syndrome, in Campylobacter jejuni Isolates from Humans, Broiler Chickens, and Wild Birds. *Microorganisms* 8 (3), 325. doi: 10.3390/microorganisms8030325

Habib, I., Ibrahim Mohamed, M.-Y., Ghazawi, A., Lakshmi, G. B., Khan, M., Li, D., et al. (2023). Genomic characterization of molecular markers associated with antimicrobial resistance and virulence of the prevalent Campylobacter coli isolated from retail chicken meat in the United Arab Emirates. *Curr. Res. Food Sci.* 6, 100434. doi: 10.1016/j.crfs.2023.100434

Hadiyan, M., Momtaz, H., and Shakerian, A. (2022). Prevalence, antimicrobial resistance, virulence gene profile and molecular typing of Campylobacter species isolated from poultry meat samples. *Vet. Med. Sci.* 8 (6), 2482–2493. doi: 10.1002/vms3.944

Hawkey, P. M. (2008). The growing burden of antimicrobial resistance. *J. Antimicrob. Chemother.* 62 (suppl_1), i1–i9. doi: 10.1093/jac/dkn241

Hodges, L. M., Taboada, E. N., Koziol, A., Mutschall, S., Blais, B. W., Douglas Inglis, G., et al. (2021). Systematic evaluation of whole-genome sequencing based prediction of antimicrobial resistance in campylobacter jejuni and C. coli. *Front. Microbiol.* 12, 776967. doi: 10.3389/fmicb.2021.776967

Huang, J. L., Xu, H. Y., Bao, G. Y., Zhou, X. H., Ji, D. J., Zhang, G., et al. (2009). Epidemiological surveillance of Campylobacter jejuni in chicken, dairy cattle and diarrhoea patients. *Epidemiol. Infection* 137 (8), 1111–1120. doi: 10.1017/S0950268809002039

Humphrey, S., Chaloner, G., Kemmett, K., Davidson, N., Williams, N., Kipar, A., et al. (2014). Campylobacter jejuni is not merely a commensal in commercial broiler chickens and affects bird welfare. *mBio* 5 (4), e01364–e01314. doi: 10.1128/mBio.01364-14

Igwaran, A., and Okoh, A. I. (2020). Occurrence, virulence and antimicrobial resistance-associated markers in campylobacter species isolated from retail fresh milk and water samples in two district municipalities in the Eastern Cape Province, South Africa. *Antibiotics* 9 (7), 426. doi: 10.3390/antibiotics9070426

Iovine, N. M. (2013). Resistance mechanisms in Campylobacter jejuni. *Virulence* 4 (3), 230–240. doi: 10.4161/viru.23753

Jones, D. R., Guard, J., Gast, R. K., Buhr, R. J., Fedorka-Cray, P. J., Abdo, Z., et al. (2016). Influence of commercial laying hen housing systems on the incidence and identification of Salmonella and Campylobacter1. *Poultry Sci.* 95 (5), 1116–1124. doi: 10.3382/ps/pew036

Ju, C. Y., Zhang, M. J., Ma, Y. P., Lu, J. R., Yu, Mu H., Chen, H., et al. (2018). Genetic and antibiotic resistance characteristics of campylobacter jejuni isolated from diarrheal patients, poultry and cattle in Shenzhen. *Biomed. Environ. Sci.* 31 (8), 579–585. doi: 10.3967/bes2018.079

Lapierre, L., Gatica, MaríaA., Riquelme, Víctor, Vergara, C., Yañez, JoséM., San Martín, B., et al. (2016). Characterization of antimicrobial susceptibility and its association with virulence genes related to adherence, invasion, and cytotoxicity in campylobacter jejuni and campylobacter coli isolates from animals, meat, and humans. *Microbial Drug Resistance* 22 (5), 432–444. doi: 10.1089/mdr.2015.0055

Lawson, A. J., Shafi, M. S., Pathak, K., and Stanley, J. (1998). Detection of campylobacter in gastroenteritis: comparison of direct PCR assay of faecal samples with selective culture. *Epidemiol. Infection* 121 (3), 547–553. doi: 10.1017/S0950268898001630

Li, B., Ma, L., Li, Y., Jia, H., Wei, J., Shao, D., et al. (2016). Antimicrobial resistance of campylobacter species isolated from broilers in live bird markets in Shanghai, China. *Foodborne Pathog. Dis.* 14 (2), 96–102. doi: 10.1089/fpd.2016.2186

Linton, D., Lawson, A. J., Owen, R. J., and Stanley, J. (1997). PCR detection, identification to species level, and fingerprinting of Campylobacter jejuni and Campylobacter coli direct from diarrheic samples. *J. Clin. Microbiol.* 35 (10), 2568–2572. doi: 10.1128/jcm.35.10.2568-2572.1997

Lopes, G. V., Ramires, T., Kleinubing, N. R., Scheik, LetíciaK., Fiorentini, ÂngelaM., and Padilha da Silva, W. (2021). Virulence factors of foodborne pathogen Campylobacter jejuni. *Microbial Pathogenesis* 161, 105265. doi: 10.1016/j.micpath.2021.105265

Luangtongkum, T., Jeon, B., Han, J., Paul, P., Logue, C. M., and Zhang, Q. (2009). Antibiotic resistance in Campylobacter: emergence, transmission and persistence. *Future Microbiol.* 4 (2), 189–200. doi: 10.2217/17460913.4.2.189

Luo, R., Liu, B., Xie, Y., Li, Z., Huang, W., Yuan, J., et al. (2012). SOAPdenovo2: an empirically improved memory-efficient short-read *de novo* assembler. *GigaScience* 1 (1), 2047–217X-1-18. doi: 10.1186/2047-217X-1-18

Ma, L., Wang, Y., Shen, J., Zhang, Q., and Wu, C. (2014). Tracking Campylobacter contamination along a broiler chicken production chain from the farm level to retail in China. *Int. J. Food Microbiol.* 181, 77–84. doi: 10.1016/j.ijfoodmicro.2014.04.023

Mancuso, G., Midiri, A., Gerace, E., and Biondo, C. (2021). Bacterial antibiotic resistance: The most critical pathogens. *Pathogens* 10 (10), 1310. doi: 10.3390/pathogens10101310

Metreveli, M., Bulia, S., Tevzadze, L., Tsanava, S., Zarske, M., Goenaga, J. C., et al. (2022). Comparison of antimicrobial susceptibility profiles of thermotolerant campylobacter spp. Isolated from human and poultry samples in Georgia (Caucasus). *Antibiotics* 11 (10), 1419. doi: 10.3390/antibiotics11101419

Modirrousta, S., Shapouri, R., Rezasoltani, S., and Molaabaszadeh, H. (2016). Prevalence of campylobacter spp. and their common serotypes in 330 cases of red-meat, chicken-meat and egg-shell in Zanjan City, Iran. *Infect. Epidemiol. Med.* 2 (1), 8–10. doi: 10.18869/modares.iem.2.1.8

Moffatt, C. R.M., Fearnley, E., Bell, R., Wright, R., Gregory, J., Sloan-Gardner, T., et al. (2019). Characteristics of campylobacter gastroenteritis outbreaks in Australia 2001 to 2016. *Foodborne Pathog. Dis.* 17 (5), 308–315. doi: 10.1089/fpd.2019.2731

Neal-McKinney, J. M., Liu, K. C., Lock, C. M., Wu, W.-H., and Hu, J. (2021). Comparison of MiSeq, MinION, and hybrid genome sequencing for analysis of Campylobacter jejuni. *Sci. Rep.* 11 (1), 5676. doi: 10.1038/s41598-021-84956-6

Newell, D. G., and Fearnley, C. (2003). Sources of campylobacter colonization in broiler chickens. *Appl. Environ. Microbiol.* 69 (8), 4343–4351. doi: 10.1128/AEM.69.8.4343-4351.2003

Painset, Anaïs, Day, M., Doumith, M., Rigby, J., Jenkins, C., Grant, K., et al. (2020). Comparison of phenotypic and WGS-derived antimicrobial resistance profiles of Campylobacter jejuni and Campylobacter coli isolated from cases of diarrhoeal disease in England and Wales 2015–16. *J. Antimicrob. Chemother.* 75 (4), 883–889. doi: 10.1093/jac/dkz539

Panzenhagen, P., Portes, A. B., dos Santos, A. M.P., Duque, S. D., and Conte Junior, C. A. (2021). The distribution of campylobacter jejuni virulence genes in genomes worldwide derived from the NCBI pathogen detection database. *Genes* 12 (10), 1538. doi: 10.3390/genes12101538

Parisi, A., Lanzilotta, S. G., Addante, N., Normanno, G., Di Modugno, G., Dambrosio, A., et al. (2007). Prevalence, molecular characterization and antimicrobial resistance of thermophilic campylobacter isolates from cattle, hens, broilers and broiler meat in south-eastern Italy. *Vet. Res. Commun.* 31 (1), 113–123. doi: 10.1007/s11259-006-3404-3

Parker, C. T., Quiñones, B., Miller, W. G., Horn, S. T., and Mandrell, R. E. (2006). Comparative genomic analysis of campylobacter jejuni strains reveals diversity due to genomic elements similar to those present in c. jejuni strain RM1221. *J. Clin. Microbiol.* 44 (11), 4125–4135. doi: 10.1128/jcm.01231-06

Pham, N. T. K., Thongprachum, A., Tran, D. N., Nishimura, S., Shimizu-Onda, Y., Duy Trinh, Q., et al. (2016). Antibiotic resistance of campylobacter jejuni and c. coli isolated from children with diarrhea in Thailand and Japan. *J. Japanese J. Infect. Dis.* 69 (1), 77–79. doi: 10.7883/yoken.JJID.2014.582

Poirel, L., Castanheira, M., Carrër, Amélie, Rodriguez, C. P., Jones, R. N., Smayevsky, J., et al. (2011). OXA-163, an OXA-48-related class D β-lactamase with extended activity toward expanded-spectrum cephalosporins. *Antimicrob. Agents Chemother.* 55 (6), 2546–2551. doi: 10.1128/aac.00022-11

Quetz, J. da S., Lima, I. F.N., Havt, A., Prata, M. M.G., Cavalcante, P. A., Medeiros, P. H.Q.S., et al. (2012). Campylobacter jejuni infection and virulence-associated genes in children with moderate to severe diarrhoea admitted to emergency rooms in northeastern Brazil. *J. Med. Microbiol.* 61 (4), 507–513. doi: 10.1099/jmm.0.040600-0

Rangaraju, V., Malla, B. A., Milton, A. A. P., Madesh, A., Balasaheb Madhukar, K., Kadwalia, A., et al. (2022). Occurrence, antimicrobial resistance and virulence properties of thermophilic Campylobacter coli originating from two different poultry settings. *Gene Rep.* 27, 101618. doi: 10.1016/j.genrep.2022.101618

Rokney, A., Valinsky, L., Vranckx, K., Feldman, N., Agmon, V., Moran-Gilad, J., et al. (2020). WGS-based prediction and analysis of antimicrobial resistance in campylobacter jejuni isolates from Israel. *Front. Cell. Infect. Microbiol.* 10, 365. doi: 10.3389/fcimb.2020.00365

Romanescu, M., Oprean, C., Lombrea, A., Badescu, B., Teodor, A., Constantin, G. D., et al(2023). Current state of knowledge regarding WHO high priority pathogens—resistance mechanisms and proposed solutions through candidates such as essential oils: a systematic review. *Int. J. Mol. Sci.* 24 (11), 9727. doi: 10.3390/ijms24119727

Schirone, M., and Visciano, P. (2021). Trends of major foodborne outbreaks in the european union during the years 2015–2019. *Hygiene* 1 (3), 106–1195. doi: 10.3390/hygiene1030010

Sheppard, S. K., McCarthy, N. D., Falush, D., and Maiden, M. C.J. (2008). Convergence of campylobacter species: Implications for bacterial evolution. *Science* 320 (5873), 237–239. doi: 10.1126/science.1155532

Snipen, L., Wassenaar, T. M., Altermann, E., Olson, J., Kathariou, S., Lagesen, K., et al. (2012). Analysis of evolutionary patterns of genes in Campylobacter jejuni and C. coli. *Microbial Inf. Experimentation* 2 (1), 8. doi: 10.1186/2042-5783-2-8

Šoprek, S., Duvnjak, S., Kompes, G., Jurinović, L., and Tambić Andrašević, A. (2022). Resistome analysis of campylobacter jejuni strains isolated from human stool and primary sterile samples in Croatia. *Microorganisms* 10 (7), 1410. doi: 10.3390/microorganisms10071410

Soro, A. B., Whyte, P., Bolton, D. J., and Tiwari, B. K. (2020). Strategies and novel technologies to control Campylobacter in the poultry chain: A review. *Compr. Rev. Food Sci. Food Saf.* 19 (4), 1353–1377. doi: 10.1111/1541-4337.12544

St. Charles, J. L., Brooks, P. T., Bell, J. A., Ahmed, H., Allen, M. V., Manning, S. D., et al. (2022). Zoonotic transmission of campylobacter jejuni to caretakers from sick pen calves carrying a mixed population of strains with and without guillain barré Syndrome-associated lipooligosaccharide loci. *Front. Microbiol.* 13, 800269. doi: 10.3389/fmicb.2022.800269

Tang, Y., Jiang, Q., Tang, H., Wang, Z., Yin, Yi, Ren, F., et al. (2020b). Characterization and prevalence of campylobacter spp. From broiler chicken rearing period to the slaughtering process in Eastern China. *Front. Vet. Sci.* 7, 227. doi: 10.3389/fvets.2020.00227

Tang, M., Zhou, Q., Zhang, X., Zhou, S., Zhang, J., Tang, X., et al. (2020a). Antibiotic resistance profiles and molecular mechanisms of campylobacter from chicken and pig in China. *Front. Microbiol.* 11, 592496. doi: 10.3389/fmicb.2020.592496

Wang, Y., Dong, Y., Deng, F., Liu, D., Yao, H., Zhang, Q., et al. (2016). Species shift and multidrug resistance of Campylobacter from chicken and swine, China 2008–14. *J. Antimicrob. Chemother.* 71 (3), 666–669. doi: 10.1093/jac/dkv382

Wang, Y., and Taylor, D. E. (1990). Natural transformation in Campylobacter species. *J. Bacteriology* 172 (2), 949–955. doi: 10.1128/jb.172.2.949-955.1990

Wang, J., Wang, Z., Zhang, J., Ding, Yu, Ma, Z., Jiang, F., et al. (2021). Prevalence, antibiotic susceptibility and genetic diversity of Campylobacter jejuni isolated from retail food in China. *LWT* 143, 111098. doi: 10.1016/j.lwt.2021.111098

Wang, T., Zhao, W., Li, S., Yao, H., Zhang, Q., and Yang, L. (2022). Characterization of erm(B)-carrying Campylobacter Spp. of retail chicken meat origin. *J. Global Antimicrobial Resistance* 30, 173–177. doi: 10.1016/j.jgar.2022.05.029

Wardak, S., Szych, J., Aleksandra, A. Z., and Gierczyński, Rafał (2007). Antibiotic Resistance of Campylobacter jejuni and Campylobacter coli Clinical Isolates from Poland. *Antimicrob. Agents Chemother.* 51 (3), 1123–1125. doi: 10.1128/aac.01187-06

WHO. (2022). *World Food Safety Day 2022 - Safer food, better health*. Available at: https://www.who.int/news/item/07-06-2022-world-food-safety-day-2022-safer-food-better-health.

Yu, H., Elbediwi, M., Zhou, X., Shuai, H., Lou, X., Wang, H., et al. (2020). Epidemiological and Genomic Characterization of Campylobacter jejuni Isolates from a Foodborne Outbreak at Hangzhou, China. *Int. J. Mol. Sci.* 21 (8), 3001. doi: 10.3390/ijms21083001

Zang, X., Lv, H., Tang, H., Jiao, X., and Huang, J. (2021). Capsular genotype and lipooligosaccharide class associated genomic characterizations of campylobacter jejuni isolates from food animals in China. *Front. Microbiol.* 12, 775090. doi: 10.3389/fmicb.2021.775090

Zeng, X., Brown, S., Gillespie, B., and Lin, J. (2014). A single nucleotide in the promoter region modulates the expression of the β-lactamase OXA-61 in Campylobacter jejuni. *J. Antimicrob. Chemother.* 69 (5), 1215–1223. doi: 10.1093/jac/dkt515

Zhang, L., Li, Yi, Shao, Y., Hu, Y., Lou, H., Chen, X., et al. (2020a). Molecular characterization and antibiotic resistant profiles of campylobacter species isolated from poultry and diarrheal patients in Southeastern China 2017–2019. *Front. Microbiol.* 11, 1244. doi: 10.3389/fmicb.2020.01244

Zhang, T., Luo, Q., Chen, Y., Li, T., Wen, G., Zhang, R., et al. (2016). Molecular epidemiology, virulence determinants and antimicrobial resistance of campylobacter spreading in retail chicken meat in central China. *Gut Pathog.* 8 (1), 48. doi: 10.1186/s13099-016-0132-2

Zhang, P., Zhang, X., Liu, Y., Cui, Q., Qin, X., Niu, Y., et al. (2022). Genomic insights into the increased occurrence of campylobacteriosis caused by antimicrobial-resistant campylobacter coli. *mBio* 13 (6), e02835–e02822. doi: 10.1128/mbio.02835-22

Zhang, P., Zhang, X., Liu, Y., Jiang, J., Shen, Z., Chen, Q., et al. (2020b). Multilocus sequence types and antimicrobial resistance of campylobacter jejuni and c. coli isolates of human patients from Beijing, China 2017–2018. *Front. Microbiol.* 11, 554784. doi: 10.3389/fmicb.2020.554784

Zhao, S., Tyson, G. H., Chen, Y., Li, C., Mukherjee, S., Young, S., et al. (2016). Whole-genome sequencing analysis accurately predicts antimicrobial resistance phenotypes in campylobacter spp. *Appl. Environ. Microbiol.* 82 (2), 459–466. doi: 10.1128/AEM.02873-15

Zhong, C., Qu, B., Hu, G., and Ning, K. (2022). Pan-genome analysis of campylobacter: Insights on the genomic diversity and virulence profile. *Microbiol. Spectr.* 10 (5), e01029-22. doi: 10.1128/spectrum.01029-22

Zilhao, R., Papadopoulou, B., and Courvalin, P. (1988). Occurrence of the Campylobacter resistance gene tetO in Enterococcus and Streptococcus spp. *Antimicrob. Agents Chemother.* 32 (12), 1793–1796. doi: 10.1128/aac.32.12.1793

frontiers | Frontiers in Cellular and Infection Microbiology

TYPE Original Research
PUBLISHED 13 October 2023
DOI 10.3389/fcimb.2023.1260066

OPEN ACCESS

EDITED BY
Luis Esau Lopez Jacome,
Instituto Nacional de Rehabilitación, Mexico

REVIEWED BY
Leonardo Gabriel Panunzi,
CEA Saclay, France
Chandra Shekhar,
University of Tennessee Health Science Center (UTHSC), United States

*CORRESPONDENCE
Dongguo Wang
wdgtzs@163.com
Liman Ma
limanma1986@163.com

†These authors have contributed equally to this work

RECEIVED 17 July 2023
ACCEPTED 29 September 2023
PUBLISHED 13 October 2023

CITATION
Qu Y, Wang W, Lu Q, Qiu J, Wang D and Ma L (2023) Occurrence and characterization of plasmids carrying *tmexCD1-toprJ1*, bla_{DHA-1}, and $bla_{CTX-M-127}$, in clinical *Klebsiella pneumoniae* strains. *Front. Cell. Infect. Microbiol.* 13:1260066. doi: 10.3389/fcimb.2023.1260066

Occurrence and characterization of plasmids carrying *tmexCD1-toprJ1*, bla_{DHA-1}, and $bla_{CTX-M-127}$, in clinical *Klebsiella pneumoniae* strains

Ying Qu[1†], Wenji Wang[2†], Qinhong Lu[3†], Jihai Qiu[4†], Dongguo Wang[5*†] and Liman Ma[5,6*†]

[1]Department of Clinical Medicine Laboratory, Taizhou Municipal Hospital Affiliated with Taizhou University, Taizhou, Zhejiang, China, [2]School of Life Sciences, Taizhou University, Taizhou, Zhejiang, China, [3]Department of Clinical Medicine Laboratory, Ningbo Medical Center Li Huili Hospital, Ningbo, Zhejiang, China, [4]Department of Infectious Diseases, Taizhou Municipal Hospital Affiliated with Taizhou University, Taizhou, Zhejiang, China, [5]Department of Central Laboratory, Taizhou Municipal Hospital Affiliated with Taizhou University, Taizhou, Zhejiang, China, [6]School of Medicine, Taizhou University, Taizhou, Zhejiang, China

Objective: Today, the emergence of *Klebsiella pneumoniae* with the *tmexCD1-toprJ1* gene cassette in patients has presented a significant clinical challenge.

Methods: To present the detailed genetic features of the *tmexCD1-toprJ1* gene cassette of *K. pneumoniae* strain F4_plasmid pA, the whole bacterial genome was sequenced by Illumina and nanopore platforms, and mobile genetic elements related to antibiotic resistance genes were analyzed with a series of bioinformatics methods.

Results: *K. pneumoniae* strain F4 was determined to be a class A+C beta-lactamase, and was resistant to routinely used antibiotics, especially tigecycline, because of the *oqxAB* gene localized on the F4_chromosome and *tmexCD1-toprJ1* on F4_plasmid A. After plasmid transfer assays, the F4_plasmid pA or F4_plasmid pB could be recovered with an average conjugation frequencies of 3.42×10^{-4} or 4.19×10^{-4}. F4_plasmid pA carried *tmexCD1-toprJ1* and bla_{DHA-1} accompanied by genetic intermixing of Tn*As1*, Tn*5393*, Tn*As3*, and In641, while F4_plasmid pB, bearing $bla_{CTX-M-174}$, had structural overlap of Tn*As3* and In641.

Conclusions: We suggested that plasmids carrying *tmexCD1- toprJ1* might be strongly related to IS*26*-integrated loop intermediates. This study showed that due to the structural evolution of F4 and related strains, their resistances were so strong that effective antibiotics were virtually unavailable, therefore their spread and prevalence should be strictly controlled.

KEYWORDS

***K. pneumoniae*, F4_plasmid pA, F4_plasmid pB, tigecycline resistance, multidrug resistance, tmexCD1-toprJ1**

Introduction

In recent years, a novel plasmid-mediated resistance-nodule-division (RND) efflux pump, *tmexCD1-toprJ1*, has emerged and been widely characterized from patient, animal, and food samples of *Klebsiella pneumoniae* (Lv et al., 2020). This novel multidrug resistance plasmid gene cluster, *tmexCD1-toprJ1*, was first reported in 2020 from animal-derived *K. pneumoniae* in China, exhibiting resistance or reduced susceptibility to several classes of antibiotics, including cephalosporins, phenolics, quinolones, and tetracyclines, and conferring resistance to the last-line antibiotics tigecycline and eravacycline (Lv et al., 2020; Wang CZ et al., 2021; Ghaheh et al., 2022).

The chromosomal or plasmid-encoded RND family *tmexCD1-toprJ1* expresses multidrug resistance (MDR) in Gram-negative bacteria (Li et al., 2015; Du et al., 2018), usually requiring the action of three gene products to be effective. Homologous transfer of the entire gene cluster encoding the RND-type tripartite drug efflux pump from chromosome to plasmid has been rarely reported thus far (Tauch et al., 2003; Li et al., 2015). The tripartite efflux system formed by the RND pump can directly export antibiotics outside the cell (Li et al., 2015), but only when regulatory genes (such as *tnfxB*, *araC*, or *tetR*) are efficiently expressed intracellularly does this lead to MDR in most clinically pathogenic bacteria carrying *tmexCD1-toprJ1* (Salehi et al., 2021).

Tigecycline is one of the limited options for the treatment of infections caused by MDR gram-negative bacteria, particularly carbapenem-resistant Enterobacteriaceae (De Oliveira et al., 2020). However, two novel plasmid-mediated mechanisms for tigecycline resistance have recently been determined, including tigecycline-resistance variants of the *tet(X), tet(A), tet(K)*, and *tet (M)* genes (Linkevicius et al., 2016; Liu et al., 2016; He et al., 2019; Lv et al., 2020; Xu et al., 2021), and the RND efflux pump gene cluster, *tmexCD1-toprJ1* (Lv et al., 2020). The *tet* variants are rarely discovered in *K. pneumoniae* (He et al., 2019; Wang et al., 2019), but *tmexCD1-toprJ1* and its variants are increasingly found in *K. pneumoniae* (Lv et al., 2020; Sun et al., 2020), and severe variants can lead to high mortality in patients (Yang et al., 2021; Wang et al., 2023). The emergence of tigecycline resistance from plasmids with *tmexCD1- toprJ1* is highly disseminated and poses a significant clinical challenge. IS26-mediated mobility of the *tmexCD1-toprJ1* plasmid may result in rapid and widespread dissemination of *tmexCD1-toprJ1* among Gram-negative bacteria (Wan et al., 2021).

Transposons could carry multiple drug-resistant genes in different plasmids, especially, Tn*3* played a crucial role in the evolution of drug-resistant plasmids in Enterobacteriaceae (Algarni et al., 2023). And Integrons could be integrated into antibiotic resistance gene cassettes with multiple IS elements or with transposons to form complex structures containing multiple resistance genes (Algarni et al., 2023), that contributed to the widespread spread of drug-resistant genes among bacteria (Algarni et al., 2022).

In this study, we compared and analyzed the MDR region of the F4 plasmids bearing *tmexCD1-toprJ1*, $bla_{\text{DHA-1}}$, and $bla_{\text{CTX-M-127}}$ accompanied by intermingling of In641 or In553 with Tn*As1*, Tn*5393*, and/or Tn*As3* with those of related plasmids, characterized the structure of the plasmids.

Materials and methods

Bacterial strains and sequencing of the 16S rRNA gene

K. pneumoniae strain F4 was isolated from a sputum sample of a patient in Taizhou Municipal Hospital affiliated with Taizhou University in 2019. EC600 and *Escherichia coli* DH5α (TaKaRa, Dalian, China) were employed as hosts for cloning. In order to verify the strain F4 belonged as *K. pneumoniae*, the nearly complete 16S rRNA gene of the strain was amplified by PCR using the following primers: 5'-AGAGTTTGATYMTGGCTCAG-3' (forward) and 5'-TACCTTGTTACGACTT-3' (Y, T or C; M, A or C) (reverse). The length of the amplicon was about 1500 bp (Frank et al., 2008). The Taq enzyme was a 3:1 mixture of Fermentas Taq : Pfu ThermoFisher Scientific, Burlington, VT, USA), and the 30 ml reaction consisted of 1.5 U of enzyme. Amplification was performed using a temperature program, including initial denaturation at 94°C for 3 min, 30 cycles of denaturation at 94°C for 40 s, annealing at 50°C for 40 s, extension at 72°C for 1 min, and final extension at 72°C for 5 min. The PCR products were identified by bidirectional sequencing.

Experiments of conjugal transfer and plasmid transfer

Conjugation experiments

Based on a previously reported (Chen et al., 2015), conjugation experiments were performed in lysogeny broth (LB) with the strain EC600 as the recipient and with the strain F4 as the donor strains. Donor and recipient cells in logarithmic phase (0.5 mL of each) were added to 4 mL of fresh LB, which was followed by incubation at 35°C for 18–24 h without shaking. The transconjugants were selected on trypticase soy agar (TSA) plates containing 10 μg/L of rifampicin and 0.02 μg/L of imipenem.

Plasmid-electroporation assays

Transformation experiments were undertaken using *E. coli* DH5α electroporated cells as recipient cells for plasmid electroporation. Conjugation frequency was calculated as the number of transconjugates per initial donor cell. To prepare electrocompetent cells, bacteria were grown to OD600 = 0.5-0.6 and precipitated by centrifugation at 4°C. Two rounds of washes and centrifugation (6,000 rpm) were performed at 4°C with 1 vol milliQ water, ending with 1/50 volume 10% glycerol. Cells were resuspended in 1/500 vol 10% glycerol and aliquoted into 50 mL samples. Aliquots were frozen on dry ice, stored at -70°C and set aside. Aliquots were mixed with less than 10 ng of DNA in a 0.2 cm cuvette (Bio-Rad, California, USA) and then electrically pulsed (2.5 kV, 25 mF and 200 Ω) in a MicroPulser (Bio-Rad, California, USA).

10.3389/fcimb.2023.1260066

Electroporated cells were added to 1 mL of LB and incubated at 37°C with shaking for antibiotic expression. After incubation, the cells were cultured on antibiotic-containing medium. When plasmids from the strain F4 were used in electroporators, it was also selected appropriately with 10 μg/L of rifampicin and 0.02 μg/L of imipenem.

Antimicrobial susceptibility test

Bacterial resistance was detected by BioMerieux VITEK2 (MICs value) and disk diffusion test (mm value) (Table 1), the results were determined in accordance with the 2022 Clinical and Laboratory Standards Institute (CLSI) Guidelines (CLSI, 2022). Twenty-two antibiotics and antibiotics + enzyme inhibitors (Table 1) were detected, and *E. coli* ATCC 25922 was used as the quality control strain.

Detection of classes A, B, C and D beta-lactamases

Dual inhibitor diffusion synergy test

Amoxicillin/clavulanic acid (AMC, 20/10 μg) was placed in the center of the plate, and cefotaxime (CTX, 30 μg), cefepime (FEP, 30 μg), ceftriaxone (CRO, 30 μg), and cloxacillin (CXC, 200 μg) were placed around the AMC, with CTX and AMC spaced 25 mm apart and the rest spaced 20 mm apart. CXC was obtained from MW & E, UK, and the others were from Oxiod, UK.

Interpretation of test results: AMC was synergistic with CRO or CTX, indicating the sample was positive for extended-spectrum beta lactamases (ESBLs); AMC was not co-operative with CRO or CTX but was in synergy with FEP, and thus positive for ESBLs and AmpC; and CXC co-interacted with CRO or FEP, showing a positive result for AmpC enzyme.

AmpC enzyme confirmatory test

Using a modified enzyme extraction three-dimensional test, colonies to be tested were picked and incubated overnight on blood plates according to the literature (Coudron et al., 2000). To make a bacterial suspension with 0.5 McFarland turbidity, 25 μL of bacterial suspension was inoculated into 6 mL trypsin-digested soy broth, incubated overnight on a constant temperature shaker at 35°C at 200 r/min, and centrifuged at 4°C at 4000 r/min for 20 min. The supernatant was discarded, the precipitate was repeatedly freeze-thawed five times at −80°C, and 1.5 mL of 0.01 mol/L phosphate buffer (pH 7.0) was added, vortexed, and mixed. The supernatant was then centrifuged at 14,000 r/min for 2 h at 4°C, thus obtaining the enzyme extract.

Based on the standard paper diffusion method, 0.5 mL of *E. coli* ATCC25922 was applied to a Mueller-Hinton (MH) agar plate. Cefoxitin (FOX, 30 μg) was placed in the center of the plate, a slit

TABLE 1 MICs and genetic profiles of *K. pneumoniae* F4 (ST15).

Antimicrobial agents	MIC (mg/L)	Mechanism of resistance/location of resistance gene
Aminoglycoside		
Amikacin	≥16	aac(6')-Ib/aadA2/aadA1/aac(3')-IV/aph(4')-Ia/aph(6')-Id/aph(4')-Ia/aph(3')-Ia/rmtB/aph(3')-Ib/tmexCD1-toprJ1 (Plasmid A), aadA16/aac(6')-Ib-cr (Plasmid B)
β-lactams		
Urtapenem	≥8	bla_{DHA-1} (Plasmid A)/$bla_{CTX-M-174}$ (Plasmid B)
Imipenem	≥2	bla_{DHA-1} (Plasmid A)/$bla_{CTX-M-174}$ (Plasmid B)
Aztreonam	≥32	bla_{DHA-1} (Plasmid A)/$bla_{CTX-M-174}$ (Plasmid B)
Cefepime	≥32	bla_{DHA-1} (Plasmid A)/$bla_{CTX-M-174}$ (Plasmid B)
Cefotaxime	≥64	bla_{DHA-1} (Plasmid A)/$bla_{CTX-M-174}$ (Plasmid B)
Ceftazidime	≥64	bla_{DHA-1} (Plasmid A)/$bla_{CTX-M-174}$ (Plasmid B)
Ceftriaxone	≥64	bla_{DHA-1} (Plasmid A)/$bla_{CTX-M-174}$ (Plasmid B)
Cefuroxime	≥64	bla_{DHA-1} (Plasmid A)/$bla_{CTX-M-174}$ (Plasmid B)
Amoxicillin/Clavulanic acid	≥32	bla_{DHA-1} (Plasmid A)/$bla_{CTX-M-174}$ (Plasmid B)
Cefoperazone/Sulbactam	≥64	bla_{DHA-1} (Plasmid A)/$bla_{CTX-M-174}$ (Plasmid B)
Cefoperazone/Avibactam (30/20 μg)	6*	bla_{DHA-1} (Plasmid A)/$bla_{CTX-M-174}$ (Plasmid B)
Cephamycin		
Cefoxitin	≥64	bla_{DHA-1} (Plasmid A)/$bla_{CTX-M-174}$ (Plasmid B)
Fluoroqinolones		
Levofloxacin	≥8	tmexCD1-toprJ1/qnrB4 (Plasmid A), qnrB2 (Plasmid B), qnrB2 (Plasmid C), oqxB/oqxA (Chromosome)
Ciprofloxacin	≥4	tmexCD1-toprJ1/qnrB4 (Plasmid A), qnrB2 (Plasmid B), qnrB2 (Plasmid C), oqxB/oqxA (Chromosome)
Tetracycline		
Tetracycline	≥64	tmexCD1-toprJ1 (Plasmid A)/tet(D) (Plasmid B)
Glycylcycline		
Tigecycline	≥8	oqxAB (Chromosome), tmexCD1-toprJ1 (Plasmid A)

(Continued)

TABLE 1 Continued

Antimicrobial agents	MIC (mg/L)	Mechanism of resistance/location of resistance gene
Phenicol		
Chloramphenicol	≥64	cmlA1 (Plasmid A), floR (plasmid B)
Sulfonamide		
Trimethoprim-sulfamethoxazole	≥320	sul1/sul3 (Plasmid A), dfrA27/sul1 (plasmid B), sul1 (plasmid C)
Disinfecting agent and antiseptic		
–	–	qacH2 (Plasmid A)

*Disc diffusion method.

was cut radiologically from inside to outside at 5 mm from the edge of the paper plate with a sterile scalpel, and 40 µL of crude enzyme extract was added to the slit from inside to outside with a microsampler to avoid the enzyme solution overflowing the slit, then incubated overnight at 35°C. If an expanded long bacterial area appeared at the junction of the slit and the inhibition circle, it was judged as a positive three-dimensional test, meaning the sample was AmpC-enzyme positive.

Confirmation test for ESBLs

The differences in the diameter of the inhibition circles between ceftazidime (CAZ, 30 µg), ceftazidime/clavulanic acid (30/30 µg), and cefotaxime/clavulanic acid (30/30 µg) were determined as a positive result for ESBLs when the difference in the diameters of the inhibition circles of either group of drugs was ≥5 mm, based on the 2022 CLSI Guidelines (CLSI, 2022).

Classes B and D beta-lactamases tests

The modified carbapenem inactivation method (mCIM) and modified carbapenem inactivation + EDTA (eCIM) methods recommended by CLSI (CLSI, 2022) were performed for the detection of metallo-β-lactamases. And the increase of the zone of inhibition by ≥5 mm of eCIM *vs.* mCIM was interpreted as a positive result for metallo-β-lactamases (class B carbapenemase).

There was no definitive report of a class D carbapenemase phenotypic assay, which could be confirmed by a process of elimination; if the strain was not inhibited by a class A or B inhibitor, it definitely belonged to class D carbapenemase (Class D beta-lactamase).

Sequencing and sequence assembly

Genomic sequencing of strain F4 was performed on the third-generation PacBio Sequel II platform (Pacific Biosciences, CA, USA) and the second-generation sequencing Illumina NovaSeq 6000 platform (Illumina, San Diego, USA) using a DNA library with an average size of ~15 kb (range 10 kb to 20 kb), and on a small fragment libraries ~400 bp (range 150 bp to 600 bp). To improve the reliability of data processing, raw data from PacBio Sequel II were trimmed to obtain the high-quality clean reads (clean data) by Canu v2.2 (https://github.com/marbl/canu). The paired-end short Illumina reads were "*de novo*" assembled using Unicycler v0.4.5 (https://github.com/rrwick/Unicycler) or SPAdes v3.15.3 (https://github.com/ablab/spades). The sequence corrections at the post-assembly level were performed using Pilon v1.24 software (https://github.com/broadinstitute/pilon) based on second-generation sequencing reads. Finally, accurate DNA sequences in the study were obtained.

Sequence annotation and comparison in detail

Open reading frames (orfs) and pseudogenes were predicted using *RAST2.0* (Brettin et al., 2015), *BLASTP/BLASTN* (Boratyn et al., 2013), *UniProtKB/Swiss-Prot* (Brettin et al., 2015), and *RefSeq* databases (Brettin et al., 2015). Resistance genes, mobile elements, and other features were annotated using online databases such as *CARD 2023* (Alcock et al., 2023), *ResFinder4.0* (Bortolaia et al., 2020), IS*finder* (Siguier et al., 2006), *INTEGRALL* (Moura et al., 2009), and the *Tn* Number Registry (Tansirichaiya et al., 2019). Clonal MLST was determinated using *MLST 2.0* (https://cge.food.dtu.dk/services/MLST/) and *BacWGSTdb 2.0* (Feng et al., 2021). *MUSCLE 3.8.31* (Edgar, 2004) and BLASTN were used for multiple and pairwise sequence comparisons such as F4_plasmid pA, F4_plasmid pB, and F4_plasmid pC with their closely related plasmids, respectively. Circos plot of plasmids were drawn with CGView (Stothard et al., 2019). All plasmids comparison figures were created by the R pacakge genoPlotR v0.8.11 sofware (http://genoplotr.r-forge.r-project.org/) and edited using Inkscape v0.48.1 (https://inkscape.org/en).

Nucleotide sequence accession numbers

The sequences of the F4_chromosome, F4_plasmid pA, F4_plasmid pB, and F4_plasmid pC were deposited on the GenBank database with the accession numbers of CP090397.1, OM144974.1, OM144975.1, and OM144976.1, respectively (Table 2). The GenBank accession numbers of the related plasmids compared with F4_plasmid pA and F4_plasmid pB were also shown in Table 2.

Results

Antimicrobial susceptibility test, enzymatic properties, and transferable features

The strain was confirmed to be *K. pneumonia* by BLAST of the 16S rRNA and genomic sequences and average nucleotide homology analysis. MICs for the drug susceptibility test of strain F4 were shown in Table 1; Results for the drug susceptibility test of BioMerieux VITEK2 without MICs using the paper diffusion method, e.g., cefoperazone/avibactam, were also listed in Table 1. Enzyme characterization was confirmed to be class A+C beta-lactamases. The MLST of the strain F4 sequence was analyzed as ST15 using *MLST 2.0* and *BacWGSTdb 2.0*.

After bacterial conjugative transfers and electroporation assays, the transconjugants integrating the F4_plasmid pA or F4_plasmid pB could be recovered with an average conjugation frequencies of 3.42×10^{-4} or 4.19×10^{-4}, respectively. However, F4_plasmid pC failed in multiple plasmid transfer experiments.

10.3389/fcimb.2023.1260066

TABLE 2 Profiles of the *K. pneumoniae* plasmids studied in the paper.

No.	Plasmid	Isolate source	Type	Size (kb)	GC%	status	Accession no.
1	F4_plasmid pA	Patient's urine (Taizhou, China)	IncFIB-IncHI1B	276.487	46.92	Complete	OM144974.1
2	pMH15-269M_1	Patient's blood (Viet Nam)	IncFIB	288.040	46.67	Complete	AP023338.1
3	pHN111RT-1	Sewage (Guangzhou, China)	IncFIB	281.670	47.06	Complete	MT647838.1
4	pSZP4-9-2-tmexCD	Pork (Shenzhen, China)	IncFIB	274.231	46.89	Complete	CP075257.1
5	P1-tmexCD	Poultry farms (Beijing, China)	IncFIB	280.953	46.86	Complete	OL348377.1
6	F4_plasmid pB	Patient's urine (Taizhou, China)	IncFIA	79.722	51.65	Complete	OM144975.1
7	pCTXM27_020046	Patient (Yibin, China)	IncFIA	74.010	51.68	Complete	CP028782.2
8	Plasmid L99-05	Swine ropharyngeal (Guangzhou, China)	IncFIA	75.320	51.65	Complete	CP063211.1
9	p19110124-2	Swine Anal swab (Zhengzhou, China)	IncFIA	73.978	51.71	Complete	CP064179.1

Overview of drug resistance genes for F4_chromosome, F4_plasmid pA, F4_plasmid pB, and F4_plasmid pC

One F4_chromosome and three plasmids, including F4_plasmid pA, F4_plasmid pB, and F4_plasmid pC, were identified in strain F4. The F4_chromosome was approximately 5.25 Mb in length and only carried four antibiotic resistance genes, *oqxB*, *oqxA*, $bla_{\text{SHV-106}}$, and $bla_{\text{CTX-M-27}}$ (Table 1, Figure S1). F4_plasmid pA is a complete plasmid with a length of about 276.5 kb, harboring 22 different categories of drug resistance genes (Table 1, Figure S2). F4_plasmid pB was also a complete plasmid with a length of about 79.7 kb, carrying nine different types of drug resistance genes (Table 1, Figure S2). The length of F4_plasmid pC was 5.721 kb, but it belonged to a plasmid fragment with only quinolone (*qnrB2*) and sulfonamide (*sul1*) resistance genes (Table 1, Figure S2). F4_plasmid pC shared identity with the back-end sequence of F4_plasmid pB and a portion of the sequence before In553 of plasmid L99-05, but in the opposite directions (Figure 1).

Comparison of F4_plasmid pA with closely related plasmids pMH15-269M_1, pHN111RT-1, pSZP4-9-2-tmexCD, and P1-tmexCD, carrying *tmexCD1-toprJ1*, $bla_{\text{DHA-1}}$, and In641

The profiles of these closely related plasmids are shown in Table 2. The identities and coverage rates between F4_plasmid pA and pMH15-269M_1, pHN111RT-1, pSZP4-9-2-tmexCD, and P1-tmexCD were all greater than 99% and 95%, respectively, with extremely high similarity. The lengths of the MDR regions from F4_plasmid pA, pMH15-269M_1, pHN111RT-1, pSZP4-9-2-tmexCD, and P1-tmexCD were estimated to be 65.8 kb, 64.3 kb, 66.6 kb, 63.1 kb, and 66.5 kb, respectively, where only an *aac(6')-Ib* gene was outside the MDR region of each plasmid (Figure S3). The most significant common feature of these plasmids is that their MDR regions carry *tmexCD1-toprJ1*, $bla_{\text{DHA-1}}$, and $bla_{\text{CTX-M-127}}$, interpenetrated with Tn*As1*, Tn*5393*, and Tn*As3*, and intercalated with incomplete In641 (Figure 2). Tn*As1* was divided by Tn*5393* and Tn*As3*, which in turn was separated by In641 and a portion of Tn*5393* containing *tmexCD1-toprJ1*, the *mphE-msrE* module, and multiple insertion sequences (IS) including IS*26* (Figure 2). The common regions of Tn*As3* and Tn*5393* contained the RND-type efflux gene cluster *tmexCD1-toprJ1*, which was linked to the same IS*26* at both ends, forming an independent and basic structure as IS*26*-hp-IS*903B*-Tn*5393*-(*toprJ1-tmexD1-tmexC1-tnfxB1*)-hp-hp-IS*26* (Figure 2), which might have separate mobile properties, with *tnfxB1* acting as a plasmid-encoded transcriptional regulator for *tmexCD1-toprJ1*. In641 located on F4_plasmid pA and pMH15-269M_1 comprised the *estX-psp-aadA2-cmlA1-aadA1- qacH2* gene cassette with 5′-CS but lacking 3′-CS; In641 on pHN111RT-1 consisted of the *estX-psp-aadA2-cmlA1-aadA1* gene cassette with 5′-CS but no 3′-CS; In641 on pSZP4-9-2-tmexCD had only the *estX-psp-emrR* gene cassette, which had 5′-CS but lacked 3′-CS; and In641 on P1-tmexCD covered the *estX-psp-aadA2-cmlA1-aadA1- emrR* gene cassette, with 5′-CS and a shortened 3′-CS (Figure 2). Tn*5393* was also compartmentalized by some elements, such as a gene array of IS*26*-hp-IS*903B*- Tn*5393*-(*toprJ1-tmexD1-tmexC1-tnfxB1*)-hp-hp-IS*26*, some IS, the *mphE-msrE* module, *psp* module, and some drug resistance genes, such as $bla_{\text{DHA-1}}$, *aph(3')-Ia*, *sul1*, and *qnB4* (Figure 2). Overall, F4_plasmid pA harbored mainly *tmexCD1-toprJ1* and $bla_{\text{DHA-1}}$, accompanied by genetic intermixing of In641 with Tn*As1*, Tn*5393*, and Tn*As3*.

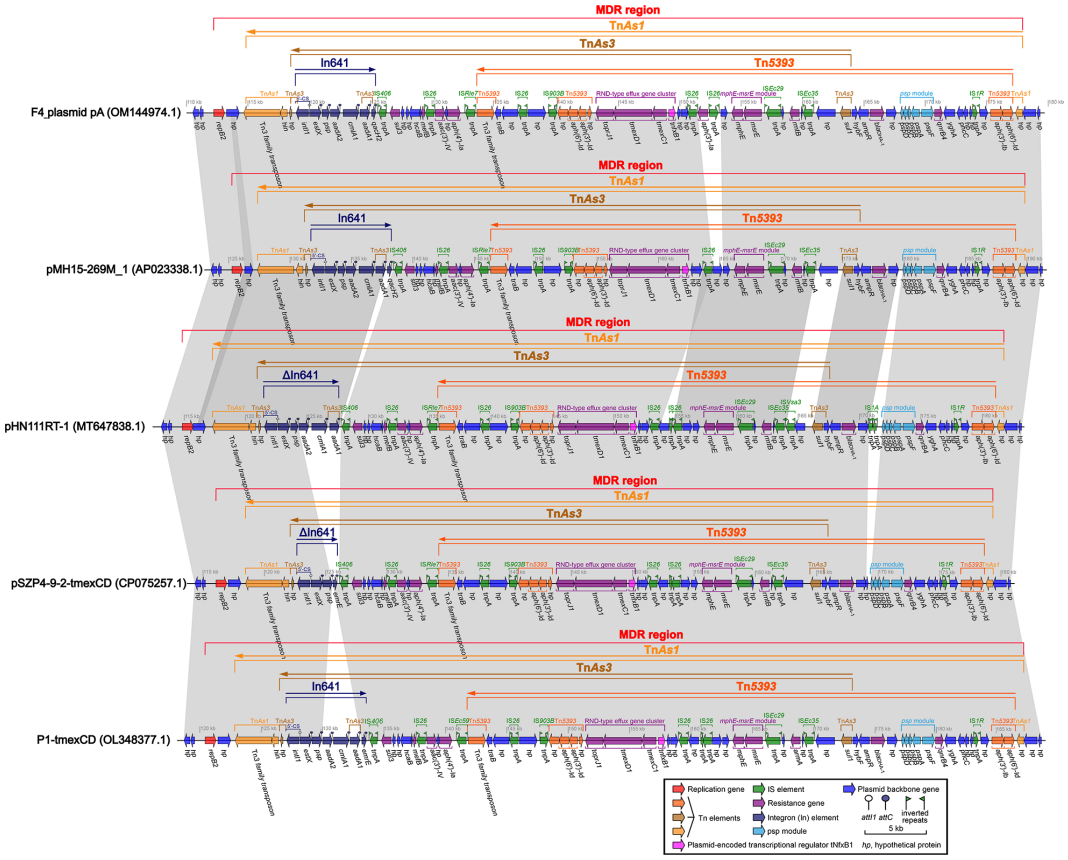

FIGURE 1
Comparison of F4_plasmid pB with related plasmids pCTXM27_ 020046, Plasmid L99-05, and p19110124-2. The shadow represents > 95% identity, while light blue represents the positive direction, and light pink refers to the opposite direction. The figure was created by the R package genoPlotR v0.8.11 software (http://genoplotr.r-forge.r-project.org/).

Comparison of F4_plasmid pB with the closely related plasmids pCTXM27_020046, Plasmid L99-05, and p19110124-2, all harboring In553 and *bla*$_{CTX-M-174}$

The profiles of F4_plasmid pB and closely related plasmids are shown in Table 2. The identities and coverage rates between F4_plasmid pB and pCTXM27_020046, Plasmid L99-05, and p19110124-2 were all greater than 99% and 92.5%, respectively, expressing extremely high similarity (Table 2).

The nearly 13.74 kb-long segment of pCTXM27_020046 from the *repA* gene to the partial 3′-CS of In553 (excluding *qacEdelta1* and *sul1*) was almost identical to the approximately 13.81 kb-long F4_plasmid pB from the 3′-CS remnant of incomplete In553 (without *qacEdelta1* and *sul1*) to the *repA* gene but in opposite directions (Figure 1). Similarly, an approximately 50.40 kb-long segment of pCTXM27_020046, from the *sul1* gene of In553 to IS*26* located at a site of approximately 64 kb, was almost identical to an approximately 47.80 kb-long segment of F4_plasmid pB, from IS26 located at a site of about 23 kb to the *sul1* gene located at site of nearly 73 kb, but in opposite directions (Figure 1).

When comparing F4_plasmid pB with Plasmid L99-05, the two plasmids were almost identical in structure and length, except for a small segment of sequence at the beginning of F4_plasmid pB that included In553, which was identical to the end of Plasmid L99-05 (Figure 1). When comparing Plasmid L99-05 with p19110124-2, the two plasmids were also nearly identical in structure and length, except that approximately a third of the final sequence length of p19110124-2 including In553 was the same as approximately a third of the length of the beginning of plasmid L99-05. F4_ plasmid pC contains five genes, two of which are the drug resistance genes *qnrB4* and *sul1*, and showed a high degree of sequence identity with the back-end sequence of F4_plasmid pB and a segment of Plasmid L99-05 located in front of In553 (Figure 1).

Structurally, Tn*As3* was divided into several parts by In553, some IS, and partial plasmid backbone genes located on F4_plasmid pB and its other closely related plasmids pCTXM27_020046, Plasmid L99-05, and p19110124-2, developing an intricate yet intersecting complex MDR region for each plasmid (Figure 1).

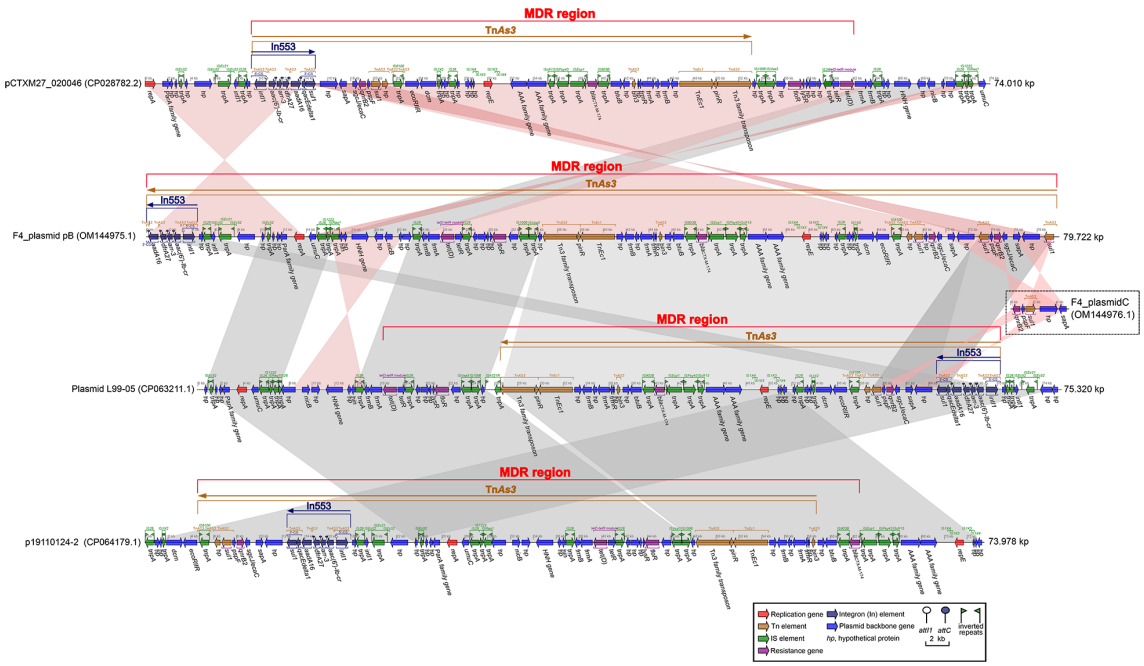

FIGURE 2
Comparison of the MDR regions from F4_plasmid pA and similar plasmids pMH15-269M_1, pHN111RT-1, pSZP4-9-2-tmexCD, and P1-tmexCD. The shadow represents >95% identity, while light blue represents the positive direction, and light pink refers to the opposite direction. The figure was created by the R package genoPlotR v0.8.11 software (http://genoplotr.r-forge.r-project.org/).

Genetic context of *toprJ1-tmexCD1-tnfxB1* from F4_plasmid pA and closely related plasmids

By finely analyzing the MDR region in Figure 2, we discovered that IS*26* was present at both the front and back of *toprJ1-tmexCD1-tnfxB1*. IS*26*-mediated translocation is the most efficient and most likely to occur when a copy of IS*26* was involved (Harmer et al., 2014).

The IS*26*s of F4_plasmid pA and closely related plasmids pMH15-269M_1, pHN111RT-1, pSZP4-9-2-tmexCD, and P1-tmexCD were consistent, and these IS*26*s were localized to the gene arrays of IS*26*-hp-IS*903B*-Tn*5393*-(*toprJ1-tmexD1- tmexC1-tnfxB1*)-hp-IS*26* and IS*26*-*aac(3')-IV*-hp-*aph(4')-Ia*-IS*26*-hp-IS*903B*-Tn*5393* -(*toprJ1-tmexD1-tmexC1-tnfxB1*)-hp-hp-IS*26* (Figure 2). Although we had not yet been able to verify this experimentally, a similar case had been confirmed in the literature (Wan et al., 2021). Thus, we assumed that the above two structures could be integrated by IS*26* to form two circular intermediates with different sequence lengths (Figure 3), implying that these intermediates might also move independently, much like the characteristics of small plasmids. Taken together, this suggests that *tmexCD1-toprJ1* might have been transferred to different plasmids including the F4_plasmid pA and closely related plasmids via IS*26*-integrated loop intermediates, representing a novel kind of dispersal dissemination. For F4_plasmid pA, in addition to carrying *tmexCD1-toprJ1*, this plasmid also carried In641, Tn*As1*, Tn*As3*, and Tn*5393* intermingled with each other, which was more complex and posed a much greater clinical threat than pHN111RT-1 and pHN111WT-1 (Wan et al., 2021).

Discussion

tmexCD-toprJ-positive bacteria are usually directly involved in multidrug resistance and can carry different drug resistance genes (Dong et al., 2022). The major functional *tmexCD* transporters have evolved into different isoforms. *tmexCD-toprJ* has a highly diverse genetic environment related to various mobile elements (Dong et al., 2022). If horizontal and vertical gene transfer of *tmexCD-toprJ* had occurred, it would likely have led to widespread clinical dissemination (Dong et al., 2022).

So far, *tmexCD-toprJ*-positive bacteria have originated largely in China from 2020, and have been occasionally discovered in Vietnam and other countries, provoking warnings of global spread (Hirabayashi et al., 2021). This may be related to the IS*26*-integrated loop intermediates described in this study (Figure 3). IS*26* could be transferred not only by a transposon consisting of two IS*26* and the related gene, but also by seamless transfer of the related gene to the end of the existing IS*26* (Harmer and Hall, 2015; Harmer and Hall, 2016). The efficiency of the second transfer was 60 times higher than that of the first transfer when the plasmid contained IS26 (Harmer et al., 2014). Furthermore, all transfer units, such as F4_plasmid pA and similar plasmids, carried the *traB* gene (Figures 2, 3), which might accelerate transfer across species (Burbank and Van Horn, 2017).

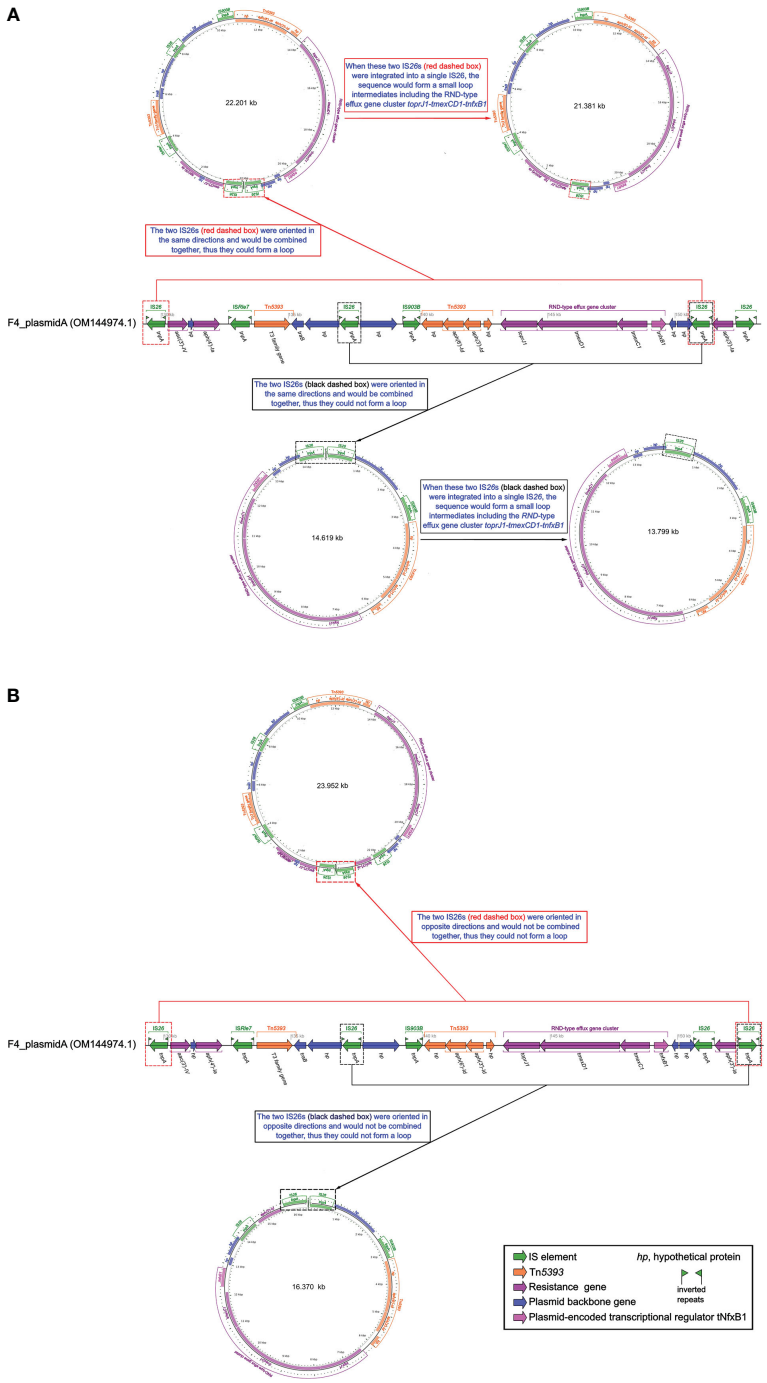

FIGURE 3
Schematic diagram of whether small loop intermediates could be formed by the integration of IS*26*s. **(A)** Schematic representation of a small loop intermediate that could be formed. **(B)** Schematic representation of a small loop intermediate that could not be formed. The diagram of F4_plasmid pA was created by the R package genoPlotR v0.8.11 software (http://genoplotr.r-forge.r-project.org/). The small loop diagrams were established using CGview v2.0.3 (https://github.com/paulstothard/cgview).

The spread of the *tmexCD-toprJ* gene cluster involves ISs (such as IS*26* and IS*903B*), transposons (such as Tn*As1*, Tn*5393*, and Tn*As3*), integrons (such as In641), integration and conjugation elements (ICEs), and plasmids (Figure 2) (Sun et al., 2020; Wang Q. et al., 2021). These mobile genetic elements have contributed significantly to the development of bacterial antibiotic resistance. Incomplete Tn*As1*, Tn*5393*, and Tn*As3* with integron components were found in the *tmexCD1-toprJ1* gene clusters in the MDR regions of F4_plasmid pA and similar plasmids (Figure 2), and a complete or incomplete In641 appeared near the *tmexCD1-toprJ1* gene clusters; we speculate that these structures of the F4_plasmid pA and similar plasmids might have accompanied the spread of the *tmexCD1-toprJ1* gene cluster at an early stage and subsequently been disrupted and partitioned by other genetic mobile elements

during the evolutionary process. Similarly, although F4_plasmid pB does not contain the *tmexCD1-toprJ1* gene cluster, incomplete Tn*As3* with In553 was also split from the MDR regions of F4_plasmid pB and similar plasmids, and complete or incomplete In553 appeared as one of the Tn*As3* components in these MDR regions (Figure 3). The presence of the *oqxAB* gene in the F4_chromosome increases the complexity of resistance to some antibiotics. A strain F4 carrying F4_plasmid pA with Tn*As1*, Tn*5393*, Tn*As3*, In641, *tmexCD1-toprJ1*, and $bla_{\text{DHA-1}}$ (Figure 2), alongside F4_plasmid pB with Tn*As3*, In641, and $bla_{\text{CTX-M-174}}$ (Figure 1) and the F4_chromosome bearing the *oqxAB* gene (Figure S1), would be extremely challenging for clinical prevention and treatment. Mobilization and dissemination of bacterial plasmids carrying *toprJ1-tmexCD1* and incorporating IS*26* as a mediator would be more dangerous in hospitals.

Overexpression of *oqxAB*, the RND-type efflux pump gene on the chromosome, plays an essential role in tigecycline resistance (Sheng et al., 2014; Bialek-Davenet et al., 2015). Strain F4 was highly resistant to 22 routinely used antibiotics and antibiotic + enzyme inhibitors, including tigecycline, and this resistance was directly associated with the *oqxAB* gene localized on the F4_chromosome (Figure S1) and *tmexCD1-toprJ1* on plasmid A (Table 1). The high resistance to β-lactams and β-lactams + enzyme inhibitors, especially the novel combination of cefoperazone + avibactam, was directly related to $bla_{\text{DHA-1}}$ on F4_plasmid pA and $bla_{\text{CTX-M-174}}$ on F4_plasmid pB (Table 1), so was cephalexin resistance (Table 1). Overall, strain F4 expressed to resistance to Aminoglycoside, β-lactams antibiotics, β-lactams antibiotics + enzyme inhibitors, Cephalexin, Fluoroqinolones, Tetracycline, Glycylcycline (tigecycline), Phenicol, Sulfonamide, Macrolide and Rifamycin (Table 1). The emergence of the plasmid-mediated multidrug resistance gene cluster *tmexCD1-toprJ1* decreases susceptibility to many clinically important antimicrobial drugs and constitutes a serious problem of multidrug resistance, which is the most troublesome issue in the human clinical setting. It's worth noting that if *tnfxB* function was absent, overexpression of *tmexCD1-toprJ1* could enhanced resistance to tetracyclines, fluoroquinolones, cephalosporins, macrolides, and chloramphenicol (Table 1), and in the presence of upstream *tnfxB*, *tmexCD1-toprJ1* would not been affected the resistance level (Lv et al., 2020). Structural differences in the composition of resistance genes between F4_plasmid pA, F4_plasmid pB and F4_plasmid pC were responsible for the differences in antibiotic resistance among strains F4 (Table 1).

Conclusion

It has risen to such a terrible extent that there are almost no effective antibiotics available, and its spread and prevalence should be effectively prevented for strain F4 and related strains, because of the intermingling of In641 with Tn*As1*, Tn*5393*, and Tn*As3* in F4_plasmid pA and closely related plasmids carrying *tmexCD1-toprJ1* and $bla_{\text{DHA-1}}$, and the structural overlaps of In553 and Tn*As3* in F4_plasmid pB and closely related plasmids bearing $bla_{\text{CTX-M-147}}$, together with the *oqxAB* genes located on the F4 chromosome.

Data availability statement

The datasets presented in this study can be found in online repositories. The names of the repository/repositories and accession number(s) can be found below: https://www.ncbi.nlm.nih.gov/genbank/, The GenBank accession numbers of the F4_chromosome, F4_plasmid pA, F4_plasmid pB, and F4_plasmid pC are CP090397.1, OM144974.1, OM144975.1, and OM144976.1, respectively.

Ethics statement

This study was approved by the Ethics Committee of Taizhou Municipal Hospital, Zhejiang, China, and written informed consent was obtained from each of the participants in accordance with the Declaration of Helsinki. The rights of the research subjects were protected throughout, and we confirm that this study was conducted in our hospital. The use of human specimens and all related experimental protocols were approved by the Committee on Human Research of the indicated institutions, and the protocols were carried out in accordance with approved guidelines.

Author contributions

YQ: Data curation, Formal Analysis, Funding acquisition, Investigation, Methodology, Project administration, Resources, Supervision, Validation, Writing – review & editing, Software. WW: Data curation, Formal Analysis, Investigation, Methodology, Project administration, Resources, Software, Supervision, Validation, Writing – review & editing. QL: Data curation, Formal Analysis, Investigation, Methodology, Project administration, Resources, Software, Supervision, Validation, Writing – review & editing. JQ: Data curation, Formal Analysis, Investigation, Methodology, Project administration, Resources, Supervision, Validation, Writing – review & editing. DW: Data curation, Formal Analysis, Investigation, Methodology, Project administration, Resources, Supervision, Validation, Writing – review & editing, Conceptualization, Funding acquisition, Writing – original draft. LM: Writing – review & editing, Data curation, Formal Analysis, Investigation, Methodology, Project administration, Resources, Software, Supervision, Validation.

Funding

The author(s) declare financial support was received for the research, authorship, and/or publication of this article. This work was supported by Zhejiang Health Department of China (2023KY1319). This work was also supported by the Science and Technology Plan Project of Taizhou City, Zhejiang Province (22ywb53).

Acknowledgments

We thank Yolanda Elisabet Gonzalez Flores, Ph.D, from Université de Limoge, for analyzing the integrons. We also thank Catherine Perfect, MA (Cantab), from Liwen Bianji (Edanz) (www.liwenbianji.cn), for editing the English text of a draft of this manuscript.

Conflict of interest

The authors declare that the research was conducted in the absence of any commercial or financial relationships that could be construed as a potential conflict of interest.

Publisher's note

All claims expressed in this article are solely those of the authors and do not necessarily represent those of their affiliated organizations, or those of the publisher, the editors and the reviewers. Any product that may be evaluated in this article, or claim that may be made by its manufacturer, is not guaranteed or endorsed by the publisher.

Supplementary material

The Supplementary Material for this article can be found online at: https://www.frontiersin.org/articles/10.3389/fcimb.2023.1260066/full#supplementary-material

SUPPLEMENTARY FIGURE 1
Circos plot of the F4_chromosome and localization of antibiotic resistance genes. **(A)** F4_chromosome of 5.249104 Mbp in length showing the location of the *oqxAB*, $bla_{CTX\text{-}M\text{-}27}$, and $bla_{SHV\text{-}106}$ genes. **(B)** Linear plots of structural features for the antibiotic resistance genes *oqxAB*, $bla_{CTX\text{-}M\text{-}27}$, and $bla_{SHV\text{-}106}$. The Circos plot of F4_chromosome was established using CGview v2.0.3 (https://github.com/paulstothard/cgview). The locations of the antibiotic resistance genes were drawn manually using Inkscape 0.48.1 (https://inkscape.org/en). Figure S1B was created by the R package genoPlotR v0.8.11 software (http://genoplotr.r-forge.r-project.org/) with hand finishing.

SUPPLEMENTARY FIGURE 2
Circos plots of F4_plasmid pA **(A)**, F4_plasmid pB **(B)**, and F4_plasmid pC **(C)**. The figure was established using CGview v2.0.3 (https://github.com/paulstothard/cgview).

SUPPLEMENTARY FIGURE 3
Comparison of F4_plasmid pA with related plasmids pMH15-269M_1, pHN111RT-1, pSZP4-9-2-tmexCD, and P1-tmexCD. The shadow represents >95% identity, while light blue represents the positive direction, and light pink refers to the opposite direction. The figure was created by the R package genoPlotR v0.8.11 software (http://genoplotr.r-forge.r-project.org/).

References

Alcock, B. P., Huynhm, W., Chalil, R., Smith, K. W., Raphenya, A. R., Wlodarski, M. A., et al. (2023). SCARD 2023: expanded curation, support for machine learning, and resistome prediction at the Comprehensive Antibiotic Resistance Database. *Nucleic Acids Res.* 51 (D1), D690–D699. doi: 10.1093/nar/gkac920

Algarni, S., Han, J., Gudeta, D. D., Khajanchi, B. K., Ricke, S. C., Kwon, Y. M., et al. (2023). In silico analyses of diversity and dissemination of antimicrobial resistance genes and mobile genetics elements, for plasmids of enteric pathogens. *Front. Microbiol.* 13. doi: 10.3389/fmicb.2022.1095128

Algarni, S., Ricke, S. C., Foley, S. L., and Han, J. (2022). The dynamics of the antimicrobial resistance mobilome of *salmonella enterica* and related enteric bacteria. *Front. Microbiol.* 13. doi: 10.3389/fmicb.2022.859854

Bialek-Davenet, S., Lavigne, J. P., Guyot, K., Mayer, N., Tournebize, R., Brisse, S., et al. (2015). Differential contribution of AcrAB and OqxAB efflux pumps to multidrug resistance and virulence in *Klebsiella pneumoniae*. *J. Antimicrob. Chemother.* 70 (1), 81–88. doi: 10.1093/jac/dku340

Boratyn, G. M., Camacho, C., Cooper, P. S., Coulouris, G., Fong, A., Ma, N., et al. (2013). BLAST: a more efficient report with usability improvements. *Nucleic Acids Res.* 41 (Web Server issue), W29–W33. doi: 10.1093/nar/gkt282

Bortolaia, V., Kaas, R. S., Ruppe, E., Roberts, M. C., Schwarz, S., Cattoir, V., et al. (2020). *ResFinder 4.0* for predictions of phenotypes from genotypes. *J. Antimicrob. Chemother.* 75 (12), 3491–3500. doi: 10.1093/jac/dkaa345

Brettin, T., Davis, J. J., Disz, T., Edwards, R. A., Gerdes, S., Olsen, G. J., et al. (2015). RASTtk: a modular and extensible implementation of the RAST algorithm for building custom annotation pipelines and annotating batches of genomes. *Sci. Rep.* 5, 8365. doi: 10.1038/srep08365

Burbank, L. P., and Van Horn, C. R. (2017). Conjugative plasmid transfer in Xylella fastidiosa is dependent on *tra* and *trb* operon functions. *J. Bacteriol.* 199 (21), e00388–e00317. doi: 10.1128/JB.00388-17

Chen, Z., Li, H., Feng, J., Li, Y., Chen, X., Guo., X., et al. (2015). NDM-1 encoded by a pNDM-BJ01-like plasmid p3SP-NDM in clinical *Enterobacter aerogenes*. *Front. Microbiol.* 6. doi: 10.3389/fmicb.2015.00294

Clinical and Laboratory Standards Institute (CLSI) (2022). *Performance standards for antimicrobial susceptibility testing. Thirty-two informational supplement. M100–S32* (Wayne, PA: Clinical and Laboratory Standards Institute).

Coudron, P. E., Moland, E. S., and Thomson, K. S. (2000). Occurrence and detection of AmpC beta-lactamases among *Escherichia coil*, *Klebsiella pneumoniae*, and *Proteus mirabilis* isolates at a veterans medical center. *J. Clin. Microbiol.* 38 (5), 1791–1796. doi: 10.1128/JCM.38.5.1791-1796.2000

De Oliveira, D. M. P., Forde, B. M., Kidd, T. J., Harris, P. N. A., Schembri, M. A., Beatson, S. A., et al. (2020). Antimicrobial resistance in ESKAPE pathogens. *Clin. Microbiol. Rev.* 33 (3), e00181–19.doi:10.1128/CMR.00181-19. doi: 10.1128/CMR.00181-19

Dong, N., Zeng, Y., Wang, Y., Liu, C., Lu, J., Cai, C., et al. (2022). Distribution and spread of the mobilised RND efflux pump gene cluster *tmexCD-toprJ* in clinical Gram-negative bacteria: a molecular epidemiological study. *Lancet Microbe* 3 (11), e846–e856. doi: 10.1016/S2666-5247(22)00221-X

Du, D., Wang-Kan, X., Neuberger, A., van Veen., H. W., Pos, K. M., Piddock, L. J. V., et al. (2018). Multidrug efflux pumps: structure, function and regulation. *Nat. Rev. Microbiol.* 16 (9), 523–539. doi: 10.1038/s41579-018-0048-6

Edgar, R. C. (2004). MUSCLE: multiple sequence alignment with high accuracy and high throughput. *Nucleic Acids Res.* 32 (5), 1792–1797. doi: 10.1093/nar/gkh340

Feng, Y., Zou, S., Chen, H., Yu, Y., and Ruan, Z. (2021). *BacWGSTdb 2.0*: a one-stop repository for bacterial whole-genome sequence typing and source tracking. *Nucleic Acids Res.* 49 (D1), D644–D650. doi: 10.1093/nar/gkaa821

Frank, J. A., Reichm, C. I., Sharma, S., Weisbaumm, J. S., Wilson, B. A., and Olsen, G. J. (2008). Critical evaluation of two primers commonly used for amplification of bacterial 16 S rRNA genes. *Appl. Environ. Microbiol.* 74 (8), 2461–2470. doi: 10.1128/aem.02272-07

Ghaheh, H. S., Damavandi, M. S., Sadeghi, P., Massah, A. R., Asl, T. H., SalariJazi, A., et al. (2022). Targeting and ultrabroad insight into molecular basis of resistance-nodulation-cell division efflux pumps. *Sci. Rep.* 12 (1), 16130. doi: 10.1038/s41598-022-20278-5

Harmer, C. J., and Hall, R. M. (2015). IS*26*-mediated precise excision of the IS*26*-*aphA1a* translocatable unit. *mBio* 6 (6), e01866–e01815. doi: 10.1128/mBio.01866-15

Harmer, C. J., and Hall, R. M. (2016). IS*26*-mediated formation of transposons carrying antibiotic resistance genes. *mSphere* 1 (2), e00038–e00016. doi: 10.1128/mSphere.00038-16

Harmer, C. J., Moran, R. A., and Hall, R. M. (2014). Movement of IS*26*-associated antibiotic resistance genes occurs via a translocatable unit that includes a single IS*26* and preferentially inserts adjacent to another IS*26*. *mBio* 5, e01801–e01814. doi: 10.1128/mBio.01801-14

He, T., Wang, R., Liu, D., Walsh, T. R., Zhang, R., Lv, Y., et al. (2019). Emergence of plasmid-mediated high-level tigecycline resistance genes in animals and humans. *Nat. Microbiol.* 4 (9), 1450–1456. doi: 10.1038/s41564-019-0445-2

Hirabayashi, A., Van Nguyen, A., Nguyen, S. T., Shibayama, K., and Suzuki, M. (2021). Emergence of a plasmid-borne tigecycline resistance in *Klebsiella pneumoniae* in Vietnam. *J. Med. Microbiol.* 70 (3), 1320. doi: 10.1099/jmm.0.001320

Li, X. Z., Plésiat, P., and Nikaido, H. (2015). The challenge of efflux-mediated antibiotic resistance in Gram-negative bacteria. *Clin. Microbiol. Rev.* 28 (2), 337–418. doi: 10.1128/CMR.00117-14

Linkevicius, M., Sandegren, L., and Andersson, D. I. (2016). Potential of tetracycline resistance proteins to evolve tigecycline resistance. *Antimicrob. Agents Chemother.* 60 (2), 789–796. doi: 10.1128/AAC.02465-15

Liu, Y.-Y., Wang, Y., Walsh, T. R., Yi, L.-X., Zhang, R., Spencer, J., et al. (2016). Emergence of plasmid-mediated colistin resistance mechanism MCR-1 in animals and human beings in China: a microbiological and molecular biological study. *Lancet Infect. Dis.* 16 (2), 161–168. doi: 10.1016/S1473-3099(15)00424-7

Lv, L., Wan, M., Wang, C., Gao, X., Yang, Q., Partridge, S., et al. (2020). Emergence of a plasmid-encoded resistance-nodulation-division efflux pump conferring resistance to multiple drugs, including tigecycline, in *Klebsiella pneumoniae*. *mBio* 11 (2), e02930–e02919. doi: 10.1128/mBio.02930-19

Moura, A., Soares, M., Pereira, C., Leitão, N., Henriques, I., and Correia, A. (2009). INTEGRALL: a database and search engine for integrons, integrases and gene cassettes. *Bioinformatics* 25 (8), 1096–1098. doi: 10.1093/bioinformatics/btp105

Salehi, B., Ghalavand, Z., Yadegar, A., and Eslami, G. (2021). Characteristics and diversity of mutations in regulatory genes of resistance-nodulation-cell division efflux pumps in association with drug-resistant clinical isolates of *Acinetobacter baumannii*. *Antimicrob. Resist. Infect. Control.* 10 (1), 1–12. doi: 10.1186/s13756-021-00924-9

Sheng, Z. K., Hu, F., Wang, W., Guo, Q., Chen, Z., Xu, X., et al. (2014). Mechanisms of tigecycline resistance among *Klebsiella pneumoniae* clinical isolates. *Antimicrob. Agents Chemother.* 58 (11), 698–6985. doi: 10.1128/AAC.03808-14

Siguier, P., Perochon, J., Lestrade, L., Mahillon, J., and Chandler, M. (2006). ISfinder: the reference centre for bacterial insertion sequences. *Nucleic Acids Res.* 34 (Database issue), D32–D36. doi: 10.1093/nar/gkj014

Stothard, P., Grant, J. R., and Van Domselaar, G. (2019). Visualizing and comparing circular genomes using the CGView family of tools. *Brief Bioinform.* 20 (4), 1576–1582. doi: 10.1093/bib/bbx081

Sun, S., Gao, H., Liu, Y., Jin, L., Wang, R., Wang, X., et al. (2020). Co-existence of a novel plasmid-mediated efflux pump with colstin resistance gene *mcr* in one plasmid confers transferable multidrug resistance in *Klebsiella pneumoniae*. *Emerg. Microbes Infect.* 9 (1), 1102–1113. doi: 10.1080/22221751.2020.1768805

Tansirichaiya, S., Rahman., M. A., and Roberts., A. P. (2019). The transposon registry. *Mob. DNA.* 10, 40. doi: 10.1186/s13100-019-0182-3

Tauch, A., Schlüter, A., Bischoff, N., Goesmann, A., Meyer, F., and Pühler, A. (2003). The 79,370-bp conjugative plasmid pB4 consists of an IncP-1 β backbone loaded with a chromate resistance transposon, the *strA-strB* streptomycin resistance gene pair, the oxacillinase gene bla_{NPS-1}, and a tripartite antibiotic efflux system of the resistance-nodulation-division family. *Mol. Genet. Genomics* 268 (5), 570–584. doi: 10.1007/s00438-002-0785-z

Wan, M., Gao, X., Lv, L., Cai, Z., and Liu, J.-H. (2021). IS*26* Mediates the acquisition of tigecycline resistance gene cluster *tmexCD1-toprJ1* by IncHI1B-FIB plasmids in *Klebsiella pneumoniae* and *Klebsiella quasipneumoniae* from food market sewage. *Antimicrob. Agents Chemother.* 65 (3), e02178–e02120. doi: 10.1128/AAC.02178-20

Wang, C.-Z., Gao, X., Yang, Q.-W., Lv, L.-C., Wan, M., Yang, J., et al. (2021). Novel transferable resistance-nodulation-division pump gene cluster *tmexCD2-toprJ2* that confers tigecycline resistance in *Raoultella ornithinolytica*. *Antimicrob. Agents Chemother.* 65 (4), e02229–e02220. doi: 10.1128/aac.02229-20

Wang, J., Jiang, Y., Lu, M.-J., Wang, Z.-Y., and Jiao, X. (2023). Emergence of a novel tigecycline resistance gene cluster *tmexC3-tmexD5-toprJ2b* in Oceanimonas sp. from chicken, China. *J. Antimicrob. Chemoth.* 78 (5), 1311–1313. doi: 10.1093/jac/dkad080

Wang, L., Liu, D., Lv, Y., Cui, L., Li, Y., Li, T., et al. (2019). Novel plasmid-mediated *tet(X5)* gene conferring resistance to tigecycline, eravacycline, and omadacycline in a clinical *Acinetobacter baumannii* isolate. *Antimicrob. Agents Chemother.* 64 (1), e01326–e01319. doi: 10.1128/AAC.01326-19

Wang, Q., Peng, K., Liu, Y., Xiao, X., Wang, Z., and Li, R. (2021). Characterization of *TMexCD3-TOprJ3*, an RND-type efflux system conferring resistance to tigecycline in *Proteus mirabilis*, and its associated integrative conjugative element. *Antimicrob. Agents Chemother.* 65 (7), e0271220. doi: 10.1128/AAC.02712-20

Xu, J., Zhu, Z., Chen, Y., Wang, W., and He, F. (2021). The Plasmid-borne *tet (A)* gene is an important factor causing tigecycline resistance in ST11 carbapenem-resistant *Klebsiella pneumoniae* under selective pressure. *Front. Microbiol.* 12. doi: 10.3389/fmicb.2021.644949

Yang, X., Dong, N., Chan, E. W., Zhang, R., and Chen, S. (2021). Carbapenem resistance- encoding and virulence-encoding conjugative plasmids in *Klebsiella pneumoniae*. *Trends Microbiol.* 29 (1), 65–83. doi: 10.1016/j.tim.2020.4.012

Frontiers in
Cellular and Infection Microbiology

Investigates how microorganisms interact with their hosts

Explores bacteria, fungi, parasites, viruses, endosymbionts, prions and all microbial pathogens as well as the microbiota and its effect on health and disease in various hosts.

Discover the latest Research Topics

See more →

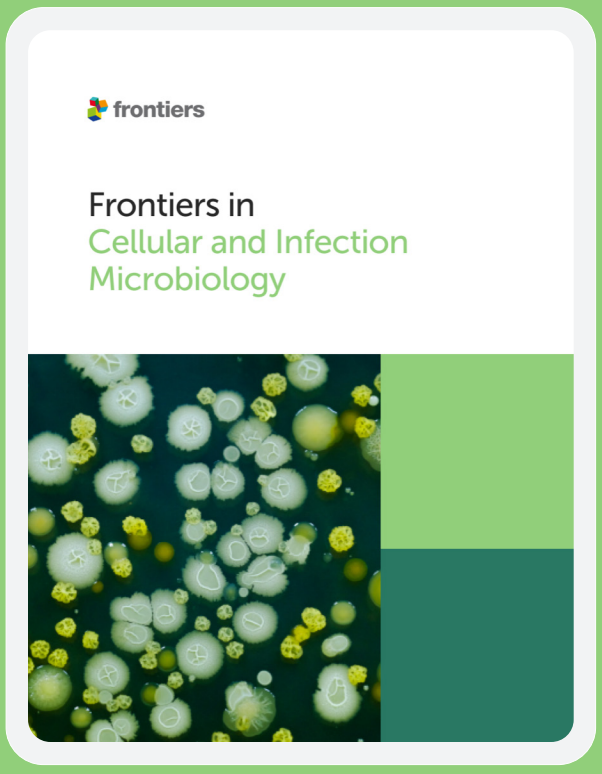

Frontiers

Avenue du Tribunal-Fédéral 34
1005 Lausanne, Switzerland
frontiersin.org

Contact us

+41 (0)21 510 17 00
frontiersin.org/about/contact